(12) INTERNATIONAL APPLICATION PUBLISHED UNDER THE PATENT COOPERATION TREATY (PCT)

(19) World Intellectual Property Organization
International Bureau

(43) International Publication Date
15 August 2019 (15.08.2019)

WIPO | PCT

(10) International Publication Number
WO 2019/157295 A1

(51) International Patent Classification:
A61K 31/01 (2006.01) *A61K 31/375* (2006.01)
A61K 31/04 (2006.01) *A61K 33/26* (2006.01)
A61K 31/015 (2006.01) *A61K 33/40* (2006.01)
A61K 31/19 (2006.01) *A61K 39/104* (2006.01)
A61K 31/197 (2006.01) *A61K 45/06* (2006.01)
A61K 31/198 (2006.01)

(21) International Application Number:
PCT/US2019/017233

(22) International Filing Date:
08 February 2019 (08.02.2019)

(25) Filing Language: English

(26) Publication Language: English

(30) Priority Data:
62/628,643 09 February 2018 (09.02.2018) US

(71) Applicant: **THE TRUSTEES OF COLUMBIA UNIVERSITY IN THE CITY OF NEW YORK** [US/US]; 412 Low Memorial Library, 535 W. 116th Street, New York, NY 10027 (US).

(72) Inventors: **DIETRICH, Lars**; 617 Fairchild Center, 1212 Amsterdam Avenue, New York, NY 10027 (US). **JO, Jeanyoung**; 617 Fairchild Center, 1212 Amsterdam Avenue, New York, NY 10027 (US).

(74) Agent: **DAVITZ, Michael, A.** et al.; Leason Ellis LLP, One Barker Avenue, Fifth Floor, White Plains, NY 10601 (US).

(81) Designated States *(unless otherwise indicated, for every kind of national protection available)*: AE, AG, AL, AM, AO, AT, AU, AZ, BA, BB, BG, BH, BN, BR, BW, BY, BZ, CA, CH, CL, CN, CO, CR, CU, CZ, DE, DJ, DK, DM, DO, DZ, EC, EE, EG, ES, FI, GB, GD, GE, GH, GM, GT, HN, HR, HU, ID, IL, IN, IR, IS, JO, JP, KE, KG, KH, KN, KP, KR, KW, KZ, LA, LC, LK, LR, LS, LU, LY, MA, MD, ME, MG, MK, MN, MW, MX, MY, MZ, NA, NG, NI, NO, NZ, OM, PA, PE, PG, PH, PL, PT, QA, RO, RS, RU, RW, SA, SC, SD, SE, SG, SK, SL, SM, ST, SV, SY, TH, TJ, TM, TN, TR, TT, TZ, UA, UG, US, UZ, VC, VN, ZA, ZM, ZW.

(84) Designated States *(unless otherwise indicated, for every kind of regional protection available)*: ARIPO (BW, GH, GM, KE, LR, LS, MW, MZ, NA, RW, SD, SL, ST, SZ, TZ, UG, ZM, ZW), Eurasian (AM, AZ, BY, KG, KZ, RU, TJ, TM), European (AL, AT, BE, BG, CH, CY, CZ, DE, DK, EE, ES, FI, FR, GB, GR, HR, HU, IE, IS, IT, LT, LU, LV, MC, MK, MT, NL, NO, PL, PT, RO, RS, SE, SI, SK, SM,

(54) Title: TREATING INFECTIONS USING INHIBITOR OF CBB3-TYPE OXIDASES

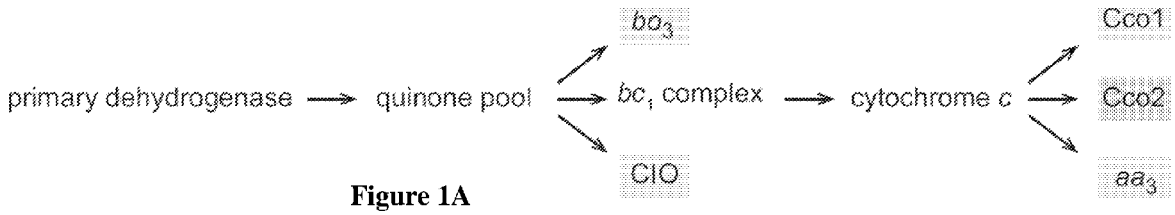


Figure 1A

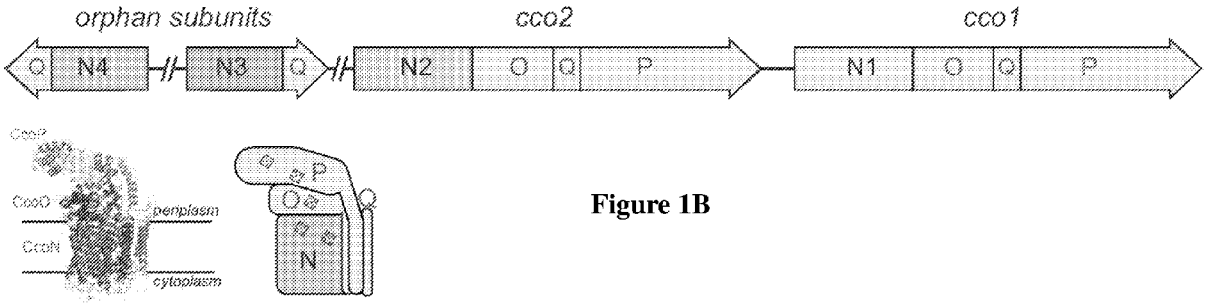


Figure 1B

(57) Abstract: The present disclosure provides for compositions and methods for inhibiting *cbb3*-type oxidases in the treatment, or prophylactic treatment, of bacterial infections and biofilm production. The cbb3-type oxidase inhibitor may be used in combination with an antibiotic.

[Continued on next page]

WO 2019/157295 A1

TR), OAPI (BF, BJ, CF, CG, CI, CM, GA, GN, GQ, GW, KM, ML, MR, NE, SN, TD, TG).

Published:

— *with international search report (Art. 21(3))*
— *with sequence listing part of description (Rule 5.2(a))*

TREATING INFECTIONS USING INHIBITOR OF CBB3-TYPE OXIDASES

Cross Reference to Related Applications

This application claims the benefit of U.S. Provisional Application No. 62/628,643 filed on February 9, 2018, the entire content of which is herein incorporated by reference.

Sequence Listing

The instant application contains a Sequence Listing which has been submitted electronically in ASCII format and is hereby incorporated by reference in its entirety. Said ASCII copy, created on February 8, 2019, is named 01001_006471-WO0_ST25.txt and is 13385 bytes in size.

Government License Rights

This invention was made with government support under AI103369 awarded by the National Institutes of Health and 1553023 awarded by the National Science Foundation. The government has certain rights in the invention.

Field of the Invention

The present invention relates to methods and compositions for the treatment of bacterial infections, and inhibiting or decreasing bacterial biofilm production. In particular, the present invention relates to the combined use of an inhibitor of a *cbb3*-type oxidase and an antibiotic in treating bacterial infections.

Background of the Invention

Pseudomonas aeruginosa is an opportunistic bacterial pathogen that is responsible for many nosocomial infections. It is also the leading cause of morbidity in patients with the genetic disease cystic fibrosis (CF). Biofilm formation contributes to *P. aeruginosa* pathogenicity and persistence during different types of infections, including the chronic lung colonization seen in individuals with cystic fibrosis (Tolker-Nielsen, 2014; Rybtke et al., 2015). See, Jo et al. An orphan *cbb3*-type cytochrome oxidase subunit supports *Pseudomonas aeruginosa* biofilm growth and virulence, eLife 2017; 6:e30205. Studies have shown that the biofilm mode of growth enables *Pseudomonas aeruginosa* (*P. aeruginosa*) to thrive in the host by providing protection against traditional methods

of treatment, such as antibiotics. *Pseudomonas aeruginosa* is also the major pathogen associated with cystic fibrosis lung infection, keratitis eye infection, and third-degree burn-associated skin infections.

The biofilm lifestyle - in which cells grow in a dense community encased in a self-produced matrix - has been linked to the establishment and persistence of infections in diverse systems, for example in hospital or other clinical settings (e.g., catheter and implant infections), and in industrial processes (e.g., clogging of cooling towers in manufacturing plants) (Edwards and Kjellerup 2012; Rybtke et al. 2015).

Growth in a crowded biofilm presents unique challenges that include restricted access to oxygen; however, *P. aeruginosa* is able to withstand this particular challenge with its highly adaptable electron transport chain that includes enzymes called terminal oxidases that are able to scavenge minute amounts of available oxygen. *Pseudomonas aeruginosa*, a colonizer of both plant and animal hosts (Rahme et al. 1995), has a branched respiratory chain with the potential to reduce O_2 to water using at least five different terminal oxidase complexes: two quinol oxidases (bo_3 (Cyo) and a *bd*-type cyanide insensitive oxidase (CIO)) and three cytochrome *c* oxidases (aa_3, cbb_3-1 or Cco1, and cbb_3-2 or Cco2). The two cbb_3-type oxidases of *P. aeruginosa* are notable for their relatively high catalytic activity at low O_2 concentrations and restriction to the bacterial domain (Brochier-Armanet, Talla, and Gribaldo 2009; Pitcher and Watmough 2004).

The cbb_3-type cytochrome c oxidase (*cbb3*) is a bacteria-specific terminal oxidase of the heme-copper oxidoreductase superfamily that catalyzes the four-electron reduction of molecular oxygen to water at the end of the aerobic respiratory chain. See, Hirai et al., Expression of multiple cbb_3 cytochrome c oxidase isoforms by combinations of multiple isosubunits in *Pseudomonas aeruginosa*, Proc Natl Acad Sci, 2016, 113(45):12815-12819. Ekici et al., (2012) Biogenesis of cbb3-type cytochrome c oxidase in Rhodobacter capsulatus. Biochim Biophys Acta 1817(6):898–910. *cbb*3-type terminal oxidases have been shown to be the predominant terminal oxidases that support *P. aeruginosa* growth. cbb_3 has a particularly high affinity for oxygen and typically functions under low-oxygen conditions in many bacteria, including several pathogens of *Helicobacter, Campylobacter*, and *Neisseria* species. Nagata et al., (1996) A cb-type cytochrome-c oxidase terminates the respiratory chain in Helicobacter pylori. Microbiology 142(Pt 7):1757–1763. Jackson et al. (2007) Oxygen reactivity of both respiratory oxidases in Campylobacter jejuni: The cydAB genes encode a cyanide-resistant, low-affinity oxidase that is not of the cytochrome bd type.

J Bacteriol 189(5):1604–1615. Li et al. (2010) Organization of the electron transfer chain to oxygen in the obligate human pathogen Neisseria gonorrhoeae: Roles for cytochromes c4 and c5, but not cytochrome c2, in oxygen reduction. J Bacteriol 192(9):2395–2406. cbb_3 oxidases are found almost exclusively in Proteobacteria. cbb_3 consists of four subunits that are encoded by the ccoNOQP operon. CcoN is the core catalytic subunit, and it contains a reaction center. CcoO and CcoP are transmembrane monoheme and diheme cytochromes c, respectively (5). CcoQ is known to affect the stability of the cbb_3 complex, but it is not necessarily a component of purified cbb_3 (6–8). Expression of cytochrome *cbb3* oxidase allows human pathogens to colonize low-oxygen environments and agronomically important diazotrophs to sustain N2 fixation.

Pseudomonas aeruginosa can survive in a wide range of environments. With an outer membrane of low permeability, a multitude of efflux pumps, and various degradative enzymes to disable antibiotics, *P. aeruginosa* is difficult to treat. As with other common pathogenic bacteria, antibiotic-resistant strains are an increasing problem.

Strong antimicrobials may be used to kill bacteria in a biofilm, controlling its development and growth. However, once biofilms are established, antimicrobials are not associated with removal of live or dead biofilm. It has been well documented that, because antimicrobials have difficulty penetrating the biofilm's surface layer, they are less effective on bacteria in an established biofilm compared to planktonic bacteria.

Therefore, there is an ongoing need to identify new methods of treating or preventing bacterial infections and disrupting biofilms.

Summary

The present disclosure provides for a method of treating a bacterial infection in a subject, comprising the step of administering to the subject an antibiotic and an inhibitor of a *cbb*$_3$-type oxidase.

The present disclosure provides for a method of treating a bacterial infection in a subject, comprising the step of administering to the subject an inhibitor of a *cbb*$_3$-type oxidase.

The present disclosure also provides for a method of disrupting a bacterial biofilm, comprising the step of contacting the bacterial biofilm with an antibiotic and an inhibitor of a *cbb*$_3$-type oxidase.

The present disclosure further provides for a method of disrupting a bacterial biofilm, comprising the step of contacting the bacterial biofilm with an inhibitor of a *cbb*$_3$-type oxidase.

Further encompassed by the present disclosure is a method of inhibiting or decreasing a bacterial biofilm production on a surface or substrate, comprising the step of contacting the surface or substrate with an antibiotic and an inhibitor of a *cbb*$_3$-type oxidase.

The present disclosure provides for method of inhibiting or decreasing a bacterial biofilm production on a surface or substrate, comprising the step of contacting the surface or substrate with an inhibitor of a *cbb*$_3$-type oxidase.

The surface may be a surface in the oral cavity, or a mammalian skin or mucosal surface.

The present disclosure provides for a method of inhibiting or decreasing bacterial biofilm production, and/or inhibiting or decreasing bacterial virulence factor production, comprising the step of contacting bacteria with an antibiotic and an inhibitor of a *cbb*$_3$-type oxidase.

The present disclosure further provides for a method of inhibiting or decreasing bacterial biofilm production, and/or inhibiting or decreasing bacterial virulence factor production, comprising the step of contacting bacteria with an inhibitor of a *cbb*$_3$-type oxidase.

The present method may further comprise administering to the subject an antifungal agent.

The present method may further comprise administering to the subject an antiviral agent.

The present method may be for therapeutic treatment, and/or for prophylactic treatment.

The present method may be for use in an industrial setting, such as a work area, a medical instrument, a chemical unit operation, a pipe, a sewage system, a pipeline, a tubing, or a filtration.

The present disclosure provides for a pharmaceutical composition comprising a first amount of an antibiotic and a second amount of an inhibitor of a *cbb*$_3$-type oxidase.

The present disclosure also provides for a pharmaceutical composition comprising an inhibitor of a *cbb*$_3$-type oxidase.

The pharmaceutical composition may be used for treating, or treating prophylactically, a bacterial infection.

The pharmaceutical composition may be for administration topically, intravenously, or intranasally.

The pharmaceutical composition may further comprise an antifungal agent, and/or an antiviral agent.

The antibiotic and the inhibitor may be administered simultaneously, sequentially or separately.

The antibiotic or the inhibitor may be administered topically, intravenously, intranasally, or through any suitable route.

In certain embodiments, the combination of the antibiotic and the inhibitor produces a synergistic effect compared to the effect of the antibiotic alone or the effect of the inhibitor alone. For example, the combination of the antibiotic and the inhibitor may result in a synergistic decrease in O_2 reduction; and/or a synergistic decrease in phenazine reduction.

The inhibitor may be a small molecule, a polynucleotide, a polypeptide, or an antibody or antigen-binding portion thereof.

In one embodiment, the inhibitor is an inhibitor of a *cbb*$_3$-type oxidase of *Pseudomonas aeruginosa*. In another embodiment, the inhibitor is an inhibitor of Cco1 and/or Cco2 of *Pseudomonas aeruginosa*. In yet another embodiment, the inhibitor is an inhibitor of catalytic subunit CcoN4 of *Pseudomonas aeruginosa*.

In one embodiment, the inhibitor is a nitrite.

Non-limiting examples of the inhibitors include diazeniumdiolate, S-Nitrosoglutathione (GSNO), S-Nitroso-N-acetylpenicillamine (SNAP), sodium nitrite, and/or potassium nitrite.

The antibiotic may be penicillin, cephalosporine, a beta-lactamase inhibitor, tetracycline, an aminoglycoside, a quinolone, a macrolide, or combinations thereof.

The antibiotic may be gentamicin, tobramycin, colistin, fluoroquinolone, or combinations thereof.

The bacterial infection may be a nosocomial infection, and/or an opportunistic infection.

The bacterial infection may be a urinary tract infection, respiratory pneumonia, a surgical site wound infection, bacteremia, a gastrointestinal infection, and/or a skin infection.

The bacterial infection may be a respiratory tract infection, a pulmonary tract infection, a urinary tract infection, a blood infection, an ear infection, an eye infection, a central nervous system infection, a gastrointestinal tract infection, a bone infection, a joint infection, a wound infection, dental plaque, gingivitis, chronic sinusitis, endocarditis, or combinations thereof.

The bacterial infection may be an implanted medical device-associated infection, a catheter-associated infection, an antibiotic resistant infection, or combinations thereof.

The bacterial infection may becaused by *Pseudomonas aeruginosa, Staphylococcus aureus, Staphylococcus aureus, Acinetobacter baumannii, Stenotrophomonas maltophilia, Clostridium difficile, Escherichia coli, Mycobacterium tuberculosis, Enterococcus, Legionella*, or combinations thereof.

The bacterial infection may be caused by *Pseudomonas* (such as *Pseudomonas aeruginosa*), *Burkholderia cepaci C. violaceum, V. harveyi, Neisseria gonorrhoeae, Neisseria meningitidis, Bordetella pertussis, Haemophilus influenzae, Legionella pneumophila, Brucella, Francisella, Xanthomonas, Agrobacterium, Escherichia coli, Salmonella, Shigella, Proteus, Yersinia pestisi*, or combinations thereof.

The subject may have cystic fibrosis, and/or primary ciliary dyskinesia.

The subject may be immunocompromised or immunosuppressed.

The subject may be undergoing, or has undergone, surgery, implantation of a medical device, and/or a dental procedure.

In one embodiment, the subject is a human.

The medical device may be a catheter, a joint prosthesis, a prosthetic cardiac valve, a ventilator, a stent, or an intrauterine device.

Any component of a cbb_3 oxidase may be inhibited by the present inhibitors. They include an inhibitor of CcoN, CcoO, CcoP, CcoQ, or combinations thereof.

Brief Description of the Drawings

Figures 1A-1C. The respiratory chain and arrangement of *cco* genes and protein products in *P. aeruginosa*, and the phylogenetic distribution of orphan *ccoN* genes. (A) Branched electron transport chain in *P. aeruginosa*, containing five terminal oxidases. (B) Organization of *cco* genes in the *P. aeruginosa* genome. The cartoon of the Cco complex is based on the Cco structure from *P. stutzeri* (PDB: 3mk7) (Buschmann et al. 2010). (C) Left: graphical representation of the portion of genomes in each bacterial phylum that contain *ccoO* and *N* homologs. The clades Chrysiogenetes, Gemmatimonadetes, and Zetaproteobacteria were omitted because they each contain only one species with *ccoO* and *N* homologs. The height of each rectangle indicates the total number of genomes included in the analysis. The width of each shaded rectangle represents the portion of genomes that contain *ccoN* homologs. Middle: genomes that contain more *ccoN* than *ccoO* homologs (indicating the presence of orphan *ccoN* genes) are listed. Right: numbers of *ccoO* and *ccoN* homologs in each genome. Blue highlights genomes containing more than one orphan *ccoN* homolog.

Figures 2A-2C. CcoN4-containing heterocomplexes make biofilm-specific contributions to morphogenesis and respiration. (A) Top: Five-day-old colony biofilms of PA14 WT and *cco* mutant strains. Biofilm morphologies are representative of more than ten biological replicates. Images were generated using a Keyence digital microscope. Scale bar is 1 cm. Bottom: 3D surface images of the biofilms shown in the top panel. Images were generated using a Keyence wide-area 3D measurement system. Height scale bar: bottom (blue) to top (red) is 0 - 0.7 mm for WT, Δ*N1*Δ*N2*, and Δ*N4*; 0 - 1.5 mm for Δ*N1*Δ*N2*Δ*N4* and Δ*cco1cco2*. (B) TTC reduction by *cco* mutant colonies after one day of growth. Upon reduction, TTC undergoes an irreversible color change from colorless to red. Bars represent the average, and error bars represent the standard deviation, of individually-plotted biological replicates (n = 5). P-values were calculated using unpaired, two-tailed t tests comparing each mutant to WT (****, $P \leq 0.0001$). For full statistical reporting, refer to Table 4. (C) Mean growth of PA14 WT and *cco* mutant strains in MOPS defined medium with 20 mM succinate. Error bars represent the standard deviation of biological triplicates.

Figures 2(IA) – 2(IC). Effects of individual and combined *cco* gene deletions on colony biofilm morphogenesis. (IA) Morphologies of WT, Δ*phz*, and *cco* single, combinatorial, and *ccoN4* complementation strains after 3 and 5 days of incubation. Images shown are representative of at least five biological replicates and were generated using a Keyence digital microscope. Scale bar is 1 cm. (IB) Development of WT, Δ*N4* and N subunit double mutants containing Δ*N4*. Images shown are representative of at least three biological replicates and were generated using a Keyence digital microscope. Scale bar is 1 cm. (IC) Development of WT and the triple mutant Δ*cox*Δ*cyo*Δ*cio* in which only the cbb_3-type terminal oxidases are present. Images were generated using a flatbed scanner (Epson Expression 11000XL) and are representative of at least three biological replicates. Scale bar is 1 cm.

Figures 2(IIA) - 2(IIB). PA14 WT, Δ*phz*, and *cco* mutant growth phenotypes are unaffected by endogenous cyanide production. (IIA) Colony development over four days for Δ*phz*, Δ*hcnABC*, and *cco* combinatorial mutants. Images were generated using a flatbed scanner (Epson Expression 11000XL) and are representative of at least three biological replicates. Scale bar is 1 cm. (IIB) Growth of Δ*phz*, Δ*hcnABC*, and *cco* combinatorial mutants in MOPS defined medium with 20 mM succinate. Error bars represent the standard deviation of biological triplicates and are not shown in cases where they would be obscured by the point marker.

Figures 2(III). Pseudomonads with CcoN homologs. We examined genomes available in the Pseudomonas Genome Database (Winsor et al. 2016) for CcoN homologs by performing a protein BLAST search on CcoN1 from *P. aeruginosa* PA14. All hits from full genomes, excluding other *P. aeruginosa* strains, were aligned using ClustalW and a tree was built using the geneious tree builder (Geneious 10 (Kearse et al. 2012)). We also included draft genomes that contained genes involved in phenazine biosynthesis (highlighted in purple). The tree revealed four clusters, each being more closely related to one of the four N subunits from PA14, which allowed us to annotate the N subunits accordingly. We next probed all genomes with N subunits for the presence of genes involved in cyanide synthesis (*hcnABC*) and phenazine biosynthesis (*phzABCDEFG*). We did not find a clear correlation between the presence of CcoN4 and Hcn proteins (Hirai et al. 2016). We note that with the exception of two *P. fluorescens* strains, those containing *phzABCDEFG* operons also contained *ccoN4*.

Figures 2(IVA) - 2(IVB). Comparison of the PA14 CcoN subunit sequences and analysis of the predicted structure of CcoN4. (IVA) Amino acid alignment (ClustalW) of the four CcoN subunits encoded by the PA14 genome. Residues conserved among all four N subunits, residues conserved among any three of the four N subunits, residues shared exclusively between CcoN1 and CcoN4, and residues unique to CcoN4, are all marked. (IVB) Predicted structure of CcoN4 from *P. aeruginosa* PA14, obtained by threading the PA14 sequence through the reported structure for the CcoN subunit of *P. stutzeri* (PDB: 5DJQ; (Buschmann et al. 2010)) using SWISS-MODELL (Biasini et al. 2014). Surface-exposed residues that are shared exclusively between CcoN1 and CcoN4, and residues that are unique to CcoN4 are shown. Ribbon structures of the CcoO and CcoP subunits from *P. stutzeri* are shown separately. Structures were generated using PyMol (Schrödinger, LLC 2015).

Figures 3A – 3D. CcoN4 confers a competitive advantage in biofilms, particularly when O_2 becomes limiting. (A) Relative fitness of various YFP-labeled *cco* mutants when co-cultured with WT in mixed-strain biofilms for three days. Error bars represent the standard deviation of biological triplicates. P-values were calculated using unpaired, two-tailed t tests (**, $P \leq 0.01$; ***, $P \leq 0.001$; ****, $P \leq 0.0001$). For full statistical reporting, refer to Table 4. (B) Time course showing relative fitness, over a period of three days, of various *cco* mutants when co-cultured with WT in mixed-strain biofilms. Results are shown for experiments in which the WT was co-cultured with various "labeled" strains, i.e. those that were engineered to constitutively express YFP. (See Figures 3(IA)-3(IC) for results from experiments in which the labeled WT was co-cultured with unlabeled mutants.) Error bars represent the standard deviation of biological triplicates. (C) Change in thickness over three days of development for colony biofilms of WT and Δ*phz* as assessed by thin sectioning and DIC microscopy. After the onset of wrinkling, thickness was determined for the base (i.e., the "valley" between wrinkles). Error bars represent the standard deviation of biological triplicates. (D) O_2 profiles of colonies at selected timepoints within the first three days of biofilm development. Circle, WT; square, Δ*phz*. Error bars denote standard deviation of biological triplicates.

Figures 3(IA) – 3(IC). CcoN4 is necessary for optimal fitness in biofilms, particularly when O_2 becomes limiting. (IA) Relative fitness of YFP-labeled WT when co-cultured with various *cco* mutant strains in mixed-strain biofilms for three days. Error bars represent the standard deviation of biological triplicates. P-values were calculated using unpaired, two-tailed t tests (***, $P \leq 0.001$; ****, $P \leq 0.0001$). For full statistical reporting, refer to Table 4. (IB) Time course showing relative fitness, over a period of three days, of YFP-labeled WT when co-cultured with various *cco* mutant strains in mixed-strain biofilms. Error bars represent the standard deviation of biological triplicates. (IC) DIC image of a three-day-old WT biofilm, which is representative of at least ten biological replicates.

Figure 4. *cco* genes are differentially expressed over biofilm depth. Left: Representative images of thin sections prepared from WT biofilms grown for three days. Each biofilm is expressing a translational GFP reporter under the control of the *cco1*, *cco2*, or *ccoQ4N4* promoter. Reporter fluorescence is overlain on respective DIC images. Right: Fluorescence values corresponding to images on the left. Fluorescence values for a strain containing the *gfp* gene without a promoter (the empty MCS control) have been subtracted from each respective plot. O_2 concentration over depth (open circles) from three-day-old WT biofilms is also shown. Error bars represent the standard deviation of biological triplicates and are not shown in cases where they would be obscured by the point markers. y-axis in the right panel provides a scale bar for the left panel. Reporter fluorescence images and values are representative of four biological replicates.

Figures 4(IA) – 4(IB). Expression of *cco* reporters in shaken liquid cultures. (IA) Fluorescence of translational reporter strains, engineered to express GFP under the control of the *cco1*, *cco2*, or *ccoN4Q4* promoter during growth in 1% tryptone. Fluorescence values for a strain containing the *gfp* gene without a promoter (the MCS control) were treated as background and subtracted from each growth curve. (IB) Liquid-culture growth of translational reporter strains in 1% tryptone. Error bars in (IA) and (IB) represent the standard deviation of biological triplicates and are not drawn in cases where they would be obscured by point markers.

Figures 5A – 5C. Characterization of chemical gradients and matrix distribution in PA14 WT and mutant colony biofilms. (A) Left: Change in O_2 concentration (blue) and redox potential (orange) with depth for WT and Δ*phz* biofilms grown for two days. For O_2 profiles, error bars represent the standard deviation of biological triplicates. For redox profiles, data are representative of at least five biological replicates. Right: model depicting the distribution of O_2 and reduced vs. oxidized phenazines in biofilms. (B) Top: Change in redox potential with depth for WT and various mutant biofilms grown for two days. Data are representative of at least five biological replicates. Bottom: Thickness of three-day-old colony biofilms of the indicated strains. Bars represent the average of the plotted data points (each point representing one biological replicate, $n \geq 4$), and error bars represent the standard deviation. P-values were calculated using unpaired, two-tailed t tests comparing each mutant to WT (n.s., not significant; **, $P \leq 0.01$; ****, $P \leq 0.0001$). For full statistical reporting, refer to Table 4. (C) Left: Representative thin sections of WT and *cco* mutant biofilms, stained with lectin and imaged by fluorescence microscopy. Biofilms were grown for two days before sampling. Right: Relative quantification of lectin stain signal intensity. Coloration of strain names in the left panel provides a key for the plotted data, and the y-axis in the right panel provides a scale bar for the left panel. Lectin-staining images and values are representative of four biological replicates.

Figures 5(IA) – 5(ID). Use of a redox microelectrode to measure phenazine reduction in colony biofilms. (IA) Change in redox potential over depth for two-day-old biofilms of PA14 WT, Δ*phz*, and Δ*phz* grown on 200 μM phenazine methosulfate (PMS). Data are representative of at least three biological replicates. To ensure that addition of PMS did not alter the baseline redox potential, a measurement was also taken of agar only. (IB) Change in redox potential with depth for WT, Δ*phz*, and Δ*cox*Δ*cyo*Δ*cio* biofilms grown for two days. Data are representative of at least two biological replicates. (IC)Levels of phenazines extracted from the agar medium underneath the colony and separated by HPLC, adjusted for biomass, for PA14 WT and various *cco* mutant biofilms grown for two days. Data represent the area under each peak in absorbance units for the phenazines indicated, and error bars represent standard deviation of at least three biological replicates. The phenazines pyocyanin (PYO), phenazine-1-carboxamide (PCN), and phenazine-1-carboxylic acid (PCA) were quantified. (ID) Colony biofilm morphologies on day four of development for WT and various *cco* mutant biofilms grown on colony morphology plates

containing 0, 10, and 40 mM potassium nitrate. Images were generated using a flatbed scanner (Epson Expression 11000XL) and are representative of at least three biological replicates. Scale bar is 1 cm.

Figures 6A - 6B. CcoN4-containing isoform(s) make unique contributions to PA14 virulence. Slow-killing kinetics of WT, *gacA*, and various *cco* mutant strains in the nematode *Caenorhabditis elegans*. Nearly 100% of the *C. elegans* population exposed to WT PA14 is killed after four days of exposure to the bacterium, while a mutant lacking GacA, a regulator that controls expression of virulence genes in *P. aeruginosa*, shows decreased killing, with ~50% of worms alive four days post-exposure. (A) *ΔN1ΔN2ΔN4* and *Δcco1cco2* show comparably attenuated pathogenicity relative to WT. Error bars represent the standard deviation of at least six biological replicates. At 2.25 days post-exposure, significantly less *C. elegans* were killed by *ΔN1ΔN2ΔN4* than by WT (unpaired two-tailed t test; $p = 0.0022$). (B) *ΔN1ΔN2* displays only slightly reduced pathogenicity when compared to WT. At 2.25 days post-exposure, significantly more *C. elegans* were killed by *ΔN1ΔN2* than by *ΔN1ΔN2ΔN4* (unpaired two-tailed t test; $p = 0.003$). For full statistical reporting, refer to Table 4. Error bars represent the standard deviation of at least four biological replicates, each with a starting sample size of 30-35 worms per replicate.

Figures 7A-7D. Cells from phenazine-null biofilms show increased sensitivity to ciprofloxacin. **a**. Four-day old colony biofilms of PA14 WT and the phenazine-null mutant (*Δphz*) grown on a defined medium containing 20 mM glucose. Scale bar is 5 mm. **b**. Schematic representing the biosynthesis of phenazines produced by glucose-grown PA14 biofilms. PCA, phenazine-1-carboxylic acid. PCN, phenazine-1-carboxamide. **c**. Schematic of experimental design used to quantify antibiotic tolerance in colony biofilms. **d**. Survival of WT and *Δphz* cells in biofilms exposed to ciprofloxacin at four concentrations. Each count is normalized to the CFU count reached without antibiotics (which corresponds to 100%). Data for growth without antibiotics does not show significant differences between strains (Figure 13). Each data point is a biological replicate, bar height indicates the mean of these replicates. P values are based on two-sided unpaired t-tests (n.s., not significant; *, $p \leq 0.05$; ***, $p \leq 0.001$).

Figures 8A-8B. Phenazine-mediated protection does not require matrix or major efflux pumps but depends on carbon source. a. Overview of known effects of phenazines on bacterial physiology. Phenazines can inhibit matrix production and induce expression of efflux pumps. Also, phenazines can alter flux through central metabolism and oxidize the cellular redox state. **b**. Quantification of ciprofloxacin tolerance observed for cells from biofilms representing various genetic or environmental conditions. The data for the parent strains (WT and Δ*phz)* grown with glucose as the carbon source are shown in grey in the left panel. Each data point (N) is a biological replicate. P values are based on unpaired one-sided t-tests (n.s., not significant; **, $p \leq 0.01$; ***, $p \leq 0.001$). Δ*pel* corresponds to Δ*pelB-G*, Δ*mex* to the triple mutant Δ*mexGHI-opmD ΔmexVW ΔmexPQ-opmE* (see **Table 5**). The center line of the boxplot shows the median, the lower and upper hinges correspond to the first and third quartiles, and the whiskers extend to the most extreme points, limited to 1.5 times the interquartile range.

Figures 9A-9C. The distribution of metabolic activity in biofilms is influenced by phenazine production and exposure to ciprofloxacin. a. Left: Section of a WT colony biofilm, prepared by paraffin embedding, stained with DAPI, and visualized by fluorescence microscopy. Scale bar is 50 μm. Data from sectioning experiments were collected at the approximate center of the colony in an area of 254x254 μm. Center and right: Microsensor and microelectrode profiling show that oxygen concentration is depleted at ~ 70 μm in WT (blue) and Δ*phz* (black) biofilms (center) and that phenazines are reduced at depth in WT biofilms (right). Data show mean and standard deviation for biological replicates for oxygen (WT: N=7, Δ*phz*: N=8) and for redox (WT: N=8, Δ*phz*: N=3). **b**. Left: Schematic of experimental design used to visualize metabolic activity in colony biofilms by stable isotope labeling. Spatially-resolved readouts were acquired by either collecting images in 5 μm steps in z-direction in an area of 254x254 μm over the biofilm depth (optical sectioning) or by subjecting biofilms to paraffin embedding and sectioning, followed by imaging signal in a 10-μm thin slice of the colony (paraffin sectioning). Right: Images and plotted deuterium signals obtained for optical and paraffin sections of colony biofilms after a 12-h incubation on D2O-containing medium. Data plots show mean deuterium signal per biofilm depth. One replicate each of WT and Δ*phz* is shown and is representative of at least five biological replicates. Deuterium signals are normalized to the signal in peak 1 within each sample. Scale bar is 50 μm. Paraffin section images are overlaid with protein signal to outline the colony. **c.** Left: Schematic of experimental design

used to visualize metabolic activity after incubation on labeled medium containing ciprofloxacin. Right: Deuterium signal for one biological replicate each of WT (blue) and Δ*phz* (black) after a 24h incubation on medium containing D2O and 0, 1, or 10 μg/ml ciprofloxacin. Deuterium signals are normalized to the signal in peak 1 within each sample. Data plots show mean deuterium signal per biofilm depth. For data of all replicates (N=3), see Figure 18b.

Figures 10A-10D. Analyses of antibiotic sensitivity and gene expression indicate that diverse redox-balancing pathways are functioning in PA14 biofilms. a. Overview of the redox balancing pathways investigated. NADH can be re-oxidized by pyruvate fermentation via LdhA or by the electron transport chain via terminal oxidases such as the *cbb*3 -type Cco complexes implicated in phenazine reduction. **b**. Ciprofloxacin (100 μg/mL) tolerance observed for cells from biofilms formed by *cco* mutants. Data for the parent strains (WT and Δ*phz*) are shown in grey. P values are based on an unpaired two-sided t-test between strain pairs as indicated (n.s., not significant; **, $p \leq 0.01$). Data for growth without antibiotics does not show significant differences between strains (Figure 13). The center line of the boxplot shows the median, the lower and upper hinges correspond to the first and third quartiles, and the whiskers extend to the most extreme points, limited to 1.5 times the interquartile range. **c**. Expression analyses of WT and Δ*phz* colony paraffin sections show lactate production (which activates expression of the *lldPDE* operon) in biofilms grown on defined medium with glucose as the sole carbon source. One representative biological replicate is shown (data for all replicates (N=x) is shown in Figure 19e). Scale bar is 25 μm. **d.** Model depicting the metabolisms that could support redox balancing in oxic (activity 1) and hypoxic (activity 2) biofilm subzones, contributing to activities detected by isotope labeling/SRS imaging and to antibiotic tolerance.

Figures 11A-11B. Representative chromatograms showing phenazines produced by *P. aeruginosa* PA14 liquid cultures and biofilms. Liquid cultures (A) were grown in 50 ml MOPS-glucose in a 250-ml Erlenmeyer flask) with shaking at 250 rpm for 16 hours before supernatant was collected for HPLC analysis. Colony biofilms (B) were each grown for 89 hours on 6 ml MOPS-glucose with 1% agar. Phenazines were extracted from a combined homogenate of the biofilm and agar-solidified medium. Phenazine-1-carboxamide (PCN) was not detected in liquid-culture samples while pyocyanin (PYO) was not detected in samples from biofilms. PCA, phenazine-1-

carboxylic acid. Chromatograms are representative of five biological replicates for liquid cultures and seven biological replicates for biofilms.

Figures 12A-12C. Survival of PA14 WT and Δ*phz* cells after exposure to antibiotics during growth in a biofilm. Circles show biological replicates, bars indicate the mean. Significant p-values are indicated and based on unpaired, two-sided t-tests (*, $p \leq 0.05$; **, $p \leq 0.01$; ***, $p \leq 0.001$). While phenazine production antagonizes killing by tobramycin and carbenicillin at higher concentrations, colistin and phenazines show a synergistic killing effect.

Figure 12D. Minimum inhibitory concentration (MIC) of ciprofloxacin, tobramycin, colistin and carbenicillin deduced from growth in MOPS-glucose. Cultures were grown in 96-well plates with shaking for 24 hours. The MIC for each antibiotic is the lowest tested concentration at which the average maximal OD is less than 0.1 (indicated by a dashed line). Circles show biological replicates.

Figure 13. Growth in the absence of ciprofloxacin. Colonies were grown for 65 hours on MOPS-glucose + 1% agar and then transferred to a fresh plate of medium and incubated for 24 additional hours. Circles show biological replicates. Boxplots indicate the median and the first and third quartile. A Kruskal-Wallis test was carried out to test the effect of strain identity on the number of CFUs per biofilm. There was no statistically significant effect of strain identity [$\chi 2(9)=10.796$, $p=0.29$]. The center line of the boxplot shows the median, the lower and upper hinges correspond to the first and third quartiles, and the whiskers extend to the most extreme points, limited to 1.5 times the interquartile range.

Figure 14. Survival of cells from stationary-phase liquid cultures after exposure to ciprofloxacin. Replicate cultures (each grown in 50 ml MOPS-glucose medium in a 250-ml flask) were started from the same preculture and grown for 16 hours to stationary phase. Ciprofloxacin was then added at the indicated concentration. Samples were taken for CFU quantification shortly before antibiotic addition and after four hours of incubation in antibiotic. Circles show biological replicates (N=3), bars indicate the mean. P-values are based on unpaired one-sided t-tests.

Figure 15. Added phenazines can enhance the growth of Δ*phz* in the presence of ciprofloxacin. Phenazine-1-carboxylic acid (PCA) or pyocyanin was added to the medium at a final concentration of 300 μM at the onset of the experiment. Liquid cultures were grown in a 96-well plate for 24 h. Circles show biological replicates (N=4 for PCA and no phenazine, N=3 for pyocyanin), crossbars indicate the mean. P values are based on unpaired one-sided t-tests (**, $p \leq 0.01$; ***. $p \leq 0.001$).

Figures 16A-16B. Raman spectra of biofilm thin sections with and without D2O metabolic labeling. a. Clear C-D peaks (dashed line) are observed in the cell spectral-silent regions in both WT and Δ*phz* biofilms. **b.** In both strains without deuterium labeling, a negligible signal is observed in the SRS images for background-free detection.

Figures 17A-17B. Measurement of metabolic activity in colony biofilms. Colonies were grown with D7-glucose and then transferred to unlabeled glucose for a 12-hour period before imaging. **a.** Experimental design for D7-glucose labeling scheme. **b.** Distribution of deuterium signal in colony biofilm optical sections prepared as described in panel a. Image and data show one biological replicate representative of N=3. In this labeling regime, metabolic activity is indicated by deuterium depletion and visible as dark zones in the biofilm images. As in the reverse labeling regime (i.e., incorporation of deuterium from D2O), the WT shows two regions of activity (valleys 1 and 2), while Δ*phz* shows one broad region of activity. Deuterium signal in data plots is corrected for light scattering using the protein channel and normalized to the minimal signal in valley 1. Scale bar is 25 μm.

Figures 18A-18E. Distribution of metabolic activity and *cco* and *mexG* expression. Distribution of metabolic activity was compared to expression of the *cco1* and *cco2* operons (encoding *cbb*3-type terminal oxidases) (**a, b**), expression from a constitutive promoter (**c**) and expression driven by the transcription factor *SoxR* (in a *mexGp-gfp* reporter strain) (**d**) in WT biofilms. For **a-c**, images and data plots show paraffin sections of one biological replicate representative of N=3 for a, b and 4 for c. Colonies were grown for three days and then incubated for 12h on medium containing 50% D2O. Deuterium and fluorescence signals in data plots are normalized to the maximum for each sample and type of signal. Scale bar is 25 μm. Panel **e** shows all replicates of experiments described in Figure 14c of *lldPDE* expression in WT (blue, N=3) and Δ*phz* (black, N=3).

Figures 19A-19B. Control experiments for the deletion mutant Δ*cco1cco2* confirm the importance of this locus for the phenazine-protective effect. a. Ciprofloxacin (100 μg/mL) tolerance observed for cells from biofilms formed by the Δ*cco1cco2* complementation strain (Δ*cco1cco2*::*cco1cco2*) as compared to WT and Δ*cco1cco2*. P value is based on an unpaired two-sided t-test between strain pairs as indicated (n.s., not significant; ***, $p \leq 0.001$). The center line of the boxplot shows the median, the lower and upper hinges correspond to the first and third quartiles, and the whiskers extend to the most extreme points, limited to 1.5 times the interquartile range. **b.** Phenazine production by Δ*cco1cco2* biofilms is similar to phenazine production by WT biofilms. Circles show biological replicates (N=7 for WT, N=8 for Δ*cco1cco2*), bars indicate mean of replicates. Biofilms were grown for four days before sampling. Phenazines were extracted from both the agar-solidified medium and the biofilm for each sample.

Figure 20. The distribution of metabolic activity across biofilm depth is altered by removal of the Cco terminal oxidases. Profiles of metabolic activity, as indicated by deuterium uptake, are shown for Δ*cco1cco2* mutants in phenazine-producing (WT) and phenazine-null (Δ*phz*) backgrounds. Colony biofilms were incubated according to the schematic shown and activity profiles are plotted in orange for Δ*cco1cco2* mutants. For comparison, the parent strains are plotted in black. The signal is normalized to the maximum signal reached in the peak closest to the air interface. The solid line shows average, dots show biological replicates (N=5 for Δ*cco1cco2*, N=3 for Δ*phz*Δ*cco1cco2*), and standard deviation is indicated by shading.

Figure 21. Deletion of *ldhA* does not significantly affect survival of cells in colony biofilms exposed to 100 μg/ml ciprofloxacin. The lack of significance was determined by an unpaired two-sided t-test (n.s., not significant). The center line of the boxplot shows the median, the lower and upper hinges correspond to the first and third quartiles, and the whiskers extend to the most extreme points, limited to 1.5 times the interquartile range.

Detailed Description of the Invention

The present disclosure provides for compositions and methods for inhibiting *cbb*$_3$-type oxidases in the treatment or prophylaxis of bacterial infections and biofilm production. Targeting *cbb*$_3$-type enzymes, which are specific to bacteria, minimizes potential cross-reactivity with host mechanisms. When their ability to form robust biofilms is attenuated, bacteria become more susceptible to conventional antibiotics, making combination therapy an effective strategy.

The present pharmaceutical composition may comprise, or consist essentially of (or consist of), an inhibitor of a *cbb*$_3$-type oxidase (or a *cbb*$_3$ oxidase inhibitor).

The present pharmaceutical composition may comprise, or consist essentially of (or consist of), an antibiotic and an inhibitor of a *cbb*$_3$-type oxidase (or a *cbb*$_3$ oxidase inhibitor).

Any component or subunit of a *cbb*$_3$-type oxidase may be inhibited or targeted by the present inhibitors. They include an inhibitor of Cco1 and/or Cco2 of *Pseudomonas aeruginosa*, an inhibitor of catalytic subunit CcoN4 of *Pseudomonas aeruginosa*, or combinations thereof. In one embodiment, the CcoN4 has a RefSeq gene symbol of PA14_10500. In another embodiment, the CcoN4 has a RefSeq gene symbol of PA14_RS04235.

The present compositions and methods may kill, inhibit the growth of, or reduce the viability of, bacteria, such as gram-negative bacteria (e.g., *Pseudomonas aeruginosa*). Bacterial infections may be treated, or treated prophylactically, by, e.g., inhibiting or decreasing biofilm production, inhibiting or decreasing pathogenicity, inhibiting or decreasing virulence factor (e.g., a phenazine such as pyocyanin) production/amount, and/or inhibiting or decreasing quorum sensing.

The present disclosure provides methods of using a combination of an antibiotic and an inhibitor of a *cbb*$_3$-type oxidase. In one embodiment, a subject having a bacterial infection is administered an antibiotic and an inhibitor of a *cbb*$_3$-type oxidase. In another embodiment, a bacterial biofilm is disrupted by contacting the bacterial biofilm with an antibiotic and an inhibitor of a *cbb*$_3$-type oxidase. In still another embodiment, a bacterial biofilm production on a surface or substrate is inhibited or decreased by contacting the surface or substrate with an antibiotic and an inhibitor of a *cbb*$_3$-type oxidase. In yet another embodiment, bacterial biofilm production and/or bacterial virulence factor production is inhibited or decreased by contacting the bacteria with an antibiotic and an inhibitor of a *cbb*$_3$-type oxidase. The combination of the antibiotic and the inhibitor of the of a *cbb*$_3$-type oxidase produces a synergistic effect on the bacterial infection, the biofilm, and/or bacteria compared to the effect of the antibiotic or the inhibitor of a *cbb*$_3$-type

oxidase alone. For example, the combination may result in a synergistic increase in bacterial killing, bacterial growth inhibition, a bacterial viability decrease, biofilm disruption, and/or a synergistic decrease in O_2 reduction and/or phenazine reduction.

The present disclosure also provides methods of using an inhibitor of a *cbb*$_3$-type oxidase. In one embodiment, a subject having a bacterial infection is administered an inhibitor of a *cbb*$_3$-type oxidase. In another embodiment, a bacterial biofilm is disrupted by contacting the bacterial biofilm with an inhibitor of a *cbb*$_3$-type oxidase. In still another embodiment, a bacterial biofilm production on a surface or substrate is inhibited or decreased by contacting the surface or substrate with an inhibitor of a *cbb*$_3$-type oxidase. In yet another embodiment, bacterial biofilm production and/or bacterial virulence factor production is inhibited or decreased by contacting the bacteria with an inhibitor of a *cbb*$_3$-type oxidase.

Methods and compositions of the present invention can be used for prophylaxis as well as treating bacterial infections (e.g., amelioration of signs and/or symptoms of bacterial infections).

For prophylaxis, the present composition can be administered to a subject in order to prevent the onset of one or more symptoms of a bacterial infection. In one embodiment, the subject can be asymptomatic. The subject may have been, or have not been, exposed to the bacterium. A prophylactically effective amount of the agent or composition is administered to such a subject. A prophylactically effective amount is an amount which prevents the onset of one or more symptoms of the bacterial infection.

The present composition can be administered to a subject to treat a bacterial infection. In one embodiment, the subject is symptomatic. In another embodiment, the subject can be asymptomatic. A therapeutically effective amount of the composition is administered to such a subject. A therapeutically effective amount is an amount effective to ameliorate one or more symptoms of the disorder.

The bacterial infections may be a nosocomial infection, and/or an opportunistic infection.

The bacterial infections may be a respiratory tract infection, a pulmonary tract infection, respiratory pneumonia, a urinary tract infection, a blood infection, an ear infection, an eye infection, a central nervous system infection, a surgical site wound infection, bacteremia, a gastrointestinal tract infection, a bone infection, a joint infection, a skin infection, a burn infection, a wound infection, dental plaque, gingivitis, chronic sinusitis, endocarditis, or combinations thereof. The infection may be of the pulmonary tract and may be pneumonia.

The subject may have cystic fibrosis, and/or primary ciliary dyskinesia. The subject may be immunocompromised or immunosuppressed. The subject may be undergoing, or has undergone, surgery, implantation of a medical device, and/or a dental procedure. For example, the medical device can be a catheter, a joint prosthesis, a prosthetic cardiac valve, a ventilator, a stent, an intrauterine device, or combinations thereof. The treatment may be therapeutic or prophylactic. In certain embodiments, the present compositions and methods are used prophylactically when the subject is undergoing surgery, a dental procedure or implantation of a medical device.

The present compositions and methods may be used on or within a medical instrument or device, a filtration device, a tubing, a pipe, a pipeline, a sewage system, water tower cooling system, or a work surface. In certain embodiments, the present compositions are applied to surfaces, tubes, pipes or devices in a fluid, aerosol, gel or cream formulation.

The present composition and methods may be used for disrupting biofilms on the surface of living entities and/or non-living things. In one embodiment, the present composition is in contact with the surface of the biofilm in a therapeutically effective amount to disrupt the biofilm, and facilitates the reduction and/or eradication of the bacteria in the biofilm once the biofilm is disrupted.

The present compositions may be used *in vitro* or administered to a subject. The administration may be topical, intravenous, intranasal, or any other suitable route as described herein.

As used herein, "antibiotic" refers to a substance that is used to treat and/or prevent bacterial infection by killing bacteria, inhibiting the growth of bacteria, or reducing the viability of bacteria.

As used herein, the term "biofilm" means a mucilaginous community of microorganisms such as bacteria, archaea, fungi, molds, algae or protozoa or mixtures thereof that grow on various surfaces when the microorganisms establish themselves on a surface and activate genes involved in producing a matrix that includes polysaccharides. In one embodiment, a biofilm may involve and/or contain more than one species of bacteria.

The biofilms can be very resistant to antibiotics and antimicrobial agents. In one embodiment, biofilms live on gingival tissues, teeth, and restorations, causing caries and periodontal disease, also known as periodontal plaque disease. In another embodiment, biofilms cause chronic middle ear infections. In still another embodiment, biofilms form on the surface of dental implants, stents, catheter lines and contact lenses. In yet another embodiment, biofilms grow

on pacemakers, heart valve replacements, artificial joints and other surgical implants. In another embodiment, fungal biofilms contaminate medical devices. They cause chronic vaginal infections and can lead to life-threatening systemic infections in people with compromised immune systems.

Biofilms may be involved in numerous diseases. For instance, cystic fibrosis patients have Pseudomonas infections that often result in antibiotic resistant biofilms. U.S. Patent No. 9,848,600.

Biofilms may cause damage to equipment such as cooling systems, or aquaculture equipment by corrosion of the equipment by microorganisms residing in the biofilm or by excessive coating or film buildup compromising the normal mechanics of the equipment.

The terms "disrupt", "disruptive" or "disruption" refer to partial or complete removal of biofilm or biofilm matrix, and/or compromising the integrity of the biofilm.

Inhibitors of *cbb*$_3$-type oxidases

The *cbb*$_3$ oxidases may be from organisms including, but not limited to, *Pseudomonas aeruginosa, Pseudomonas mendocina*, *Achromobacter xylosoxidans*, *Pseudomonas putida, Pseudomonas syringae pv. Tomato str., Caulobacter crescentus, Ralstonia solanacearum, Neisseria meningitidis, Neisseria gonorrhoeae, Helicobacter pylori, Helicobacter pylori, Vibrio cholerae, Campylobacter jejuni, Gemmata obscuriglobus, Cytophaga hutchinsonii P. denitrificans*, *R. sphaeroides*, *Rhodobacter capsulatus*, and *Bradyrhizobium japonicum*, *Azorhizobium caulinodans, Campylobacter jejuni, Helicobacter pylori,* and *Neisseria meningitidis*. Pitcher et al., The bacterial cytochrome *cbb*$_3$ oxidases, Biochimica et Biophysica Acta 1655 (2004) 388– 399.

Any component of a *cbb*$_3$ oxidase may be inhibited by the present inhibitors. They include an inhibitor of CcoN, CcoO, CcoP, CcoQ, or combinations thereof.

Any isoform of any *cbb*$_3$ oxidase may be inhibited by the present inhibitors. They include, but are not limited to: an inhibitor of an isoform of *cbb*$_3$, e.g., as in Hirai et al. 2016, or Example 1 of the present disclosure. In certain embodiments, the inhibitor is an inhibitor of an isoform of *cbb*$_3$ containing CcoN4.

The present inhibitors may target the wild-type or mutant component of a *cbb*$_3$ oxidase.

As used herein, the term "inhibitor" refers to agents capable of down-regulating or otherwise decreasing or suppressing the amount and/or activity of a *cbb*$_3$ oxidase.

The mechanism of inhibition may be at the genetic level (e.g., interference with or inhibit expression, transcription or translation, etc.) or at the protein level (e.g., binding, competition, etc.). In one embodiment, the inhibitor reduces O_2 reduction.

A wide variety of suitable inhibitors may be employed, guided by art-recognized criteria such as efficacy, toxicity, stability, specificity, half-life, etc.

The present inhibitor may be a small molecule, a nucleic acid, a protein or polypeptide, an antibody or antigen-binding portion thereof, or combinations thereof.

The nucleic acid targeting *cbb3* DNA or RNA (e.g., mRNA) may be a small interfering RNA (siRNA), a short hairpin RNA (shRNA), small temporal RNAs (stRNAs), and micro-RNAs (miRNAs), an antisense oligonucleotide, and combinations thereof.

Small Molecule Inhibitors

As used herein, the term "small molecules" encompasses molecules other than proteins or nucleic acids without strict regard to size. Non-limiting examples of small molecules that may be used according to the methods and compositions of the present invention include, small organic molecules, peptide-like molecules, peptidomimetics, carbohydrates, lipids or other organic (carbon containing) or inorganic molecules.

For example, the inhibitor may be nitric oxide, a nitric oxide-generating system, or a nitric oxide donor. Arjona et al., Nitric oxide is a potent inhibitor of the *cbb*$_3$-type heme-copper oxidases, FEBS Letters, 2015, 589(11):1214-1218. In one embodiment, the inhibitor is a nitrite, a thionitrite or S-Nitrosothiols, an organic nitrate, and/or an iron-nitrosyl complex.

Non-limiting examples of nitrites include, but are not limited to, alkali metal nitrites (e.g., sodium nitrite, potassium nitrite), and organic nitrites. In some embodiments, the inhibitor is an organic nitrite having the formula RONO (or RNO_2) where R is an aryl or alkyl group. In one embodiment, the inhibitor is amyl nitrite.

The inhibitor may be a thionitrite or S-Nitrosothiols, e.g., having the formula RSNO where R denotes an organic group. including, but not limited to, S-Nitrosoglutathione (GSNO), S-Nitroso-N-acetylpenicillamine (SNAP), etc.

In one embodiment, the inhibitor is diazeniumdiolate.

Non-limiting examples of *cbb3* oxidase inhibitors also include: diazeniumdiolate, S-Nitrosoglutathione (GSNO), S-Nitroso-N-acetylpenicillamine (SNAP), sodium nitrite, potassium nitrite, etc.

In certain embodiments, the *cbb3* oxidase inhibitor used in the present methods and compositions is a polynucleotide that reduces expression of a *cbb3* oxidase. Thus, the method involves administering an effective amount of a polynucleotide that specifically targets nucleotide sequence(s) within a *cbb3* oxidase. The polynucleotides reduce expression of a *cbb3* oxidase, to yield reduced levels of the gene product (the translated polypeptide).

The nucleic acid target of the polynucleotides (e.g., antisense oligonucleotides, and ribozymes) may be any location within the gene or transcript of any component of a *cbb3* oxidase.

Endonucleases

A *cbb3* oxidase may be inhibited by using a sequence-specific endonuclease that target the gene encoding a *cbb3* oxidase or a subunit of a *cbb3* oxidase.

Non-limiting examples of the endonucleases include a zinc finger nuclease (ZFN), a ZFN dimer, a ZFNickase, a transcription activator-like effector nuclease (TALEN), or a RNA-guided DNA endonuclease (e.g., CRISPR/Cas9). Meganucleases are endonucleases characterized by their capacity to recognize and cut large DNA sequences (12 base pairs or greater). Any suitable meganuclease may be used to in the present methods to introduce transgenes to the donor animal's genome, such as endonucleases in the LAGLIDADG family.

An example of sequence-specific endonucleases includes RNA-guided DNA nucleases, e.g., the CRISPR/Cas system. Geurts et al., Science 325, 433 (2009); Mashimo et al., PLoS ONE 5, e8870 (2010); Carbery et al., Genetics 186, 451-459 (2010); Tesson et al., Nat. Biotech. 29, 695-696 (2011). Wiedenheft et al. Nature 482,331-338 (2012); Jinek et al. Science 337,816-821 (2012); Mali et al. Science 339,823-826 (2013); Cong et al. Science 339,819-823 (2013).

The sequence-specific endonuclease of the methods and compositions described herein can be engineered, chimeric, or isolated from an organism. Endonucleases can be engineered to recognize a specific DNA sequence, by, e.g., mutagenesis. Seligman et al. (2002) Mutations altering the cleavage specificity of a homing endonuclease, Nucleic Acids Research 30: 3870–3879. Combinatorial assembly is a method where protein subunits form different enzymes can be associated or fused. Arnould et al. (2006) Engineering of large numbers of highly specific homing

endonucleases that induce recombination to novel DNA targets, Journal of Molecular Biology 355: 443–458. These two approaches, mutagenesis and combinatorial assembly, may be combined to produce an engineered endonuclease with desired DNA recognition sequence.

The sequence-specific nuclease can be introduced into the cell in the form of a protein or in the form of a nucleic acid encoding the sequence-specific nuclease, such as an mRNA or a cDNA. Nucleic acids can be delivered to a bacterial cell by transformation, e.g., heat shock, electroporation, etc. In one embodiment, bacterial cells are incubated in a solution containing divalent cations (e.g., calcium chloride) under cold conditions, before being exposed to a heat pulse (heat shock).

Antisense Polynucleotides

The polynucleotide of the invention may be an antisense nucleic acid sequence that is complementary to a target region within the mRNA of a *cbb*$_3$ oxidase, or any component of a *cbb*$_3$ oxidase (e.g., a subunit of a *cbb*$_3$ oxidase). The antisense polynucleotide may bind to the target region and inhibit translation. The antisense oligonucleotide may be DNA or RNA, or comprise synthetic analogs of ribo-deoxynucleotides. Thus, the antisense oligonucleotide inhibits expression of a *cbb*$_3$ oxidase, or any component of a *cbb*$_3$ oxidase (e.g., a subunit of a *cbb*$_3$ oxidase).

An antisense oligonucleotide can be, for example, about 7, 10, 15, 20, 25, 30, 35, 40, 45, 50, 55, 60, 65, 70, 75, 80, or more nucleotides in length.

The antisense nucleic acid molecules of the invention may be administered to a subject, or generated in situ such that they hybridize with or bind to the mRNA of a *cbb*$_3$ oxidase, or any component of a *cbb*$_3$ oxidase (e.g., a subunit of a cbb3 oxidase).

Ribozyme

The inhibitor may be a ribozyme that inhibits expression of the gene of a *cbb*$_3$ oxidase, or any component of a *cbb*$_3$ oxidase (e.g., a subunit of a *cbb*$_3$ oxidase).

Ribozymes can be chemically synthesized and structurally modified to increase their stability and catalytic activity using methods known in the art. Ribozyme encoding nucleotide sequences can be introduced into host cells through gene-delivery mechanisms known in the art.

Antibodies

The present inhibitors can be an antibody or antigen-binding portion thereof that is specific

to a *cbb3* oxidase, or any component of a *cbb3* oxidase (e.g., a subunit of a *cbb3* oxidase).

The antibody or antigen-binding portion thereof may be the following: (a) a whole immunoglobulin molecule; (b) an scFv; (c) a Fab fragment; (d) an F(ab')2; and (e) a disulfide linked Fv. The antibody or antigen-binding portion thereof may be monoclonal, polyclonal, chimeric and humanized. The antibodies may be murine, rabbit or human/humanized antibodies.

Antibiotics

The antibiotic may target one or more of the following pathways in bacteria: DNA replication and cell growth; protein biosynthesis; cell wall biosynthesis; transport and membrane function or biosynthesis; metabolism; redox homeostasis, stress response, cell signaling; transcription; translation; tetrahydrofolic acid synthesis; and DNA modification, repair, and maintenance.

Non-limiting examples of antibiotics include, penicillin (e.g. flucloxacillin, amoxicillin, ampicillin, carbenicillin, mezlocillin, penicillin), cephalosporine (e.g. cefazolin, cefuroxim, cefotaxim, cefaclor, cefalexin, cefepime), beta-lactamase inhibitor (e.g. sulbactam, tazobactam), tetracycline (e.g. doxycyclin, minocyclin, tetracyclin, oxytetracyclin), aminoglycoside (e.g. gentamicin, neomycin, streptomycin, kanamycin), makrolid antibiotics (e.g. azithromycin, clarithromycin, erythromycin, roxithromycin, spiramycin, clindamycin), lincosamide (e.g. lincomycin), gyrase inhibitor (e.g. ciprofloxacin, ofloxacin, norfloxacin), sulfonamides (such a Bactrim), trimethoprim, glycopeptides (e.g. vancomycin), polypeptide antibiotics (e.g. colistin, polymyxin), carbapenems (such as meropenem); quinolines (such a levaquin); carbacephems; cephamycins; monobactams; quinolones; macrolides; fluoroquinolones; and amphenicole (e.g. chloramphenicol).

In one embodiment, the antibiotic is an antisense antibiotic oligomer.

Non-limiting examples of antibiotics also include amoxicillin, tetracycline, metronidazole, rifabutin, clarithromycin, clofazimine, vancomycin, rifampicin, nitroimidazole, chloramphenicol, and a combination thereof. In certain aspects, an antibiotic may be selected from the group consisting of rifaximin, rifamycin derivative, rifampicin, rifabutin, rifapentine, rifalazil, bicozamycin, aminoglycoside, gentamycin, neomycin, streptomycin, paromomycin, verdamicin, mutamicin, sisomicin, netilmicin, retymicin, kanamycin, aztreonam, aztreonam macrolide, clarithromycin, dirithromycin, roxithromycin, telithromycin, azithromycin, bismuth subsalicylate,

vancomycin, streptomycin, fidaxomicin, amikacin, arbekacin, neomycin, netilmicin, paromomycin, rhodostreptomycin, tobramycin, apramycin, daptomycin, and a combination thereof.

Additional examples of antibiotics include, but are not limited to, Penicillin G (CAS Registry No.: 61-33-6); Methicillin (CAS Registry No.: 61-32-5); Nafcillin (CAS Registry No.: 147-52-4); Oxacillin (CAS Registry No.: 66-79-5); Cloxacillin (CAS Registry No.: 61-72-3); Dicloxacillin (CAS Registry No.; 3116-76-5); Ampicillin (CAS Registry No.: 69-53-4); Amoxicillin (CAS Registry No.: 26787-78-0); Ticarcillin (CAS Registry No.: 34787-01-4); Carbenicillin (CAS Registry No.: 4697-36-3); Mezlocillin (CAS Registry No.: 51481-65-3); Azlocillin (CAS Registry No.: 37091-66-0); Piperacillin (CAS Registry No.: 61477-96-1); Imipenem (CAS Registry No.: 74431-23-5); Aztreonam (CAS Registry No.: 78110-38-0); Cephalothin (CAS Registry No.: 153-61-7); Cefazolin (CAS Registry No.: 25953-19-9); Cefaclor (CAS Registry No.: 70356-03-5); Cefamandole formate sodium (CAS Registry No.: 42540-40-9); Cefoxitin (CAS Registry No.: 35607-66-0); Cefuroxime (CAS Registry No.: 55268-75-2); Cefonicid (CAS Registry No.: 61270-58-4); Cefinetazole (CAS Registry No.: 56796-20-4); Cefotetan (CAS Registry No.: 69712-56-7); Cefprozil (CAS Registry No.: 92665-29-7); Lincomycin (CAS Registry No.: 154-21-2); Linezolid (CAS Registry No.: 165800-03-3); Loracarbef (CAS Registry No.: 121961-22-6); Cefetamet (CAS Registry No.: 65052-63-3); Cefoperazone (CAS Registry No.: 62893-19-0); Cefotaxime (CAS Registry No.: 63527-52-6); Ceftizoxime (CAS Registry No.: 68401-81-0); Ceftriaxone (CAS Registry No.: 73384-59-5); Ceftazidime (CAS Registry No.: 72558-82-8); Cefepime (CAS Registry No.: 88040-23-7); Cefixime (CAS Registry No.: 79350-37-1); Cefpodoxime (CAS Registry No.: 80210-62-4); Cefsulodin (CAS Registry No.: 62587-73-9); Fleroxacin (CAS Registry No.: 79660-72-3); Nalidixic acid (CAS Registry No.: 389-08-2); Norfloxacin (CAS Registry No.: 70458-96-7); Ciprofloxacin (CAS Registry No.: 85721-33-1); Ofloxacin (CAS Registry No.: 82419-36-1); Enoxacin (CAS Registry No.: 74011-58-8); Lomefloxacin (CAS Registry No.: 98079-51-7); Cinoxacin (CAS Registry No.: 28657-80-9); Doxycycline (CAS Registry No.: 564-25-0); Minocycline (CAS Registry No.: 10118-90-8); Tetracycline (CAS Registry No.: 60-54-8); Amikacin (CAS Registry No.: 37517-28-5); Gentamicin (CAS Registry No.: 1403-66-3); Kanamycin (CAS Registry No.: 8063-07-8); Netilmicin (CAS Registry No.: 56391-56-1); Tobramycin (CAS Registry No.: 32986-56-4); Streptomycin (CAS Registry No.: 57-92-1); Azithromycin (CAS Registry No.: 83905-01-5); Clarithromycin (CAS Registry No.: 81103-11-9);

Erythromycin (CAS Registry No.: 114-07-8); Erythromycin estolate (CAS Registry No.: 3521-62-8); Erythromycin ethyl succinate (CAS Registry No.: 41342-53-4); Erythromycin glucoheptonate (CAS Registry No.: 23067-13-2); Erythromycin lactobionate (CAS Registry No.: 3847-29-8); Erythromycin stearate (CAS Registry No.: 643-22-1); Vancomycin (CAS Registry No.: 1404-90-6); Teicoplanin (CAS Registry No.: 61036-64-4); Chloramphenicol (CAS Registry No.: 56-75-7); Clindamycin (CAS Registry No.: 18323-44-9); Trimethoprim (CAS Registry No.: 738-70-5); Sulfamethoxazole (CAS Registry No.: 723-46-6); Nitrofurantoin (CAS Registry No.: 67-20-9); Rifampin (CAS Registry No.: 13292-46-1); Mupirocin (CAS Registry No.: 12650-69-0); Metronidazole (CAS Registry No.: 443-48-1); Cephalexin (CAS Registry No.: 15686-71-2); Roxithromycin (CAS Registry No.: 80214-83-1); Co-amoxiclavuanate; combinations of Piperacillin and Tazobactam; and their various salts, acids, bases, and other derivatives.

The beta-lactam antibiotic agent may be any antibiotic agent which comprises a beta-lactam and is therefore susceptible to degradation by beta-lactamases. Examples include carbapenems (e.g. meropenem, faropenem, imipenem, ertapenem, doripenem, panipenem/betamipron and biapenem as well as razupenem, tebipenem, lenapenem and tomopenem), ureidopenicillins (e.g. piperacillin), carbacephems (e.g. loracarbef) and cephalosporins (e.g. cefpodoxime, ceftazidime, cefotaxime, ceftriaxone, ceftobiprole, and ceftaroline). Specific examples of beta-lactam antibiotic agents include temocillin, piperacillin, cefpodoxime, ceftazidime, cefotaxime, ceftriaxone, meropenem, faropenem, imipenem, loracarbef, ceftobiprole, ceftaroline. Drawz, Clin Microbiol Rev. January 2010; 23(1): 160-201.

Non-limiting examples of penicillins include, Amdinocillin, Amoxicillin (e.g. NOVAMOX, AMOXIL); Ampicillin (e.g. PRINCIPEN); Azlocillin; Carbenicillin (e.g. GEOCILLIN); Cloxacillin (e.g. TEGOPEN); Cyclacillin, Dicloxacillin (e.g. DYNAPEN); Flucloxacillin (e.g. FLOXAPEN); Mezlocillin (e.g. MEZLIN); Methicillin (e.g. STAPHCILLIN); Nafcillin (e.g. UNIPEN); Oxacillin (e.g. PROSTAPHLIN); Penicillanic Acid, Penicillin G (e.g. PENTIDS or PFIZERPEN); Penicillin V (e.g. VEETIDS (PEN-VEE-K)); Piperacillin (e.g. PIPRACIL); Sulbactam, Temocillin (e.g. NEGABAN); and Ticarcillin (e.g. TICAR).

Non-limiting examples of cephalosporins include, a first generation cephalosporin (e.g. Cefadroxil (e.g. DURICEF); Cefazolin (e.g. ANCEF); Ceftolozane, Cefalotin/Cefalothin (e.g. KEFLIN); Cefalexin (e.g. KEFLEX); a second generation cephalosporin (e.g. Cefaclor (e.g. DISTACLOR); Cefamandole (e.g. MANDOL); Cefoxitin (e.g. MEFOXIN); Cefprozil (e.g.

CEFZIL); Cefuroxime (e.g. CEFTIN, ZINNAT)); a third generation cephalosporin (e.g. Cefixime (e.g. SUPRAX); Cefdinir (e.g. OMNICEF, CEFDIEL); Cefditoren (e.g. SPECTRACEF); Cefoperazone (e.g. CEFOBID); Cefotaxime (e.g. CLAFORAN); Cefpodoxime (e.g. VANTIN); Ceftazidime (e.g. FORTAZ); Ceftibuten (e.g. CEDAX) Ceftizoxime (e.g. CEFIZOX); and Ceftriaxone (e.g. ROCEPHIN)); a fourth generation cephalosporin (e.g. Cefepime (e.g. MAXIPIME)); or a fifth generation cephalosporin (e.g. Ceftaroline fosamil (e.g. TEFLARO); Ceftobiprole (e.g. ZEFTERA)). Also included is Latamoxef (or moxalactam). In a specific embodiment, cephalosporins include, for example, cefoperazone, ceftriaxone or cefazolin.

Non-limiting examples of monobactams include, aztreonam (e.g. AZACTAM, CAYSTON), tigemonam, nocardicin A, and tabtoxin.

Non-limiting examples of carbapenems include, meropenem, imipenem (by way of non-limiting example, imipenem/cilastatin), ertapenem, doripenem, panipenem/betamipron, biapenem, razupenem (PZ-601), tebipenem, lenapenem, thienamycins, and tomopenem.

Bacterial Infections

The present compositions and methods may be used to treat, or treat prophylactically, bacterial infection. The bacterial infection may be caused by, or associated with, Gram-negative or Gram-positive bacteria. For example, the bacterial infection may be caused by, or associated with, bacteria from one or more of the families *Clostridium, Pseudomonas, Escherichia, Klebsiella, Enterococcus, Enterobacter, Serratia, Morganella, Yersinia, Salmonella, Proteus, Pasteurella, Haemophilus, Citrobacter, Burkholderia, Brucella, Moraxella, Mycobacterium, Streptococcus or Staphylococcus*. Particular examples include *Clostridium, Pseudomonas, Escherichia, Klebsiella, Enterococcus, Enterobacter, Streptococcus* and *Staphylococcus*. The bacterial infection may be caused by, or associated with, one or more bacteria selected from *Moraxella catarrhalis, Brucella abortus, Burkholderia cepacia, Citrobacter species, Escherichia coli, Haemophilus Pneumonia, Klebsiella Pneumonia, Pasteurella multocida, Proteus mirabilis, Salmonella typhimurium, Clostridium difficile, Yersinia enterocolitica Mycobacterium tuberculosis, Staphylococcus aureus, group B streptococci, Streptococcus Pneumonia*, and *Streptococcus pyogenes*, e.g., from *E. coli* and *K. pneumoniae*.

Gram-negative bacteria are typically free-living organisms often found in soil and water, and play an important role in decomposition, biodegradation, and the C and N cycles. However, many gram-negative bacteria are pathogenic.

For example, the bacterial infection may be caused by, or associated with, gram-negative bacteria including, but not limited to, *Pseudomonas* (including, but not limited to *Pseudomonas aeruginosa*), *Burkholderia cepaci, C. violaceum, V harveyi, Neisseria gonorrhoeae, Neisseria meningitidis, Bordetell pertussis, Haemophilus influenzae, Legionella pneuinophila, Brucella, Francisella, Xanthomonas, Agrobacterium, enteric bacteria,* such as *Escherichia coli* and its relatives, the members of the family *Enterobacteriaceae,* such as *Salmonella* and *Shigella, Proteus,* and *Yersinia pestis*. U.S. Patent No. 9,751,851.

Gram-negative bacteria that can be inhibited by the present compositions include, but are not limited to, *Pseudomonas* (including, but not limited to *Pseudomonas aeruginosa*), *Burkholderia cepaci, C. violaceum, V harveyi, Neisseria gonorrhoeae, Neisseria meningitidis, Bordetell pertussis, Haemophilus influenzae, Legionella pneuinophila, Brucella, Francisella, Xanthomonas, Agrobacterium, enteric bacteria,* such as *Escherichia coli* and its relatives, the members of the family *Enterobacteriaceae,* such as *Salmonella* and *Shigella, Proteus,* and *Yersinia pestis*.

Medical/Industrial Uses

The present compositions and methods can be used to treat, or treat prophylactically, infections of the pulmonary tract, urinary tract, burns, and wounds, caused by, or associated with, gram negative bacteria such as *P. aeruginosa*. The present compositions and methods can be used to treat, or treat prophylactically, catheter-associated infections, blood infections, middle ear infections, formation of dental plaque, gingivitis, chronic sinusitis, endocarditis, coating of contact lenses, and infections associated with implanted devices (e.g., catheters, joint prostheses, prosthetic cardiac valves and intrauterine devices), caused by, or associated with, gram negative bacteria such as *P. aeruginosa*. The present compositions and methods can be used to treat, or treat prophylactically, infections of the central nervous system, gastrointestinal tract, bones, joints, ears and eyes, caused by, or associated with, gram negative bacteria such as *P. aeruginosa*.

The present compositions and methods can be used to treat, or treat prophylactically, inhibit, and/or ameliorate infections including opportunistic infections and/or antibiotic resistant bacterial infections caused by gram negative bacteria. Examples of such opportunistic infections, include,

but are not limited to *P. aeruginosa*. or poly-microbial infections of P. aeruginosa with, for example, Staphylococcus aureus or Burkholderia cepacia. Examples of patients who may acquire such opportunistic and/or resistant infections include, but are not limited to, patients who are immunocompromised or immunosuppressed, who have cystic fibrosis or HIV, who have implanted medical devices, subcutaneous devices or who are on ventilators, patients who have been intubated, patients who have catheters, patients who have nosocomial infections, patients who are undergoing bone marrow transplant or other types of surgery, including, but not limited to dental surgery, and patients who are IV drug users, especially with regard to heart valve infection.

The present compositions and methods can be used to treat, or treat prophylactically, burns and/or other traumatic wounds as well as common or uncommon infections. Examples of such wounds and infection disorders include, but are not limited to puncture wounds, radial keratotomy, ecthyma gangrenosum, osteomyelitis, external otitis, and/or dermatitis.

In one embodiment, the present compositions and methods can be used to treat, treat prophylactically, prevent, and/or ameliorate pulmonary infections. In one embodiment, the present compositions and methods can be used to treat, treat prophylactically, prevent, and/or ameliorate pneumonia. Pneumonia can be caused by colonization of medical devices, such as ventilator-associated pneumonia, and other nosocomial pneumonia. In one embodiment, the present compositions and methods can be used to treat, treat prophylactically, prevent, and/or ameliorate lung infections, such as pneumonia, in cystic fibrosis patients. In one embodiment, the present compositions and methods can be used to treat, treat prophylactically, prevent, and/or ameliorate an infection caused by, or associated with, gram negative bacteria (such as by P. aeruginosa) in cystic fibrosis patients.

The present compositions and methods can be used to treat, treat prophylactically, prevent, and/or ameliorate septic shock. The present compositions and methods can be used to treat, treat prophylactically, prevent, and/or ameliorate septic shock in neutropenic, immunocompromised, and/or immunosuppressed patients or patients infected with antibiotic resistant bacteria, such as, for example, antibiotic resistant P. aeruginosa.

The present compositions and methods can be used to treat, treat prophylactically, prevent, and/or ameliorate urinary tract or pelvic infections. The present compositions and methods can be used to treat, treat prophylactically, prevent, and/or ameliorate gastrointestinal infections, such as necrotizing enterocolitis, often seen in premature infants and/or neutropenic cancer patients.

The present compositions and methods can be used to treat, treat prophylactically, prevent, and/or ameliorate urinary dysentery (for example, dysentery caused by bacillary dysentery), food poisoning and/or gastroenteritis (for example, caused by Salmonella enterica), typhoid fever (for example, caused by Salmonella typhi), whooping cough (or pertussis) as is caused by Bordetella pertussis, Legionnaires' pneumonia, caused by Legionella pneumophila, sexually transmitted diseases, such as gonorrhea, caused by Neisseria gonorrhoeae, or meningitis, caused by, for example, Neisseria meningitidis or Haemophilus influenzae, brucellosis which is caused by brucellae, and more specifically, Brucella abortus.

The present compositions are used to treat articles, devices, substrates and surfaces (mammalian or inanimate) to disrupt the formation of, or disrupt already formed, biofilms.

The present compositions and methods may be used to attenuate bacterial virulence.

In one embodiment, the present compositions are administered to a subject who is free of bacterial disease. Administration may be in advance of an anticipated health-related procedure known to increase susceptibility to gram-negative bacteria (e.g., P. aeruginosa) pathogenicity, for example, in advance of a surgical procedure, including dental procedures, procedures involving implants, and/or insertion of catheters or other devices.

In another embodiment, the present compositions are used to contact or coat surfaces of work areas, medical instruments (e.g., intubation equipment), medical devices (e.g., implants), hospital bed frames, and the like in order to attenuate the virulence of gram-negative bacteria, such as *P. aeruginosa*, that may come into contact with these surfaces.

In still another embodiment, the present compositions are deployed to prevent the failure of devices that are prone to fouling by biofilms. These compounds are useful in industrial settings and in contexts requiring medical implants.

The present compositions may be administered in the liquid phase, may be embedded in materials used for production of such devices, or may coat such devices resulting in products that are innately resistant to biofilms. These compounds also may be used to inhibit biofilms from forming in situations where liquids are flowing, as, for example, through pipes, pipelines, tubing, water cooling systems, stents or filtration devices.

Surface to be treated with the present compositions may include medical devices such as catheters, respirators, and ventilators. In other embodiments, the surface can be that of implanted

medical devices, including stents, artificial valves, joints, pins, bone implants, sutures, staples, pacemakers, and other temporary or permanent medical devices.

The present disclosure further relates to a method of using the present compositions to treat and/or prevent dental plaque, dental carries, gingival disease, periodontal disease, and oral infection in a subject. In such embodiments, the method involves treating the surfaces of the oral cavity of the subject with the present compositions. In particular embodiments, treatment can be carried out with a dentifrice, mouthwash, mouth rinse, dental floss, gum, strip, toothpaste, a toothbrush containing the biofilm disruptor, and other preparations containing the biofilm disruptor. In certain other embodiments, the composition may also contain other compounds known in the dental arts that are typically added to dental compositions. For example, in some embodiments, the present composition may also include such oral care actives as fluoride, desensitizing agents, anti-tartar agents, anti-bacterial agents, remineralization agents, whitening agents, abrasives and anti-caries agents.

The present compositions may also be incorporated into or used to form an encapsulated system to allow for a controlled release. In these embodiments, the present composition can optionally be in the form of a plurality of small microspheres that encapsulate the inhibitor and/or antibiotic. The microspheres can optionally have an outer coating of dissolvable material that enables the inhibitor and/or antibiotic to slowly release over a time period.

The present methods and compositions may be used for cleaning and/or disinfecting articles such as contact lenses. The method involves treating contact lenses with a cleaning and/or disinfecting solution containing the present compositions. In some embodiments, the contact lens may be treated in this manner while being stored in solution or while being used. In alternative embodiments, the present compositions can be used in eye drops.

The present disclosure provides for a method of treating and/or preventing acne or other biofilm-associated skin infections on the skin of a subject. The methods involve treating the skin of the subject systemically or the skin surface topically with the present compositions under conditions effective to treat and/or prevent the acne or biofilm-associated skin infections. In some embodiments, the present compositions may be present in an ointment, cream, liniment, salves, shaving lotion, or aftershave. In these embodiments, the present compositions may also be present in a powder, cosmetic, ointment, cream, liquid, soap, gel, suspension, lotion, solution, paste, spray, aerosol, oil, cosmetic applicator, and/or solid, woven or non-woven material intended to contact or

be proximate with the skin. In other embodiments, the present compositions may be present in suspensions, syrups, elixirs, solutions, pills, capsules, suppositories and tablets for oral systemic use.

The present invention also relates to a method of treating and/or preventing a chronic biofilm-associated disease in a subject. The methods of these embodiments involve administering to the subject the present compositions under conditions effective to treat and/or prevent the chronic biofilm-associated disease. The chronic biofilm-associated diseases to be treated and/or prevented include, but are not limited to, middle ear infections, osteomyelitis, prostatitis, colitis, vaginitis, urethritis, arterial plaques, sinovial infections, infections along tissue fascia, respiratory tract infections (e.g., infections associated with lung infections of cystic fibrosis patients, pneumonia, pleurisy, pericardial infections), genito-urinary infections, and gastric or duodenal ulcer infections. In some embodiments, the present compositions may be administered in combination with an antimicrobial agent.

The present compositions can be used in industrial settings to inhibit biofilm production and/or to remove antibiotic resistant bacteria, such as in a hospital or other public setting. For example, the present compositions can be used to remove biofilms that have grown in moist and warm environments, such as showers, water and sewage pipes, cooling or heating water systems, (e.g., cooling towers), marine engineering systems, such as, for example, pipelines of the offshore oil and gas industry. The present compositions can also be used, for example, to remove and/or prevent bacterial adhesion to boat hulls, since once a biofilm of bacteria forms, it is easier for other marine organisms such as barnacles to attach. The present compositions can be used to reduce, for example, the time a boat is in dry dock for refitting and repainting, thereby increasing productivity of shipping assets, and useful life of the ships. The present compositions can also be used to remove biofilm production intentionally used to eliminate petroleum oil from contaminated oceans or marine systems, once the contamination is removed.

Additionally, the present compositions can be used to wash, rinse or swab floors and counters, such as in food preparation areas or medical facilities, as well as medical devices, including but not limited to, stents, catheters, intubation tubes, or ventilator equipment. Still further the present compositions can be used as a hand wash to help eliminate spread of virulent bacteria by health workers, patients and others.

Surface to be treated with the present compositions may also include articles such as drains, tubs, kitchen appliances, countertops, shower curtains, grout, toilets, industrial food and beverage production facilities, flooring, and food processing equipment and the like.

Surface to be treated with the present compositions includes article surfaces such as filter or heat exchanger surfaces, providing means for reducing and/or eliminating biofouling of heat exchangers or filters.

In one embodiment, surface to be treated with the present compositions includes articles, devices, substrates or surfaces associated marine structures including, but not limited to, boats, piers, oil platforms, water intake ports, sieves, and viewing ports.

Articles, substrate or device surface being treated with the present compositions can alternatively be associated with a system for water treatment and/or distribution (like drinking water treatment and/or distributing systems, pool and spa water treatment systems, water treatment and/or distribution systems in manufacturing operations, and a system for dental water treatment and/or distribution).

Article, substrate or device surface treated by the present compositions can also be associated with a system for petroleum drilling, storage, separation, refining and/or distribution (like petroleum separation trains, a petroleum container, petroleum distributing pipes, and petroleum drilling equipment). In other embodiments, the biofilm disruptor can also be included in formulations directed at reducing or eliminating biofilm deposits or biofouling in porous medium, such as with oil and gas bearing geological formations. In particular embodiments, the present composition treatment may be accomplished by applying a coating of the present composition, such as by painting, to the surface of articles, substrate or device.

In one embodiment, the present composition can be impregnated in a surface in order to inhibit formation of a biofilm on the surface. Alternatively, the present composition can be in a copolymer or a gel coating over the surface.

Combination Therapy

The *cbb*$_3$ oxidase inhibitor may be administered alone or in combination with other compounds, such as an antibiotic, an antimicrobial agent, and/or an anti-inflammatory agent. In certain embodiments, the *cbb*$_3$ oxidase inhibitor may be administered in combination with one or more antibiotics, for example, gentamicin, tobramycin, colistin, and fluoroquinolins. Combinations

may be administered either concomitantly, e.g., as an admixture, separately but simultaneously or concurrently; or sequentially. This includes presentations in which the combined agents are administered together as a therapeutic mixture, and also procedures in which the combined agents are administered separately but simultaneously, e.g., as through separate intravenous lines into the same individual. Administration "in combination" further includes the separate administration of one of the compounds or agents given first, followed by the second.

The present method for treating a bacterial infection may comprise the step of administering to a subject an antibiotic and an inhibitor of a *cbb*$_3$-type oxidase.

This may be achieved by administering a pharmaceutical composition that includes both agents (e.g., an antibiotic and an inhibitor of a *cbb*$_3$-type oxidase, or an antimicrobial agent and an inhibitor of a *cbb*$_3$-type oxidase), or by administering two pharmaceutical compositions, at the same time or within a short time period, wherein one composition comprises an antibiotic, and the other composition includes an inhibitor of a *cbb*$_3$-type oxidase.

Antimicrobial agents include, but are not limited to, triclosan, metronidazole, tetracyclines, quinolones, plant essential oils, camphor, thymol, carvacrol, menthol, eucalyptol, methyl salicylate, tobramycin, cetylpyridinium chloride, neomycin, polymyxin, bacitracin, clindamycin, ciprofloxacin, rifampin, oxfloxacin, macrolides, penicillins, cephalosporins, amoxicillin/clavulanate, quinupristin/dalfopristin, amoxicillin/sulbactum, fluoroquinolones, ketolides, aminoglycosides and mixtures thereof.

Antimicrobial agents also include, but are not limited to, Aerucin (AR-105), LST007, and phosphorodiamidate morpholino oligomers (PPMOs). Aerucin (AR-105) is a broadly active, fully human IgG1 monoclonal antibody targeting *P. aeruginosa* alginate, a widely distributed cell surface polysaccharide involved in surface adhesion, biofilm formation, and protection against the human immune system. LST007 is a monoclonal antibody that targets the exposed virulence factor flagellin type b on *P. aeruginosa* cells. Peptide-conjugated phosphorodiamidate morpholino oligomers (PPMOs) inhibit translation of complementary mRNA from specific, essential genes in *P. aeruginosa*.

Anti-inflammatory agents include, but are not limited to, steroidal anti-inflammatory actives, non-steroidal anti-inflammatory actives and mixtures thereof. Suitable steroidal anti-inflammatory agents include, but are not limited to, hydrocortisone, fluocinolone acetonide, halcinonide, halobetasol propionate, clobetasol propionate, betamethasone dipropionate, betamethasone valerate,

triamcinolone acetonide and mixtures thereof. Suitable non-steroidal anti-inflammatory actives include, but are not limited to, salicylic acid derivatives such as aspirin, sodium salicylate, choline magnesium salicylate, salsalate, diflunisal, salicylsalicylic acid, sulfasalazine, and olsalazine; para-aminophenol derivatives such as acetaminophen; indole and indene acetic acids such as indomethacin, sulindac, and etodolac; heteroaryl acetic acids such as tolmetin, diclofenac, and ketorolac; arylpropionic acids such as ibuprofen, naproxen, flurbiprofen, ketoprofen, fenoprofen, and oxaprozin; anthranilic acids (fenamates) such as oxicams (piroxicam, tenoxicam), pyrazolidineones (phenylbutazone, oxyphenthatrazone); alkanones such as nabumetone; apazone (azapropazone); nimesulide; and mixtures thereof.

In certain embodiments, the combination of the antibiotic (an antimicrobial agent, and/or an anti-inflammatory agent) and the inhibitor of the *cbb*$_3$-type oxidase produces an additive or synergistic effect (i.e., greater than additive effect) in treating the bacterial infection, disrupting a biofilm, and/or inhibiting or reducing biofilm production and/or growth, compared to the effect of the antibiotic (an antimicrobial agent, and/or an anti-inflammatory agent) or the inhibitor of the *cbb*$_3$-type oxidase alone. For example, the combination may result in a synergistic disruption of biofilms, and/or a synergistic reduction or inhibition in biofilm production and/or growth, and/or a synergistic reduction or inhibition in quorum sensing, and/or a synergistic reduction or inhibition in pathogenicity, and/or a synergistic reduction or inhibition in virulence factor (such as toxins, e.g., phenazines such as pyocyanin, etc.) production or amount.

In various embodiments, the present invention provides methods to disrupt biofilms, reduce or inhibit biofilm production and/or growth, reduce or inhibit quorum sensing, reduce or inhibit pathogenicity, and/or reduce or inhibit virulence factor (such as toxins, e.g., phenazines such as pyocyanin, etc.) production or amount., as measured according to routine techniques in the art.

The phenazine may be any suitable phenazine. Mavrodi et al., Diversity and Evolution of the Phenazine Biosynthesis Pathway, Appl. Environ. Microbiol. 2010, vol. 76, no. 3:866-879.

In one embodiment, the antibacterial effect (e.g., disrupting, reducing or inhibiting bacterial biofilm growth and/or development) of the present composition is assayed by a colony morphology assay (Dietrich et al. 2013). For example, the antibacterial effect (e.g., reducing or inhibiting bacterial biofilm growth and/or development) of the present composition may be demonstrated by a biofilm with a smaller diameter, a smaller thickness, and/or other growth defects or altered

phenotypes (e.g., see, Example 1 below). In one embodiment, bacteria treated with the present composition show decreased formation of the hypoxic and anoxic zones.

In one embodiment, the antibacterial effect (e.g., disrupting, reducing or inhibiting bacterial biofilm growth and/or development) of the present composition is assayed by a competition assay in which bacteria treated with the present composition are grown as mixed-strain biofilms with control bacteria (e.g., bacteria not treated with the present composition, the wild type bacteria, etc.). For example, competitive fitness of the bacteria treated with the present composition can be associated with a fitness disadvantage in early or late colony development.

The antibacterial effect (e.g., disrupting, reducing or inhibiting bacterial biofilm growth and/or development) of the present composition may be assayed by respiratory activity in biofilms. For example, bacteria treated with the present composition may be measured for reduction of triphenyl tetrazolium chloride (TTC), an activity that is often associated with cytochrome *c* oxidase-dependent respiration (Rich et al. 2001). In one embodiment, bacteria treated with the present composition may show decreased respiratory activity in biofilms or colonies. In one embodiment, bacteria treated with the present composition show decreased O_2 reduction and/or phenazine reduction. In one embodiment, bacteria treated with the present composition show decreased cytochrome *c* oxidation.

The antibacterial effect (e.g., disrupting, reducing or inhibiting bacterial biofilm growth and/or development) of the present composition may be assayed by measuring biofilm-specific phenazine production (Dietrich et al. 2008, 2013). For example, bacteria treated with the present composition may show a defect in biofilm-specific phenazine production. In one embodiment, the antibacterial effect (e.g., reducing or inhibiting bacterial virulence and/or bacterial pathogenicity) of the present composition is assayed in a microelectrode-based redox profiling which reveals differential phenazine reduction activity. For example, a Unisense platinum microelectrode may be used to measure the extracellular redox potential in biofilms as a function of depth. This electrode measures the inclination of the sample to donate or accept electrons relative to a Ag/AgCl reference electrode.

The antibacterial effect (e.g., disrupting, reducing or inhibiting bacterial biofilm growth and/or development) of the present composition may be assayed by matrix profiling/production. For example, thin sections from colonies may be prepared and stained with fluorescein-labeled lectin, which binds preferentially to the Pel polysaccharide component of the matrix (Jennings et al.

2015). In one embodiment, bacteria treated with the present composition may show increased Pel polysaccharide production.

In one embodiment, the antibacterial effect (e.g., disrupting, reducing or inhibiting bacterial virulence and/or bacterial pathogenicity) of the present composition is assayed in a *Caenorhabditis elegans* ("slow killing") model of infection. It has been shown that *P. aeruginosa* is pathogenic to *C. elegans* and that the slow killing assay mimics an infection-like killing of *C. elegans* by the bacterium (Tan, Mahajan-Miklos, and Ausubel 1999). For example, bacteria treated with the present composition may show impaired killing relative to control bacteria (e.g., bacteria not treated with the present composition, the wild type bacteria, etc.).

In one embodiment, the antibacterial effect (e.g., reducing or inhibiting bacterial virulence and/or bacterial pathogenicity) of the present composition is assayed in a murine model of acute pulmonary infection (Recinos et al. 2012).

In some embodiments, the combination therapy results in a synergistic effect, for example, the antibiotic (or the antimicrobial agent, or the anti-inflammatory agent) and the inhibitor of the cbb_3 oxidase act synergistically, for example, in the antibacterial effect (e.g., disrupting, reducing or inhibiting bacterial biofilm growth and/or development, and/or reducing or inhibiting bacterial virulence and/or bacterial pathogenicity).

As used herein, the term "synergy" (or "synergistic") means that the effect achieved with the methods and combinations of the combination therapy is greater than the sum of the effects that result from using the individual agents alone, e.g., using the antibiotic (or the antimicrobial agent, or the anti-inflammatory agent) alone and the inhibitor of the cbb_3 oxidase alone. For example, the antibacterial effect (e.g., disruption, reduction or inhibition of bacterial biofilm growth and/or development, and/or reduction or inhibition of bacterial virulence and/or bacterial pathogenicity etc. as described herein) achieved with the combination of an antibiotic (or an antimicrobial agent, and/or an anti-inflammatory agent) and an inhibitor of a cbb_3 oxidase is about 1.1 fold, about 1.2 fold, about 1.3 fold, about 1.4 fold, about 1.5 fold, about 1.6 fold, about 1.7 fold, about 1.8 fold, about 1.9 fold, about 2 fold, about 2.5 fold, about 3 fold, about 3.5 fold, about 4 fold, about 4.5 fold, about 5 fold, about 5.5 fold, about 6 fold, about 6.5 fold, about 7 fold, about 8 fold, about 9 fold, about 10 fold, about 12 fold, about 15 fold, about 20 fold, about 25 fold, about 30 fold, about 50 fold, about 100 fold, at least about 1.2 fold, at least about 1.5 fold, at least about 2 fold, at least about 2.5 fold, at least about 3 fold, at least about 3.5 fold, at least about 4 fold, at least about 4.5

fold, at least about 5 fold, at least about 5.5 fold, at least about 6 fold, at least about 6.5 fold, at least about 7 fold, at least about 8 fold, at least about 9 fold, at least about 10 fold, of the sum of the effects that result from using the antibiotic (or the antimicrobial agent, or the anti-inflammatory agent) alone and the inhibitor of a *cbb*$_3$ oxidase alone.

Synergistic effects of the combination may also be evidenced by additional, novel effects that do not occur when either agent is administered alone, or by reduction of adverse side effects when either agent is administered alone.

In one embodiment, advantageously, such synergy provides greater efficacy at the same doses, lower side effects, and/or prevents or delays the build-up of antibiotic-resistance.

The antibiotic (or the antimicrobial agent, or the anti-inflammatory agent) and the inhibitor of a *cbb*$_3$ oxidase may be administered simultaneously, separately or sequentially. They may exert an advantageously combined effect (e.g., additive or synergistic effects).

For sequential administration, either an antibiotic (or an antimicrobial agent, and/or an anti-inflammatory agent) is administered first and then a *cbb*$_3$ oxidase inhibitor, or the *cbb*$_3$ oxidase inhibitor is administered first and then an antibiotic (or an antimicrobial agent, and/or an anti-inflammatory agent). In embodiments where the antibiotic (or an antimicrobial agent, and/or an anti-inflammatory agent) and an inhibitor of a *cbb*$_3$ oxidase are administered separately, administration of a first agent can precede administration of a second agent by seconds, minutes, hours, days, or weeks. The time difference in non-simultaneous administrations may be greater than 1 minute, and can be, for example, precisely, at least, up to, or less than 5 minutes, 10 minutes, 15 minutes, 30 minutes, 45 minutes, 60 minutes, 2 hours, 3 hours, 6 hours, 9 hours, 12 hours, 24 hours, 36 hours, or 48 hours, or more than 48 hours. The two or more agents can be administered within minutes of each other or within about 0.5, about 1, about 2, about 3, about 4, about 6, about 9, about 12, about 15, about 18, about 24, or about 36 hours of each other or within about 1, 2, 3, 4, 5, 6, 7, 8, 9, 10, 12, 14 days of each other or within about 2, 3, 4, 5, 6, 7, 8, 9, or 10 weeks of each other. In some cases, longer intervals are possible.

Pharmaceutical Compositions

The present invention provides for a pharmaceutical composition comprising a first amount of an antibiotic (or an antimicrobial agent, and/or an anti-inflammatory agent) and a second amount of an inhibitor of a *cbb*$_3$ oxidase. The combination of the first amount of an antibiotic (or an

antimicrobial agent, and/or an anti-inflammatory agent) and the second amount of the inhibitor of a *cbb*$_3$ oxidase produces a synergistic effect on a bacterial infection compared to the effect of the first amount of antibiotic (or an antimicrobial agent, and/or an anti-inflammatory agent) alone or the effect of the second amount of the inhibitor of a *cbb*$_3$ oxidase alone.

The amount of an antibiotic (or an antimicrobial agent, and/or an anti-inflammatory agent) or the amount of the inhibitor of a *cbb*$_3$ oxidase that may be used in the combination therapy may be a therapeutically effective amount, a sub-therapeutically effective amount or a synergistically effective amount.

An antibiotic (or an antimicrobial agent, and/or an anti-inflammatory agent), and/or an inhibitor of a *cbb*$_3$ oxidase may be present in the pharmaceutical composition in an amount ranging from about 0.005% (w/w) to about 100% (w/w), from about 0.01% (w/w) to about 90% (w/w), from about 0.1% (w/w) to about 80% (w/w), from about 1% (w/w) to about 70% (w/w), from about 10% (w/w) to about 60% (w/w), from about 0.01% (w/w) to about 15% (w/w), or from about 0.1% (w/w) to about 20% (w/w).

An antibiotic (or an antimicrobial agent, and/or an anti-inflammatory agent) and an inhibitor of a *cbb*$_3$ oxidase may be present in two separate pharmaceutical compositions to be used in a combination therapy.

The present agents or pharmaceutical compositions may be administered by any route, including, without limitation, oral, transdermal, ocular, intraperitoneal, intravenous, ICV, intracisternal injection or infusion, subcutaneous, implant, sublingual, subcutaneous, intramuscular, intravenous, rectal, mucosal, ophthalmic, intrathecal, intra-articular, intra-arterial, sub-arachinoid, bronchial and lymphatic administration. The present composition may be administered parenterally or systemically.

The pharmaceutical compositions of the present invention can be, e.g., in a solid, semi-solid, or liquid formulation. Intranasal formulation can be delivered as a spray or in a drop; inhalation formulation can be delivered using a nebulizer or similar device; topical formulation may be in the form of gel, ointment, paste, lotion, cream, poultice, cataplasm, plaster, dermal patch aerosol, etc.; transdermal formulation may be administered via a transdermal patch or iontorphoresis. Compositions can also take the form of tablets, pills, capsules, semisolids, powders, sustained release formulations, solutions, emulsions, suspensions, elixirs, aerosols, chewing bars or any other appropriate compositions.

The composition may be administered locally via implantation of a membrane, sponge, or another appropriate material on to which the desired molecule has been absorbed or encapsulated. Where an implantation device is used, the device may be implanted into any suitable tissue or organ, and delivery of the desired molecule may be via diffusion, timed release bolus, or continuous administration.

To prepare such pharmaceutical compositions, one or more of compound of the present invention may be mixed with a pharmaceutical acceptable excipient, e.g., a carrier, adjuvant and/or diluent, according to conventional pharmaceutical compounding techniques.

Pharmaceutically acceptable carriers that can be used in the present compositions encompass any of the standard pharmaceutical carriers, such as a phosphate buffered saline solution, water, and emulsions, such as an oil/water or water/oil emulsion, and various types of wetting agents. The compositions can additionally contain solid pharmaceutical excipients such as starch, cellulose, talc, glucose, lactose, sucrose, gelatin, malt, rice, flour, chalk, silica gel, magnesium stearate, sodium stearate, glycerol monostearate, sodium chloride, dried skim milk and the like. Liquid and semisolid excipients may be selected from glycerol, propylene glycol, water, ethanol and various oils, including those of petroleum, animal, vegetable or synthetic origin, e.g., peanut oil, soybean oil, mineral oil, sesame oil, etc. Liquid carriers, particularly for injectable solutions, include water, saline, aqueous dextrose, and glycols. For examples of carriers, stabilizers, preservatives and adjuvants, see Remington's Pharmaceutical Sciences, edited by E. W. Martin (Mack Publishing Company, 18th ed., 1990). Additional excipients, for example sweetening, flavoring and coloring agents, may also be present.

The pharmaceutically acceptable excipient may be selected from the group consisting of fillers, e.g. sugars and/or sugar alcohols, e.g. lactose, sorbitol, mannitol, maltodextrin, etc.; surfactants, e.g. sodium lauryle sulfate, Brij 96 or Tween 80; disintegrants, e.g. sodium starch glycolate, maize starch or derivatives thereof; binder, e.g. povidone, crosspovidone, polyvinylalcohols, hydroxypropylmethylcellulose; lubricants, e.g. stearic acid or its salts; flowability enhancers, e.g. silicium dioxide; sweeteners, e.g. aspartame; and/or colorants. Pharmaceutically acceptable carriers include any and all clinically useful solvents, dispersion media, coatings, antibacterial and antifungal agents, isotonic and absorption delaying agents and the like.

The pharmaceutical composition may contain excipients for modifying, maintaining or preserving, for example, the pH, osmolarity, viscosity, clarity, color, isotonicity, odor, sterility,

stability, rate of dissolution or release, adsorption or penetration of the composition. Suitable excipients include, but are not limited to, amino acids (such as glycine, glutamine, asparagine, arginine or lysine); antimicrobials; antioxidants (such as ascorbic acid, sodium sulfite or sodium hydrogen sulfite); buffers (such as borate, bicarbonate, Tris HCl, citrates, phosphates, other organic acids); bulking agents (such as mannitol or glycine), chelating agents (such as ethylenediamine tetraacetic acid (EDTA), ethylene glycol tetraacetic acid (EGTA)); complexing agents (such as caffeine, polyvinylpyrrolidone, beta cyclodextrin or hydroxypropyl beta cyclodextrin); fillers; monosaccharides; disaccharides and other carbohydrates (such as glucose, mannose, or dextrins); proteins (such as serum albumin, gelatin or immunoglobulins); coloring; flavoring and diluting agents; emulsifying agents; hydrophilic polymers (such as polyvinylpyrrolidone); low molecular weight polypeptides; salt forming counterions (such as sodium); preservatives (such as benzalkonium chloride, benzoic acid, salicylic acid, thimerosal, phenethyl alcohol, methylparaben, propylparaben, chlorhexidine, sorbic acid or hydrogen peroxide); solvents (such as glycerin, propylene glycol or polyethylene glycol); sugar alcohols (such as mannitol or sorbitol); suspending agents; surfactants or wetting agents (such as pluronics, PEG, sorbitan esters, polysorbates such as polysorbate 20, polysorbate 80, triton, tromethamine, lecithin, cholesterol, tyloxapal); stability enhancing agents (sucrose or sorbitol); tonicity enhancing agents (such as alkali metal halides (in one aspect, sodium or potassium chloride, mannitol sorbitol); delivery vehicles; diluents; excipients and/or pharmaceutical adjuvants. (Remington's Pharmaceutical Sciences, 18th Edition, A. R. Gennaro, ed., Mack Publishing Company, 1990).

Oral dosage forms may be tablets, capsules, bars, sachets, granules, syrups and aqueous or oily suspensions. Tablets may be formed form a mixture of the active compounds with fillers, for example calcium phosphate; disintegrating agents, for example maize starch, lubricating agents, for example magnesium stearate; binders, for example microcrystalline cellulose or polyvinylpyrrolidone and other optional ingredients known in the art to permit tabletting the mixture by known methods. Similarly, capsules, for example hard or soft gelatin capsules, containing the active compound, may be prepared by known methods. The contents of the capsule may be formulated using known methods so as to give sustained release of the active compounds. Other dosage forms for oral administration include, for example, aqueous suspensions containing the active compounds in an aqueous medium in the presence of a non-toxic suspending agent such as sodium carboxymethylcellulose, and oily suspensions containing the active compounds in a

suitable vegetable oil, for example arachis oil. The active compounds may be formulated into granules with or without additional excipients. The granules may be ingested directly by the patient or they may be added to a suitable liquid carrier (e.g. water) before ingestion. The granules may contain disintegrants, e.g. an effervescent pair formed from an acid and a carbonate or bicarbonate salt to facilitate dispersion in the liquid medium. U.S. Patent No. 8,263,662.

Intravenous forms include, but are not limited to, bolus and drip injections. Examples of intravenous dosage forms include, but are not limited to, Water for Injection USP; aqueous vehicles including, but not limited to, Sodium Chloride Injection, Ringer's Injection, Dextrose Injection, Dextrose and Sodium Chloride Injection, and Lactated Ringer's Injection; water-miscible vehicles including, but not limited to, ethyl alcohol, polyethylene glycol and polypropylene glycol; and non-aqueous vehicles including, but not limited to, corn oil, cottonseed oil, peanut oil, sesame oil, ethyl oleate, isopropyl myristate and benzyl benzoate.

Additional compositions include formulations in sustained or controlled delivery, such as using liposome or micelle carriers, bioerodible microparticles or porous beads and depot injections.

The present compound(s) or composition may be administered as a single dose, or as two or more doses (which may or may not contain the same amount of the desired molecule) over time, or as a continuous infusion via implantation device or catheter. The pharmaceutical composition can be prepared in single unit dosage forms.

Appropriate frequency of administration can be determined by one of skill in the art and can be administered once or several times per day (e.g., twice, three, four or five times daily). The compositions of the invention may also be administered once each day or once every other day. The compositions may also be given twice weekly, weekly, monthly, or semi-annually. In the case of acute administration, treatment is typically carried out for periods of hours or days, while chronic treatment can be carried out for weeks, months, or even years. U.S. Patent No. 8,501,686.

Administration of the compositions of the invention can be carried out using any of several standard methods including, but not limited to, continuous infusion, bolus injection, intermittent infusion, inhalation, or combinations of these methods. For example, one mode of administration that can be used involves continuous intravenous infusion. The infusion of the compositions of the invention can, if desired, be preceded by a bolus injection.

The amount of an antibiotic (or an antimicrobial agent, and/or an anti-inflammatory agent) (e.g., a first amount) or the amount of the inhibitor of a *cbb*$_3$ oxidase (e.g., a second amount) that may be used in the combination therapy may be a therapeutically effective amount, a sub-therapeutically effective amount or a synergistically effective amount. The amounts are dosages that achieve the desired synergism.

As used herein, the term "therapeutically effective amount" is an amount sufficient to treat a specified disorder or disease or alternatively to obtain a pharmacological response treating a disorder or disease.

Methods of determining the most effective means and dosage of administration can vary with the composition used for therapy, the purpose of the therapy, the target cell being treated, and the subject being treated. Single or multiple administrations can be carried out with the dose level and pattern being selected by the treating physician. The specific dose level for any particular subject depends upon a variety of factors including the activity of the specific peptide, the age, body weight, general health, sex, diet, time of administration, route of administration, and rate of excretion, drug combination and the severity of the particular disease undergoing therapy.

For example, the antibiotic (or an antimicrobial agent, and/or an anti-inflammatory agent) or the inhibitor of a *cbb*$_3$ oxidase may be administered at about 0.0001 mg/kg to about 500 mg/kg, about 0.01 mg/kg to about 200 mg/kg, about 0.01 mg/kg to about 0.1 mg/kg, about 0.1 mg/kg to about 100 mg/kg, about 10 mg/kg to about 200 mg/kg, about 10 mg/kg to about 20 mg/kg, about 5 mg/kg to about 15 mg/kg, about 0.0001 mg/kg to about 0.001 mg/kg, about 0.001 mg/kg to about 0.01 mg/kg, about 0.01 mg/kg to about 0.1 mg/kg, about 0.1 mg/kg to about 0.5 mg/kg, about 0.5 mg/kg to about 1 mg/kg, about 1 mg/kg to about 2.5 mg/kg, about 2.5 mg/kg to about 10 mg/kg, about 10 mg/kg to about 50 mg/kg, about 50 mg/kg to about 100 mg/kg, about 100 mg/kg to about 250 mg/kg, about 0.1 µg/kg to about 800 µg/kg, about 0.5 µg/kg to about 500 µg/kg, about 1 µg/kg to about 20 µg/kg, about 1 µg/kg to about 10 µg/kg, about 10 µg/kg to about 20 µg/kg, about 20 µg/kg to about 40 µg/kg, about 40 µg/kg to about 60 µg/kg, about 60 µg/kg to about 100 µg/kg, about 100 µg/kg to about 200 µg/kg, about 200 µg/kg to about 300 µg/kg, or about 400 µg/kg to about 600 µg/kg. In some embodiments, the dose is within the range of about 250 mg/kg to about 500 mg/kg, about 0.5 mg/kg to about 50 mg/kg, or any other suitable amounts.

The effective amount of the antibiotic (or an antimicrobial agent, and/or an anti-inflammatory agent) or the inhibitor of a *cbb*$_3$ oxidase for the combination therapy may be less than, equal to, or greater than when the agent is used alone.

In certain embodiments, the amount or dose of an antibiotic (or an antimicrobial agent, and/or an anti-inflammatory agent) or the inhibitor of a *cbb*$_3$ oxidase may range from about 0.01 mg to about 10 g, from about 0.1 mg to about 9 g, from about 1 mg to about 8 g, from about 1 mg to about 7 g, from about 5 mg to about 6 g, from about 10 mg to about 5 g, from about 20 mg to about 1 g, from about 50 mg to about 800 mg, from about 100 mg to about 500 mg, from about 600 mg to about 800 mg, from about 800 mg to about 1 g, from about 0.01mg to about 10 g, from about 0.05 μg to about 1.5 mg, from about 10 μg to about 1 mg protein, from about 0.1mg to about 10 mg, from about 2 mg to about 5 mg, from about 1 mg to about 20 mg, from about 30 μg to about 500 μg, from about 40 pg to about 300 pg, from about 0.1 μg to about 200 mg, from about 0.1 μg to about 5 μg, from about 5 μg to about 10 μg, from about 10 μg to about 25 μg, from about 25 μg to about 50 μg, from about 50 μg to about 100 μg, from about 100 μg to about 500 μg, from about 500 μg to about 1 mg, from about 1 mg to about 2 mg, e.g., in the pharmaceutical composition.

The dose of an antibiotic (or an antimicrobial agent, and/or an anti-inflammatory agent) or the inhibitor of a *cbb*$_3$ oxidase may range from about 0.1 μg/day to about 1 mg/day, from about 10 μg/day to about 200 μg/day, from about 20 μg/day to about 150 μg/day, from about 0.1 μg/day to about 125 μg/day, from about 1 μg/day to about 20 μg/day, or about 4.5 μg/day to about 30 μg/day.

Different dosage regimens may be used. In some embodiments, a daily dosage, such as any of the exemplary dosages described above, is administered once, twice, three times, or four times a day for at least three, four, five, six, seven, eight, nine, or ten days. Depending on the stage and severity of the cancer, a shorter treatment time (e.g., up to five days) may be employed along with a high dosage, or a longer treatment time (e.g., ten or more days, or weeks, or a month, or longer) may be employed along with a low dosage. In some embodiments, a once- or twice-daily dosage is administered every other day.

Kits

The present invention also provides for a kit for use in the treatment or prevention of a bacterial infection. Kits according to the invention include package(s) (e.g., vessels) comprising the present agents or compositions. The kit may include (i) an antibiotic (or an antimicrobial agent,

and/or an anti-inflammatory agent), and (ii) an inhibitor of a *cbb3* oxidase. In one embodiment, the kit may include an inhibitor of a *cbb3* oxidase. The antibiotic (or an antimicrobial agent, and/or an anti-inflammatory agent) and/or the inhibitor of a *cbb3* oxidase may be present in the pharmaceutical compositions as described herein. The antibiotic (or an antimicrobial agent, and/or an anti-inflammatory agent) and/or the inhibitor of a *cbb3* oxidase may be present in unit dosage forms.

Examples of pharmaceutical packaging materials include, but are not limited to, bottles, tubes, inhalers, pumps, bags, vials, containers, syringes, bottles, and any packaging material suitable for a selected formulation and intended mode of administration and treatment.

The kit can contain instructions for administering the present agents or compositions to a patient. The kit can comprise instructions for uses of the present agents or compositions. The kit can contain labeling or product inserts for the present agents or compositions. The kits also can include buffers for preparing solutions for conducting the methods. The instruction of the kits may state that the combination of the antibiotic (or an antimicrobial agent, and/or an anti-inflammatory agent) and the inhibitor of a *cbb3* oxidase produces a synergistic effect on treating, or treating prophylactically, a bacterial infection compared to the effect of the antibiotic (or an antimicrobial agent, and/or an anti-inflammatory agent) alone or the effect of the inhibitor of a *cbb3* oxidase alone.

Subjects, which may be treated according to the present invention include all animals which may benefit from administration of the agents of the present invention. Such subjects include mammals, preferably humans, but can also be an animal such as dogs and cats, farm animals such as cows, pigs, sheep, horses, goats and the like, and laboratory animals (e.g., rats, mice, guinea pigs, and the like).

The following are examples of the present invention and are not to be construed as limiting.

Example 1

Summary

Hypoxia is a common challenge faced by bacteria during associations with hosts due in part to the formation of densely packed communities (biofilms). *cbb*$_3$-type cytochrome *c* oxidases, which catalyze the terminal step in respiration and have a high affinity for oxygen, have been linked to bacterial pathogenesis. The pseudomonads are unusual in that they often contain multiple full and partial (i.e., "orphan") operons for *cbb*$_3$-type oxidases and oxidase subunits. Here, we

describe a unique role for the orphan catalytic subunit CcoN4 (PA14_10500) in colony biofilm development and respiration in the opportunistic pathogen *Pseudomonas aeruginosa* PA14. Our work has shown that a particular subunit of the *cbb*3-type enzymes, CcoN4 (PA14_10500), is necessary for optimal biofilm survival.

Another aspect of biofilm growth that confers a survival advantage to this bacterium is the production of redox-active antibiotics called phenazines. Our research has shown that the synthesis and utilization of phenazines by *P. aeruginosa* allows it to withstand the challenges associated with decreased access to oxygen. We have also shown that phenazines are important virulence factors in a murine pathogenicity model. Although the electron-shuttling capability of phenazines is integral to their function, the mechanisms by which phenazines are reduced and oxidized remain largely unknown. Our work shows the electron transport chain, specifically *cbb*3-type terminal oxidases and the CcoN4 (RefSeq gene symbol: PA14_10500) subunit, in mediation of phenazine reduction. We also show that CcoN4 contributes to the reduction of phenazines, antibiotics that support redox balancing for cells in biofilms, and to virulence in a *Caenorhabditis elegans* model of infection. When *P. aeruginosa* cells lack the *cbb*3-type terminal oxidases, phenazines are not utilized as efficiently. These results highlight the relevance of the colony biofilm model to pathogenicity and using cbb_3-type oxidases as therapeutic targets.

Among the oxidants available for biological reduction, molecular oxygen (O_2) provides the highest free energy yield. Since the accumulation of O_2 in the atmosphere between ~2.4-0.54 billion years ago (Kirschvink and Kopp 2008; Dietrich, Tice, and Newman 2006), organisms that can use it for growth and survival, and tolerate its harmful byproducts, have evolved to exploit this energy and increased in complexity (Knoll and Sperling 2014; Falkowski 2006). At small scales and in crowded environments, rapid consumption of O_2 leads to competition for this resource and has promoted diversification of bacterial and archaeal mechanisms for O_2 reduction that has not occurred in eukaryotes (Brochier-Armanet, Talla, and Gribaldo 2009). The various enzymes that allow bacteria to respire O_2 exhibit a range of affinities and proton-pumping efficiencies and likely contribute to competitive success in hypoxic niches (Morris and Schmidt 2013). Such environments include the tissues of animal and plant hosts that are colonized by bacteria of high agricultural (Preisig et al. 1996) and clinical (Way et al. 1999; Weingarten, Grimes, and Olson 2008) significance.

The opportunistic pathogen *Pseudomonas aeruginosa*, a colonizer of both plant and animal hosts (Rahme et al. 1995), has a branched respiratory chain with the potential to reduce O_2 to water using at least five different terminal oxidase complexes: two quinol oxidases (bo_3 (Cyo) and a *bd*-type cyanide insensitive oxidase (CIO)) and three cytochrome *c* oxidases (aa_3, cbb_3-1, and cbb_3-2) (**Figure 1A**). Several key publications have described *P. aeruginosa*'s complement of terminal oxidases and oxidase subunits, revealing features specific to this organism (Williams, Zlosnik, and Ryall 2007; Comolli and Donohue 2004; Alvarez-Ortega and Harwood 2007; Arai et al. 2014; Kawakami et al. 2010; Jo, Price-Whelan, and Dietrich 2014). *P. aeruginosa* is somewhat unusual in that it encodes two oxidases belonging to the cbb_3-type family. These enzymes are notable for their relatively high catalytic activity at low O_2 concentrations and restriction to the bacterial domain (Brochier-Armanet, Talla, and Gribaldo 2009; Pitcher and Watmough 2004). (The *P. aeruginosa* cbb_3-type oxidases are often referred to as cbb_3-1 and cbb_3-2; however, we will use "Cco1" and "Cco2" for these enzymes, consistent with the annotations of their encoding genes.) Most bacterial genomes that encode cbb_3-type oxidases contain only one operon for such a complex, which is induced specifically under conditions of O_2 limitation (Cosseau and Batut 2004). In *P. aeruginosa*, the *cco2* operon is induced during growth at low O_2 concentrations, but the *cco1* operon is expressed constitutively at high levels (Comolli and Donohue 2004; Kawakami et al. 2010).

An additional quirk of the *P. aeruginosa* terminal oxidase complement lies in the presence of genes for "orphan" cbb_3-type subunits at chromosomal locations distinct from the *cco1* and *cco2* operons. While the *cco1* and *cco2* operons, which are chromosomally adjacent, each contain four genes encoding a functional Cco complex (consisting of subunits N, O, P, and Q), the two additional partial operons *ccoN3Q3* and *ccoN4Q4* each contain homologs coding for only the Q and catalytic N subunits (**Figure 1B**). Expression of the *ccoN3Q3* operon is induced under anaerobic denitrification conditions (Alvarez-Ortega and Harwood 2007), and by nitrite exposure during growth under 2% O_2 (Hirai et al. 2016). During aerobic growth in liquid cultures, *ccoN4Q4* is induced by cyanide, which is produced in stationary phase (Hirai et al. 2016). However, additional expression studies indicate that *ccoN4Q4* transcription is influenced by redox conditions, as this operon is induced by O_2 limitation (Alvarez-Ortega and Harwood 2007) and slightly downregulated in response to pyocyanin, a redox-active antibiotic produced by *P. aeruginosa* (Dietrich et al. 2006).

In a recent study, Hirai et al. characterized the biochemical properties and physiological roles of *P. aeruginosa* cbb_3 isoforms containing combinations of canonical and orphan subunits

(Hirai et al. 2016). In a strain lacking all of the aerobic terminal oxidases, expression of any isoform conferred the ability to grow using O_2, confirming that isoforms containing the orphan N subunits are functional. When preparations from wild-type, stationary-phase *P. aeruginosa* cells were separated on 2D gels and probed with anti-CcoN4 antibody, this subunit was detected at the same position as the assembled CcoNOP complex, showing that CcoN4-containing heterocomplexes form in vivo. Furthermore, the authors found that the products of *ccoN3Q3* and *ccoN4Q4* contributed resistance to nitrite and cyanide, respectively, during growth in liquid cultures under low-O_2 conditions. While these results provide insight into contributions of the cbb_3 heterocomplexes to growth in liquid cultures, potential roles for N3- and N4-containing isoforms in biofilm growth and pathogenicity have yet to be explored.

The biofilm lifestyle—in which cells grow in a dense community encased in a self-produced matrix—has been linked to the establishment and persistence of infections in diverse systems (Edwards and Kjellerup 2012; Rybtke et al. 2015). Biofilm development promotes the formation of O_2 gradients such that cells at a distance from the biofilm surface are subjected to hypoxic or anoxic conditions (Werner et al. 2004). Using a colony morphology assay to study redox metabolism and its relationship to community behavior, we have shown that O_2 limitation for cells in biofilms leads to an imbalance in the intracellular redox state. This can be relieved by a change in community morphology, which increases the surface area-to-volume ratio of the biofilm and therefore access to O_2 for resident cells (Kempes et al. 2014). For *P. aeruginosa* cells in biofilms, the intracellular accumulation of reducing power can also be prevented by production and reduction of endogenous antibiotics called phenazines, which mediate extracellular electron transfer to oxidants available at a distance (Dietrich et al. 2013). We have found that biofilm-specific phenazine production contributes to pathogenicity in a murine model of acute pulmonary infection (Recinos et al. 2012), further underscoring the importance of phenazine-mediated redox balancing for *P. aeruginosa* cells in communities.

Because of the formation of an O_2 gradient inherent to the biofilm lifestyle, we hypothesized that the differential regulation of the *P. aeruginosa cco* operons affects their contributions to metabolic electron flow in biofilm subzones. We evaluated the roles of various cbb_3-type oxidase isoforms in multicellular behavior and virulence. Our results indicate that isoforms containing the orphan subunit CcoN4 can support survival in biofilms via O_2 and

phenazine reduction and contribute to *P. aeruginosa* pathogenicity in a *Caenorhabditis elegans* "slow killing" model of infection.

RESULTS

A small minority of bacterial genomes encode cbb$_3$*-type oxidase subunits in partial ("orphan") operons*

Biochemical, genetic, and genomic analyses suggest that the CcoN and CcoO subunits, typically encoded by an operon, form the minimal functional unit of *cbb*$_3$-type oxidases (Ducluzeau, Ouchane, and Nitschke 2008; de Gier et al. 1996; Zufferey et al. 1996). CcoN is the membrane-integrated catalytic subunit and contains two *b*-type hemes and a copper ion. CcoO is membrane-anchored and contains one *c*-type heme. Additional redox subunits and/or subunits implicated in complex assembly, such as CcoQ and CcoP, can be encoded by adjacent genes (**Figure 1B**). *ccoNO*-containing clusters are widely distributed across phyla of the bacterial domain (Ducluzeau, Ouchane, and Nitschke 2008). We used the EggNOG database, which contains representative genomes for more than 3000 bacterial species (Huerta-Cepas et al. 2016) to obtain an overview of the presence and frequency of *cco* genes. Out of 3318 queried bacterial genomes we found 467 with full *cco* operons (encoding potentially functional *cbb*$_3$-type oxidases with O and N subunits). Among these, 78 contain more than one full operon. We also used EggNOG to look for orphan *ccoN* genes by examining the relative numbers of *ccoO* and *ccoN* homologs in individual genomes. We found 14 genomes, among which *Pseudomonas* species are overrepresented, that contain orphan *ccoN* genes (**Figure 1C**), and our analysis yielded 3 species that contain more than one orphan *ccoN* gene: *Pseudomonas mendocina*, *Pseudomonas aeruginosa*, and *Achromobacter xylosoxidans*. *P. mendocina* is a soil bacterium and occasional nosocomial pathogen that is closely related to *P. aeruginosa*, based on 16S rRNA gene sequence comparison (Anzai et al. 2000). *A. xylosoxidans*, in contrast, is a member of a different proteobacterial class but nevertheless is often mistaken for *P. aeruginosa* (Saiman et al. 2001). Like *P. aeruginosa*, it is an opportunistic pathogen that can cause pulmonary infections in immunocompromised individuals and patients with cystic fibrosis (De Baets et al. 2007; Firmida et al. 2016). Hirai et al. previously reported a ClustalW-based analysis of CcoN homologs specifically from pseudomonads, which indicated the presence of orphan genes in additional species not represented in the EggNOG database. These include *P. denitrificans*, which contains two orphan genes (Hirai et al. 2016).

CcoN4-containing isoforms function specifically in biofilms to support community morphogenesis and respiration

During growth in a biofilm, subpopulations of cells are subjected to regimes of electron donor and O_2 availability that may create unique metabolic demands and require modulation of the respiratory chain for survival (Alvarez-Ortega and Harwood 2007; Borriello et al. 2004; Werner et al. 2004). We therefore investigated the contributions of individual *cco* genes and gene clusters to *P. aeruginosa* PA14 biofilm development using a colony morphology assay, which has demonstrated sensitivity to electron acceptor availability and utilization (Dietrich et al. 2013). Because the Cco1 and Cco2 complexes are the most important cytochrome oxidases for growth of *P. aeruginosa* in fully aerated and O_2-limited liquid cultures (Alvarez-Ortega and Harwood 2007; Arai et al. 2014), we predicted that mutations disabling the functions of Cco1 and Cco2 would affect colony growth. Indeed, a mutant lacking both the *cco1* and *cco2* operons ("Δ*cco1cco2*") produced thin biofilms with a smaller diameter than the wild type. After five days of development, this mutant displayed a dramatic phenotype consisting of a tall central ring feature surrounded by short ridges that emanate radially (**Figure 2A**, **Figure 2(IA)**). Δ*cco1cco2* colonies were also darker in color, indicating increased uptake of the dye Congo red, which binds to the extracellular matrix produced by biofilms (Friedman and Kolter 2004). Surprisingly, a strain specifically lacking the catalytic subunits of Cco1 and Cco2 ("Δ*N1*Δ*N2*"), while showing a growth defect similar to that of Δ*cco1cco2* when grown in liquid culture (**Figure 2C**), showed biofilm development that was similar to that of the wild type (**Figure 2A**, **Figure 2(IA)**).

As it is known that CcoN3 and CcoN4 can form functional complexes with subunits of the Cco1 and Cco2 oxidases in *P. aeruginosa* PAO1 (Hirai et al. 2016), this led us to hypothesize that Cco isoforms containing the orphan subunits CcoN3 and/or CcoN4 could substitute for Cco1 and Cco2 in the biofilm context. Deleting *ccoN3* ("Δ*N3*" or "Δ*N1*Δ*N2*Δ*N3*") did not have an observable effect on biofilm development when mutants were compared to respective parent strains (**Figure 2(IA)**). However, the phenotype of a "Δ*N1*Δ*N2*Δ*N4*" mutant was consistent with our model, as it mimicked that of the Δ*cco1cco2* mutant in both liquid-culture and biofilm growth (**Figures 2A** and **2C**, **Figure 2(IA)**). Furthermore, we found that a mutant lacking only *ccoN4* ("Δ*N4*") displayed an altered phenotype in that it began to form wrinkle structures earlier than the wild type (**Figure 2(IA)**), which developed into a disordered region of wrinkles inside a central ring, surrounded by

long, radially emanating ridges (**Figure 2A**). Reintroduction of the *ccoN4* gene into either of these strains restored the phenotypes of the respective parent strains (**Figure 2(IA)**). Deletion of either *ccoN2* or *ccoN3* in the Δ*N4* background did not exacerbate the colony phenotype seen in Δ*N4* alone. However, the "Δ*N1*Δ*N4*" double mutant showed an intermediate phenotype relative to Δ*N4* and Δ*N1*Δ*N2*Δ*N4* (**Figure 2(IB)**), suggesting some functional redundancy for CcoN1 and CcoN4. The developmental pattern of the Δ*N4* colony is reminiscent of those displayed by mutants defective in phenazine production and sensing (**Figure 2(IA)**) (Dietrich et al. 2008, 2013; Sakhtah et al. 2016; Okegbe et al. 2017). Although Δ*N4* itself showed a unique phenotype in the colony morphology assay, its growth in shaken liquid cultures was indistinguishable from that of the wild type (**Figure 2C**). Deleting the three non-cbb_3-type terminal oxidases ("Δ*cox*Δ*cyo*Δ*cio*"), did not affect biofilm morphology. These results suggest that CcoN4-containing Cco isoform(s) play physiological roles that are specific to the growth conditions encountered in biofilms.

Next, we asked whether CcoN4 contributes to respiration in biofilms. We tested a suite of *cco* mutants for reduction of triphenyl tetrazolium chloride (TTC), an activity that is often associated with cytochrome *c* oxidase-dependent respiration (Rich et al. 2001). The Δ*cco1cco2* mutant showed a severe defect in TTC reduction, which was recapitulated by the Δ*N1*Δ*N2*Δ*N4* mutant. As in the colony morphology assay, this extreme phenotype was not recapitulated in a mutant lacking only CcoN1 and CcoN2, indicating that CcoN4 contributes to respiratory activity in PA14 biofilms. Although we did not detect a defect in TTC reduction for the Δ*N4* mutant, we saw an intermediate level of TTC reduction for Δ*N1*Δ*N4* compared to Δ*N1*Δ*N2* and Δ*N1*Δ*N2*Δ*N4*, further implicating the CcoN4 subunit in this activity (**Figure 2B**).

A recent study implicated CcoN4 in resistance to cyanide, a respiratory toxin that is produced by *P. aeruginosa* (Hirai et al. 2016). The altered biofilm phenotypes of Δ*N4* mutants could therefore be attributed to an increased sensitivity to cyanide produced during biofilm growth. We deleted the *hcn* operon, coding for cyanide biosynthetic enzymes, in the wild-type, phenazine-null, and various *cco* mutant backgrounds. The biofilm morphologies and liquid-culture growth of these strains were unaffected by the Δ*hcnABC* mutation, indicating that the biofilm-specific role of CcoN4 explored in this work is independent of its role in mediating cyanide resistance (**Figures 2(IIA)-2(IIB)**). Additionally, we examined genomes available in the Pseudomonas Genome Database for the presence of homologs encoding CcoN subunits (*ccoN* genes) and enzymes for

cyanide synthesis (*hcnABC*) (Winsor et al. 2016) and did not find a clear correlation between the presence of *hcnABC* and *ccoN4* homologs (**Figure 2(III)**).

Together, the effects of *cco* gene mutations that we observed in assays for colony morphogenesis and TTC reduction suggest that one or more CcoN4-containing Cco isoform(s) support respiration and redox balancing, and is/are utilized preferentially in comparison to CcoN1- and CcoN2-containing Cco complexes, in biofilms. We performed a sequence alignment of the CcoN subunits encoded by the PA14 genome and identified residues that are unique to CcoN4 or shared uniquely between CcoN4 and CcoN1, which showed the strongest functional redundancy with CcoN4 in our assays (**Figure 2(IVA)**). We also threaded the CcoN4 sequence using the available structure of the CcoN subunit from *P. stutzeri (Buschmann et al. 2010)* and highlighted these residues (**Figure 2(IVB)**). It is noteworthy that most of the highlighted residues are surface-exposed, specifically on one half of the predicted CcoN4 structure, where they may engage in binding an unknown protein partner or specific lipids. In contrast, sites that have been described as points of interaction with CcoO and CcoP are mostly conserved, further supporting the notion that CcoN4 can interact with these subunits in Cco complexes.

Different CcoN subunits are required for competitive fitness in early or late colony development

To further test CcoN4's contribution to growth in biofilms, we performed competition assays in which Δ*N4* and other mutants were grown as mixed-strain biofilms with the wild type. In each of these assays, one strain was labeled with constitutively-expressed YFP so that the strains could be distinguished during enumeration of colony forming units (CFUs). Experiments were performed with the label on each strain to confirm that YFP expression did not affect fitness (**Figures 3(IA)-3(IB)**). When competitive fitness was assessed after three days of colony growth (**Figure 3A**), Δ*N4* cells showed a disadvantage, with the wild type outcompeting Δ*N4* by a factor of two. This was similar to the disadvantage observed for the Δ*N1*Δ*N2* mutant, further suggesting that the orphan subunit CcoN4 plays a significant role in biofilm metabolism. Remarkably, deletion of *ccoN4* in mutants already lacking *ccoN1* and *ccoN2* led to a drastic decrease in fitness, with the wild type outcompeting Δ*N1*Δ*N2*Δ*N4* by a factor of 16. This disadvantage was comparable to that observed for the mutant lacking the full *cco* operons (Δ*cco1cco2*), underscoring the importance of CcoN4-containing isoforms during biofilm growth.

To further explore the temporal dynamics of N subunit utilization, we repeated the competition assay, but sampled each day over the course of three days (**Figure 3B**). The fitness disadvantage that we had found for strains lacking CcoN1 and CcoN2 was evident after only one day of growth and did not significantly change after that. In contrast, the Δ*N4*-specific decline in fitness did not occur before the second day. These data suggest that the contributions of the various N subunits to biofilm metabolism differ depending on developmental stage.

DIC imaging of thin sections from wild-type colonies reveals morphological variation over depth that may result from decreasing O_2 availability (**Figure 3(IC)**). We have previously reported that three-day-old PA14 colony biofilms are hypoxic at depth (Dietrich et al. 2013) and that O_2 availability is generally higher in thinner biofilms, such as those formed by a phenazine-null mutant (Δ*phz*). We have proposed that the utilization of phenazines as electron acceptors in wild-type biofilms enables cellular survival in the hypoxic zone and promotes colony growth (Okegbe, Price-Whelan, and Dietrich 2014). The relatively late-onset phenotype of the Δ*N4* mutant in the competition assay suggested to us that CcoN4 may play a role in survival during formation of the hypoxic colony subzone and that this zone could arise at a point between one and two days of colony growth. We measured O_2 concentrations in wild-type and Δ*phz* biofilms at specific time points over development, and found that O_2 declined similarly with depth in both strains (**Figure 3D**). The rate of increase in height of Δ*phz* tapered off when a hypoxic zone began to form, consistent with our model that the base does not increase in thickness when electron acceptors (O_2 or phenazines) are not available. Although we cannot pinpoint the exact depth at which the O_2 microsensor leaves the colony base and enters the underlying agar, we can estimate these values based on colony thickness measurements (**Figure 3C**). When we measured the thickness of wild-type and Δ*phz* biofilms over three days of incubation, we found that the values began to diverge between 30 and 48 hours of growth, after the colonies reached ~70 μm in height, which coincides with the depth at which O_2 becomes undetectable. Δ*phz* colonies reached a maximum thickness of ~80 μm, while wild-type colonies continued to grow to ~150 μm (**Figure 3C**). In this context, it is interesting to note that the point of divergence for the increase in wild-type and Δ*phz* colony thickness corresponds to the point at which CcoN4 becomes important for cell viability in our mixed-strain colony growth experiments (**Figure 3B**). We hypothesize that this threshold thickness leads to a level of O_2 limitation that is physiologically relevant for the roles of phenazines and CcoN4 in biofilm metabolism.

cco *genes show differential expression across biofilm subzones*

P. aeruginosa's five canonical terminal oxidases are optimized to function under and in response to distinct environmental conditions, including various levels of O_2 availability (Arai et al. 2014; Kawakami et al. 2010; Alvarez-Ortega and Harwood 2007; Comolli and Donohue 2004). Furthermore, recent studies, along with our results, suggest that even within the Cco terminal oxidase complexes, the various N subunits may perform different functions (Hirai et al. 2016). We sought to determine whether differential regulation of *cco* genes could lead to uneven expression across biofilm subzones. To test this, we engineered reporter strains in which GFP expression is regulated by the *cco1*, *cco2*, or *ccoN4Q4* promoters. Biofilms of these strains were grown for three days, thin-sectioned, and imaged by fluorescence microscopy. Representative results are shown in the left panel of **Figure 4**. The right panel of **Figure 4** contains plotted GFP signal intensity and O_2 concentration measurements over depth for PA14 wild-type colonies. *cco1* and *ccoN4* expression patterns indicate that the Cco1 oxidase and the CcoN4 subunit are produced throughout the biofilm (**Figure 4**). *cco2* expression, on the other hand, is relatively low in the top portion of the biofilm and shows a sharp induction starting at a depth of ~45 μm. This observation is consistent with previous studies showing that *cco2* expression is regulated by Anr, a global transcription factor that controls gene expression in response to a shift from oxic to anoxic conditions (Comolli and Donohue 2004; Kawakami et al. 2010; Ray and Williams 1997).

Though previous studies have evaluated expression as a function of growth phase in shaken liquid cultures for *cco1* and *cco2*, this property has not been examined for *ccoN4Q4*. We monitored the fluorescence of our engineered *cco* gene reporter strains during growth under this condition in a nutrient-rich medium. As expected based on the known constitutive expression of *cco1* and Anr-dependence of *cco2* induction, we saw *cco1*-associated fluorescence increase before that associated with *cco2*. Induction of *ccoN4Q4* occurred after that of *cco1* and *cco2* (**Figures 4(IA)-4(IB)**), consistent with microarray data showing that this locus is strongly induced by O_2 limitation (Alvarez-Ortega and Harwood 2007). However, our observation that *ccoN4Q4* is expressed in the aerobic zone, where *cco2* is not expressed, in biofilms (**Figure 4**) suggests that an Anr-independent mechanism functions to induce this operon during multicellular growth.

Our results indicate that different Cco isoforms may function in specific biofilm subzones, but that CcoN4-containing isoforms could potentially form throughout the biofilm. These data,

together with our observation that Δ*N4* biofilms exhibit a fitness disadvantage from day two (**Figure 3B**), led us to more closely examine the development and chemical characteristics of the biofilm over depth.

Microelectrode-based redox profiling reveals differential phenazine reduction activity in wild-type and cco *mutant biofilms*

The results shown in **Figure 2B** implicate CcoN4-containing isoforms in the reduction of TTC, a small molecule that interacts with the respiratory chain (Rich et al. 2001). Similar activities have been demonstrated for phenazines, including the synthetic compound phenazine methosulfate (PMS) (Nachlas, Margulies, and Seligman 1960) and those produced naturally by *P. aeruginosa* (Armstrong and Stewart-Tull 1971). Given that CcoN4 and phenazines function to influence morphogenesis at similar stages of biofilm growth (**Figures 2A**, **3**, **Figures 2(IA)-2(IC)**, **Figures 3(IA)-3(IB)**), we wondered whether the role of CcoN4 in biofilm development was linked to phenazine metabolism. We used a Unisense platinum microelectrode with a 20-30 μm tip to measure the extracellular redox potential in biofilms as a function of depth. This electrode measures the inclination of the sample to donate or accept electrons relative to an Ag/AgCl reference electrode. We found that wild-type colonies showed a decrease in redox potential over depth, indicating an increased ratio of reduced to oxidized phenazines, while the redox potential of Δ*phz* colonies remained unchanged (**Figure 5A**). To confirm that phenazines are the primary determinant of the measured redox potential in the wild type, we grew Δ*phz* colonies on medium containing PMS (which resembles the natural phenazines that regulate *P. aeruginosa* colony morphogenesis (Sakhtah et al. 2016)), and found that these colonies yielded redox profiles similar to those of the wild type (**Figure 5(IA)**). Therefore, though the microelectrode we employed is capable of interacting with many redox-active substrates, we found that its signal was primarily determined by phenazines in our system. In addition, while wild-type colonies showed rapid decreases in O_2 availability starting at the surface, the strongest decrease in redox potential was detected after ~50 μm (**Figure 5A**). These results suggest that the bacteria residing in the biofilm differentially utilize O_2 and phenazines depending on their position and that O_2 is the preferred electron acceptor.

We hypothesized that one or more of the CcoN subunits encoded by the PA14 genome is required for phenazine reduction and tested this by measuring the redox potential over depth for a

series of *cco* mutants (**Figure 5B**, **top**). We saw very little reduction of phenazines in the Δ*cco1cco2* colony, suggesting that cbb_3-type oxidases are required for this activity. In contrast, the mutant lacking the catalytic subunits of Cco1 and Cco2, Δ*N1*Δ*N2*, showed a redox profile similar to the wild type, indicating that isoforms containing one or both of the orphan CcoN subunits could support phenazine reduction activity. Indeed, although redox profiles obtained for the Δ*N1*Δ*N2* and Δ*N4* mutants were similar to those obtained for the wild type, the redox profile of the Δ*N1*Δ*N2*Δ*N4* mutant recapitulated that of Δ*cco1cco2*. These results indicate redundancy in the roles of some of the CcoN subunits. Consistent with this, Δ*N1*Δ*N4* showed an intermediate defect in phenazine reduction. We note that the triple mutant Δ*cox*Δ*cyo*Δ*cio* showed a wild-type-like redox profile, indicating that the cbb_3-type terminal oxidases are sufficient for normal phenazine reduction (**Figure 5(IB)**). Extraction and measurement of phenazines released from wild-type and *cco* mutant biofilms showed that variations in redox profiles could not be attributed to differences in phenazine production (**Figure 5(IC)**).

Our group has previously shown that a Δ*phz* mutant compensates for its lack of phenazines by forming thinner colonies, thus limiting the development of the hypoxic subzone seen in the wild type (Dietrich et al. 2013). We therefore hypothesized that mutants unable to reduce phenazines would likewise result in thinner colonies. Indeed, we observed that the *cco* mutants that lacked phenazine reduction profiles in the top panel of **Figure 5B** produced biofilms that were significantly thinner than wild-type and comparable to that of the Δ*phz* mutant (**Figure 5B**, **bottom**).

Our group has also reported that reduction of nitrate, an alternate electron acceptor for *P. aeruginosa* (Williams, Zlosnik, and Ryall 2007), can serve as an additional redox-balancing strategy for cells in biofilms (Dietrich et al. 2013). Colony wrinkling is stimulated by a reduced cellular redox state; thus, provision of nitrate in the growth medium inhibits colony feature formation. We hypothesized that nitrate reduction could compensate for defects in O_2 and phenazine reduction and inhibit colony wrinkling in the *cco* mutants that are the focus of this study. To test this, we grew strains on medium containing 10 or 40 mM potassium nitrate. We found that 10 mM nitrate was sufficient to inhibit wrinkling for up to 4 days of incubation in the wild type, Δ*N4*, and Δ*N1*Δ*N4*, but that Δ*phz* and Δ*N1*Δ*N2*Δ*N4* had initiated wrinkling at this point (**Figure 5(ID)**). When we grew these strains on medium containing 40 mM nitrate, we saw increased inhibition of wrinkling such that the wild type, Δ*phz*, Δ*N4*, and Δ*N1*Δ*N4* remained completely

smooth at 4 days of incubation. Though *ΔN1ΔN2ΔN4* had shown some feature formation after 4 days on this medium, it was diminished relative to the same point on 10 mM nitrate. These results suggest that O_2 reduction, phenazine reduction, and nitrate reduction can operate in synchrony to oxidize the redox states of cells in biofilms and that provision of nitrate can compensate for defects in O_2 and phenazine reduction to enable maintenance of redox homeostasis.

Wild-type and cco *mutant colony biofilms show increased matrix production at a consistent depth*

We have recently demonstrated that extracellular matrix production, a hallmark of biofilm formation, is regulated by redox state in PA14 colony biofilms. Increased matrix production correlates with the accumulation of reducing power (as indicated by higher cellular NADH/NAD^+ ratios) due to electron acceptor limitation and is visible in the hypoxic region of *Δphz* colonies (Dietrich et al. 2013; Okegbe et al. 2017). The morphologies of our *cco* mutants (**Figure 2A**) suggest that matrix production can also be induced by respiratory chain dysfunction, which may be linked to defects in phenazine utilization (**Figure 5B**). To further examine the relationships between Cco isoforms and redox imbalance in biofilms, we prepared thin sections from two day-old colonies and stained with fluorescein-labeled lectin, which binds preferentially to the Pel polysaccharide component of the matrix (Jennings et al. 2015). Consistent with their similar gross morphologies, the wild-type and *ΔN1ΔN2* biofilms showed similar patterns of staining, with a faint band of higher intensity at a depth of ~40 μm (**Figure 5C**). *ΔN4* also showed a similar pattern, with a slightly higher intensity of staining in this band. *ΔN1ΔN2ΔN4* and *Δcco1cco2* showed more staining throughout each sample, with wider bands of greater intensity at the ~40 μm point. These data suggest that deletion of the Cco complexes leads to a more reduced biofilm, which induces production of more matrix, and that CcoN4 contributes significantly to maintaining redox homeostasis when O_2 is limiting.

ccoN4 contributes to P. aeruginosa *virulence in a* C. elegans *slow killing model*

We have previously shown that a mutant defective in biofilm-specific phenazine production, which also shows altered colony morphology (Dietrich et al. 2008, 2013), exhibits decreased virulence (Recinos et al. 2012). We and others have suggested that one way in which phenazines could contribute to virulence is by acting as electron acceptors to balance the intracellular redox state in the hypoxic conditions that are encountered during infection (Price-Whelan, Dietrich, and

Newman 2006; Newman 2008; Dietrich et al. 2013). Because CcoN4 is required for wild-type biofilm architecture and respiration (**Figures 2A**, **2C**, and **5C**), we hypothesized that it could also contribute to virulence. To test this, we conducted virulence assays using the nematode *Caenorhabditis elegans* as a host. It has been shown that *P. aeruginosa* is pathogenic to *C. elegans* and that the slow killing assay mimics an infection-like killing of *C. elegans* by the bacterium (Tan, Mahajan-Miklos, and Ausubel 1999). While Δ*N1*Δ*N2* killed with wild type-like kinetics, Δ*N1*Δ*N2*Δ*N4* and Δ*cco1cco2* both showed comparably-impaired killing relative to wild-type PA14 (**Figures 6A-6B**).

DISCUSSION

Biofilm formation contributes to *P. aeruginosa* pathogenicity and persistence during different types of infections, including the chronic lung colonizations seen in individuals with cystic fibrosis (Tolker-Nielsen 2014; Rybtke et al. 2015). The conditions found within biofilm microenvironments are distinct from those in well-mixed liquid cultures with respect to availability of electron donors and acceptors. We have previously described the roles of phenazines, electron-shuttling antibiotics produced by *P. aeruginosa*, in biofilm-specific metabolism. In this study, we focused on *P. aeruginosa*'s large complement of genes encoding cbb_3-type cytochrome oxidase subunits and set out to test their contributions to metabolic electron flow in biofilms.

The *P. aeruginosa* genome contains four different homologs of *ccoN*, encoding the catalytic subunit of cbb_3-type oxidase. Only two of these (*ccoN1* and *ccoN2*) are co-transcribed with a *ccoO* homolog, encoding the other critical component of an active cbb_3-type oxidase (**Figure 1B**). However, genetic studies have demonstrated that all four versions of CcoN can form functional complexes when expressed with either of the two CcoO homologs (Hirai et al. 2016). In well-mixed liquid cultures, mutants lacking the "orphan" subunits did not show growth defects (**Figure 2C**) (Hirai et al. 2016). We were therefore surprised to find that the Δ*N4* mutant showed a unique morphotype in a colony biofilm assay (**Figure 2A**, **Figure 2(IA)**). We have applied this assay extensively in our studies of the mechanisms underlying cellular redox balancing and sensing and noted that the phenotype of Δ*N4* was similar to that of mutants with defects in electron shuttling and redox signaling (Dietrich et al. 2013; Okegbe et al. 2017).

We characterized the effects of a Δ*N4* mutation on biofilm physiology through a series of assays. In well-mixed liquid cultures, Δ*cco1cco2* showed a growth phenotype similar to that of

Δ*N1*Δ*N2*. While Hirai et al. have shown that wild-type *P. aeruginosa* cultures grown planktonically do form Cco heterocomplexes containing CcoN4, our observations suggest that such complexes do not contribute significantly to growth under these conditions. Consistent with this, deleting *ccoN4* in the Δ*N1*Δ*N2* background had no effect on planktonic growth (**Figure 2C**). However, in biofilm-based experiments, we found that deleting *N4* alone was sufficient to cause an altered morphology phenotype (**Figure 2A** and **Figure 2(IA)**), and that deleting *N4* in either a Δ*N1* or a Δ*N1*Δ*N2* background profoundly affected biofilm physiology. These experiments included quantification of respiratory activity in colonies, in which deletion of CcoN4 led to a significant decrease (**Figure 2B**); biofilm co-culturing, in which CcoN4 was required for competitive fitness (**Figures 3A** and **3B**, **Figures 3(IA) – 3(IC)**); redox profiling, which showed that CcoN4 can contribute to phenazine reduction (**Figure 5B, top**); colony thickness measurements, which showed that CcoN4 is required for the formation of the hypoxic and anoxic zones (**Figure 5B, bottom**); and matrix profiling, which showed that CcoN4 contributes to the repression of Pel polysaccharide production (**Figure 5C**). The overlap in zones of expression between *cco1*, *cco2*, and *ccoN4Q4* seen in colony thin sections (**Figure 4**) implies that CcoN4 can form heterocomplexes with Cco1 and Cco2 subunits that span the depth of the colony and function to influence the physiology of *P. aeruginosa* biofilms in these ways.

The mutant phenotypes and gene expression profiles reported in this study suggest roles for CcoN4 in O_2 and phenazine reduction specifically in the biofilm context, and allow us to draw conclusions about the roles of other CcoN subunits. The expression of *ccoN4Q4* throughout the biofilm depth suggests that CcoN4-containing isoforms could contribute to cytochrome *c* oxidation in both oxic and hypoxic zones (**Figure 4**). This constitutes a deviation from the previously published observation that these genes are specifically induced in hypoxic liquid cultures when compared to well-aerated ones (Alvarez-Ortega and Harwood 2007). Therefore, the *ccoN4Q4* expression we observed in the relatively oxic, upper portion of the colony may be specific to biofilms.

Δ*N4* displayed a colony morphology indicative of redox stress and had a fitness disadvantage compared to the wild type (**Figures 2A**, **3A** and **3B**, **Figure 5B**, **bottom**, **Figure 3(IA)**). However, because it did not show a defect in phenazine reduction (**Figure 5B**, **top**), we attribute its colony morphology and impaired fitness phenotypes to its proposed role in O_2 reduction (Hirai et al. 2016). Similarly, Δ*N1*Δ*N2* showed reduced fitness compared to the wild type

(**Figures 3A** and **3B**, **Figures 3(IA) – 3(IC)**) while showing phenazine reduction comparable to that of the wild type (**Figure 5B**), implying that one or both of these subunits contribute to oxygen reduction in biofilms. When CcoN4 was deleted in conjunction with CcoN1 and CcoN2, however, the resulting strain showed a severe phenazine reduction defect, a phenotype recapitulated by deleting both *cco* operons (**Figure 5B**). Thus, our observations suggest a role for the cbb_3-type oxidases in phenazine reduction in addition to their established roles in O_2 reduction, thereby expanding our understanding of their overall contributions *P. aeruginosa*'s physiology and viability.

The results described here can inform our model of how cells survive under distinct conditions in the microenvironments within biofilms. Previous work has shown that pyruvate fermentation can support survival of *P. aeruginosa* under anoxic conditions (Eschbach et al. 2004) and that phenazines facilitate this process (Glasser, Kern, and Newman 2014). Additional research suggests that phenazine reduction is catalyzed adventitiously by *P. aeruginosa* flavoproteins and dehydrogenases (Glasser et al. 2017). Our observation that cbb_3-type cytochrome oxidases, particularly those containing the CcoN1 or CcoN4 subunits, were required for phenazine reduction in hypoxic biofilm subzones (**Figure 5B**) further implicates the electron transport chain in utilization of these compounds. It is also interesting in light of the historical roles of phenazines acting as mediators in biochemical studies of the cytochrome bc_1 complex and cytochrome oxidases (King 1963; Armstrong and Stewart-Tull 1971; Davidson et al. 1992). Based on this earlier work, we can speculate that different CcoN subunits may indirectly influence phenazine reduction, which could occur at the cytochrome *c* binding site of the CcoO subunit or elsewhere in the electron transport chain, through effects these CcoN subunits have on the overall function or stability of respiratory complexes. Ultimately, various mechanisms of phenazine reduction and phenazine-related metabolisms may be relevant at different biofilm depths or depending on electron donor availability. Our results suggest that, in the colony biofilm system, enzyme complexes traditionally considered to be specific to oxygen reduction may contribute to anaerobic survival.

Because biofilm formation is often associated with colonization of and persistence in hosts, we tested whether CcoN4 contributes to *P. aeruginosa* pathogenicity in *C. elegans*. Similar to our observations in biofilm assays, we found that the Δ*cco1cco2* mutant displayed a more severe phenotype than the Δ*N1*Δ*N2* mutant, suggesting that an orphan subunit can substitute for those encoded by the *cco1* and *cco2* operons. We also found that deleting *ccoN4* in Δ*N1*Δ*N2* led to a Δ*cco1cco2*-like phenotype, suggesting that CcoN4 is the subunit that can play this role (**Figure 6**).

In host microenvironments where O_2 is available, CcoN4-containing isoforms could contribute to its reduction. Additionally, in hypoxic zones, CcoN4-containing isoforms could facilitate the reduction of phenazines, enabling cellular redox balancing. Both of these functions would contribute to persistence of the bacterium within the host. The contributions of the cbb_3-type oxidases to *P. aeruginosa* pathogenicity raise the possibility that compounds interfering with Cco enzyme function could be effective therapies for these infections. Such drugs would be attractive candidates due to their specificity for bacterial respiratory chains and, as such, would not affect the host's endogenous respiratory enzymes.

Our discovery that an orphan cbb_3-type oxidase subunit contributes to growth in biofilms further expands the picture of *P. aeruginosa*'s remarkable respiratory flexibility. Beyond modularity at the level of the terminal enzyme complex (e.g., utilization of an aa_3- vs. a cbb_3-type oxidase), the activity of *P. aeruginosa*'s respiratory chain is further influenced by substitution of orphan cbb_3-type catalytic subunits for native ones. Utilization of CcoN4-containing isoforms promotes phenazine reduction activity and may influence aerobic respiration in *P. aeruginosa* biofilms. For the exceptional species that contain orphan cbb_3-type catalytic subunits, this fine level of control could be particularly advantageous during growth and survival in environments covering a wide range of electron acceptor availability (Cowley et al. 2015).

MATERIALS AND METHODS

Resources Table			
Reagent type (species) or resource	**Designation**	**Source or reference**	**Additional information**
strain, strain background (UCBPP-PA14 *Pseudomonas aeruginosa*)	wild type (WT)	PMID: 7604262	
strain, strain background (UCBPP-PA14 *P. aeruginosa*)	Δ*phz*	PMID: 16879411	LD24
strain, strain background (UCBPP-PA14 *P. aeruginosa*)	Δ*ccoN1*; Δ*N1*	this study	LD1784
strain, strain background (UCBPP-PA14 *P. aeruginosa*)	Δ*ccoN2; ΔN2*	this study	LD1614

strain, strain background (UCBPP-PA14 *P. aeruginosa*)	*ΔccoN3; ΔN3*	this study	LD1620
strain, strain background (UCBPP-PA14 *P. aeruginosa*)	*ΔccoN4; ΔN4*	this study	LD2833
strain, strain background (UCBPP-PA14 *P. aeruginosa*)	*ΔccoN1ΔccoN2*; *ΔN1ΔN2*	this study	LD1888
strain, strain background (UCBPP-PA14 *P. aeruginosa*)	*ΔccoN1ΔccoN4; ΔN1ΔN4*	this study	LD1951
strain, strain background (UCBPP-PA14 *P. aeruginosa*)	*ΔccoN2ΔccoN4; ΔN2ΔN4*	this study	LD1692
strain, strain background (UCBPP-PA14 *P. aeruginosa*)	*ΔccoN3ΔccoN4; ΔN3ΔN4*	this study	LD1649
strain, strain background (UCBPP-PA14 *P. aeruginosa*)	*ΔccoN1ΔccoN2ΔccoN3; ΔN1ΔN2ΔN3*	this study	LD1977
strain, strain background (UCBPP-PA14 *P. aeruginosa*)	*ΔccoN1ΔccoN2ΔccoN4; ΔN1ΔN2ΔN4*	this study	LD1976
strain, strain background (UCBPP-PA14 *P. aeruginosa*)	*ΔccoN1ΔccoN2ΔccoN4ΔccoN3; ΔN1ΔN2ΔN4ΔN3*	this study	LD2020
strain, strain background (UCBPP-PA14 *P. aeruginosa*)	*Δcco1cco2*	this study	LD1933
strain, strain background (UCBPP-PA14 *P. aeruginosa*)	*ΔcoxΔcyoΔcio*	this study	LD2587
strain, strain background (UCBPP-PA14 *P. aeruginosa*)	*Δhcn*	this study	LD2827
strain, strain background (UCBPP-PA14 *P. aeruginosa*)	*ΔphzΔhcn*	this study	LD2828
strain, strain background (UCBPP-PA14 *P. aeruginosa*)	*ΔccoN4Δhcn; ΔN4Δhcn*	this study	LD2829
strain, strain background (UCBPP-PA14 *P. aeruginosa*)	*ΔccoN1ΔccoN2Δhcn; ΔN1ΔN2Δhcn*	this study	LD2830
strain, strain background (UCBPP-PA14 *P. aeruginosa*)	*ΔccoN1ΔccoN2ΔccoN4Δhcn; ΔN1ΔN2ΔN4Δhcn*	this study	LD2831
strain, strain background (UCBPP-PA14 *P. aeruginosa*)	*Δcco1cco2Δhcn*	this study	LD2832
strain, strain background	*gacA::Tn*	PMID:	LD1560

(UCBPP-PA14 *P. aeruginosa*)		16477005	

strain, strain background (UCBPP-PA14 *P. aeruginosa*)	Δ*ccoN4*::*ccoN4; ΔN4*::*N4*	this study	LD1867
strain, strain background (UCBPP-PA14 *P. aeruginosa*)	Δ*ccoN1*Δ*ccoN2*Δ*ccoN4*::*ccoN4; ΔN1ΔN2ΔN4*::*N4*	this study	LD2576
strain, strain background (UCBPP-PA14 *P. aeruginosa*)	MCS-*gfp*	this study	LD2820
strain, strain background (UCBPP-PA14 *P. aeruginosa*)	*Pcco1-gfp*; *cco1Pr-gfp*	this study	LD2784
strain, strain background (UCBPP-PA14 *P. aeruginosa*)	*Pcco2-gfp*; *cco2Pr-gfp*	this study	LD2786
strain, strain background (UCBPP-PA14 *P. aeruginosa*)	*PccoN4-gfp; ccoN4Pr-gfp*	this study	LD2788
strain, strain background (UCBPP-PA14 *P. aeruginosa*)	PA14-*yfp*	this study	LD2780
strain, strain background (UCBPP-PA14 *P. aeruginosa*)	Δ*ccoN1*Δ*ccoN2-yfp*; *ΔN1ΔN2-yfp*	this study	LD2013
strain, strain background (UCBPP-PA14 *P. aeruginosa*)	Δ*ccoN4-yfp*; *ΔN4-yfp*	this study	LD2834
strain, strain background (UCBPP-PA14 *P. aeruginosa*)	Δ*ccoN1*Δ*ccoN2*Δ*ccoN4-yfp; ΔN1ΔN2ΔN4-yfp*	this study	LD2136
strain, strain background (UCBPP-PA14 *P. aeruginosa*)	Δ*cco1cco2-yfp*	this study	LD2012
strain, strain background (*Escherichia coli*)	UQ950	other	LD44
strain, strain background (*E. coli*)	BW29427	other	LD661
strain, strain background (*E. coli*)	β2155	PMID: 8990308	LD69
strain, strain background (*E. coli*)	S17-1	doi:10.1038/nbt1183-784	LD2901
strain, strain background (*Saccharomyces cerevisiae*)	InvSc1	Invitrogen	LD676

recombinant DNA reagent	pMQ30 (plasmid)	PMID: 16820502	For generation of deletion constructs listed above
recombinant DNA reagent	pAKN69 (plasmid)	PMID: 15186351	For generation of strains constitutively expression *eyfp*
recombinant DNA reagent	pLD2722 (plasmid)	this study	For generation of gfp reporter constructs
recombinant DNA reagent	pFLP2 (plasmid)	PMID: 9661666	For generation of *gfp* reporter constructs
software, algorithm	EggNOG Database	PMID: 26582926	http://eggnogdb.embl.de/#/app/home
software, algorithm	SensorTrace Profiling	Unisense	For data acquisition for redox and oxygen microprofiling
other	Agar	Teknova	For colony morphology assays
other	Lectin	Vector Laboratories	For visualization of matrix

Bacterial strains and growth conditions. *P. aeruginosa* strain UCBPP-PA14 (Rahme et al. 1995) was routinely grown in lysogeny broth (LB; 1% tryptone, 1% NaCl, 0.5% yeast extract) (Bertani 2004) at 37 ˚C with shaking at 250 rpm unless otherwise indicated. Overnight cultures were grown for 12-16 hours. For genetic manipulation, strains were typically grown on LB solidified with 1.5% agar. Strains used in this study are listed in Table 3. In general, liquid precultures served as inocula for experiments. Overnight precultures for biological replicates were started from separate clonal source colonies on streaked agar plates. For technical replicates, a single preculture served as the source inoculum for subcultures.

Construction of mutant *P. aeruginosa* strains. For making markerless deletion mutants in *P. aeruginosa* PA14 (Table 3) 1 kb of flanking sequence from each side of the target gene were amplified using the primers listed in Table 1 and inserted into pMQ30 through gap repair cloning in *Saccharomyces cerevisiae* InvSc1 (Shanks et al. 2006). Each plasmid listed in Table 2 was

transformed into *Escherichia coli* strain UQ950, verified by restriction digests, and moved into PA14 using biparental conjugation. PA14 single recombinants were selected on LB agar plates containing 100 µg/ml gentamicin. Double recombinants (markerless deletions) were selected on LB without NaCl and modified to contain 10% sucrose. Genotypes of deletion mutants were confirmed by PCR. Combinatorial mutants were constructed by using single mutants as hosts for biparental conjugation, with the exception of Δ*cco1cco2*, which was constructed by deleting the *cco1* and *cco2* operons simultaneously as one fragment. *ccoN4* complementation strains were made in the same manner, using primers LD438 and LD441 listed in Table 1 to amplify the coding sequence of *ccoN4*, which was verified by sequencing and complemented back into the site of the deletion.

Colony biofilm morphology assays. Overnight precultures were diluted 1:100 in LB (Δ*N1*Δ*N2*, Δ*N1*Δ*N2*Δ*N3*, Δ*N1*Δ*N2*Δ*N4*, Δ*N1*Δ*N2*Δ*N4*Δ*N3*, Δ*N1*Δ*N2*Δ*N4::N4*, Δ*cco1cco2*, Δ*N1*Δ*N2*Δ*hcn*, Δ*N1*Δ*N2*Δ*N4*Δ*hcn*, Δ*cco1cco2*Δ*hcn*, and Δ*cox*Δ*cyo*Δ*cio* were diluted 1:50) and grown to mid-exponential phase (OD at 500 nm ≈ 0.5). Ten microliters of subcultures were spotted onto 60 mL of colony morphology medium (1% tryptone, 1% agar [Teknova A7777] containing 40 µg/ml Congo red dye [VWR AAAB24310-14] and 20 µg/ml Coomassie blue dye [Omnipur; VWR EM-3300]) in a 10 cm x 10 cm x 1.5 cm square Petri dish (LDP D210-16). For preparation of biofilms grown on on phenazine methosulfate (PMS), colony morphology medium was supplemented with 200 µM PMS (Amresco 0361) after autoclaving. For nitrate experiments, colony morphology medium was supplemented with 0, 10, or 40 mM potassium nitrate. Plates were incubated for up to five days at 25 °C with > 90% humidity (Percival CU-22L) and imaged daily using a Keyence VHX-1000 digital microscope. Images shown are representative of at least ten biological replicates. 3D images of biofilms were taken on day 5 of development using a Keyence VR-3100 wide-area 3D measurement system. Δ*cox*Δ*cyo*Δ*cio*, *hcn* deletion mutants, and strains grown for the nitrate experiment were imaged using a flatbed scanner (Epson E11000XL-GA) and are representative of at least three biological replicates

TTC reduction assay. One microliter of overnight cultures (five biological replicates), grown as described above, was spotted onto a 1% tryptone, 1.5% agar plate containing 0.001% (w/v) TTC (2,3,5-triphenyl-tetrazolium chloride [Sigma-Aldrich T8877]) and incubated in the dark at 25 °C for 24 hours. Spots were imaged using a scanner (Epson E11000XL-GA) and TTC reduction, normalized to colony area, was quantified using Adobe Photoshop CS5. Colorless TTC undergoes

an irreversible color change to red when reduced. Pixels in the red color range were quantified and normalized to colony area using Photoshop CS5.

Liquid culture growth assays. **(i)** Overnight precultures were diluted 1:100 (*ΔN1ΔN2*, *ΔN1ΔN2ΔN4*, and *Δcco1cco2* were diluted 1:50) in 1% tryptone in a clear, flat-bottom polystyrene 96-well plate (VWR 82050-716) and grown for two hours ($OD_{500nm} \approx 0.2$). These cultures were then diluted 100-fold in 1% tryptone in a new 96-well plate and incubated at 37 °C with continuous shaking on the medium setting in a Biotek Synergy 4 plate reader. Growth was assessed by taking OD readings at 500 nm every thirty minutes for at least 24 hours. **(ii) *hcn* mutants:** Overnight precultures were diluted 1:100 (*ΔN1ΔN2Δhcn*, *ΔN1ΔN2ΔN4Δhcn*, and *Δcco1cco2Δhcn* were diluted 1:50) in MOPS minimal medium (50 mM 4-morpholinepropanesulfonic acid (pH 7.2), 43 mM NaCl, 93 mM NH_4Cl, 2.2 mM KH_2PO4, 1 mM $MgSO_4•7H_2O$, 1 µg/ml $FeSO_4•7H_2O$, 20 mM sodium succinate hexahydrate) and grown for 2.5 hours until OD at 500 nm ≈ 0.1. These cultures were then diluted 100-fold in MOPS minimal medium in a clear, flat-bottom polystyrene 96-well plate and incubated at 37 °C with continuous shaking on the medium setting in a Biotek Synergy 4 plate reader. Growth was assessed by taking OD readings at 500 nm every thirty minutes for at least 24 hours. **(iii) Terminal oxidase reporters:** Overnight precultures were grown in biological triplicate; each biological triplicate was grown in technical duplicate. Overnight precultures were diluted 1:100 in 1% tryptone and grown for 2.5 hours until OD at 500 nm ≈ 0.1. These cultures were then diluted 100-fold in 1% tryptone in a clear, flat-bottom, polystyrene black 96-well plate (VWR 82050-756) and incubated at 37 °C with continuous shaking on the medium setting in a Biotek Synergy 4 plate reader. Expression of GFP was assessed by taking fluorescence readings at excitation and emission wavelengths of 480 nm and 510 nm, respectively, every hour for 24 hours. Growth was assessed by taking OD readings at 500 nm every 30 minutes for 24 hours. Growth and RFU values for technical duplicates were averaged to obtain the respective values for each biological replicate. RFU values for a strain without a promoter inserted upstream of the *gfp* gene (MCS-*gfp*) were considered background and subtracted from the fluorescence values of each reporter.

Competition assays. Overnight precultures of fluorescent (YFP-expressing) and non-fluorescent strains were diluted 1:100 in LB (*ΔN1ΔN2*, *ΔN1ΔN2ΔN4* and *Δcco1cco2* were diluted 1:50) and grown to mid-exponential phase (OD at 500 nm ≈ 0.5). Exact OD at 500 nm values were read in a Spectronic 20D+ spectrophotometer (Thermo Scientific) and cultures were adjusted to the same

OD. Adjusted cultures were then mixed in a 1:1 ratio of fluorescent:non-fluorescent cells and ten µl of this mixture were spotted onto colony morphology plates and grown for three days as described above. At specified time points, biofilms were collected, suspended in one mL of 1% tryptone, and homogenized on the "high" setting in a bead mill homogenizer (Omni Bead Ruptor 12); day one colonies were homogenized for 35 seconds while days two and three colonies were homogenized for 99 seconds. Homogenized cells were serially diluted and 10^{-6}, 10^{-7}, and 10^{-8} dilutions were plated onto 1% tryptone plates and grown overnight at 37 °C. Fluorescent colony counts were determined by imaging plates with a Typhoon FLA7000 fluorescent scanner (GE Healthcare) and percentages of fluorescent vs. non-fluorescent colonies were determined.

Construction of terminal oxidase reporters. Translational reporter constructs for the Cco1, Cco2, and CcoN4Q4 operons were constructed using primers listed in Table 1. Respective primers were used to amplify promoter regions (500 bp upstream of the operon of interest), adding an SpeI digest site to the 5' end of the promoter and an XhoI digest site to the 3' end of the promoter. Purified PCR products were digested and ligated into the multiple cloning site (MCS) of the pLD2722 vector, upstream of the *gfp* sequence. Plasmids were transformed into *E. coli* strain UQ950, verified by sequencing, and moved into PA14 using biparental conjugation with *E. coli* strain S17-1. PA14 single recombinants were selected on M9 minimal medium agar plates (47.8 mM Na_2HPO_4•$7H_2O$, 22 mM KH_2PO_4, 8.6 mM NaCl, 18.6 mM NH_4Cl, 1 mM $MgSO_4$, 0.1 mM $CaCl_2$, 20 mM sodium citrate dihydrate, 1.5% agar) containing 100 µg/ml gentamicin. The plasmid backbone was resolved out of PA14 using Flp-FRT recombination by introduction of the pFLP2 plasmid (Hoang et al. 1998) and selected on M9 minimal medium agar plates containing 300 µg/ml carbenicillin and further on LB agar plates without NaCl and modified to contain 10% sucrose. The presence of *gfp* in the final clones was confirmed by PCR.

Thin sectioning analyses. Two layers of 1% tryptone with 1% agar were poured to depths of 4.5 mm (bottom) and 1.5 mm (top). Overnight precultures were diluted 1:100 (*ΔN1ΔN2*, *ΔN1ΔN4*, *ΔN1ΔN2ΔN4*, *Δcco1cco2* were diluted 1:50) in LB and grown for two hours, until early-mid exponential phase. Five to ten µL of subculture were then spotted onto the top agar layer and colonies were incubated in the dark at 25 °C with > 90% humidity (Percival CU-22L) and grown for up to three days. At specified time points to be prepared for thin sectioning, colonies were covered by a 1.5-mm-thick 1% agar layer. Colonies sandwiched between two 1.5-mm agar layers were lifted from the bottom layer and soaked for four hours in 50 mM L-lysine in phosphate

buffered saline (PBS) (pH 7.4) at 4 ˚C, then fixed in 4% paraformaldehyde, 50 mM L-lysine, PBS (pH 7.4) for four hours at 4˚C, then overnight at 37 °C. Fixed colonies were washed twice in PBS and dehydrated through a series of ethanol washes (25%, 50%, 70%, 95%, 3x 100% ethanol) for 60 minutes each. Colonies were cleared via three 60-minute incubations in Histoclear-II (National Diagnostics HS-202) and infiltrated with wax via two separate washes of 100% Paraplast Xtra paraffin wax (Electron Microscopy Sciences; Fisher Scientific 50-276-89) for two hours each at 55 ˚C, then colonies were allowed to polymerize overnight at 4 ˚C. Tissue processing was performed using an STP120 Tissue Processor (Thermo Fisher Scientific 813150). Trimmed blocks were sectioned in ten µm-thick sections perpendicular to the plane of the colony using an automatic microtome (Thermo Fisher Scientific 905200ER), floated onto water at 45 ˚C, and collected onto slides. Slides were air-dried overnight, heat-fixed on a hotplate for one hour at 45 ˚C, and rehydrated in the reverse order of processing. Rehydrated colonies were immediately mounted in TRIS-Buffered DAPI:Fluorogel (Electron Microscopy Sciences; Fisher Scientific 50-246-93) and overlaid with a coverslip. Differential interference contrast (DIC) and fluorescent confocal images were captured using an LSM700 confocal microscope (Zeiss). Each strain was prepared in this manner in at least biological triplicates.

Colony thickness measurements. Colonies were prepared for thin sectioning as described above, but growth medium was supplemented with 40 µg/ml Congo Red dye and 20 µg/ml Coomassie Blue dye. Colony height measurements were obtained from confocal DIC images using Fiji image processing software (Schindelin et al. 2012).

Lectin staining. Two-day-old colonies were prepared for thin sectioning as described above. Rehydrated colonies were post-stained in 100 µg/mL fluorescein-labeled *Wisteria floribunda* lectin (Vector Laboratories FL-1351) in PBS before being washed twice in PBS, mounted in TRIS-buffered DAPI and overlaid with a coverslip. Fluorescent confocal images were captured using an LSM700 confocal microscope (Zeiss).

Redox profiling of biofilms. A 25 µm-tip redox microelectrode and external reference (Unisense RD-25 and REF-RM) were used to measure the extracellular redox state of day two (~ 48 h) biofilms (grown as for the **colony biofilm morphology assays**). The redox microelectrode measures the tendency of a sample to take up or release electrons relative to the reference electrode, which is immersed in the same medium as the one on which the sample is grown. The redox microelectrode was calibrated according to manufacturer's instructions using a two-point

calibration to 1% quinhydrone in pH 4 buffer and 1% quinhydrone in pH 7 buffer. Redox measurements were taken every five μm throughout the depth of the biofilm using a micromanipulator (Unisense MM33) with a measurement time of three seconds and a wait time between measurements of five seconds. Profiles were recorded using a multimeter (Unisense) and the SensorTrace Profiling software (Unisense).

Oxygen profiling of biofilms. A 25 μm-tip oxygen microsensor (Unisense OX-25) was used to measure oxygen concentrations within biofilms during the first two days of development, grown as described above. For oxygen profiling on three-day-old colonies (**Figure 4**), biofilms were grown as for the thin sectioning analyses. To calibrate the oxygen microsensor, a two-point calibration was used. The oxygen microsensor was calibrated first to atmospheric oxygen using a calibration chamber (Unisense CAL300) containing water continuously bubbled with air. The microsensor was then calibrated to a "zero" point using an anoxic solution of water thoroughly bubbled with N_2; to ensure complete removal of all oxygen, N_2 was bubbled into the calibration chamber for a minimum of 30 minutes before calibrating the microsensor to the zero calibration point. Oxygen measurements were then taken throughout the depth of the biofilm using a measurement time of three seconds and a wait time between measurements of five seconds. For six-hour-old colonies, a step size of one μm was used to profile through the entire colony; for 12-hour and 24-hour colonies, two μm; for 48-hour colonies, five μm. A micromanipulator (Unisense MM33) was used to move the microsensor within the biofilm and profiles were recorded using a multimeter (Unisense) and the SensorTrace Profiling software (Unisense).

Phenazine quantification. Overnight precultures were diluted 1:10 in LB and spotted onto a 25-mm 0.2 μm filter disk (pore size: 0.2 μm; GE Healthcare 110606) placed into the center of one 35 x 10 mm round Petri dish (Falcon 351008). Colonies were grown for two days in the dark at 25 °C with > 90% humidity. After two days of growth, each colony (with filter disk) was lifted off its respective plate and weighed. Excreted phenazines were then extracted from the agar medium overnight in five mL of 100% methanol (in the dark, nutating at room temperature). Three hundred μl of this overnight phenazine/methanol extraction were then filtered through a 0.22 μm cellulose Spin-X column (Thermo Fisher Scientific 07-200-386) and 200 μl of the flow-through were loaded into an HPLC vial. Phenazines were quantified using high-performance liquid chromatography (Agilent 1100 HPLC System) as described previously (Dietrich et al. 2006; Sakhtah et al. 2016).

***C. elegans* pathogenicity (slow killing) assays.** Slow killing assays were performed as described previously (Tan, Mahajan-Miklos, and Ausubel 1999; Powell and Ausubel 2008). Briefly, ten µl of overnight PA14 cultures (grown as described above) were spotted onto slow killing agar plates (0.3% NaCl, 0.35% Bacto-Peptone, 1 mM $CaCl_2$, 1 mM $MgSO_4$, 5 µg/ml cholesterol, 25 mM KPO_4, 50 µg/ml FUDR, 1.7% agar) and plates were incubated for 24 hours at 37 °C followed by 48 hours at room temperature (~23 °C). Larval stage 4 (L4) nematodes were picked onto the PA14-seeded plates and live/dead worms were counted for up to four days. Each plate was considered a biological replicate and had a starting sample size of 30-35 worms.

Statistical analysis. Data analysis was performed using GraphPad Prism version 7 (GraphPad Software, La Jolla California USA). Values are expressed as mean ± SD. Statistical significance of the data presented was assessed with the two-tailed unpaired Student's t-test. Values of $P \leq 0.05$ were considered significant (*, $P \leq 0.05$; **, $P \leq 0.01$; ***, $P \leq 0.001$; ****, $P \leq 0.0001$).

Table 1. Primers used in this study.

primer number	sequence	used to make plasmid number
LD717	ccaggcaaattctgttttatcagaccgcttctgcgttctgatCAGGACAAGCAGTGGGAAC (SEQ ID No. 1)	pLD1852
LD718	aggtgttgtaggccatcagcTGGCGGACCACCTTATAGTT (SEQ ID No. 2)	
LD958	aactataaggtggtccgccaCGGTGGTTTCTTCCTCACC (SEQ ID No. 3)	
LD959	ggaattgtgagcggataacaatttcacacaggaaacagctGGTCCAGCCTTTTTCCTTGT (SEQ ID No. 4)	
LD725	ccaggcaaattctgttttatcagaccgcttctgcgttctgatCCCCTCAGAGAAGTCAGTCG (SEQ ID No. 5)	pLD1610
LD726	aggtgttgtaggccatcaggGGCGGACCACCTTGTAGTTA (SEQ ID No. 6)	
LD727	taactacaaggtggtccgccCCTGATGGCCTACAACACCT (SEQ ID No. 7)	
LD728	ggaattgtgagcggataacaatttcacacaggaaacagctCAGCGGGTTGTCATACTCCT (SEQ ID No. 8)	
LD741	ccaggcaaattctgttttatcagaccgcttctgcgttctgatTCGAGGGCTTCGAGAAGAT (SEQ ID No. 9)	pLD1616
LD742	aggtgttgtaggccatcagcCAGGGTCATCAGGGTGAACT (SEQ ID	

	No. 10)	
LD743	agttcaccctgatgaccctgGCTGATGGCCTACAACACCT (SEQ ID No. 11)	
LD744	ggaattgtgagcggataacaatttcacacaggaaacagctCGGGTGATGTCGACGTATTC (SEQ ID No. 12)	
LD438	ggaattgtgagcggataacaatttcacacaggaaacagctCCGTTGATTTCCTTCTGCAT (SEQ ID No. 13)	pLD1264 (LD438 - LD441) pLD1853 (LD438 and LD441)
LD439	ctacaaggtggttcgccagtCGCTGACCTACTCCTTCGTC (SEQ ID No. 14)	
LD440	gacgaaggagtaggtcagcgACTGGCGAACCACCTTGTAG (SEQ ID No. 15)	
LD441	ccaggcaaattctgttttatcagaccgcttctgcgttctgatCATCGACCTGGAAGTGCTC (SEQ ID No. 16)	
LD725	ccaggcaaattctgttttatcagaccgcttctgcgttctgatCCCCTCAGAGAAGTCAGTCG (SEQ ID No. 17)	pLD1929
LD1063	gttgcccaggtgttcctgtGGCGGACCACCTTGTAGTTA (SEQ ID No. 18)	
LD949	ggaattgtgagcggataacaatttcacacaggaaacagctTGTAGTCGAGGGACTTCTTGC (SEQ ID No. 19)	
LD1064	taactacaaggtggtccgccACAGGAACACCTGGGCAAC (SEQ ID No. 20)	
LD2168	ccaggcaaattctgttttatcagaccgcttctgcgttctgatATGTAGGGATCGAGCGACAG (SEQ ID No. 21)	pLD2791
LD2169	acacgatatccagcccctctTGGACATCGCGCCGTTCCTC (SEQ ID No. 22)	
LD2170	gaggaacggcgcgatgtccaAGAGGGGCTGGATATCGTGT (SEQ ID No. 23)	
LD2171	ggaattgtgagcggataacaatttcacacaggaaacagctAAGAGGTCATAATCGGCGGT (SEQ ID No. 24)	
LD2120	gattcgacatcactagtACGCCCAGCTCCAACAAA (SEQ ID No. 25)	pLD2777
LD2121	gattcgatgccctcgaGCTAGGGGTTCCACGGTTAAT (SEQ ID No. 26)	
LD2122	gattcgactgcactagtCATCGACTTGCCGCCCAG (SEQ ID No. 27)	pLD2778
LD2123	gattcgatgccctcgaGCTATGGGCTTCCATCCAC (SEQ ID No. 28)	
LD2124	gattcgactgcactagtGGCTACTTCCTCTGGCTGG (SEQ ID No. 29)	pLD2779
LD2125	gattcgactgcctcgagCTGTACAGTCCCGAAAGAAATGAAC (SEQ ID No. 30)	

Table 1 (continued). Primers used in this study.

primer number	sequence	used to make plasmid number
LD1118	ccaggcaaattctgttttatcagaccgcttctgcgttctgatTCTTCAGGTTCTCG CGGTAG (SEQ ID No. 31)	pLD1966
LD1119	aagtgccagtaccaactggcGCAGATCCAGAAGATGGTCA (SEQ ID No. 32)	
LD1120	tgaccatcttctggatctgcGCCAGTTGGTACTGGCACTT (SEQ ID No. 33)	
LD1121	ggaattgtgagcggataacaatttcacacaggaaacagctATCGCGAGACTCA TGGTTTT (SEQ ID No. 34)	
LD1134	ccaggcaaattctgttttatcagaccgcttctgcgttctgatCGCTGCTTGTCGAT CTGTT (SEQ ID No. 35)	pLD1967
LD1135	gcgacatgaccctgttcaacCTGACCGGCTACTGGACC (SEQ ID No. 36)	
LD1136	ggtccagtagccggtcagGTTGAACAGGGTCATGTCGC (SEQ ID No. 37)	
LD1137	ggaattgtgagcggataacaatttcacacaggaaacagctCCTCGGCGACCAT GAATAC (SEQ ID No. 38)	
LD1126	ccaggcaaattctgttttatcagaccgcttctgcgttctgatTTCAGGTTCTTCGG GTTCTC (SEQ ID No. 39)	pLD2044
LD1187	aacagcgcgccgaccagcatCTCTTCGTTCGTTTTCAGCC (SEQ ID No. 40)	
LD1188	ggctgaaaacgaacgaagagATGCTGGTCGGCGCGCTGTT (SEQ ID No. 41)	
LD1189	ggaattgtgagcggataacaatttcacacaggaaacagctGCGTTGATGAAGC GGATAAC (SEQ ID No. 42)	

Table 2. Plasmids used in this study.

plasmid	description	source
pMQ30	7.5 kb mobilizable vector; oriT, sacB, Gm^R.	Shanks et al. 2006
pAKN69	Contains mini-Tn7(Gm)PA1/04/03::eyfp fusion.	Lambertsen et al. 2004
pLD2722	Gm^R, Tet^R flanked by Flp recombinase target (FRT) sites to resolve out resistance casettes.	this study
pFLP2	Site-specific excision vector with cI857-controlled FLP recombinase encoding sequence, sacB, Ap^R.	Hoang et al. 1998
pLD1852	Δ*ccoN1* PCR fragment introduced into pMQ30 by gap repair cloning in yeast strain InvSc1.	this study
pLD1610	Δ*ccoN2* PCR fragment introduced into pMQ30 by gap repair cloning in yeast strain InvSc1.	this study
pLD1616	Δ*ccoN3* PCR fragment introduced into pMQ30 by gap repair cloning in yeast strain InvSc1.	this study
pLD1264	Δ*ccoN4* PCR fragment introduced into pMQ30 by gap repair cloning in yeast strain InvSc1.	this study
pLD1929	Δ*cco1 cco2* PCR fragment introduced into pMQ30 by gap repair cloning in yeast strain InvSc1.	this study
pLD2791	Δ*hcn* PCR fragment introduced into pMQ30 by gap repair cloning in yeast strain InvSc1.	this study
pLD1853	Full genomic sequence of *ccoN4* PCR fragment introduced into pMQ30 by gap repair cloning in yeast strain InvSc1. Verified by sequencing.	this study
pLD1966	Δaa_3 PCR fragment introduced into pMQ30 by gap repair cloning in yeast strain IncSc1.	this study
pLD1967	Δbo_3 PCR fragment introduced into pMQ30 by gap repair cloning in yeast strain IncSc1.	this study
pLD2044	Δ*cio* PCR fragment introduced into pMQ30 by gap repair cloning in yeast strain IncSc1.	this study
pLD2777	PCR-amplified *cco1* promoter ligated into pSEK103 using SpeI and XhoI.	this study
pLD2778	PCR-amplified *cco2* promoter ligated into pSEK103 using SpeI and XhoI.	this study
pLD2779	PCR-amplified *ccoN4* promoter ligated into pSEK103 using SpeI and XhoI.	this study

Table 3. Strains used in this study.

strain	number	description	source
Pseudomonas aeruginosa strains			
UCBPP-PA14		Clinical isolate UCBPP-PA14.	Rahme et al. 1995
PA14 Δphz	LD24	PA14 with deletions in *phzA1-G1* and *phzA2-G2* operons.	Dietrich et al. 2006
PA14 Δ*ccoN1*	LD1784	PA14 with deletion in PA14_44370.	this study
PA14 Δ*ccoN2*	LD1614	PA14 with deletion in PA14_44340.	this study
PA14 Δ*ccoN3*	LD1620	PA14 with deletion in PA14_40510.	this study
PA14 Δ*ccoN4*	LD2833	PA14 with deletion in PA14_10500.	this study
PA14 Δ*ccoN1* Δ*ccoN2*	LD1888	PA14 with deletions in PA14_44370 and PA14_44340. Made by mating pLD1610 into LD1784.	this study
PA14 Δ*ccoN1* Δ*ccoN4*	LD1951	PA14 with deletions in PA14_44370 and PA14_10500. Made by mating pLD1264 into LD1784.	this study
PA14 Δ*ccoN2* Δ*ccoN4*	LD1692	PA14 with deletions in PA14_44340 and PA14_10500. Made by mating pLD1264 into LD1614.	this study
PA14 Δ*ccoN3* Δ*ccoN4*	LD1649	PA14 with deletions in PA14_40510 and PA14_10500. Made by mating pLD1264 into LD1620.	this study
PA14 Δ*ccoN1* Δ*ccoN2* Δ*ccoN3*	LD1977	PA14 with deletions in PA14_443470, PA14_44340, and PA14_40510. Made by mating pLD1616 into LD1888.	this study
PA14 Δ*ccoN1* Δ*ccoN2* Δ*ccoN4*	LD1976	PA14 with deletions in PA14_443470, PA14_44340, and PA14_10500. Made by mating pLD1264 into LD1888.	this study
PA14 Δ*ccoN1* Δ*ccoN2* Δ*ccoN4* Δ*ccoN3*	LD2020	PA14 with deletions in PA14_443470, PA14_44340, PA14_10500, and PA14_40510. Made by mating pLD1264 into LD1977.	this study
PA14 Δ*cco1cco2*	LD1933	PA14 with both *cco* operons (PA14_44340-PA14_44400) deleted simultaneously.	this study
PA14 Δ*cox* Δ*cyo* Δ*cio*	LD2587	PA14 with deletions in PA14_01290-01320 (*cox*/*aa*3 operon), PA14_47150-47210 (*cyo*/*bo*3 operon), and PA14_13030-13040 (*cio* operon). Made by mating pLD1966, pLD1967, and pLD2044, in that order, to PA14.	this study
PA14 Δ*hcn*	LD2827	PA14 with deletion in *hcnABC* operon (PA14_36310-36330).	this study

PA14 Δ*phz* Δ*hcn*	LD2828	PA14 with deletions in *phzA1-G1, phzA2-G2,* and *hcnABC* operons. Made by mating pLD2791 into LD24.	this study
PA14 Δ*ccoN4* Δ*hcn*	LD2829	PA14 with deletions in PA14_10500 and *hcnABC* operon. Made by mating pLD2791 into LD2833.	this study
PA14 Δ*ccoN1* Δ*ccoN2* Δ*hcn*	LD2830	PA14 with deletions in PA14_44370, PA14_44340, and *hcnABC* operon. Made by mating pLD2791 into LD1888.	this study
PA14 Δ*ccoN1* Δ*ccoN2* Δ*ccoN4* Δ*hcn*	LD2831	PA14 with deletions in PA14_44370, PA14_44340, PA14_10500 and *hcnABC* operon. Made by mating pLD2791 into LD1976.	this study

Table 3 (continued). Strains used in this study.

strain	number	description	source
Pseudomonas aeruginosa strains			
PA14 Δ*cco1cco2* Δ*hcn*	LD2832	PA14 with deletions in *cco1*, *cco2*, and *hcnABC* operons. Made by mating pLD2791 into LD1933.	this study
PA14 *gacA*::*Tn*	LD1560	MAR2xT7 transposon insertion into PA14_30650.	Liberati et al. 2006
PA14 Δ*ccoN4*::*ccoN4*	LD1867	PA14 Δ*ccoN4* strain with wild-type *ccoN4* complemented back into the site of deletion. Made by mating pLD1853 into LD2833.	this study
PA14 Δ*ccoN1* Δ*ccoN2* Δ*ccoN4*::*ccoN4*	LD2576	PA14 Δ*ccoN1* Δ*ccoN2* Δ*ccoN4* strain with wild-type *ccoN4* complemented back into the site of deletion. Made by mating pLD1853 into LD1976.	this study
PA14 MCS-gfp	LD2820	PA14 without a promoter driving *gfp* expression.	this study
PA14 $P_{cco\text{-}1}$-gfp	LD2784	PA14 with promoter of *cco1* operon driving *gfp* expression.	this study
PA14 $P_{cco\text{-}2}$-gfp	LD2786	PA14 with promoter of *cco2* operon driving *gfp* expression.	this study
PA14 P_{ccoN4}-gfp	LD2788	PA14 with promoter of *ccoN4Q4* operon driving *gfp* expression.	this study
PA14-yfp	LD2780	WT PA14 constitutively expressing *eyfp*.	this study
PA14 Δ*ccoN1* Δ*ccoN2*-yfp	LD2013	PA14 Δ*ccoN1* Δ*ccoN2* constitutively expressing *eyfp*. Made by mating pAKN69 into LD1888.	this study
PA14 Δ*ccoN4*-yfp	LD2834	PA14 Δ*ccoN4* constitutively expressing *eyfp*. Made by mating pAKN69 into LD2833.	this study

PA14 Δ*ccoN1* Δ*ccoN2* Δ*ccoN4*-yfp	LD2136	PA14 Δ*ccoN1* Δ*ccoN2* Δ*ccoN4* constitutively expressing *eyfp*. Made by mating pAKN69 into LD1976.	this study
PA14 Δ*cco1cco2*-yfp	LD2012	PA14 Δ*cco1cco2* constitutively expressing *eyfp*. Made by mating pAKN69 into LD1933.	this study
Escherichia coli strains			
UQ950	LD44	*E. coli* DH5 λpir strain for cloning. F-Δ(argF- lac) 169φ80 dlacZ58(ΔM15) glnV44(AS) rfbD1 gyrA96(NaI^R) recA1 endA1 spoT thi-1 hsdR17 deoR λpir$^+$	
BW29427	LD661	Donor strain for conjugation. thrB1004 pro thi rpsL hsdS lacZ ΔM15RP4-1360 Δ(araBAD)567 ΔdapA1314::[erm pir(wt)]	
β2155	LD69	Helper strain. thrB1004 pro thi strA hsdsS lacZΔM15 (F'lacZΔM15 laclq traD36 proA+ proB+) ΔdapA::erm (Ermr)pir::RP4 [::kan (Kmr) from SM10]	Dehio and Meyer, 1997
S17-1	LD2901	Str^R , Tp^R , F$^-$ RP4-2-Tc::Mu aphA::Tn7 recA λpir lysogen	Simon et al. 1983
Saccharomyces cerevisiae strains			
InvSc1	LD676	MATa/MATalpha leu2/leu2 trp1-289/trp1-289 ura3-52/ ura3-52 his3-Δ1/his3-Δ1	Invitrogen

Table 4. Statistical analysis.

Figure 2B	**number of values (biological replicates)**	**mean**	**median**	**SD**	**SEM**	**lower 95% confidence interval of mean**	**upper 95% confidence interval of mean**
WT	5	73.22	72.94	3.387	1.515	69.02	77.43
Δ*N4*	5	68.97	70.6	6.44	2.88	60.97	76.96
Δ*N1*Δ*N2*	5	52.18	50.46	5.142	2.3	45.79	58.56
Δ*N1*Δ*N4*	5	11.57	12.42	2.011	0.8991	9.074	14.07
Δ*N1*Δ*N2*Δ*N4*	5	0.001958	0.001117	0.001696	0.0007586	-0.0001481	0.004064
Δ*cco1cco2*	5	0.001367	0.0008644	0.001237	0.0005532	-0.0001686	0.002903
t-test	**P value**	**P value summary**					

WT vs. Δ*N4*	0.2273	ns					
WT vs. Δ*N1*Δ*N2*	<0.0001	****					
WT vs. Δ*N1*Δ*N4*	<0.0001	****					
WT vs. Δ*N1*Δ*N2*Δ*N4*	<0.0001	****					
WT vs. Δ*cco1cco2*	<0.0001	****					

Figure 3A	**number of values (biological replicates)**	**mean**	**median**	**SD**	**SEM**	**lower 95% confidence interval of mean**	**upper 95% confidence interval of mean**
WT-YFP	12	54.95	54.92	4.387	1.266	52.16	57.74
Δ*N4*-YFP	3	29.92	30.83	2.234	1.29	24.37	35.46
Δ*N1*Δ*N2*-YFP	3	30.49	31.91	3.527	2.036	21.73	39.25
Δ*N1*Δ*N2*Δ*N4*-YFP	3	4.408	4.296	3.23	1.865	-3.617	12.43
Δ*cco1cco2*-YFP	3	7.097	5.306	4.093	2.363	-3.072	17.27
t-test	**P value**	**P value summary**					
WT-YFP vs. Δ*N4*-YFP	<0.0001	****					
WT-YFP vs. Δ*N1*Δ*N2*-YFP	<0.0001	****					
Δ*N1*Δ*N2*-YFP vs. Δ*N1*Δ*N2*Δ*N4*-YFP	0.0007	***					
Δ*N1*Δ*N2*-YFP vs. Δ*cco1cco2*-YFP	0.0017	**					

Table 4 (continued). Statistical analysis.

Figure 3(IA)	**number of values (biological replicates)**	**mean**	**median**	**SD**	**SEM**	**lower 95% confidence interval of mean**	**upper 95% confidence interval of mean**
WT	12	45.05	45.08	4.387	1.266	42.26	47.84
Δ*N4*	3	28.22	31.31	7.442	4.297	9.731	46.71
Δ*N1*Δ*N2*	3	27.81	28.57	2.514	1.451	21.56	34.05
Δ*N1*Δ*N2*Δ*N4*	3	7.002	6.973	0.7508	0.4335	5.137	8.867

Δ*cco1cco2*	3	5.38	4.183	2.146	1.239	0.05034	10.71
t-test	**P value**	**P value summary**					
WT vs. Δ*N4*	0.0002	***					
WT vs. Δ*N1*Δ*N2*	<0.0001	****					
Δ*N1*Δ*N2* vs. Δ*N1*Δ*N2*Δ*N4*	0.0002	***					
Δ*N1*Δ*N2* vs. Δ*cco1cco2*	0.0003	***					

Figure 5	number of values (biological replicates)	mean	median	SD	SEM	lower 95% confidence interval of mean	upper 95% confidence interval of mean
WT	8	150.3	151.2	10.31	3.644	141.7	158.9
Δ*N1*Δ*N2*	4	139.3	137.6	12.33	6.166	119.6	158.9
Δ*N4*	7	131.9	127.8	8.915	3.369	123.7	140.2
Δ*N1*Δ*N4*	4	99.96	99.34	2.726	1.363	95.62	104.3
Δ*cco1cco2*	4	95.19	95.56	1.559	0.7793	92.71	97.67
Δ*N1*Δ*N2*Δ*N4*	4	102.8	99.79	8.664	4.332	88.98	116.6
Δ*phz*	7	84.98	84.23	10.93	4.131	74.87	95.09
t-test	**P value**	**P value summary**					
WT vs. Δ*N1*Δ*N2*	0.1302	ns					
WT vs. Δ*N4*	0.0028	**					
WT vs. Δ*N1*Δ*N4*	<0.0001	****					
WT vs. Δ*cco1cco2*	<0.0001	****					
WT vs. Δ*N1*Δ*N2*Δ*N4*	<0.0001	****					
WT vs. Δ*phz*	<0.0001	****					

Table 4 (continued). Statistical analysis.

Figure 6	number of values (biological replicates)	mean	median	SD	SEM	lower 95% confidence interval of mean	upper 95% confidence interval of mean
WT	9	27.44	39	18.48	6.16	13.24	41.65
gacA::Tn	9	92.56	93	8.546	2.849	85.99	99.12
Δ*N1*Δ*N2*	4	19	21.5	14.07	7.036	-3.39	41.39
Δ*N1*Δ*N2*Δ*N4*	6	64.17	68	18	7.35	45.27	83.06
Δ*cco1cco2*	9	70.56	76	22.69	7.565	53.11	88
t-test	**P value**	**P value summary**					
WT vs. Δ*N1*Δ*N2*Δ*N4*	0.0022	**					
Δ*N1*Δ*N2* vs. Δ*N1*Δ*N2*Δ*N4*	0.0030	**					
WT vs. Δ*N1*Δ*N2*	0.4362	ns					

References

Alvarez-Ortega, Carolina, and Caroline S. Harwood. 2007. "Responses of Pseudomonas Aeruginosa to Low Oxygen Indicate That Growth in the Cystic Fibrosis Lung Is by Aerobic Respiration." Molecular Microbiology 65 (1): 153–65.

Anzai, Y., H. Kim, J. Y. Park, H. Wakabayashi, and H. Oyaizu. 2000. "Phylogenetic Affiliation of the Pseudomonads Based on 16S rRNA Sequence." International Journal of Systematic and Evolutionary Microbiology 50 Pt 4 (July): 1563–89.

Arai, Hiroyuki, Takuro Kawakami, Tatsuya Osamura, Takehiro Hirai, Yoshiaki Sakai, and Masaharu Ishii. 2014. "Enzymatic Characterization and in Vivo Function of Five Terminal Oxidases in Pseudomonas Aeruginosa." Journal of Bacteriology 196 (24): 4206–15.

Armstrong, A. V., and D. E. Stewart-Tull. 1971. "The Site of the Activity of Extracellular Products of Pseudomonas Aeruginosa in the Electron-Transport Chain in Mammalian Cell Respiration." Journal of Medical Microbiology 4 (2): 263–70.

Bertani, Giuseppe. 2004. "Lysogeny at Mid-Twentieth Century: P1, P2, and Other Experimental Systems." Journal of Bacteriology 186 (3): 595–600.

Biasini, Marco, Stefan Bienert, Andrew Waterhouse, Konstantin Arnold, Gabriel Studer, Tobias Schmidt, Florian Kiefer, et al. 2014. "SWISS-MODEL: Modelling Protein Tertiary and Quaternary Structure Using Evolutionary Information." Nucleic Acids Research 42 (Web Server issue): W252–58.

Borriello, Giorgia, Erin Werner, Frank Roe, Aana M. Kim, Garth D. Ehrlich, and Philip S. Stewart. 2004. "Oxygen Limitation Contributes to Antibiotic Tolerance of Pseudomonas Aeruginosa in Biofilms." Antimicrobial Agents and Chemotherapy 48 (7): 2659–64.

Brochier-Armanet, Celine, Emmanuel Talla, and Simonetta Gribaldo. 2009. "The Multiple Evolutionary Histories of Dioxygen Reductases: Implications for the Origin and Evolution of Aerobic Respiration." Molecular Biology and Evolution 26 (2): 285–97.

Buschmann, Sabine, Eberhard Warkentin, Hao Xie, Julian D. Langer, Ulrich Ermler, and Hartmut Michel. 2010. "The Structure of cbb3 Cytochrome Oxidase Provides Insights into Proton Pumping." Science 329 (5989): 327–30.

Comolli, James C., and Timothy J. Donohue. 2004. "Differences in Two Pseudomonas Aeruginosa cbb3 Cytochrome Oxidases." Molecular Microbiology 51 (4): 1193–1203.

Cosseau, Céline, and Jacques Batut. 2004. "Genomics of the ccoNOQP-Encoded cbb3 Oxidase Complex in Bacteria." Archives of Microbiology 181 (2): 89–96.

Cowley, Elise S., Sebastian H. Kopf, Alejandro LaRiviere, Wiebke Ziebis, and Dianne K. Newman. 2015. "Pediatric Cystic Fibrosis Sputum Can Be Chemically Dynamic, Anoxic, and Extremely Reduced Due to Hydrogen Sulfide Formation." mBio 6 (4): e00767.

Davidson, E., T. Ohnishi, M. Tokito, and F. Daldal. 1992. "Rhodobacter Capsulatus Mutants Lacking the Rieske FeS Protein Form a Stable Cytochrome bc1 Subcomplex with an Intact Quinone Reduction Site." Biochemistry 31 (13): 3351–58.

De Baets, Frans, Petra Schelstraete, Sabine Van Daele, Filomeen Haerynck, and Mario Vaneechoutte. 2007. "Achromobacter Xylosoxidans in Cystic Fibrosis: Prevalence and Clinical Relevance." Journal of Cystic Fibrosis: Official Journal of the European Cystic Fibrosis Society 6 (1): 75–78.

Dehio, C., and M. Meyer. 1997. "Maintenance of Broad-Host-Range Incompatibility Group P and Group Q Plasmids and Transposition of Tn5 in Bartonella Henselae Following Conjugal Plasmid Transfer from Escherichia Coli." Journal of Bacteriology 179 (2): 538–40.

Dietrich, Lars E. P., Chinweike Okegbe, Alexa Price-Whelan, Hassan Sakhtah, Ryan C. Hunter, and Dianne K. Newman. 2013. "Bacterial Community Morphogenesis Is Intimately Linked to the Intracellular Redox State." Journal of Bacteriology 195 (7): 1371–80.

Dietrich, Lars E. P., Alexa Price-Whelan, Ashley Petersen, Marvin Whiteley, and Dianne K. Newman. 2006. "The Phenazine Pyocyanin Is a Terminal Signalling Factor in the Quorum Sensing Network of Pseudomonas Aeruginosa." Molecular Microbiology 61 (5): 1308–21.

Dietrich, Lars E. P., Tracy K. Teal, Alexa Price-Whelan, and Dianne K. Newman. 2008. "Redox-Active Antibiotics Control Gene Expression and Community Behavior in Divergent Bacteria." Science 321 (5893): 1203–6.

Dietrich, Lars E. P., Michael M. Tice, and Dianne K. Newman. 2006. "The Co-Evolution of Life and Earth." Current Biology: CB 16 (11): R395–400.

Ducluzeau, Anne-Lise, Soufian Ouchane, and Wolfgang Nitschke. 2008. "The cbb3 Oxidases Are an Ancient Innovation of the Domain Bacteria." Molecular Biology and Evolution 25 (6): 1158–66.

Edwards, Sarah, and Birthe V. Kjellerup. 2012. "Exploring the Applications of Invertebrate Host-Pathogen Models for in Vivo Biofilm Infections." FEMS Immunology and Medical Microbiology 65 (2): 205–14.

Eschbach, Martin, Kerstin Schreiber, Katharina Trunk, Jan Buer, Dieter Jahn, and Max Schobert. 2004. "Long-Term Anaerobic Survival of the Opportunistic Pathogen Pseudomonas Aeruginosa via Pyruvate Fermentation." Journal of Bacteriology 186 (14): 4596–4604.

Falkowski, Paul G. 2006. "Evolution. Tracing Oxygen's Imprint on Earth's Metabolic Evolution." Science 311 (5768): 1724–25.

Firmida, M. C., R. H. V. Pereira, E. A. S. R. Silva, E. A. Marques, and A. J. Lopes. 2016. "Clinical Impact of Achromobacter Xylosoxidans Colonization/infection in Patients with Cystic Fibrosis." Brazilian Journal of Medical and Biological Research = Revista Brasileira de Pesquisas Medicas E Biologicas / Sociedade Brasileira de Biofisica ... [et Al.] 49 (4): e5097.

Friedman, Lisa, and Roberto Kolter. 2004. "Genes Involved in Matrix Formation in Pseudomonas Aeruginosa PA14 Biofilms." Molecular Microbiology 51 (3): 675–90.

Gier, J. W. de, M. Schepper, W. N. Reijnders, S. J. van Dyck, D. J. Slotboom, A. Warne, M. Saraste, et al. 1996. "Structural and Functional Analysis of aa3-Type and cbb3-Type

Cytochrome c Oxidases of Paracoccus Denitrificans Reveals Significant Differences in Proton-Pump Design." Molecular Microbiology 20 (6): 1247–60.

Glasser, Nathaniel R., Suzanne E. Kern, and Dianne K. Newman. 2014. "Phenazine Redox Cycling Enhances Anaerobic Survival in Pseudomonas Aeruginosa by Facilitating Generation of ATP and a Proton-Motive Force." Molecular Microbiology 92 (2). Wiley Online Library: 399–412.

Glasser, Nathaniel R., Benjamin X. Wang, Julie A. Hoy, and Dianne K. Newman. 2017. "The Pyruvate and α-Ketoglutarate Dehydrogenase Complexes of Pseudomonas Aeruginosa Catalyze Pyocyanin and Phenazine-1-Carboxylic Acid Reduction via the Subunit Dihydrolipoamide Dehydrogenase." The Journal of Biological Chemistry 292 (13): 5593–5607.

Hirai, Takehiro, Tatsuya Osamura, Masaharu Ishii, and Hiroyuki Arai. 2016. "Expression of Multiple cbb3 Cytochrome c Oxidase Isoforms by Combinations of Multiple Isosubunits in Pseudomonas Aeruginosa." Proceedings of the National Academy of Sciences of the United States of America, October. doi:10.1073/pnas.1613308113.

Hoang, T. T., R. R. Karkhoff-Schweizer, A. J. Kutchma, and H. P. Schweizer. 1998. "A Broad-Host-Range Flp-FRT Recombination System for Site-Specific Excision of Chromosomally-Located DNA Sequences: Application for Isolation of Unmarked Pseudomonas Aeruginosa Mutants." Gene 212 (1): 77–86.

Huerta-Cepas, Jaime, Damian Szklarczyk, Kristoffer Forslund, Helen Cook, Davide Heller, Mathias C. Walter, Thomas Rattei, et al. 2016. "eggNOG 4.5: A Hierarchical Orthology Framework with Improved Functional Annotations for Eukaryotic, Prokaryotic and Viral Sequences." Nucleic Acids Research 44 (D1): D286–93.

Jennings, Laura K., Kelly M. Storek, Hannah E. Ledvina, Charlène Coulon, Lindsey S. Marmont, Irina Sadovskaya, Patrick R. Secor, et al. 2015. "Pel Is a Cationic Exopolysaccharide That Cross-Links Extracellular DNA in the Pseudomonas Aeruginosa Biofilm Matrix." Proceedings of the National Academy of Sciences of the United States of America 112 (36): 11353–58.

Jo, Jeanyoung, Alexa Price-Whelan, and Lars E. P. Dietrich. 2014. "An Aerobic Exercise: Defining the Roles of Pseudomonas Aeruginosa Terminal Oxidases." Journal of Bacteriology 196 (24): 4203–5.

Kawakami, Takuro, Miho Kuroki, Masaharu Ishii, Yasuo Igarashi, and Hiroyuki Arai. 2010. "Differential Expression of Multiple Terminal Oxidases for Aerobic Respiration in Pseudomonas Aeruginosa." Environmental Microbiology 12 (6): 1399–1412.

Kearse, Matthew, Richard Moir, Amy Wilson, Steven Stones-Havas, Matthew Cheung, Shane Sturrock, Simon Buxton, et al. 2012. "Geneious Basic: An Integrated and Extendable Desktop Software Platform for the Organization and Analysis of Sequence Data." Bioinformatics 28 (12): 1647–49.

Kempes, Christopher P., Chinweike Okegbe, Zwoisaint Mears-Clarke, Michael J. Follows, and Lars E. P. Dietrich. 2014. "Morphological Optimization for Access to Dual Oxidants in Biofilms." Proceedings of the National Academy of Sciences of the United States of America 111 (1): 208–13.

King, T. E. 1963. "Reconstitution f Respiratory Chain Enzyme Systems. Xii. Some Observations On The Reconstitution Of The Succinate Oxidase System From Heart Muscle." The Journal of Biological Chemistry 238 (December): 4037–51.

Kirschvink, Joseph L., and Robert E. Kopp. 2008. "Palaeoproterozoic Ice Houses and the Evolution of Oxygen-Mediating Enzymes: The Case for a Late Origin of Photosystem II." Philosophical Transactions of the Royal Society of London. Series B, Biological Sciences 363 (1504): 2755–65.

Knoll, Andrew H., and Erik A. Sperling. 2014. "Oxygen and Animals in Earth History." Proceedings of the National Academy of Sciences of the United States of America 111 (11): 3907–8.

Lambertsen, Lotte, Claus Sternberg, and Søren Molin. 2004. "Mini-Tn7 Transposons for Site-Specific Tagging of Bacteria with Fluorescent Proteins." Environmental Microbiology 6 (7): 726–32.

Liberati, Nicole T., Jonathan M. Urbach, Sachiko Miyata, Daniel G. Lee, Eliana Drenkard, Gang Wu, Jacinto Villanueva, Tao Wei, and Frederick M. Ausubel. 2006. "An Ordered, Nonredundant Library of Pseudomonas Aeruginosa Strain PA14 Transposon Insertion Mutants." Proceedings of the National Academy of Sciences of the United States of America 103 (8): 2833–38.

Morris, Rachel L., and Thomas M. Schmidt. 2013. "Shallow Breathing: Bacterial Life at Low O(2)." Nature Reviews. Microbiology 11 (3): 205–12.

Nachlas, M. M., S. I. Margulies, and A. M. Seligman. 1960. "A Colorimetric Method for the Estimation of Succinic Dehydrogenase Activity." The Journal of Biological Chemistry 235 (February): 499–503.

Newman, D. K. 2008. "From Iron Oxides to Infections." Geobiology 6 (3): 196–200.

Okegbe, Chinweike, Blanche L. Fields, Stephanie J. Cole, Christopher Beierschmitt, Chase J. Morgan, Alexa Price-Whelan, Richard C. Stewart, Vincent T. Lee, and Lars E. P. Dietrich. 2017. "Electron-Shuttling Antibiotics Structure Bacterial Communities by Modulating Cellular Levels of c-Di-GMP." Proceedings of the National Academy of Sciences of the United States of America 114 (26): E5236–45.

Okegbe, Chinweike, Alexa Price-Whelan, and Lars E. P. Dietrich. 2014. "Redox-Driven Regulation of Microbial Community Morphogenesis." Current Opinion in Microbiology 18 (April): 39–45.

Pitcher, Robert S., and Nicholas J. Watmough. 2004. "The Bacterial Cytochrome cbb3 Oxidases." Biochimica et Biophysica Acta 1655 (1-3): 388–99.

Powell, Jennifer R., and Frederick M. Ausubel. 2008. "Models of Caenorhabditis Elegans Infection by Bacterial and Fungal Pathogens." Methods in Molecular Biology 415: 403–27.

Preisig, O., R. Zufferey, L. Thöny-Meyer, C. A. Appleby, and H. Hennecke. 1996. "A High-Affinity cbb3-Type Cytochrome Oxidase Terminates the Symbiosis-Specific Respiratory Chain of Bradyrhizobium Japonicum." Journal of Bacteriology 178 (6): 1532–38.

Price-Whelan, Alexa, Lars E. P. Dietrich, and Dianne K. Newman. 2006. "Rethinking 'Secondary' Metabolism: Physiological Roles for Phenazine Antibiotics." Nature Chemical Biology 2 (2): 71–78.

Rahme, L. G., E. J. Stevens, S. F. Wolfort, J. Shao, R. G. Tompkins, and F. M. Ausubel. 1995. "Common Virulence Factors for Bacterial Pathogenicity in Plants and Animals." Science 268 (5219): 1899–1902.

Ray, A., and H. D. Williams. 1997. "The Effects of Mutation of the Anr Gene on the Aerobic Respiratory Chain of Pseudomonas Aeruginosa." FEMS Microbiology Letters 156 (2): 227–32.

Recinos, David A., Matthew D. Sekedat, Adriana Hernandez, Taylor Sitarik Cohen, Hassan Sakhtah, Alice S. Prince, Alexa Price-Whelan, and Lars E. P. Dietrich. 2012. "Redundant Phenazine Operons in Pseudomonas Aeruginosa Exhibit Environment-Dependent Expression

and Differential Roles in Pathogenicity." Proceedings of the National Academy of Sciences of the United States of America 109 (47): 19420–25.

Rich, P. R., L. A. Mischis, S. Purton, and J. T. Wiskich. 2001. "The Sites of Interaction of Triphenyltetrazolium Chloride with Mitochondrial Respiratory Chains." FEMS Microbiology Letters 202 (2): 181–87.

Rybtke, Morten, Louise Dahl Hultqvist, Michael Givskov, and Tim Tolker-Nielsen. 2015. "Pseudomonas Aeruginosa Biofilm Infections: Community Structure, Antimicrobial Tolerance and Immune Response." Journal of Molecular Biology 427 (23): 3628–45.

Saiman, L., Y. Chen, S. Tabibi, P. San Gabriel, J. Zhou, Z. Liu, L. Lai, and S. Whittier. 2001. "Identification and Antimicrobial Susceptibility of Alcaligenes Xylosoxidans Isolated from Patients with Cystic Fibrosis." Journal of Clinical Microbiology 39 (11): 3942–45.

Sakhtah, Hassan, Leslie Koyama, Yihan Zhang, Diana K. Morales, Blanche L. Fields, Alexa Price-Whelan, Deborah A. Hogan, Kenneth Shepard, and Lars E. P. Dietrich. 2016. "The Pseudomonas Aeruginosa Efflux Pump MexGHI-OpmD Transports a Natural Phenazine That Controls Gene Expression and Biofilm Development." Proceedings of the National Academy of Sciences of the United States of America 113 (25): E3538–47.

Schindelin, Johannes, Ignacio Arganda-Carreras, Erwin Frise, Verena Kaynig, Mark Longair, Tobias Pietzsch, Stephan Preibisch, et al. 2012. "Fiji: An Open-Source Platform for Biological-Image Analysis." Nature Methods 9 (7): 676–82.

Schrödinger, LLC. 2015. "The PyMOL Molecular Graphics System, Version 1.8."

Shanks, Robert M. Q., Nicky C. Caiazza, Shannon M. Hinsa, Christine M. Toutain, and George A. O'Toole. 2006. "Saccharomyces Cerevisiae-Based Molecular Tool Kit for Manipulation of Genes from Gram-Negative Bacteria." Applied and Environmental Microbiology 72 (7). Am Soc Microbiol: 5027–36.

Simon, R., U. Priefer, and A. Pühler. 1983. "A Broad Host Range Mobilization System for In Vivo Genetic Engineering: Transposon Mutagenesis in Gram Negative Bacteria." Nature Biotechnology 1 (9). Nature Publishing Group: 784–91.

Tan, M. W., S. Mahajan-Miklos, and F. M. Ausubel. 1999. "Killing of Caenorhabditis Elegans by Pseudomonas Aeruginosa Used to Model Mammalian Bacterial Pathogenesis." Proceedings of the National Academy of Sciences of the United States of America 96 (2): 715–20.

Tolker-Nielsen, Tim. 2014. "Pseudomonas Aeruginosa Biofilm Infections: From Molecular Biofilm Biology to New Treatment Possibilities." APMIS. Supplementum, no. 138 (December): 1–51.

Way, S. S., S. Sallustio, R. S. Magliozzo, and M. B. Goldberg. 1999. "Impact of Either Elevated or Decreased Levels of Cytochrome Bd Expression on Shigella Flexneri Virulence." Journal of Bacteriology 181 (4): 1229–37.

Weingarten, Rebecca A., Jesse L. Grimes, and Jonathan W. Olson. 2008. "Role of Campylobacter Jejuni Respiratory Oxidases and Reductases in Host Colonization." Applied and Environmental Microbiology 74 (5): 1367–75.

Werner, Erin, Frank Roe, Amandine Bugnicourt, Michael J. Franklin, Arne Heydorn, Søren Molin, Betsey Pitts, and Philip S. Stewart. 2004. "Stratified Growth in Pseudomonas Aeruginosa Biofilms." Applied and Environmental Microbiology 70 (10): 6188–96.

Williams, Huw D., James E. A. Zlosnik, and Ben Ryall. 2007. "Oxygen, Cyanide and Energy Generation in the Cystic Fibrosis Pathogen Pseudomonas Aeruginosa." Advances in Microbial Physiology 52: 1–71.

Winsor, Geoffrey L., Emma J. Griffiths, Raymond Lo, Bhavjinder K. Dhillon, Julie A. Shay, and Fiona S. L. Brinkman. 2016. "Enhanced Annotations and Features for Comparing Thousands of Pseudomonas Genomes in the Pseudomonas Genome Database." Nucleic Acids Research 44 (D1): D646–53.

Zufferey, Rachel, Oliver Preisig, Hauke Hennecke, and Linda Thöny-Meyer. 1996. "Assembly and Function of the Cytochrome Cbb Oxidase Subunits in Bradyrhizobium Japonicum." The Journal of Biological Chemistry 271 (15): 9114–19.

Example 2 Phenazine production promotes antibiotic tolerance and metabolic heterogeneity in *Pseudomonas aeruginosa* biofilms

Antibiotic efficacy can be antagonized by bioactive metabolites and other drugs present at infection sites. *Pseudomonas aeruginosa*, a common cause of biofilm-based infections, releases metabolites called phenazines that accept electrons to support cellular redox balancing. Here, we find that phenazines promote tolerance to clinically relevant antibiotics, such as ciprofloxacin, in *P. aeruginosa* biofilms and that this effect depends on the carbon source provided for growth. We couple stable isotope labeling with stimulated Raman scattering

microscopy to visualize biofilm metabolic activity *in situ*. This approach shows that phenazines promote metabolism in microaerobic biofilm regions and influence metabolic responses to ciprofloxacin treatment. Consistent with roles of specific respiratory complexes in supporting phenazine utilization in biofilms, phenazine-dependent survival on ciprofloxacin is diminished in mutants lacking these enzymes. Our work introduces a technique for the chemical imaging of biosynthetic activity in biofilms and highlights complex interactions between bacterial products, their effects on biofilm metabolism, and the antibiotics we use to treat infections.

High-throughput screens of drug-drug combinations have revealed that synergistic, antagonistic or suppressive interactions arise frequently[1–3]. Small molecules produced by bacteria similarly have the potential to influence bacterial susceptibility to antibiotic treatment. These compounds, commonly released during the stationary phase of growth in liquid cultures, during growth in biofilms, and during infection, can impact the physiology of their bacterial producers as well as other microbes or eukaryotic hosts, in line with their numerous functions such as nutrient acquisition, signaling or inhibition of competitors[4–6]. One of the few well-described examples of a small molecule metabolite that alters antibiotic efficacy is that of indole, a signaling molecule released by *Escherichia coli* and other bacteria[7,8]. Indole antagonizes the effect of antibiotic treatment by inducing expression of efflux pumps and oxidative stress responses.

Pseudomonas aeruginosa produces redox-active pigments called phenazines that affect gene expression, metabolic flux, and redox balancing in their producers[9,10] and that have the potential to alter antibiotic susceptibility. *P. aeruginosa* is a major cause of hospital-acquired infections and chronic lung infections in patients with the inherited disease cystic fibrosis. In addition to phenazine production, a salient feature of *P. aeruginosa* infections is the formation of biofilms, densely packed communities with limited oxygen at depth. *P. aeruginosa* has few metabolic strategies to support redox homeostasis under anoxic conditions (including the use of nitrate[11] or, to a limited degree, arginine[12] or pyruvate[13] fermentation). Analyses of biofilm growth and gene expression have indeed indicated that denitrification and pyruvate fermentation occur in biofilms grown under an oxic atmosphere[10,14,15] and that components of these pathways are not uniformly expressed over biofilm depth. Furthermore, as endogenous phenazines constitute an alternate electron acceptor[16–18], it has also been proposed that they support metabolic activity in hypoxic biofilm subregions[16,19,20]. Consistent with this model,

microelectrode measurements of intact biofilms show that the extracellular phenazine pool becomes more reduced at depth[21], suggesting that cells in the oxygen limited biofilm base carry out phenazine reduction. Studies of metabolic mutants have also implicated *P. aeruginosa*'s *cbb*3-type terminal oxidases Cco1 and Cco2, important components of the respiratory chain, in this activity[21]. Collectively, these results provide indirect evidence that metabolism is qualitatively heterogeneous over biofilm depth.

Metabolic heterogeneity in biofilms could equate to differences in antibiotic susceptibility and impede treatment of biofilm-based infections. Here, we investigate the effect of *P. aeruginosa* phenazine production on the survival of cells in biofilms that have been exposed to antibiotics. By combining stable isotope labeling and stimulated Raman scattering (SRS) microscopy, we develop a chemical imaging technique to visualize biofilm metabolic activity *in situ*. We use this technique to assess the influence of phenazine synthesis and antibiotic treatment on metabolism across biofilm depth. Finally, we use metabolic mutants to test whether specific phenazine-fostered pathways contribute to survival during antibiotic exposure. Our results underscore the relevance of endogenous bacterial products to community behavior and potential therapeutic approaches.

Results

Phenazine synthesis aids survival in antibiotic-exposed biofilms. To test the effect of phenazine production on antibiotic treatment, we chose to work with *P. aeruginosa* PA14 colony biofilms grown on a chemically-defined medium with glucose as the sole carbon source. Under these conditions, wild-type colonies produced phenazine-1-carboxylic acid (PCA) and phenazine-1-carboxamide (PCN; **Figures 7A, 7B**), visible as yellow coloration, while the methylated phenazines commonly associated with *P. aeruginosa* cultures and infections were not detectable (WT; **Figures 11A, 11B**). For the following experiments, we quantified the effect of these endogenously produced phenazines on metabolism and antibiotic efficacy by comparing WT and a strain that completely lacks phenazine production (Δ*phz*)[22].

Pre-grown colony biofilms were exposed for 24 hours to antibiotics from different classes and then collected, homogenized, and plated for colony-forming units (CFUs) (**Figure 7C**). We use herein the terms "survival" and "tolerance" to describe the formation of CFUs by *P. aeruginosa* cells from such antibiotic-treated biofilms. We observed broad antagonistic effects: phenazines diminished killing by the aminoglycoside tobramycin, the beta-lactam carbenicillin

(**Figures 12A, 12B**), and the fluoroquinolone ciprofloxacin (**Figure 7D**). The polymyxin colistin was the only antibiotic for which phenazines acted synergistically (**Figure 12C**), i.e. increased susceptibility. Notably, the minimum inhibitory concentration (MIC) determined in shaken liquid cultures did not differ between WT and Δ*phz* for any of the antibiotics (**Figure 12D**), nor was there any significant difference in CFU counts between strains for untreated biofilms (**Figure 13**). For further experiments, we focused on the clinically relevant antibiotic ciprofloxacin, because it was the most effective at killing biofilm cells and because it was the antibiotic for which phenazines had the strongest antagonistic effect. Protection by phenazines was not significant when stationary-phase liquid cultures were subjected to ciprofloxacin treatment (**Figure 14**), and though the addition of pure phenazines provided some protection in liquid culture, it was only detectable in a limited range (**Figure 15**). Together, these results show that phenazines antagonize the effects of ciprofloxacin on cells grown in colony biofilms; i.e., phenazine exposure allows more cells from antibiotic-treated biofilms to survive treatment and subsequently form CFUs when plated on fresh medium. We use the term antagonistic to indicate that phenazine production counteracts the killing efficiencies of antibiotics applied to biofilms exogenously. We note that this definition of antagonism is not in line with classic definitions from the clinical drug-drug interaction field[23], which rely on conditions not directly applicable to our biofilm system (e.g. MIC testing in liquid culture, where the protective effect of phenazines is diminished). The effect of phenazines on ciprofloxacin tolerance is biofilm-specific, as it was low or undetectable in liquid-culture experiments.

Protection from antibiotics is linked to metabolism. Phenazines have various effects on *P. aeruginosa* biofilm physiology, some of which could affect survival during exposure to antibiotics (**Figure 8A**): (1) they inhibit production of matrix, the exopolysaccharide scaffold that can support biofilm structure formation[24]; (2) they induce expression of efflux pumps[22]; and (3) they affect flux through central metabolism and balance the intracellular redox state[9,10]. To assess whether matrix or efflux pump production contribute to the antagonistic effect of phenazines on ciprofloxacin, we measured the in-biofilm survival of mutant strains after antibiotic exposure. To test the contribution of matrix production, we used a strain background lacking genes for production of the exopolysaccharide Pel, which is the main polysaccharide component of the biofilm matrix in PA14 (Δ*pel*)[25,26]. To test the contribution of efflux pumps, we used a strain lacking the operons *mexGHI-opmD*, *mexPQ-opmE,* and *mexVW* (Δ*mex*).

mexGHI-opmD and *mexPQ-opmE* encode RND efflux pumps that are upregulated by phenazines[22], while *mexVW* encodes the closest homolog to *mexHI*[27]. We found that phenazine-mediated ciprofloxacin tolerance was maintained in both of these strain backgrounds (**Figure 8B**), indicating a limited effect of expression of efflux pumps or matrix production. However, when biofilms were grown on succinate, a carbon source that enters central metabolism downstream of glucose, the protective effect of phenazines was abolished (**Figure 8B**). Influencing metabolism by altering the carbon source therefore has a stronger effect on phenazine-mediated tolerance than matrix production or efflux, suggesting that ciprofloxacin antagonism is linked to the effect of phenazines on metabolism and redox-balancing.

SRS imaging reveals phenazine-dependent metabolism in biofilms. The relationship between metabolic status and susceptibility to antibiotics has emerged as a prominent theme in recent literature, especially in the contexts of redox balancing and/or effects on the proton motive force[28–32]. For phenazines, the metabolic effects are potentially most significant in biofilm subzones where cells are limited by the electron acceptor oxygen and rely on phenazine reduction as an alternate redox-balancing strategy[10,21]. We thus used microsensors and microelectrodes to measure oxygen and extracellular redox potential, respectively, across depth in colony biofilms. As observed previously for biofilms grown on tryptone, we found that oxygen was depleted and became undetectable at a depth of ~70 μm (**Figure 9A**)[10,21]. We also found that cells across depth in these biofilms carry out reduction of phenazines[21] (**Figure 9A**, compare WT to Δ*phz*). Interestingly, in contrast to results obtained for tryptone-grown biofilms[21], we observed that growth on glucose supported reduction of phenazines across the whole biofilm, including the oxygen-rich region.

The links we observed between metabolic status and the antagonistic effect of phenazines suggested to us that metabolic heterogeneity, induced by resource gradients, between biofilm subpopulations may lead to differential susceptibility to antibiotic treatment. To characterize metabolic heterogeneity, previous biofilm studies have mostly relied on the expression of inducible or unstable fluorescent proteins as readouts for metabolic activity as a function of depth[33–35]. Here, we employed a technique that quantifies biosynthetic activity more globally as incorporation of stable isotopes into biomass (such as proteins, lipids, and carbohydrates). Stable isotopes like deuterium have previously been used to study metabolism by mass spectrometry and Raman spectroscopy in an unbiased and minimally perturbing way in single bacterial and

eukaryotic cells[36–38]. To directly examine metabolism in colony biofilms in a spatially resolved manner, we coupled stable isotope labeling with the emerging stimulated Raman scattering (SRS) microscopy[39,40]. SRS microscopy is a nonlinear optical imaging technique that provides a 108-fold enhancement in spontaneous Raman scattering signal and 103-106 times higher imaging speed than conventional Raman microscopy[41,42]. Using deuterium labeling, we can directly visualize the global metabolic activity as incorporated deuterium signal in colony biofilms with high sensitivity and specificity through SRS imaging of carbon-deuterium bonds (C-D) in the cell Raman170 silent window (**Figures 16A, 16B**). A deuterium incorporation level as low as 0.1% of total biomass can be detected[43,44]. Compared to other Raman imaging techniques, SRS has a well-preserved spectrum that is free from non-resonant background, has linear dependence on the analyte concentration for quantitative analysis and endows 3D-sectioning capability[42].

We confirmed the robustness of our method by separately examining deuterium incorporation from two different substrates, D7-glucose and D2O, via SRS imaging of live biofilms by optical sectioning (**Figure 9B and Figures 17A, 17B**). We also compared optical sectioning to an alternate method in which colonies are subjected to paraffin-embedding and thin sectioning[45] ("paraffin sectioning", **Figure 9B**) and SRS imaging is performed on the 10-μm thin sections. All techniques yielded qualitatively similar results, and although we observed considerable variation in the absolute deuterium signal between experiments, the relative distribution patterns were reproducible. Both WT and Δ*phz* colonies showed peaks of metabolic activity at a depth of ~30-40 μm, while activity in the bottom third of biofilms (>100 μm depth) was below detection in both strains (**Figure 9B and Figures 17A, 17B**), consistent with previous studies describing a dichotomy between metabolically active cells at the biofilm-air interface and inactive cells at the biofilm substrate interface[33–35,46]. Our results are unique, however, in that they show a complex distribution of metabolically active cells that is influenced by the presence of phenazines. Most notably, the metabolic patterns for WT and Δ*phz* biofilms differed in that WT samples displayed a more prominent peak of activity below 50 μm. Our microsensor measurements indicate that the second population visible in the WT is located in an oxygen-depleted region of the biofilm where extracellular phenazines are in the reduced state (**Figure 9A**). Finally, we also used SRS imaging and fluorescence microscopy to analyze biofilms containing a GFP-based reporter for the intracellular presence of oxidized phenazines[47], which showed maximal expression in the metabolically active, hypoxic region (**Figure 19D**). The co-

localization of reduced (**Figure 9A**) and oxidized phenazines indicates that cells are catalyzing their redox cycling. Phenazines have been shown to accept metabolic electrons and facilitate redox balancing, ATP production and survival in *P. aeruginosa*[9,18,48]; these physiological effects could contribute to the maintenance of phenazine-dependent metabolic activity we observe via SRS imaging of deuterium incorporation.

To further investigate the relationship between phenazine-dependent metabolism and ciprofloxacin efficacy, we exposed biofilms to ciprofloxacin in the presence of D2O labeling (**Figure 9C and Figure 18B**). The protocol used for deuterium labeling was modified to mirror the setup used for measuring ciprofloxacin tolerance (**Figure 7C**), i.e., colonies were transferred to the D2O-containing medium 12 h earlier than for the experiments shown in **Figure 9B** and incubated for 24 h after the transfer. In contrast to **Figure 9B**, the modified protocol yielded similar metabolic activity profiles for WT and Δ*phz* in the absence of ciprofloxacin (**Figure 9C**). We attribute this discrepancy to the longer incubation time with D2O, which allows both strains to reach steady-state deuterium incorporation and diminishes differences in metabolic turnover rates. Nevertheless, incubation on 1 μg/ml ciprofloxacin yielded different labeling patterns for WT and Δ*phz* colonies (**Figure 9C**). We were particularly intrigued by the emergence of distinct activity peaks in hypoxic biofilm regions for both WT and Δ*phz* colonies. While metabolic activity in the presence of phenazines is maximized at ~60 μm (in WT), in their absence activity peaks at ~90-μm (in Δ*phz*). The activity in Δ*phz* might arise from the enhancement of phenazine-independent redox-balancing mechanisms, such as high-affinity terminal oxidases that function at low oxygen concentrations, and/or fermentation[9] (see also **Figures 10A-10D**). We also note that the activity at 90-μm depth in Δ*phz* is susceptible to 10 μg/ml ciprofloxacin. Although we cannot definitively identify the biofilm subpopulations that are responsible for the differential tolerances of ciprofloxacin observed for WT and Δ*phz* biofilms (**Figure 7D**), our findings provide insight into how antibiotics influence metabolic activity *in situ*, and show that this relationship is affected by phenazines. Also, these data highlight that the largest changes in metabolic profiles induced by ciprofloxacin and phenazines are visible at depth, i.e. their effects are strongest in oxygen-limited biofilm regions.

Cco complexes support phenazine-mediated antibiotic resistance. Our observations suggest that phenazines support metabolic activity in oxygen-depleted biofilm subzones and that metabolic state influences the antibiotic susceptibility of cells in biofilms. To identify pathways

that could enhance the survival of biofilm cells during antibiotic exposure, we tested mutants representing unique branches of energy metabolism: Δ*cco1cco2* and Δ*ldhA*. Δ*cco1cco2* lacks the major terminal oxidases that catalyze O2 reduction (i.e., respiration) and that are required for phenazine reduction in *P. aeruginosa* biofilms[21], while Δ*ldhA* lacks an enzyme that converts pyruvate to lactate during survival by fermentation (**Figure 10A**). Measurement of survival for cells from Δ*cco1cco2* biofilms revealed that the *cbb*3-type terminal oxidases (i.e., Cco complexes) contribute to ciprofloxacin tolerance when phenazines are produced but not in the phenazine-null background (**Figure 10B**). Genetic complementation confirmed that altered survival of Δ*cco1cco2* biofilms can be attributed to the function of this locus (**Figure 19A**). Furthermore, the difference in survival between WT and Δ*cco1cco2* cannot be attributed to effects on phenazine production, because phenazine measurements for Δ*cco1cco2* biofilms yielded results that were similar to those for the WT (**Figure 19B**). When we applied our SRS imaging technique to Δ*cco1cco2* biofilms, we found that, in agreement with a phenazine-dependent role for Cco terminal oxidases, the Δ*cco1cco2* mutation led to complete loss of the lower peak of metabolic activity (50-90 μm biofilm depth) that is visible in WT biofilms (**Figure 20A, 20B**). Also, we detected expression of both terminal oxidases at the corresponding depth (**Figure 18A, 18B**). The peak of activity in the oxygen-depleted zone could thus be attributed to Cco-dependent phenazine reduction, indicating that this type of metabolism contributes to ciprofloxacin tolerance. These observations suggest that the previously described role of the *cbb*3-type terminal oxidases in reducing phenazines[21] supports a metabolic state that contributes to ciprofloxacin tolerance in biofilms.

We next tested the contribution of pyruvate fermentation to antibiotic resistance by measuring survival upon ciprofloxacin treatment for cells from Δ*ldhA* biofilms. Δ*ldhA* biofilms showed a modest decrease in resistance that was not statistically significant (**Figure 21**). However, as previous studies from our group have indicated that colonies grown on a complex medium containing tryptone and pyruvate carry out pyruvate fermentation[49], we sought to test whether this metabolism is operating in the biofilms grown on the defined, glucose-containing medium used here. We grew colonies of reporter strains that express *gfp* under the control of a promoter that is induced by lactate and examined thin sections by fluorescence microscopy. We observed GFP fluorescence throughout both biofilms but saw maximal levels in their microaerobic zone, particularly in the Δ*phz* background (**Figure 10C**). These results indicate that

electron acceptor-limited cells in biofilms route a portion of the glucose provided in the medium to lactate, possibly as a redox-balancing mechanism, and are consistent with previous observations of stationary-phase liquid cultures grown with glucose as the sole carbon source[9]. The more pronounced role of this metabolism in the Δ*phz* background could account for the relatively subtle effect of the Δ*ldhA* mutation that we observed in the WT (i.e. phenazine-producing) background. More broadly, it supports a model in which respiratory, rather than fermentative, metabolism is primarily responsible for the phenazine-dependent ciprofloxacin tolerance observed for cells in PA14 biofilms (**Figure 10C**).

Discussion

Previous literature describing metabolic heterogeneity in biofilms has generally differentiated between a metabolically active region at the oxygen-exposed interface and an inactive region at depth, where oxygen is limiting[33–35,46]. Based on our data from *P. aeruginosa* PA14 biofilms, the hypoxic region itself is metabolically diverse. In this zone (below 60-μm depth, where oxygen becomes undetectable), cells reduce pyruvate (**Figure 10C**) and express high affinity terminal oxidases in parallel[21] (**Figures 18A, 18B**). The presence of phenazines further expands the metabolic versatility in this region and leads to the formation of a distinct metabolically active subpopulation that we detected by stable isotope labeling and SRS imaging (**Figure 9B**).

Furthermore, our data suggest that metabolic versatility in redox balancing contributes to tolerance to ciprofloxacin. We propose that Cco-mediated phenazine reduction constitutes a redox-balancing pathway that confers a physiological condition of enhanced ciprofloxacin tolerance (**Figure 10D**), in line with previous reports highlighting links between respiration and antibiotic tolerance[28,30,32]. We note that, while the Δ*cco1cco2* mutant shows decreased antibiotic tolerance relative to the WT, it nevertheless shows survival levels that are higher than that of the Δ*phz* mutant, indicating that additional mechanisms contribute to the antagonistic effect of phenazines (**Figure 10B**). In the presence of phenazines, pyruvate fermentation is attenuated (**Figure 10C**), highlighting the role of phenazines in determining the metabolic organization of different subpopulations within a biofilm (**Figure 10D**). For aminoglycoside antibiotics like tobramycin, for which we also observed an antagonistic effect of phenazines, reduction of the proton motive force as a result of respiration has been shown to protect cells by diminishing drug

uptake[28], though currently the mechanistic basis whereby respiration supports ciprofloxacin tolerance is less clear.

Our results represent the first direct visualization of the heterogeneous distribution of metabolism inside biofilms by *in situ* SRS metabolic imaging of stable isotope incorporation. This technique can be generally applied for studying microbial metabolism and antibiotic treatment in complex settings with high spatial resolution and minimal perturbation, which is of great importance considering that biofilms are one of the main contributors to persistent and antibiotic-resistant infections[50]. In addition, our data suggest that treatment of *P. aeruginosa* biofilm infections is influenced by interactions of antibiotics and phenazines, compounds widely detectable in cystic fibrosis patients[51]. Our findings thus highlight the interactions between small molecule metabolites, primary metabolism, and antibiotics that can impact the survival of microbes that cause biofilm-based infections.

Methods

Bacterial strains and growth conditions

Strains and plasmids used are listed in **Tables 5 and 6**. Biological replicates were started from a single colony streaked out from a frozen glycerol stock on lysogeny broth agar (LB52; 1% tryptone, 1% NaCl, 0.5% yeast extract, 1% agar). Colonies were inoculated in 2 ml LB and grown for 12-13 h (37 °C, shaking at 250 rpm). Cells were subcultured for around 4 hours in 20 mM glucose MOPS minimal medium (50 mM 4-morpholinepropanesulfonic acid (pH 7.2), 43 mM NaCl, 93 mM NH4Cl, 2.2 mM KH2PO4, 1 µg/ml FeSO4·7H2O, 1 mM MgSO4·7H2O) in a 1:100 dilution until they reached exponential phase, with an optical density at 500 nm between 0.25-0.5. The terminal oxidase mutants (Δ*cco1cco2*) grew slower in subculture and were hence started with a dilution of 1:60. Optical density was adjusted to 0.25 with phosphate buffered saline (PBS), and cells were washed (centrifugation for 5 min, 6800x g) and resuspended in PBS for further use. For most experiments, 5 µl cells were consequently spotted on 1% agar solidified media and incubated at 25 °C and >90% humidity to form colony biofilms.

Strain construction

Strains containing markerless deletions in efflux pumps and Cco1 and Cco2 terminal oxidases were made by homologous recombination53. In brief, 1 kb flanking sequence was amplified from each side of the target gene (for primers, see **Table 7**) and inserted into the

plasmid pMQ30 using the yeast gap repair method in *Saccharomyces cerevisiae* InvSc154. The plasmid was moved into PA14 by biparental mating with *Escherichia coli* strain UQ950. Following initial selection on 100 μg/ml Gentamicin, markerless mutants resulting from double recombination were further selected on 10% sucrose LB plates without NaCl. Mutants were confirmed by PCR. Multiple deletions were generated stepwise by using strains already containing mutations as host for biparental mating. The *cco1cco2* complementation strain was made in a similar manner: the coding sequences of *cco1* and *cco2* were cloned, verified by sequencing, and inserted at the deletion site.

Use of high-pressure liquid chromatography to quantify phenazines

To extract phenazines from biofilms, colonies were grown on filter paper overlaid by a thin 1% agar layer as for the CFU count experiments. Phenazines were extracted from this filter paper as well as the agar below the colony (with a volume of 6 ml) by nutating the biofilm and the agar in 5 ml HPLC-grade methanol overnight at room temperature in the dark. Phenazines from liquid culture were directly quantified in the supernatant, from which cells had been removed by centrifugation (5 minutes, 16870x g). 300 μl of supernatant or phenazine extract were filtered through a 0.22 μm cellulose Spin-X column (Thermo Fisher Scientific 07-200-386) and 200 μl of the flow-through were loaded into an HPLC vial. Phenazines were quantified using reversed-phase high performance liquid chromatography (Agilent [Santa Clara, CA] 1100 HPLC System) with a biphenyl column (Kinetex 00F-4622-E0, 4.6 x 150 mm, 2.6 μm). A gradient method was used with (a) deionized water (containing 0.02% formic acid) and (b) methanol (containing 0.02% formic acid) by increasing (b) from 40% to 100% within 25 minutes with a flow rate of 0.4 mL min-1 at room temperature, followed by a hold at 100% methanol for 5 minutes. Absorption was quantified at 366 nm. The identity of phenazine peaks was verified by the absorption spectrum as well as comparison with the retention time of phenazine standards.

Quantification of ciprofloxacin tolerance in biofilms

To start biofilm colonies, 5 μl washed cell culture, prepared as explained above, was spotted onto 20 mM glucose MOPS minimal medium with 1% agar (40 ml in a 100 mm x 15 mm Petri dish). Cells were spotted onto a filter disk (diameter: 25 mm; pore size: 0.2 μm; GE Healthcare 110606) that was covered with a thin (~ 1 mm high) 1% agar layer to reduce effects of the filter on colony morphology. For survival tests on succinate, 20 mM sodium succinate hexahydrate was used. Biofilms were incubated at 25 °C with >90% humidity (Percival [Perry,

IA] CU-22L). Colony images were obtained with a flatbed scanner (Epson [Japan] E11000XL-GA). Colonies were incubated for around 3 days (64-65 hours) and then moved with the filter to a 35x10mm Petri dish (VWR 25373-041) containing 6 ml of 20 mM glucose MOPS minimal medium and 1% agar as well as antibiotics. Ciprofloxacin (Sigma-Aldrich 17850) was dissolved in acidified sterile water and stocks were stored at -20 °C. Carbenicillin disodium salt (Teknova, C2105) was dissolved in sterile water and stocks were stored at -20 °C. Tobramycin sulfate (VWR AAJ62995-03) and colistin sulfate (VWR 10791-860) were dissolved in sterile water and directly used. Biofilms were exposed to ciprofloxacin for 24h at 25 °C with >90% humidity and then homogenized in 1 ml PBS using a bead mill homogenizer (Omni [Kennesaw, GA] Bead Ruptor 12; at high setting for 99 seconds) and ceramic beads (Thermo Fisher 15 340 159, diameter of 1.4 mm). The cell suspension was serially diluted in PBS, plated onto 1% tryptone plates and incubated overnight at 37 °C before CFU counting.

Quantification of ciprofloxacin tolerance in stationary phase

To quantify survival of cells to ciprofloxacin in stationary phase liquid culture, cells were grown in 50 ml 20 mM glucose MOPS minimal medium in a 250-ml flask for 16 hours, shaking at 250 rpm at 37 °C. Cultures were started with a 1:50 dilution from the washed subculture prepared as described above. After 16h, when cells had reached stationary phase, ciprofloxacin was added to the cultures, and samples were taken for CFU counts at 0h and 4h to quantify survival over time. Cells were serially diluted in PBS and plated onto 1% tryptone plates for CFU counting. To quantify the effect of phenazines on ciprofloxacin-exposed liquid culture, cells were grown in a 96-well plate as explained above. Pyocyanin standard (dissolved in DSMO; Cayman Chemical 10009594, >98%) and PCA standard (dissolved in DMSO; Apexmol, 95%) were stored at -80 °C and added to the wells prior to inoculation.

Determination of minimal inhibitory concentration

To determine the minimal inhibitory concentration (MIC) cells were grown in a clear, flat bottom polystyrene 96-well plate (Greiner Bio-One 655001). Starting concentrations for testing the MIC were based on literature values46,55–57. MIC was determined as the lowest antibiotic concentration tested at which blanked optical density at 500 nm stayed below 0.1 and no clumps had formed after an incubation of 24h in 20 mM glucose MOPS minimal medium at 37 °C. Growth was quantified with a plate reader (Biotek Synergy H1, linear continuous shaking with a frequency of 731 cycles per minute). Cultures were started from a 1:100 dilution of the washed

subculture, prepared as explained above. Growth was quantified as optical density at 500 nm, read every 10 minutes for 24 hours.

Spontaneous Raman spectroscopy

Raman spectra of biofilm thin sections were collected on a confocal Raman microscope (Xplora, Horiba) using the LabSpec 6 software. The samples were excited by a 532 nm diode laser through a 50× air objective (Mplan N, 0.75 NA, Olympus) at room temperature. The power was 27 mW after the objective and the acquisition time for the spectra was 20 s.

SRS microscopy

An integrated laser source (picoEMERALD, Applied Physics & Electronics, Inc.) was used to produce both a Stokes beam (1064 nm, 6 ps, intensity modulated at 8 MHz) and a tunable pump beam (720 to 990 nm, 5–6 ps) at a 80 MHz repetition rate. The spectral resolution of SRS is FWHM = 6-7 cm-1. Two spatially and temporally overlapped beams with optimized near-IR throughput were coupled into an inverted multiphoton laser-scanning microscope (FV1200MPE, Olympus). Both beams were focused on the cell samples through a 25× water objective (XLPlan N, 1.05 N.A. MP, Olympus) and collected with a high N.A. oil condenser lens (1.4 N.A., Olympus) after the sample. By removing the Stokes beam with a high O.D. bandpass filter (890/220 CARS, Chroma Technology), the pump beam is detected with a large area Si photodiode (FDS1010, Thorlabs) reverse-biased by 64 DC voltage. The output current of the photodiode was electronically filtered (KR 2724, KR electronics), terminated with 50 Ω, and demodulated with a RF lock-in amplifier (SR844, Stanford Research Systems) to achieve near shot-noise-limited sensitivity. The stimulated Raman loss signal at each pixel was sent to the analog interface box (FV10-ANALOG, Olympus) of the microscope to generate the image. All images were acquired with 30 μs time constant at the lock-in amplifier and 100 μs pixel dwell time (~7 s per frame of 256 × 256 pixels). Measured after the objectives, 12 mW pump power and 40 mW Stokes power were used to image the protein CH3 2940 and off-resonance 2650 cm^{-1} channel. 24 mW pump beam and 120 mW Stokes beam were used to image the carbon deuterium 2165, 2175, and off-resonance 2000 cm^{-1} channels.

Stable isotope labeling

To image metabolic activity as incorporation of deuterium isotopes, 20 mM glucose MOPS minimal medium was amended with either 20 mM deuterated D7-glucose (Sigma Aldrich) or 50% deuterated water (Sigma Aldrich; 2 ml volume in a 35x10mm Petri dish). For pulse

experiments with deuterated water, biofilms were grown on unlabeled medium for 76h or, in the case of the antibiotic tests for 64h, followed by incubation on medium with 50% D2O for 12h or 24h, respectively. For optical sectioning, deuterated water in the media was removed by incubation on 1% agar with unlabeled H2O for 30 minutes prior to SRS imaging. Chase experiments were conducted by growing biofilms for three days on MOPS minimal medium containing 20 mM deuterated D7-glucose, which was then chased by incubation on 20 mM glucose MOPS minimal medium for 12h.

Preparation of biofilms for SRS imaging via optical sectioning

Colonies were grown on a 1.5% thin agar layer on top of a filter in media described above. After deuterium labeling, the colony was transferred onto a coverslip using the thin agar layer. Spacers (Sigma Aldrich) were used to create an imaging chamber with a microscopy glass slide on top of the spacer for SRS imaging of live biofilms.

Paraffin-embedded thin sectioning for imaging

Thin sectioning was performed similar to as previously described45. Colony biofilms were moved onto a two-layer agar plate using the thin (~ 1 mm high) 1.5% agar layer biofilms had grown on. The two-layer agar consisted of a bottom layer of 32 ml and a top layer of 8 ml of 1% agar in a 100 mm x 15 mm Petri dish. After transfer of the colony, the plate was covered with 8 ml of 1% agar. After polymerization of the agar, the embedded colony was cut out including the surrounding agar and pre-fixated at 4 °C in 50 mM L-lysine Hydrochloride and PBS, followed by fixation in 50 mM L-lysine Hydrochloride, PBS, and 4% paraformaldehyde, first for 4 hours at 4 °C and then at 37 °C for 24 hours in the dark. Dehydration, sectioning to 10 µm-thin sections, and rehydration were performed as described previously45. Sections were mounted in TRIS Buffered DAPI:Fluorogel (Thermo Fisher Scientific 50-246-93) or TRIS-Buffered Fluorogel without DAPI (Thermo Fisher Scientific 50-247-04) for correlative SRS and fluorescence imaging. Fluorescence imaging was performed using the Olympus FV1200 confocal microscope with standard laser excitation and bandpass filter set for each fluorescent reporter.

Oxygen and redox gradient measurements

Four-days old colony biofilms directly grown on 20 mM glucose MOPS minimal medium without filter were used for oxygen- and redox profiling as described previously[21].

Image analysis

For optical sections, images collected were imported into Fiji and deuterium and protein images from the same biofilm depth were manually aligned. Mean signal per height was exported as a csv file and further analyzed in R58. Data plots shown are based on protein-corrected deuterium signal.

For paraffin sections, signal profiles over height were assembled using a combination of Fiji59 and R58. Raw images were imported in Fiji and rotated such that the bottom of the biofilm was aligned to the bottom of the image. A mask of the biofilm section was created based on either fluorescence (for fluorescence images) or the protein channel (for protein and deuterium signal). In cases where no masks could be generated by thresholding, the mask was manually drawn around the biofilm section. Raw data from within this mask were exported as csv and further analyzed in R. In a custom-written R script, the biofilm section was aligned at the top interface of the biofilm and average signals per height were calculated. Images of paraffin sections show background subtracted-deuterium signal overlayed with background-subtracted protein channel (whereby we target the methyl group vibration in proteins with a frequency of 2940 cm-1) to visualize the outline of the biofilm section. For fluorescence images, the background was subtracted as the average auto-fluorescence signal measured in a promoterless reporter control.

Statistical analysis

Statistical analyses were conducted with R58. Levene's test for homogeneity of variance was carried about for data subjected to t tests.

Table 5. Bacterial and fungal strains used in this study.

Number	Strain	Description	Source
Pseudomonas aeruginosa PA14 strains			
	PA14 (WT)	Clinical isolate UCBPP-PA14 *Pseudomonas aeruginosa*	60
LD24	Δ*phz*	PA14 with deletions in *phzA1-G1* and *phzA2-G2* operons	61

LD2329	Δ*mexGHI-opmD* Δ*mexVW*Δ*mexPQ-opmE*	PA14 with deletions in PA14_09500-PA14_09540, PA14_56880 -PA14_56890 and PA14_18760-PA14_18790	This study
LD2330	Δ*phz*Δ*mexGHI-opmD* Δ*mexVW*Δ*mexPQ-opmE*	LD24 (Δ*phz*) with deletions in PA14_09500-PA14_09540, PA14_56880 -PA14_56890 and PA14_18760-PA14_18790	This study
LD82	Δ*pel*	PA14 with deletions in *pelB-G*	62
LD83	Δ*phz*Δ*pel*	PA14Δ*phz* with deletions in *pelB-G*	62
LD1933	Δ*cco1cco2*	PA14 with deletions in PA14_44340-PA14_44400	63
LD3182	Δ*cco1cco2*::*cco1cco2*	LD1933 (Δ*cco1cco2*) with *cco1cco2* complemented back into the site of deletion. Made by mating pLD3175 into LD1933.	This study
LD1938	Δ*phz*Δ*cco1cco2*	LD24 (Δ*phz*) with deletions in PA14_44340-PA14_44400	This study
LD2729	Δ*ldhA*	PA14 with deletion in PA14_52270	64
LD2820	MCS-gfp	PA14 with promoterless *gfp* expression reporter	63
LD2784	*cco1pr-gfp*	PA14 with promoter of *cco1* operon driving *gfp*-expression	63
LD2786	*cco2pr-gfp*	PA14 with promoter of *cco2* operon driving *gfp*-expression	63

LD2798	P*lldPDEpr-gfp*	PA14 with promoter of *lldP* operon driving *gfp*-expression	64
LD2799	Δ*phz*P*lldPDEpr-gfp*	PA14 with promoter of *lldP* operon driving *gfp*-expression in Δ*phz* background	64
LD36	*PA1/04/03p*-yfp	PA14 with constitutive tac promoter driving *yfp*-expression	65
LD808	P*mexG-gfp*	PA14 with mexG promoter driving gfp expression	This study
Escherichia coli			
LD44	UQ950	*E. coli* DH5 λpir strain for cloning. F^- Δ(*argF- lac*) 169φ80d*lacZ58*(ΔM15) *glnV44*(AS) *rfbD1 gyrA96*(NaI^R) *recA1 endA1 spoT thi-1 hsdR17 deoR* λpir^+	
LD661	BW29427	Donor strain for conjugation; *thrB1004 pro thi rpsL hsdS lacZ* ΔM15RP4-1360 Δ(*araBAD*)*567* Δ*dapA1314::*[*erm pir*(wt)]	
LD69	β2155	Helper strain. thrB1004 pro thi strA hsdsS lacZDM15 (F'lacZDM15 lacIq traΔ36 $proA^+$ $proB^+$) ΔdapA:: erm (Ermr)pir::RP4 [::kan (Kmr) from SM10]	66
LD2901	S17-1	Str^R, Tp^R, F^- RP4-2-Tc::Mu *aphA*::Tn7 *recA* λpir lysogen	67
Saccharomyces cerevisiae			
LD676	InvSc	*MATα/MATα leu2/leu2 trp1-289/trp1-289*	Invitrogen

		ura3-52/ura3-52 his3-Δ1/his3-Δ1	

Table 6. Plasmids used in this study.

Plasmid	Description	Source
pMQ30	Yeast-based allelic-exchange vector; *sacB*$^+$, CEN/ARSH, URA3$^+$, Gm^R	9
pLD2722	Gm^R, Tet^R flanked by Flp recombinase target (FRT) sites to resolve out resistance cassettes	4
pFLP2	Site-specific excision vector with cI857-controlled FLP recombinase encoding sequence, sacB$^+$, Amp^R	10
pLD2297	Δ3522 PCR fragment introduced into pMQ30 by gap repair cloning in yeast strain InvSc1.	This study
pLD2285	Δ*mexVW* PCR fragment introduced into pMQ30 by gap repair cloning in yeast strain InvSc1.	This study
pLD2273	Δ*mexAB-oprM* PCR fragment introduced into pMQ30 by gap repair cloning in yeast strain InvSc1.	This study
pLD1929	Δ*cco1cco2* PCR fragment introduced into pMQ30 by gap repair cloning in yeast strain InvSc1.	4
pLD3175	*cco1cco2* PCR fragments introduced into pMQ30 by gap repair cloning in yeast strain InvSc1.	This study
pLD1599	*mexG* promoter PCR fragment ligated into pYL122 using HindIII and EcoRI.	This study

5

Table 7. Primers used in this study.

Primers for plasmid pLD2297 (used to make Δ3522)	
LD1403	ccaggcaaattctgttttatcagaccgcttctgcgttctgaCCTACAACCAGGCCGATGC (SEQ ID No. 43)
LD1404	ggagaggtatcgtcggtagcGATAAGGGCCGCGACACCTA (SEQ ID No. 44)
LD1405	taggtgtcgcggcccttatcGCTACCGACGATACCTCTCC (SEQ ID No. 45)
LD1406	ggaattgtgagcggataacaatttcacacaggaaacagcAGCGTTCTTTCCACAATAGCC (SEQ ID No. 46)
Primers for plasmid pLD2285 (used to make Δ*mexVW*)	
LD1411	ccaggcaaattctgttttatcagaccgcttctgcgttctgaAACGACACTACCGATCCCG (SEQ ID No. 47)
LD1412	aggacgaacagggtgaagagCTGACGGATGGAGTAGAC (SEQ ID No. 48)
LD1413	gtctactccatccgtcagCTCTTCACCCTGTTCGTCCT (SEQ ID No. 49)
LD1414	ggaattgtgagcggataacaatttcacacaggaaacagctGCACTCTGGCTGTCGATCA (SEQ ID No. 50)
Primers for plasmid pLD2273 (used to make Δmex*AB-oprM*)	
LD1371	ccaggcaaattctgttttatcagaccgcttctgcgttctgCATCCCAGGAAGTCGAGCTG (SEQ ID No. 51)
LD1372	cacggtctgctggttccaTTCCAGGGTCACGATTCC (SEQ ID No. 52)
LD1373	ggaatcgtgaccctggaaTGGAACCAGCAGACCGTG (SEQ ID No. 53)
LD1374	ggaattgtgagcggataacaatttcacacaggaaacagctGATGCCCAGGGTTTCGACC (SEQ ID No. 54)
Primers for plasmid pLD1929 (used to make Δ*cco1cco2*)	
LD725	ccaggcaaattctgttttatcagaccgcttctgcgttctgatCCCCTCAGAGAAGTCAGTCG (SEQ ID No. 55)

LD1063	gttgcccaggtgttcctgtGGCGGACCACCTTGTAGTTA (SEQ ID No. 56)
LD949	ggaattgtgagcggataacaatttcacacaggaaacagctTGTAGTCGAGGGACTTCTTGC (SEQ ID No. 57)
LD1064	taactacaaggtggtccgccACAGGAACACCTGGGCAAC (SEQ ID No. 58)
Primers for plasmid pLD3175 (used to make Δ*cco1cco2*::*cco1cco2*)	
LD725	ccaggcaaattctgttttatcagaccgcttctgcgttctgatCCCCTCAGAGAAGTCAGTCG (SEQ ID No. 59)
LD2540	ACCACGGCATCCATTTCGGTCTTGCCTTTCAGCGAGTC (SEQ ID No. 60)
LD2541	GACTCGCTGAAAGGCAAGACCGAAATGGATGCCGTGGT (SEQ ID No. 61)
LD2542	TTTCGGGATCAGGTGGTAGAGCGAGCCGATGGAGATCAT (SEQ ID No. 62)
LD2543	ATGATCTCCATCGGCTCGCTCTACCACCTGATCCCGAAA (SEQ ID No. 63)
LD949	ggaattgtgagcggataacaatttcacacaggaaacagctTGTAGTCGAGGGACTTCTTGC (SEQ ID No. 64)
Primers for plasmid pLD1599 (used to make P*mexG-gfp*)	
LD2596	taccaagcttCTCGTGGCCAACCAGAATAG (SEQ ID No. 65)
LD2597	ttgcgaattcGTCGTTCCTTGTGCTGGTC (SEQ ID No. 66)

References

1. Yeh, P., Tschumi, A. I. & Kishony, R. Functional classification of drugs by properties of their pairwise interactions. *Nat. Genet.* **38**, 489–494 (2006).

2. Bollenbach, T. Antimicrobial interactions: mechanisms and implications for drug discovery and resistance evolution. *Curr. Opin. Microbiol.* **27**, 1–9 (2015).

3. Brochado, A. R. *et al.* Species-specific activity of antibacterial drug combinations. *Nature* (2018). doi:10.1038/s41586-018-0278-9

4. Martin, J. Organization and expression of genes involved in the biosynthesis of antibiotics and other secondary metabolites. *Annu. Rev. Microbiol.* **43**, 173–206 (1989).

5. Vining, L. C. Functions of secondary metabolites. *Annu. Rev. Microbiol.* **44**, 395–427 (1990).

6. Miller, M. B. & Bassler, B. L. Quorum sensing in bacteria. *Annu. Rev. Microbiol.* **55**, 165–199 (2001).

7. Lee, H. H., Molla, M. N., Cantor, C. R. & Collins, J. J. Bacterial charity work leads to population-wide resistance. *Nature* **467**, 82–85 (2010).

8. Lee, J.-H., Wood, T. K. & Lee, J. Roles of indole as an interspecies and interkingdom signaling molecule. *Trends Microbiol.* **23**, 707–718 (2015).

9. Price-Whelan, A., Dietrich, L. E. P. & Newman, D. K. Pyocyanin alters redox homeostasis and carbon flux through central metabolic pathways in *Pseudomonas aeruginosa* PA14. *J. Bacteriol.* **189**, 6372–6381 (2007).

10. Dietrich, L. E. P. *et al.* Bacterial community morphogenesis is intimately linked to the intracellular redox state. *J. Bacteriol.* **195**, 1371–1380 (2013).

11. Carlson, C. A. & Ingraham, J. L. Comparison of denitrification by *Pseudomonas stutzeri*, *Pseudomonas aeruginosa*, and *Paracoccus denitrificans*. *Appl. Environ. Microbiol.* **45**, 1247–1253 (1983).

12. Vander Wauven, C., Piérard, A., Kley-Raymann, M. & Haas, D. *Pseudomonas aeruginosa* mutants affected in anaerobic growth on arginine: evidence for a four gene cluster encoding the arginine deiminase pathway. *J. Bacteriol.* **160**, 928–934 (1984).

13. Eschbach, M. *et al.* Long-term anaerobic survival of the opportunistic pathogen *Pseudomonas aeruginosa* via pyruvate fermentation. *J. Bacteriol.* **186**, 4596–4604 (2004).

14. Lin, Y.-C. *et al.* Phenazines regulate Nap-dependent denitrification in *Pseudomonas aeruginosa* biofilms. *J. Bacteriol.* (2018). doi:10.1128/JB.00031-18

15. Lin, Y. C., Cornell, W. C., Price-Whelan, A. & Dietrich, L. E. P. The *Pseudomonas aeruginosa* complement of lactate dehydrogenases enables use of D-and L-lactate and metabolic crossfeeding. *bioRxiv* (2018).

16. Price-Whelan, A., Dietrich, L. E. P. & Newman, D. K. Rethinking 'secondary' metabolism: physiological roles for phenazine antibiotics. *Nat. Chem. Biol.* **2**, 71–78 (2006).

17. Wang, Y., Kern, S. E. & Newman, D. K. Endogenous Phenazine Antibiotics Promote Anaerobic Survival of *Pseudomonas aeruginosa* via Extracellular Electron Transfer. *J. Bacteriol.* **192**, 365–369 (2009).

18. Glasser, N. R., Kern, S. E. & Newman, D. K. Phenazine redox cycling enhances anaerobic survival in *Pseudomonas aeruginosa* by facilitating generation of ATP and a proton-motive force. *Mol. Microbiol.* **92**, 399–412 (2014).

19. Stewart, P. S. & Franklin, M. J. Physiological heterogeneity in biofilms. *Nat. Rev. Microbiol.* **6**, 199–210 (2008).

20. Dietrich, L. E. P. *et al.* Bacterial community morphogenesis is intimately linked to the intracellular redox state. *J. Bacteriol.* **195**, 1371–1380 (2013).

21. Jo, J., Cortez, K. L., Cornell, W. C., Price-Whelan, A. & Dietrich, L. E. An orphan cbb3-type cytochrome oxidase subunit supports *Pseudomonas aeruginosa* biofilm growth and virulence. *Elife* **6**, (2017).

22. Dietrich, L. E. P., Price-Whelan, A., Petersen, A., Whiteley, M. & Newman, D. K. The phenazine pyocyanin is a terminal signalling factor in the quorum sensing network of *Pseudomonas aeruginosa*. *Mol. Microbiol.* **61**, 1308–1321 (2006).

23. Odds, F. C. Synergy, antagonism, and what the chequerboard puts between them. *J. Antimicrob. Chemother.* **52**, 1 (2003).

24. Okegbe, C. *et al.* Electron-shuttling antibiotics structure bacterial communities by modulating cellular levels of c-di-GMP. *Proc. Natl. Acad. Sci. U. S. A.* **114**, E5236–E5245 (2017).

25. Friedman, L. & Kolter, R. Two genetic loci produce distinct carbohydrate-rich structural components of the *Pseudomonas aeruginosa* biofilm matrix. *J. Bacteriol.* **186**, 4457–4465 (2004).

26. Jennings, L. K. *et al.* Pel is a cationic exopolysaccharide that cross-links extracellular DNA in the *Pseudomonas aeruginosa* biofilm matrix. *Proceedings of the National Academy of Sciences* **112**, 11353–11358 (2015).

27. Li, Y. *et al.* A new member of the tripartite multidrug efflux pumps, MexVW-OprM, in *Pseudomonas aeruginosa*. *J. Antimicrob. Chemother.* **52**, 572–575 (2003).

28. Allison, K. R., Brynildsen, M. P. & Collins, J. J. Metabolite-enabled eradication of bacterial persisters by aminoglycosides. *Nature* **473**, 216–220 (2011).

29. Peng, B. *et al.* Exogenous alanine and/or glucose plus kanamycin kills antibiotic resistant bacteria. *Cell Metab.* **21**, 249–261 (2015).

30. Kim, J.-S. *et al.* Fumarate-mediated persistence of *Escherichia coli* against antibiotics. *Antimicrob. Agents Chemother.* **60**, 2232–2240 (2016).

31. Meylan, S. *et al.* Carbon sources tune antibiotic susceptibility in *Pseudomonas aeruginosa* via tricarboxylic acid cycle control. *Cell Chemical Biology* **24**, 195–206 (2017).

32. Gutierrez, A. *et al.* Understanding and sensitizing density-dependent persistence to quinolone antibiotics. *Mol. Cell* **68**, 1147–1154.e3 (2017).

33. Walters, M. C., Roe, F., Bugnicourt, A., Franklin, M. J. & Stewart, P. S. Contributions of antibiotic penetration, oxygen limitation, and low metabolic activity to tolerance of *Pseudomonas aeruginosa* biofilms to ciprofloxacin and tobramycin. *Antimicrob. Agents Chemother.* **47**, 317–323 (2003).

34. Pamp, S. J., Gjermansen, M., Johansen, H. K. & Tolker-Nielsen, T. Tolerance to the antimicrobial peptide colistin in *Pseudomonas aeruginosa* biofilms is linked to metabolically active cells, and depends on the pmr and mexAB-oprM genes. *Mol. Microbiol.* **68**, 223–240 (2008).

35. Williamson, K. S. *et al.* Heterogeneity in *Pseudomonas aeruginosa* biofilms includes expression of ribosome hibernation factors in the antibiotic-tolerant subpopulation and hypoxia-induced stress response in the metabolically active population. *J. Bacteriol.* **194**, 2062–2073 (2012).

36. Berry, D. *et al.* Tracking heavy water (D2O) incorporation for identifying and sorting active microbial cells. *Proceedings of the National Academy of Sciences* **112**, E194–E203 (2014).

37. Hong, W. *et al.* Antibiotic Susceptibility Determination within One Cell Cycle at Single-Bacterium Level by Stimulated Raman Metabolic Imaging. *Anal. Chem.* **90**, 3737–3743 (2018).

38. Tao, Y. *et al.* Metabolic-Activity-Based Assessment of Antimicrobial Effects by D2O-Labeled Single-Cell Raman Microspectroscopy. *Anal. Chem.* **89**, 4108–4115 (2017).

39. Freudiger, C. W. *et al.* Label-free biomedical imaging with high sensitivity by stimulated Raman scattering microscopy. *Science* **322**, 1857–1861 (2008).

40. Cheng, J.-X. & Xie, X. S. Vibrational spectroscopic imaging of living systems: An emerging platform for biology and medicine. *Science* **350**, aaa8870 (2015).

41. Wakisaka, Y. *et al.* Probing the metabolic heterogeneity of live *Euglena gracilis* with stimulated Raman scattering microscopy. *Nature Microbiology* 1–4 (2016).

42. Min, W., Freudiger, C. W., Lu, S. & Xie, X. S. Coherent nonlinear optical imaging: beyond fluorescence microscopy. *Annu. Rev. Phys. Chem.* **62**, 507–530 (2011).

43. Wei, L., Yu, Y., Shen, Y., Wang, M. C. & Min, W. Vibrational imaging of newly synthesized proteins in live cells by stimulated Raman scattering microscopy. *Proc. Natl. Acad. Sci. U. S. A.* **110**, 11226–11231 (2013).

44. Shi, L. *et al.* Optical imaging of metabolic dynamics in animals. *Nat. Commun.* **9**, 2995 (2018).

45. Cornell, W. C. *et al.* Paraffin embedding and thin sectioning of microbial colony biofilms for microscopic analysis. *JoVE (Journal of Visualized Experiments)* e57196–e57196 (2018).

46. Borriello, G. *et al.* Oxygen limitation contributes to antibiotic tolerance of *Pseudomonas aeruginosa* in biofilms. *Antimicrob. Agents Chemother.* **48**, 2659–2664 (2004).

47. Sakhtah, H. *et al.* The *Pseudomonas aeruginosa* efflux pump MexGHI-OpmD transports a natural phenazine that controls gene expression and biofilm development. *Proc. Natl. Acad. Sci. U. S. A.* **113**, E3538–47 (2016).

48. Wang, Y., Kern, S. E. & Newman, D. K. Endogenous phenazine antibiotics promote anaerobic survival of *Pseudomonas aeruginosa* via extracellular electron transfer. *J. Bacteriol.* **192**, 365–369 (2010).

49. Lin, Y.-C., Cornell, W. C., Jo, J., Price-Whelan, A. & Dietrich, L. E. P. The Pseudomonas aeruginosa Complement of Lactate Dehydrogenases Enables Use of d- and l-Lactate and Metabolic Cross-Feeding. *MBio* **9**, (2018).

50. Høiby, N., Bjarnsholt, T., Givskov, M., Molin, S. & Ciofu, O. Antibiotic resistance of bacterial biofilms. *Int. J. Antimicrob. Agents* **35**, 322–332 (2010).

51. Hunter, R. C. *et al.* Phenazine content in the cystic fibrosis respiratory tract negatively correlates with lung function and microbial complexity. *Am. J. Respir. Cell Mol. Biol.* **47**, 738–745 (2012).

52. Bertani, G. Lysogeny at mid-twentieth century: P1, P2, and other experimental systems. *J. Bacteriol.* **186**, 595–600 (2004).

53. Recinos, D. A. *et al.* Redundant phenazine operons in *Pseudomonas aeruginosa* exhibit environment-dependent expression and differential roles in pathogenicity. *Proceedings of the National Academy of Sciences* **109**, 19420–19425 (2012).

54. Shanks, R. M. Q., Caiazza, N. C., Hinsa, S. M., Toutain, C. M. & O'Toole, G. A. *Saccharomyces cerevisiae*-based molecular tool kit for manipulation of genes from gram-negative bacteria. *Appl. Environ. Microbiol.* **72**, 5027–5036 (2006).

55. Herrmann, G. *et al.* Colistin-tobramycin combinations are superior to monotherapy concerning the killing of biofilm *Pseudomonas aeruginosa*. *J. Infect. Dis.* **202**, 1585–1592 (2010).

56. Llanes, C. *et al.* Role of the MexEF-OprN efflux system in low-level resistance of *Pseudomonas aeruginosa* to ciprofloxacin. *Antimicrob. Agents Chemother.* **55**, 5676–5684 (2011).

57. Tseng, B. S. *et al.* The extracellular matrix protects *Pseudomonas aeruginosa* biofilms by limiting the penetration of tobramycin. *Environ. Microbiol.* **59**, (2013).

58. Team, R. C. & Others. R: A language and environment for statistical computing. (2013).

59. Schindelin, J. *et al.* Fiji: an open-source platform for biological-image analysis. *Nat. Methods* **9**, 676–682 (2012).

60. Rahme, L. G., Stevens, E. J., Wolfort, S. F., Shao, J., Tompkins, R. G. & Ausubel, F. M. Common virulence factors for bacterial pathogenicity in plants and animals. *Science* **268** (5219), 1899–1902 (1995).

61. Dietrich, L. E. P., Price-Whelan, A., Petersen, A., Whiteley, M. & Newman, D. K. The phenazine pyocyanin is a terminal signalling factor in the quorum sensing network of Pseudomonas aeruginosa. *Mol. Microbiol.* **61** (5), 1308–1321 (2006).

62. Dietrich, L. E. P., Okegbe, C., Price-Whelan, A., Sakhtah, H., Hunter, R. C. & Newman, D. K. Bacterial Community Morphogenesis Is Intimately Linked to the Intracellular Redox State. *J. Bacteriol.* **195** (7), 1371–1380 (2013).

63. Jo, J., Cortez, K. L., Cornell, W. C., Price-Whelan, A. & Dietrich, L. E. An orphan cbb3-type cytochrome oxidase subunit supports Pseudomonas aeruginosa biofilm growth and virulence. *Elife* **6**, doi: 10.7554/eLife.30205 (2017).

64. Lin, Y. C., Cornell, W. C., Price-Whelan, A. & Dietrich, L. E. P. The Pseudomonas aeruginosa complement of lactate dehydrogenases enables use of D-and L-lactate and metabolic crossfeeding. *mBio* . **9** (5) e00961-18; doi:10.1128/mBio.00961-18 (2018).

65. Ramos, I., Dietrich, L. E. P., Price-Whelan, A. & Newman, D. K. Phenazines affect biofilm formation by Pseudomonas aeruginosa in similar ways at various scales. *Res. Microbiol.* **161** (3), 187–191 (2010).

66. Dehio, C. & Meyer, M. Maintenance of broad-host-range incompatibility group P and group Q plasmids and transposition of Tn5 in Bartonella henselae following conjugal plasmid transfer from Escherichia coli. *J. Bacteriol.* **179** (2), 538–540 (1997).

67. Simon, R., Priefer, U. & Pühler, A. A Broad Host Range Mobilization System for In Vivo Genetic Engineering: Transposon Mutagenesis in Gram Negative Bacteria. *Biotechnology* **1**, 784 (1983).

68. Shanks, R. M. Q., Caiazza, N. C., Hinsa, S. M., Toutain, C. M. & O'Toole, G. A. Saccharomyces cerevisiae-based molecular tool kit for manipulation of genes from gram-negative bacteria. *Appl. Environ. Microbiol.* **72** (7), 5027–5036 (2006).

69. Hoang, T. T., Karkhoff-Schweizer, R. R., Kutchma, A. J. & Schweizer, H. P. A broad-host-range Flp-FRT recombination system for site-specific excision of chromosomally-located DNA sequences: application for isolation of unmarked Pseudomonas aeruginosa mutants. *Gene* **212** (1), 77–86 (1998).

The scope of the present invention is not limited by what has been specifically shown and described hereinabove. Those skilled in the art will recognize that there are suitable alternatives to the depicted examples of materials, configurations, constructions and dimensions. Numerous references, including patents and various publications, are cited and discussed in the description of this invention. The citation and discussion of such references is provided merely to clarify the description of the present invention and is not an admission that any reference is prior art to the invention described herein. All references cited and discussed in this specification are incorporated herein by reference in their entirety. Variations, modifications and other implementations of what is described herein will occur to those of ordinary skill in the art without departing from the spirit and scope of the invention. While certain embodiments of the present invention have been shown and described, it will be obvious to those skilled in the art that changes and modifications may be made without departing from the spirit and scope of the invention. The matter set forth in the foregoing description and accompanying drawings is offered by way of illustration only and not as a limitation.

What is claimed is:

1. A method of treating a bacterial infection in a subject, comprising the step of administering to the subject an antibiotic and an inhibitor of a *cbb*$_3$-type oxidase.
2. A method of disrupting a bacterial biofilm, comprising the step of contacting the bacterial biofilm with an antibiotic and an inhibitor of a *cbb*$_3$-type oxidase.
3. A method of inhibiting or decreasing a bacterial biofilm production on a surface or substrate, comprising the step of contacting the surface or substrate with an antibiotic and an inhibitor of a *cbb*$_3$-type oxidase.
4. A method of inhibiting or decreasing bacterial biofilm production, and/or inhibiting or decreasing bacterial virulence factor production, comprising the step of contacting bacteria with an antibiotic and an inhibitor of a *cbb*$_3$-type oxidase.
5. The method of claim 1, wherein the bacterial infection is a nosocomial infection.
6. The method of claim 1, wherein the bacterial infection is an opportunistic infection.
7. The method of claim 1, wherein the bacterial infection is a urinary tract infection, respiratory pneumonia, a surgical site wound infection, bacteremia, a gastrointestinal infection, and/or a skin infection.
8. The method of claim 1, wherein the bacterial infection is a respiratory tract infection, a pulmonary tract infection, a urinary tract infection, a blood infection, an ear infection, an eye infection, a central nervous system infection, a gastrointestinal tract infection, a bone infection, a joint infection, a wound infection, dental plaque, gingivitis, chronic sinusitis, endocarditis, or combinations thereof.
9. The method of claim 1, wherein the bacterial infection is an implanted medical device-associated infection, a catheter-associated infection, an antibiotic resistant infection, or combinations thereof.
10. The method of claim 1, wherein the subject has cystic fibrosis, and/or primary ciliary dyskinesia.
11. The method of claim 1, wherein the subject is immunocompromised or immunosuppressed.
12. The method of claim 1, wherein the subject is undergoing, or has undergone, surgery, implantation of a medical device, and/or a dental procedure.

13. The method of claim 12, wherein the medical device is a catheter, a joint prosthesis, a prosthetic cardiac valve, a ventilator, a stent, or an intrauterine device.
14. The method of any of claims 1-4, wherein the antibiotic or the inhibitor is administered topically, intravenously, or intranasally.
15. The method of claim 1, wherein the bacterial infection is caused by *Pseudomonas aeruginosa, Staphylococcus aureus, Staphylococcus aureus, Acinetobacter baumannii, Stenotrophomonas maltophilia, Clostridium difficile, Escherichia coli, Mycobacterium tuberculosis, Enterococcus, Legionella*, or combinations thereof.
16. The method of claim 1, wherein the bacterial infection is caused by *Pseudomonas, Burkholderia cepaci C. violaceum, V. harveyi, Neisseria gonorrhoeae, Neisseria meningitidis, Bordetella pertussis, Haemophilus influenzae, Legionella pneumophila, Brucella, Francisella, Xanthomonas, Agrobacterium, Escherichia coli, Salmonella, Shigella, Proteus, Yersinia pestisi*, or combinations thereof.
17. The method of claim 16, wherein the *Pseudomonas* is *Pseudomonas aeruginosa.*
18. The method of any of claims 1-4, wherein the combination of the antibiotic and the inhibitor produces a synergistic effect compared to the effect of the antibiotic alone or the effect of the inhibitor alone.
19. The method of claim 18, wherein the combination results in a synergistic decrease in O_2 reduction.
20. The method of claim 18, wherein the combination results in a synergistic decrease in phenazine reduction.
21. The method of any of claims 1-4, wherein the inhibitor is an inhibitor of a *cbb*$_3$-type oxidase of *Pseudomonas aeruginosa.*
22. The method of any of claims 1-4, wherein the inhibitor is an inhibitor of Cco1 and/or Cco2 of *Pseudomonas aeruginosa.*
23. The method of any of claims 1-4, wherein the inhibitor is an inhibitor of catalytic subunit CcoN4 of *Pseudomonas aeruginosa.*
24. The method of any of claims 1-4, wherein the inhibitor is a small molecule, a polynucleotide, a polypeptide, or an antibody or antigen-binding portion thereof.
25. The method of any of claims 1-4, wherein the inhibitor is a nitrite.

26. The method of any of claims 1-4, wherein the inhibitor is diazeniumdiolate, S-Nitrosoglutathione (GSNO), S-Nitroso-N-acetylpenicillamine (SNAP), sodium nitrite, and/or potassium nitrite.
27. The method of any of claims 1-4, wherein the antibiotic is penicillin, cephalosporine, a beta-lactamase inhibitor, tetracycline, an aminoglycoside, a quinolone, a macrolide, or combinations thereof.
28. The method of any of claims 1-4, wherein the antibiotic is gentamicin, tobramycin, colistin, fluoroquinolone, or combinations thereof.
29. The method of claim 3, wherein the surface is a surface in the oral cavity.
30. The method of claim 3, wherein the surface is a mammalian skin or mucosal surface.
31. The method of any of claims 1-4, wherein the antibiotic and the inhibitor are administered simultaneously, sequentially or separately.
32. The method of claim 1, further comprising administering to the subject an antifungal agent.
33. The method of claim 1, further comprising administering to the subject an antiviral agent.
34. The method of claim 1, wherein the subject is a human.
35. The method of any of claims 1-4, for therapeutic treatment.
36. The method of any of claims 1-4, for prophylactic treatment.
37. The method of any of claims 1-4, for use in an industrial setting.
38. The method of claim 37, wherein the industrial setting is a work area, a medical instrument, a chemical unit operation, a pipe, a sewage system, a pipeline, a tubing, or a filtration device.
39. A method of treating a bacterial infection in a subject, comprising the step of administering to the subject an inhibitor of a *cbb*$_3$-type oxidase.
40. A method of disrupting a bacterial biofilm, comprising the step of contacting the bacterial biofilm with an inhibitor of a *cbb*$_3$-type oxidase.
41. A method of inhibiting or decreasing a bacterial biofilm production on a surface or substrate, comprising the step of contacting the surface or substrate with an inhibitor of a *cbb*$_3$-type oxidase.
42. A method of inhibiting or decreasing bacterial biofilm production, and/or inhibiting or decreasing bacterial virulence factor production, comprising the step of contacting bacteria with an inhibitor of a *cbb*$_3$-type oxidase.
43. The method of claim 39, wherein the bacterial infection is a nosocomial infection.

44. The method of claim 39, wherein the bacterial infection is an opportunistic infection.

45. The method of claim 39, wherein the bacterial infection is a urinary tract infection, respiratory pneumonia, a surgical site wound infection, bacteremia, a gastrointestinal infection, and/or a skin infection.

46. The method of claim 39, wherein the bacterial infection is a respiratory tract infection, a pulmonary tract infection, a urinary tract infection, a blood infection, an ear infection, an eye infection, a central nervous system infection, a gastrointestinal tract infection, a bone infection, a joint infection, a wound infection, dental plaque, gingivitis, chronic sinusitis, endocarditis, or combinations thereof.

47. The method of claim 39, wherein the bacterial infection is an implanted medical device-associated infection, a catheter-associated infection, an antibiotic resistant infection, or combinations thereof.

48. The method of claim 39, wherein the subject has cystic fibrosis, and/or primary ciliary dyskinesia.

49. The method of claim 39, wherein the subject is immunocompromised or immunosuppressed.

50. The method of claim 39, wherein the subject is undergoing, or has undergone, surgery, implantation of a medical device, and/or a dental procedure.

51. The method of claim 50, wherein the medical device is a catheter, a joint prosthesis, a prosthetic cardiac valve, a ventilator, a stent, or an intrauterine device.

52. The method of any of claims 39-42, wherein the antibiotic or the inhibitor is administered topically, intravenously, or intranasally.

53. The method of claim 39, wherein the bacterial infection is caused by *Pseudomonas aeruginosa, Staphylococcus aureus, Staphylococcus aureus, Acinetobacter baumannii, Stenotrophomonas maltophilia, Clostridium difficile, Escherichia coli, Mycobacterium tuberculosis, Enterococcus, Legionella*, or combinations thereof.

54. The method of claim 39, wherein the bacterial infection is caused by *Pseudomonas, Burkholderia cepaci C. violaceum, V. harveyi, Neisseria gonorrhoeae, Neisseria meningitidis, Bordetella pertussis, Haemophilus influenzae, Legionella pneumophila, Brucella, Francisella, Xanthomonas, Agrobacterium, Escherichia coli, Salmonella, Shigella, Proteus, Yersinia pestisi*, or combinations thereof.

55. The method of claim 54, wherein the *Pseudomonas* is *Pseudomonas aeruginosa.*

56. The method of any of claims 39-42, wherein the combination of the antibiotic and the inhibitor produces a synergistic effect compared to the effect of the antibiotic alone or the effect of the inhibitor alone.

57. The method of claim 56, wherein the combination results in a synergistic decrease in O_2 reduction.

58. The method of claim 56, wherein the combination results in a synergistic decrease in phenazine reduction.

59. The method of any of claims 39-42, wherein the inhibitor is an inhibitor of a *cbb*$_3$-type oxidase of *Pseudomonas aeruginosa*.

60. The method of any of claims 39-42, wherein the inhibitor is an inhibitor of Cco1 and/or Cco2 of *Pseudomonas aeruginosa*.

61. The method of any of claims 39-42, wherein the inhibitor is an inhibitor of catalytic subunit CcoN4 of *Pseudomonas aeruginosa*.

62. The method of any of claims 39-42, wherein the inhibitor is a small molecule, a polynucleotide, a polypeptide, or an antibody or antigen-binding portion thereof.

63. The method of any of claims 39-42, wherein the inhibitor is a nitrite.

64. The method of any of claims 39-42, wherein the inhibitor is diazeniumdiolate, S-Nitrosoglutathione (GSNO), S-Nitroso-N-acetylpenicillamine (SNAP), sodium nitrite, and/or potassium nitrite.

65. The method of any of claims 39-42, wherein the antibiotic is penicillin, cephalosporine, a beta-lactamase inhibitor, tetracycline, an aminoglycoside, a quinolone, a macrolide, or combinations thereof.

66. The method of any of claims 39-42, wherein the antibiotic is gentamicin, tobramycin, colistin, fluoroquinolone, or combinations thereof.

67. The method of claim 41, wherein the surface is a surface in the oral cavity.

68. The method of claim 41, wherein the surface is a mammalian skin or mucosal surface.

69. The method of any of claims 39-42, wherein the antibiotic and the inhibitor are administered simultaneously, sequentially or separately.

70. The method of claim 39, further comprising administering to the subject an antifungal agent.

71. The method of claim 39, further comprising administering to the subject an antiviral agent.

72. The method of claim 39, wherein the subject is a human.

73. The method of any of claims 39-42, for therapeutic treatment.
74. The method of any of claims 39-42, for prophylactic treatment.
75. The method of any of claims 39-42, for use in an industrial setting.
76. The method of claim 75, wherein the industrial setting is a work area, a medical instrument, a chemical unit operation, a pipe, a sewage system, a pipeline, a tubing, or a filtration device.
77. A pharmaceutical composition comprising a first amount of an antibiotic and a second amount of an inhibitor of a *cbb*$_3$-type oxidase.
78. A pharmaceutical composition comprising an inhibitor of a *cbb*$_3$-type oxidase.
79. The pharmaceutical composition of claims 77 or 78, for treating, or treating prophylactically, a bacterial infection.
80. The pharmaceutical composition of claim 79, wherein the bacterial infection is caused by *Pseudomonas aeruginosa, Staphylococcus aureus, Staphylococcus aureus, Acinetobacter baumannii, Stenotrophomonas maltophilia, Clostridium difficile, Escherichia coli, Mycobacterium tuberculosis, Enterococcus, Legionella*, or combinations thereof.
81. The pharmaceutical composition of claim 79, wherein the bacterial infection is caused by *Pseudomonas, Burkholderia cepaci C. violaceum, V. harveyi, Neisseria gonorrhoeae, Neisseria meningitidis, Bordetella pertussis, Haemophilus influenzae, Legionella pneumophila, Brucella, Francisella, Xanthomonas, Agrobacterium, Escherichia coli, Salmonella, Shigella, Proteus, Yersinia pestisi*, or combinations thereof.
82. The pharmaceutical composition of claim 79, wherein the *Pseudomonas* is *Pseudomonas aeruginosa*.
83. The pharmaceutical composition of claims 77 or 78, for administration topically, intravenously, or intranasally.
84. The pharmaceutical composition of claims 77 or 78, wherein the inhibitor is an inhibitor of a *cbb*$_3$-type oxidase of *Pseudomonas aeruginosa*.
85. The pharmaceutical composition of claims 77 or 78, wherein the inhibitor is an inhibitor of Cco1 and/or Cco2 of *Pseudomonas aeruginosa*.
86. The pharmaceutical composition of claims 77 or 78, wherein the inhibitor is an inhibitor of catalytic subunit CcoN4 of *Pseudomonas aeruginosa*.
87. The pharmaceutical composition of claims 77 or 78, wherein the inhibitor is a small molecule, a polynucleotide, a polypeptide, or an antibody or antigen-binding portion thereof.

88. The pharmaceutical composition of claims 77 or 78, wherein the inhibitor is a nitrite.

89. The pharmaceutical composition of claims 77 or 78, wherein the inhibitor is diazeniumdiolate, S-Nitrosoglutathione (GSNO), S-Nitroso-N-acetylpenicillamine (SNAP), sodium nitrite, and/or potassium nitrite.

90. The pharmaceutical composition of claims 77 or 78, further comprising an antifungal agent.

91. The pharmaceutical composition of claims 77 or 78, further comprising an antiviral agent.

92. The method of any of claims 1-4, wherein the inhibitor is an inhibitor of CcoN, CcoO, CcoP, CcoQ, or combinations thereof.

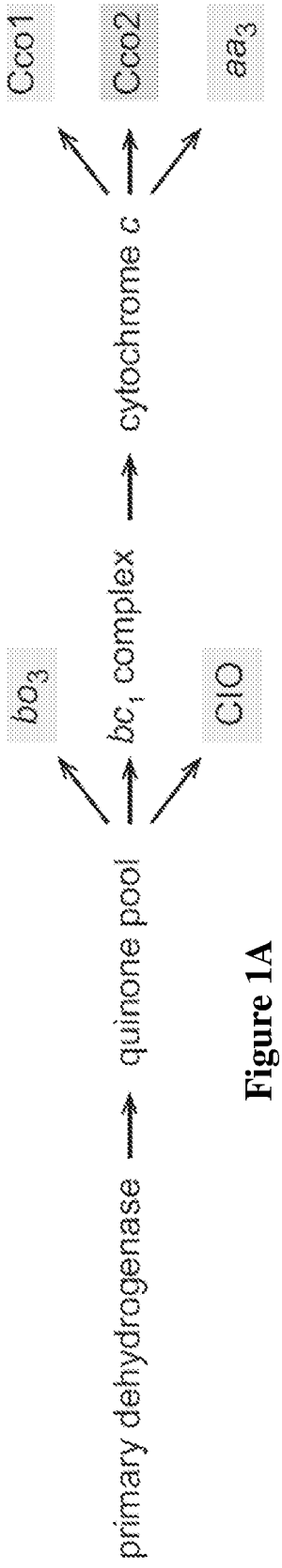


Figure 1A

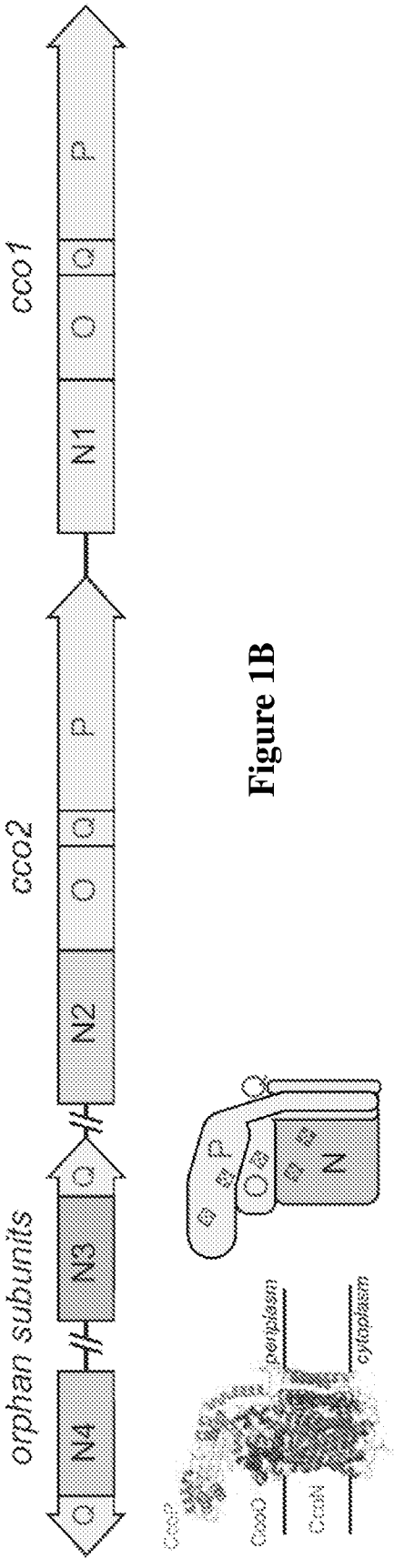


Figure 1B

Figure 1C

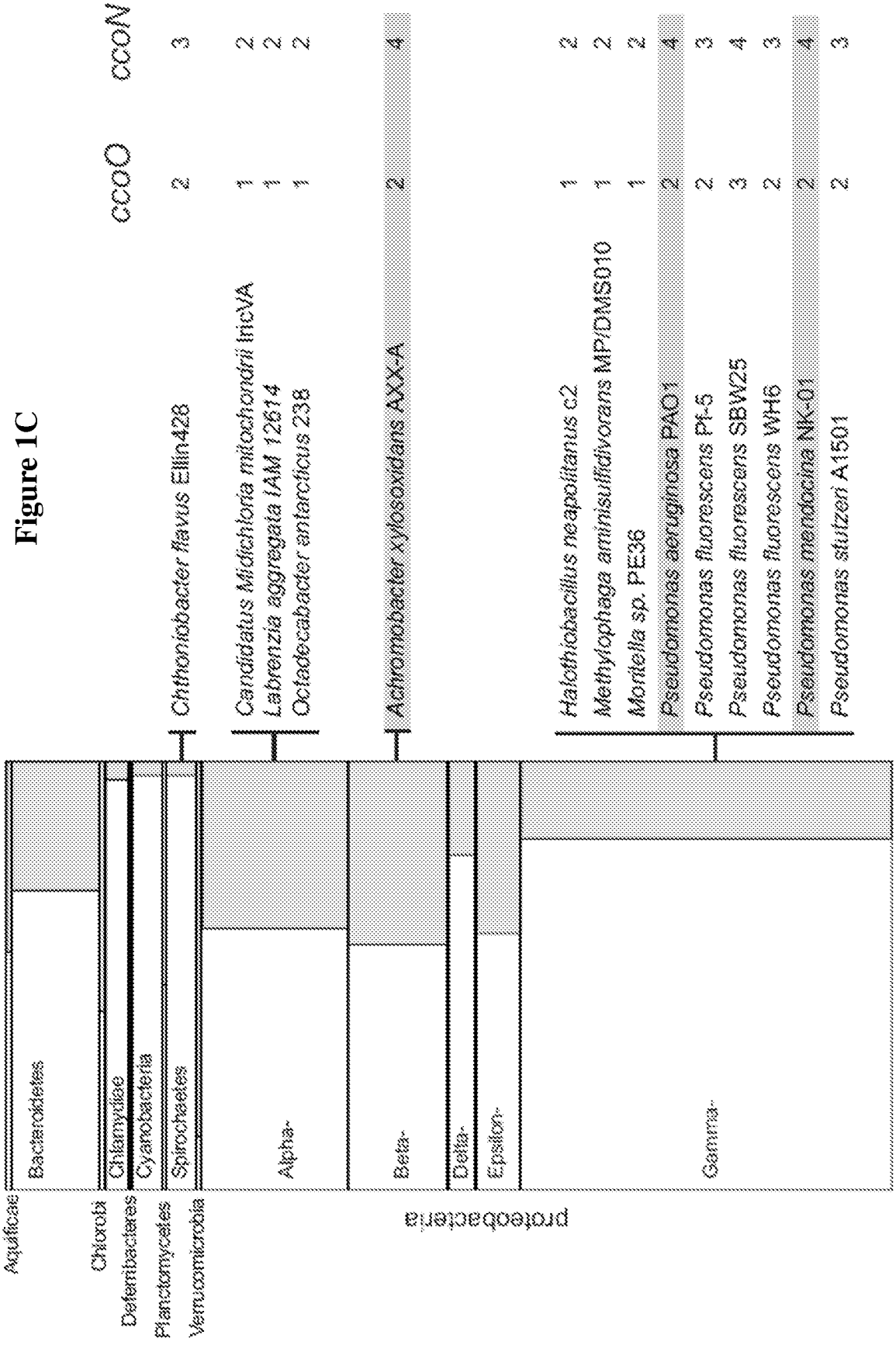
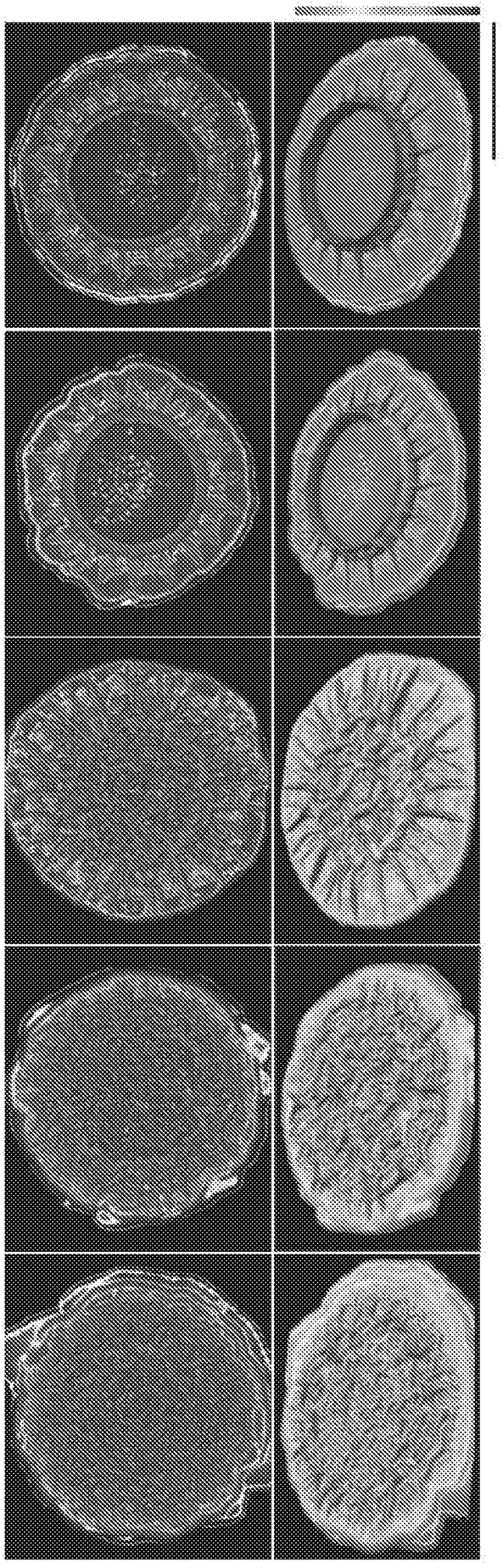

ccoO
ccoN
Aquificae
Bacteroidetes
Chlorobi
Chlamydiae
Deferribacteres
Cyanobacteria
Planctomycetes
Spirochaetes
Verrucomicrobia
Alpha-
Beta-
Delta-
Epsilon-
Gamma-
proteobacteria
Chthoniobacter flavus Ellin428 2 3
Candidatus Midichloria mitochondrii IricVA 1 2
Labrenzia aggregata IAM 12614 1 2
Octadecabacter antarcticus 238 1 2
Achromobacter xylosoxidans AXX-A 2 4
Halothiobacillus neapolitanus c2 1 2
Methyliophaga aminisulfidivorans MP/DMS010 1 2
Moritella sp. PE36 1 2
Pseudomonas aeruginosa PAO1 2 4
Pseudomonas fluorescens Pf-5 2 3
Pseudomonas fluorescens SBW25 3 4
Pseudomonas fluorescens WH6 2 3
Pseudomonas mendocina NK-01 2 4
Pseudomonas stutzeri A1501 2 3

Figure 2A



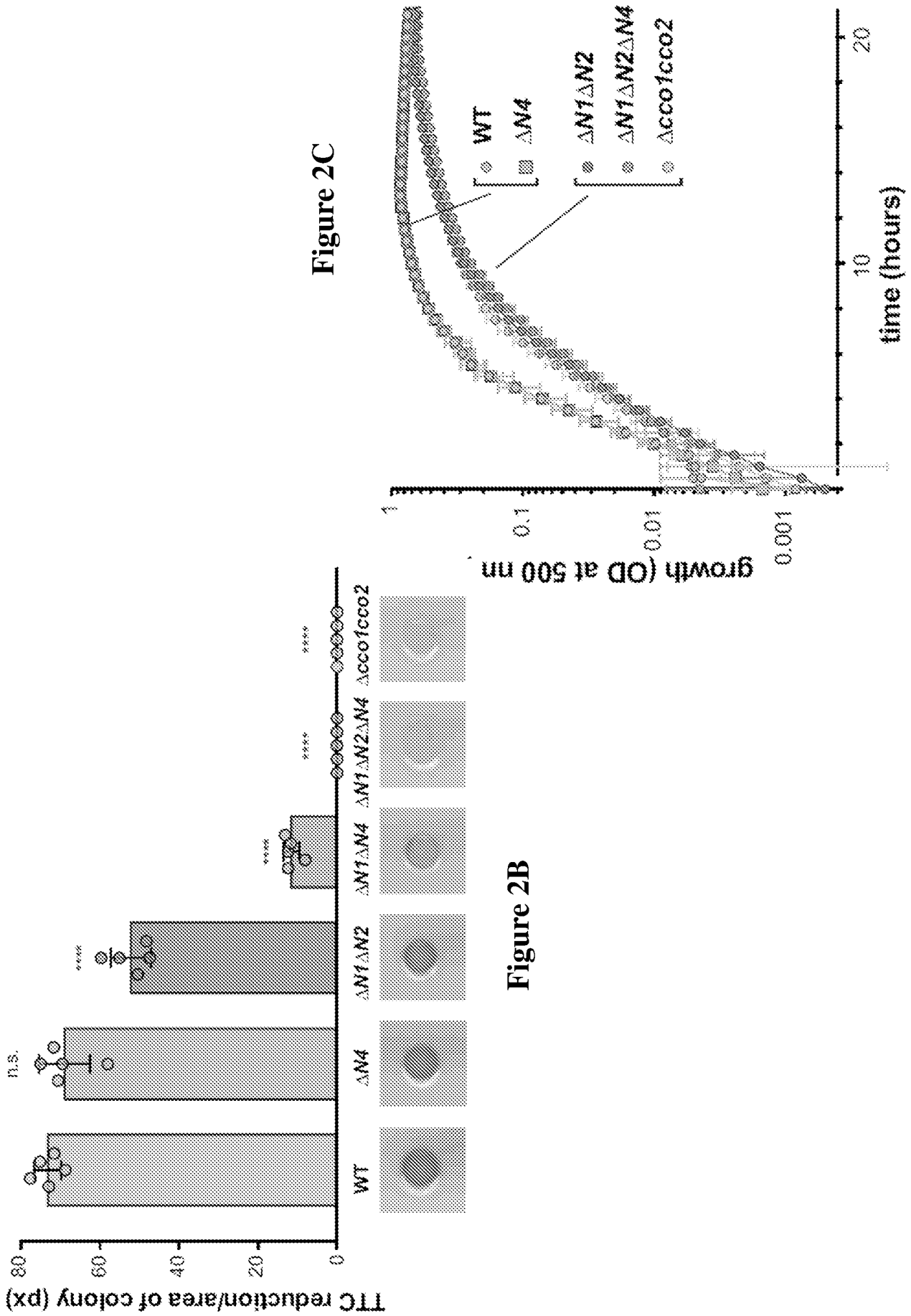


Figure 2B

Figure 2C

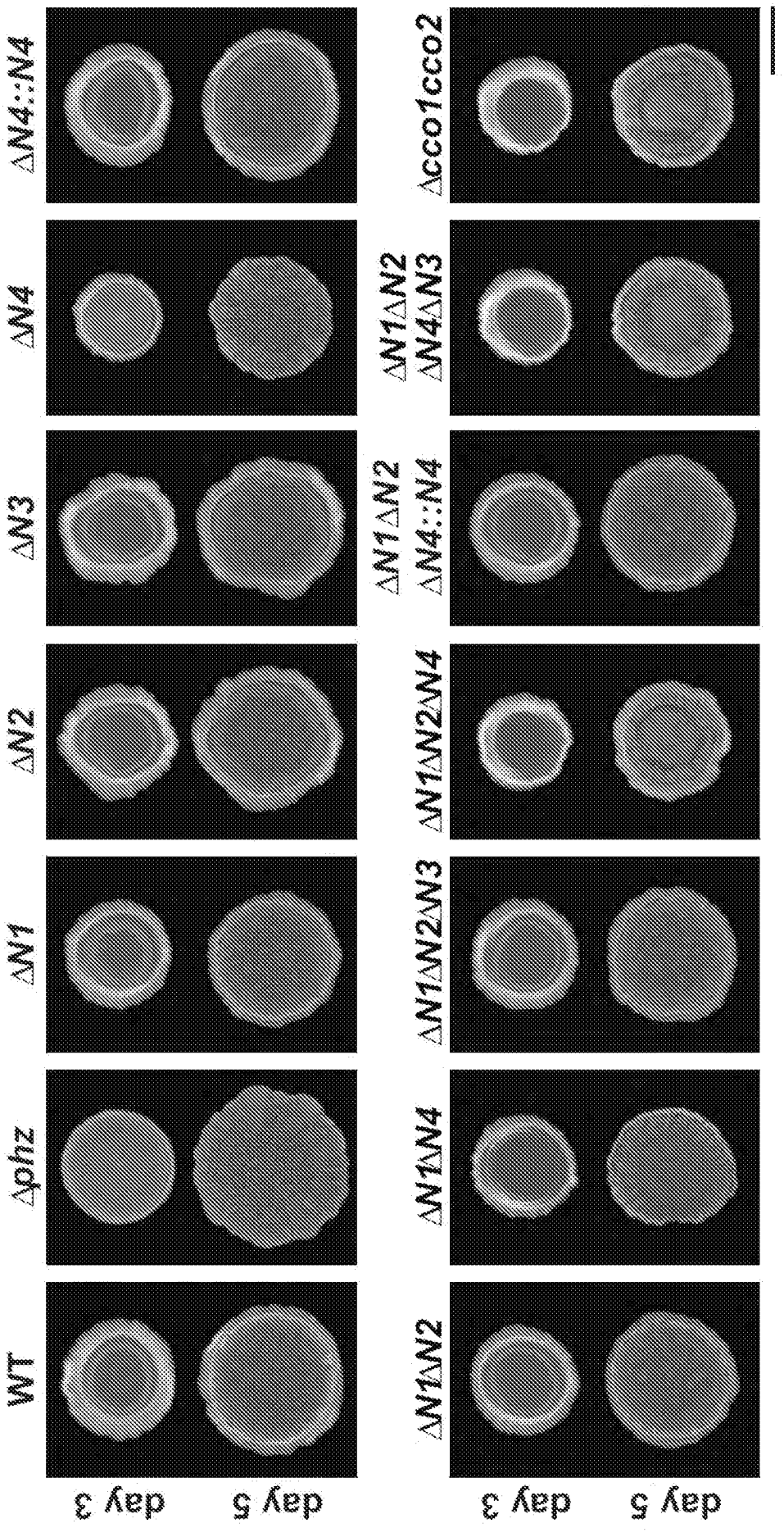

WT
Δphz
ΔN1
ΔN2
ΔN3
ΔN4
ΔN4::N4
ΔN1ΔN2
ΔN1ΔN2ΔN3
ΔN1ΔN2ΔN4
ΔN1ΔN2
ΔN4::N4
ΔN1ΔN2
ΔN4ΔN3
Δcco1cco2
day 3
day 5
day 3
day 5

Figure 2(IA)

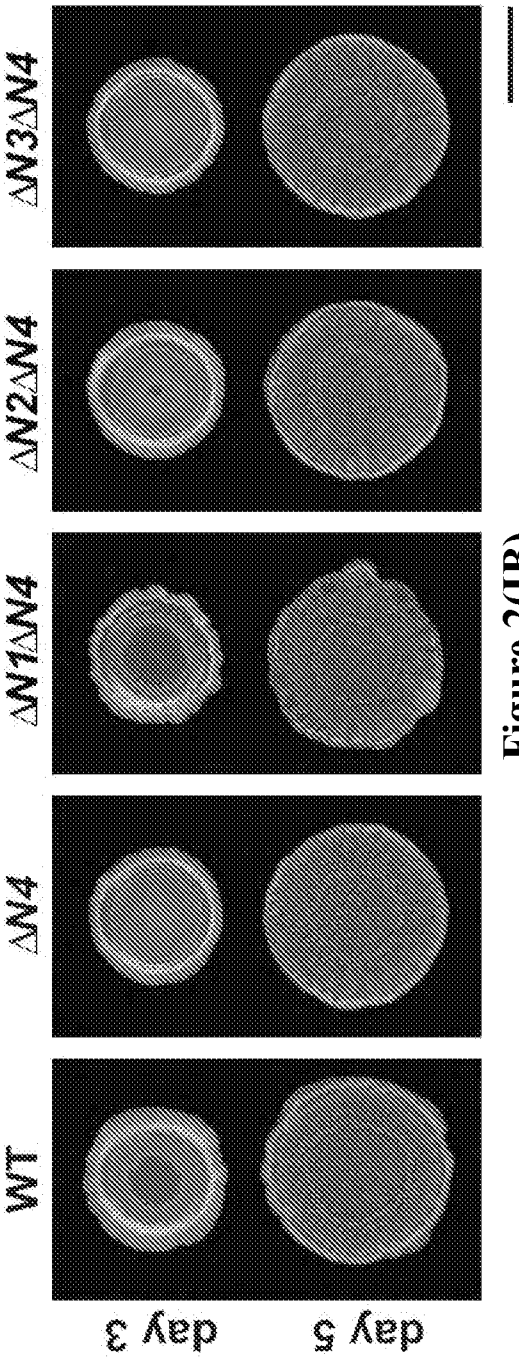


Figure 2(IB)

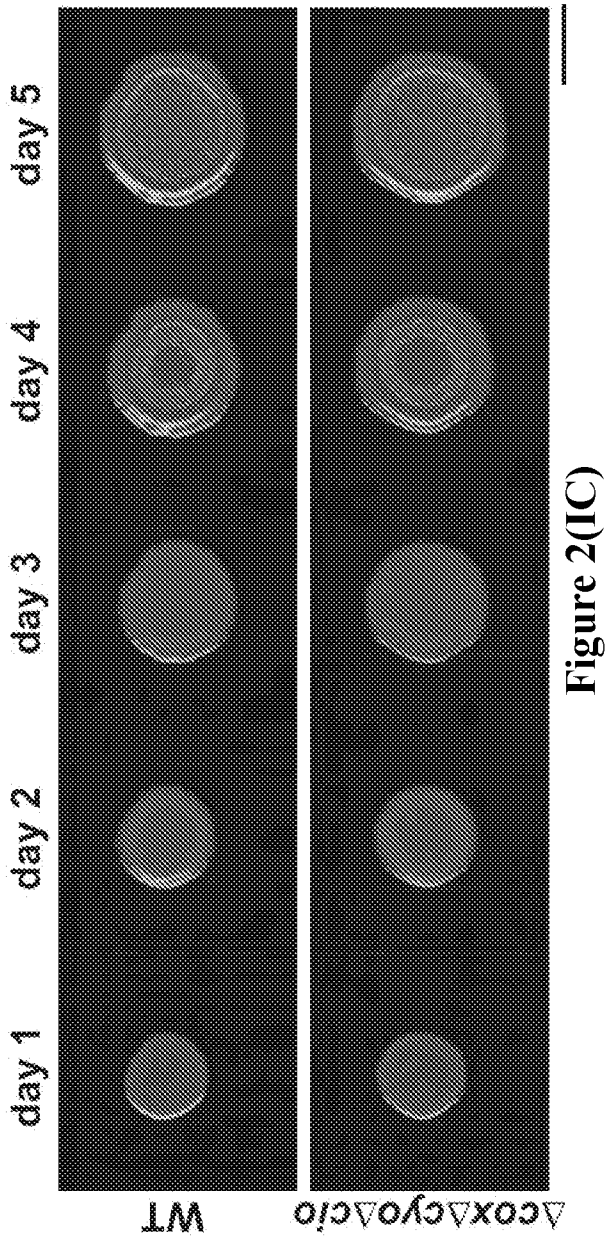


Figure 2(IC)

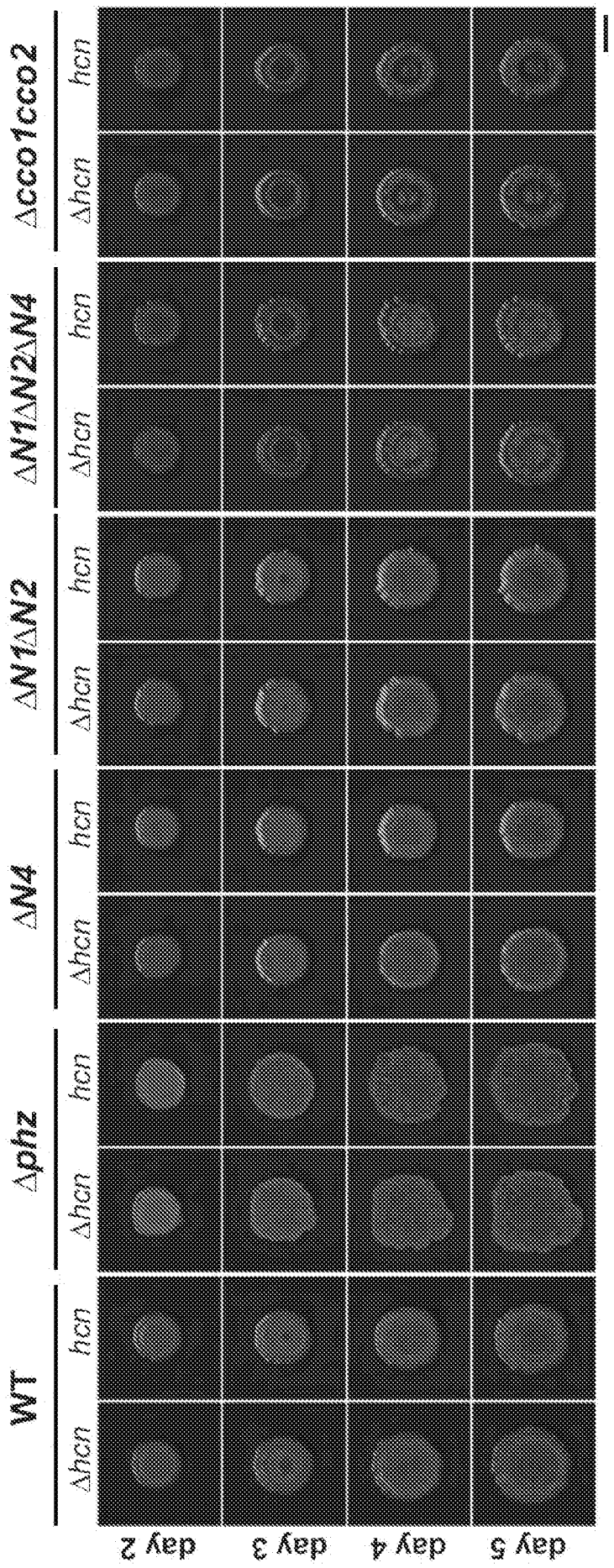

WT
Δphz
ΔN4
ΔN1ΔN2
ΔN1ΔN2ΔN4
Δcco1cco2
Δhcn
hcn
day 2
day 3
day 4
day 5

Figure 2(IIA)

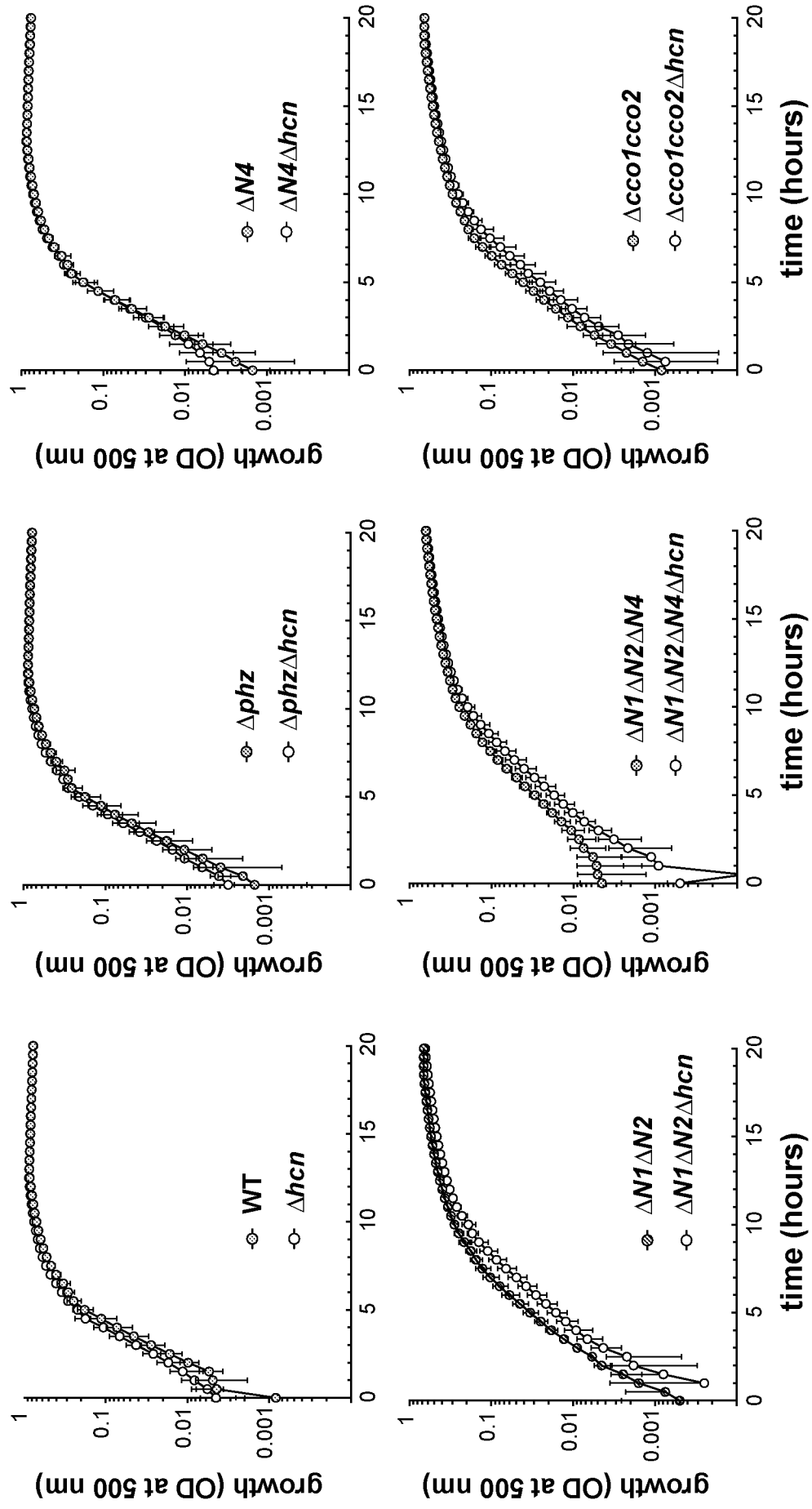

growth (OD at 500 nm)
time (hours)
WT
Δhcn
ΔN1ΔN2
ΔN1ΔN2Δhcn
Δphz
Δphzhcn
ΔN1ΔN2ΔN4
ΔN1ΔN2ΔN4Δhcn
ΔN4
ΔN4Δhcn
Δcco1cco2
Δcco1cco2Δhcn

Figure 2(IIB)

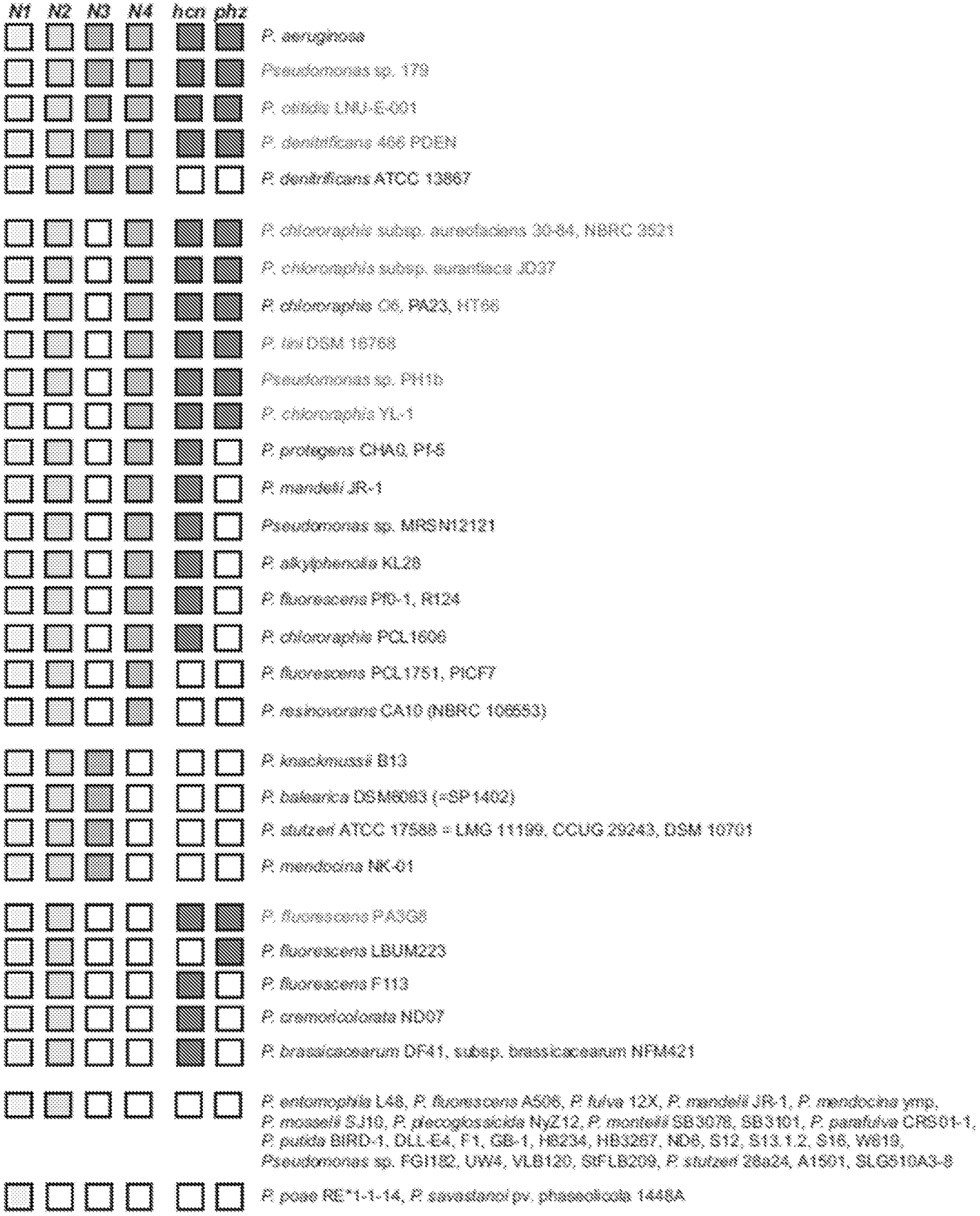

N1
N2
N3
N4
hcn
phz
P. aeruginosa
Pseudomonas sp. 179
P. citrea LMU-E-001
P. denitrificans 486 PDEN
P. denitrificans ATCC 13867
P. chlororaphis subsp. aurantiaca 30-84, NBRC 3521
P. chlororaphis subsp. aurantiaca JD37
P. chlororaphis O6, PA23, HT66
P. lini DSM 18788
Pseudomonas sp. PH1b
P. chlororaphis YL-1
P. protegens CHA0, Pf-5
P. mandelii JR-1
Pseudomonas sp. MRSN12121
P. alkylphenolia KL28
P. fluorescens Pf0-1, R124
P. chlororaphis PCL1606
P. fluorescens PCL1751, PICF7
P. resinovorans CA10 (NBRC 106553)
P. knackmussii B13
P. balearica DSM6083 (=SP1402)
P. stutzeri ATCC 17588 = LMG 11199, CCUG 29243, DSM 10701
P. mendocina NK-01
P. fluorescens PA3G8
P. fluorescens LBUM223
P. fluorescens F113
P. cremoricolorata ND07
P. brassicacearum DF41, subsp. brassicacearum NFM421
P. entomophila L48, P. fluorescens A506, P. fulva 12X, P. mandelii JR-1, P. mendocina ymp, P. mosselii SJ10, P. plecoglossicida NyZ12, P. monteilii SB3078, SB3101, P. parafulva CRS01-1, P. putida BIRD-1, DLL-E4, F1, GB-1, H8234, HB3267, ND6, S12, S13.1.2, S16, W619, Pseudomonas sp. FGI182, UW4, VLB120, StFLB209, P. stutzeri 28a24, A1501, SLG510A3-8
P. poae RE*1-1-14, P. savastanoi pv. phaseolicola 1448A

Figure 2(III)

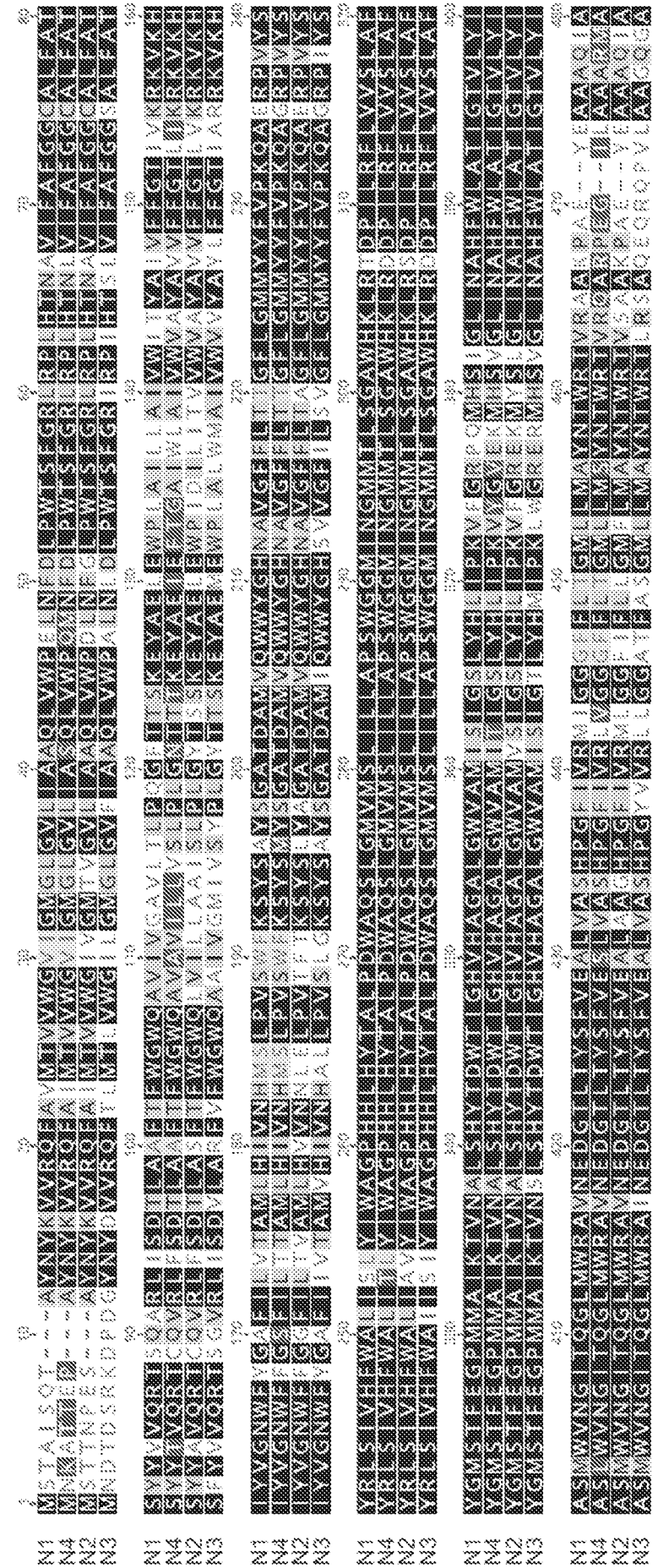


Figure 2(IVA)

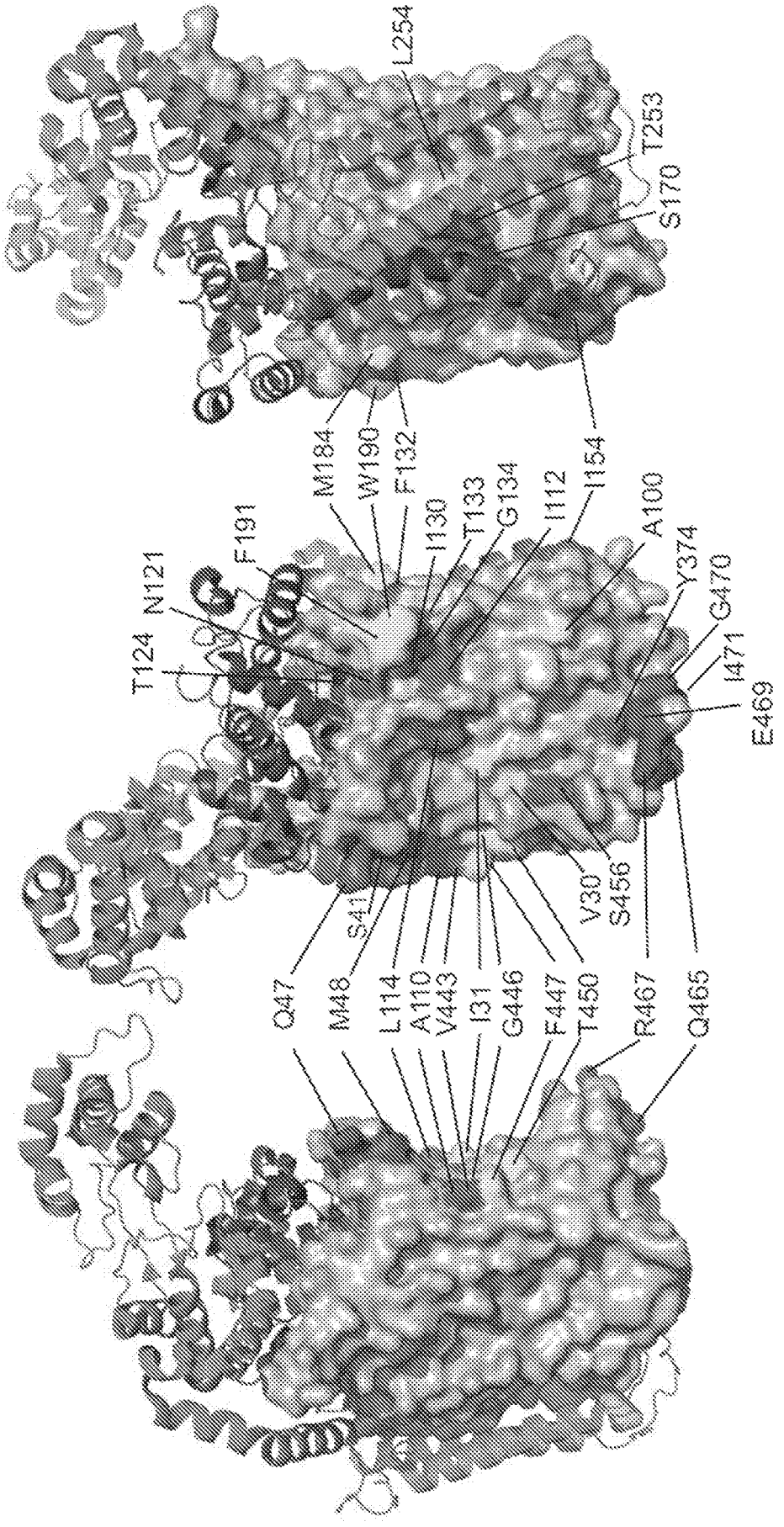

L254
T253
S170
M184
W190
F132
I154
T133
G134
I130
I112
A100
Y374
G470
I471
E469
F191
N121
T124
V30
S456
S41
M48
Q47
L114
A110
V443
I31
G446
F447
T450
R467
Q465

Figure 2(IVB)

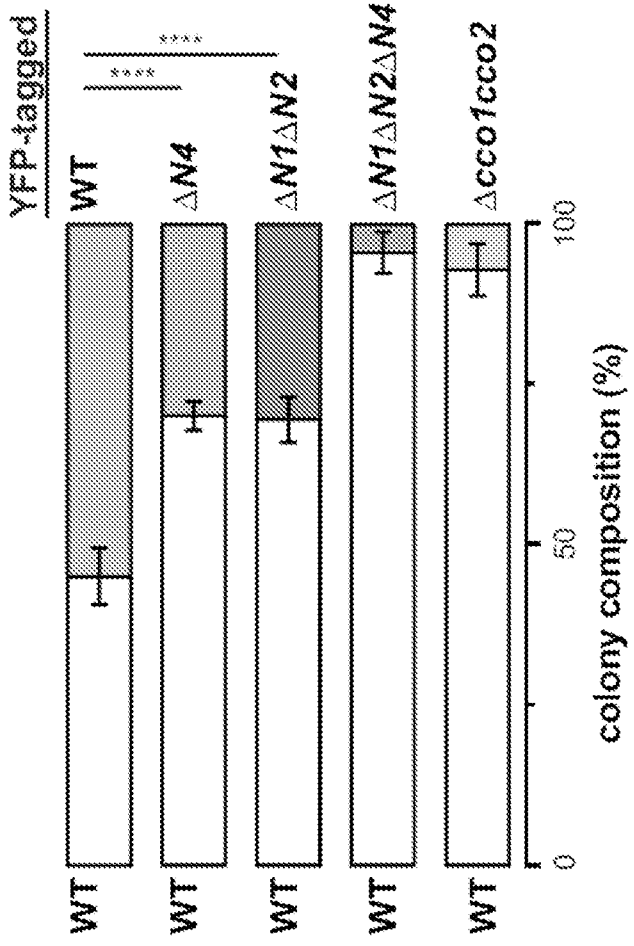


Figure 3A

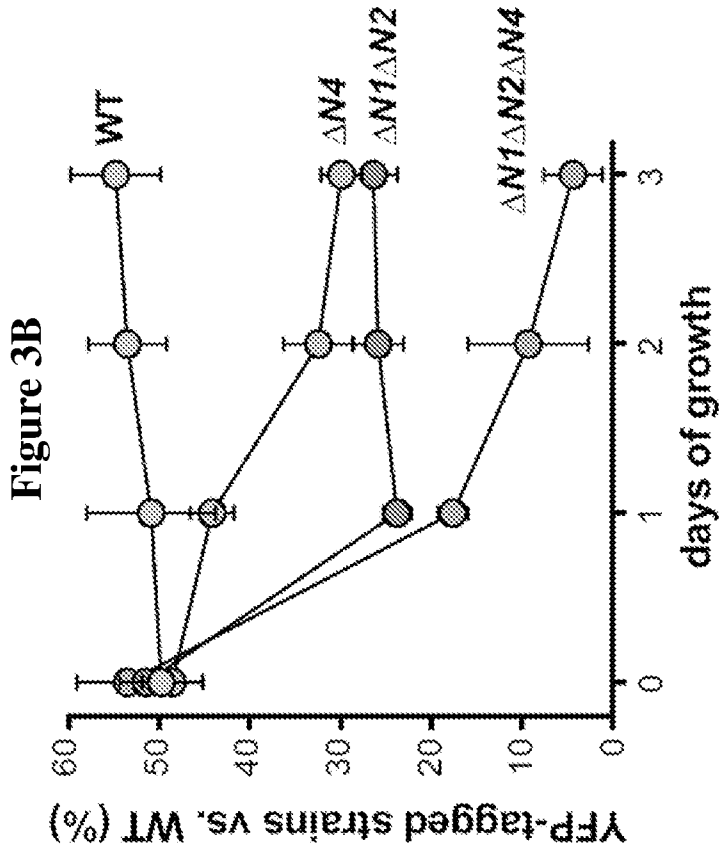


Figure 3B

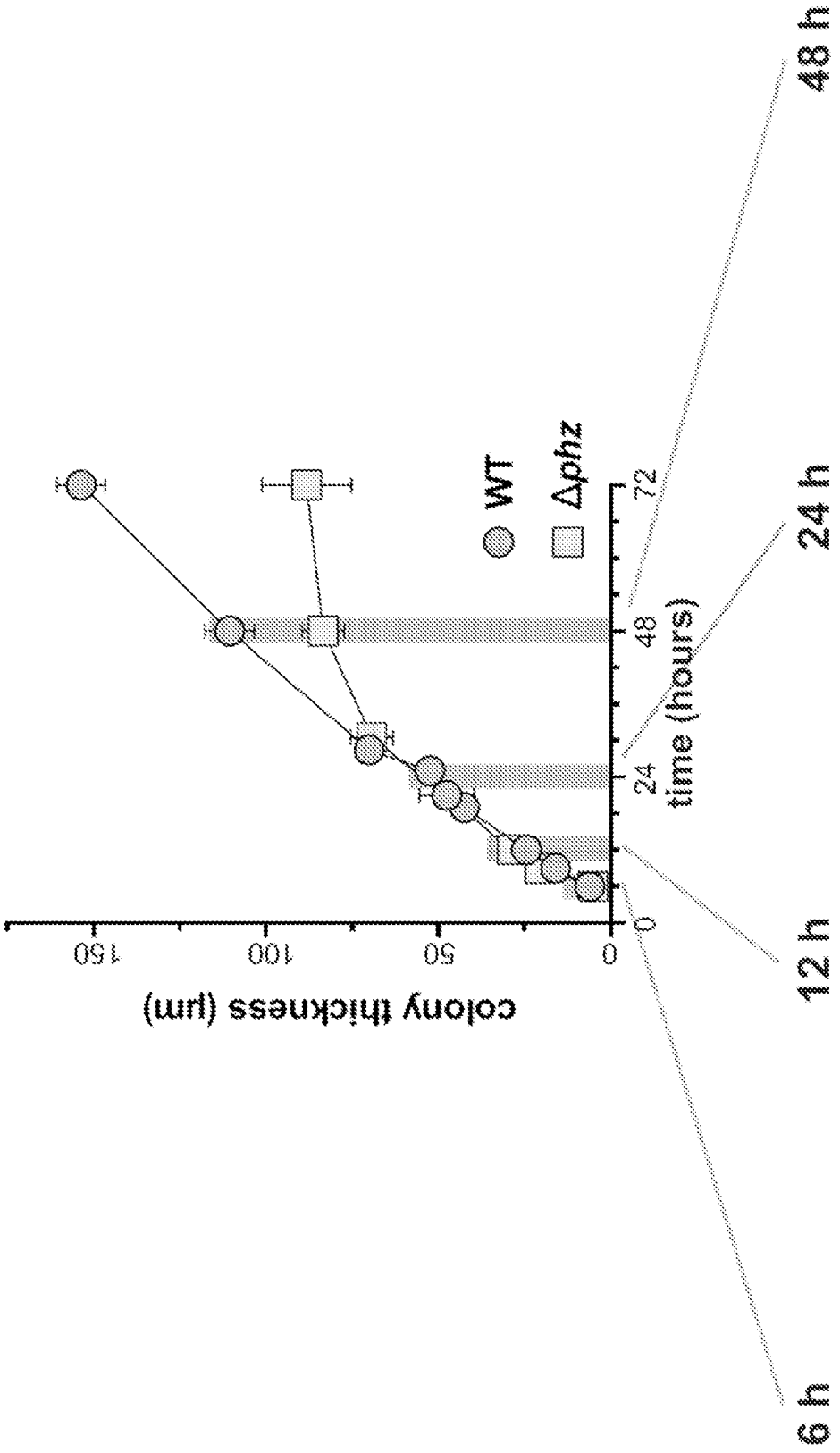

48 h
24 h
12 h
6 h
WT
Δphz
colony thickness (μm)
150
100
50
0
time (hours)
0
24
48
72

Figure 3C

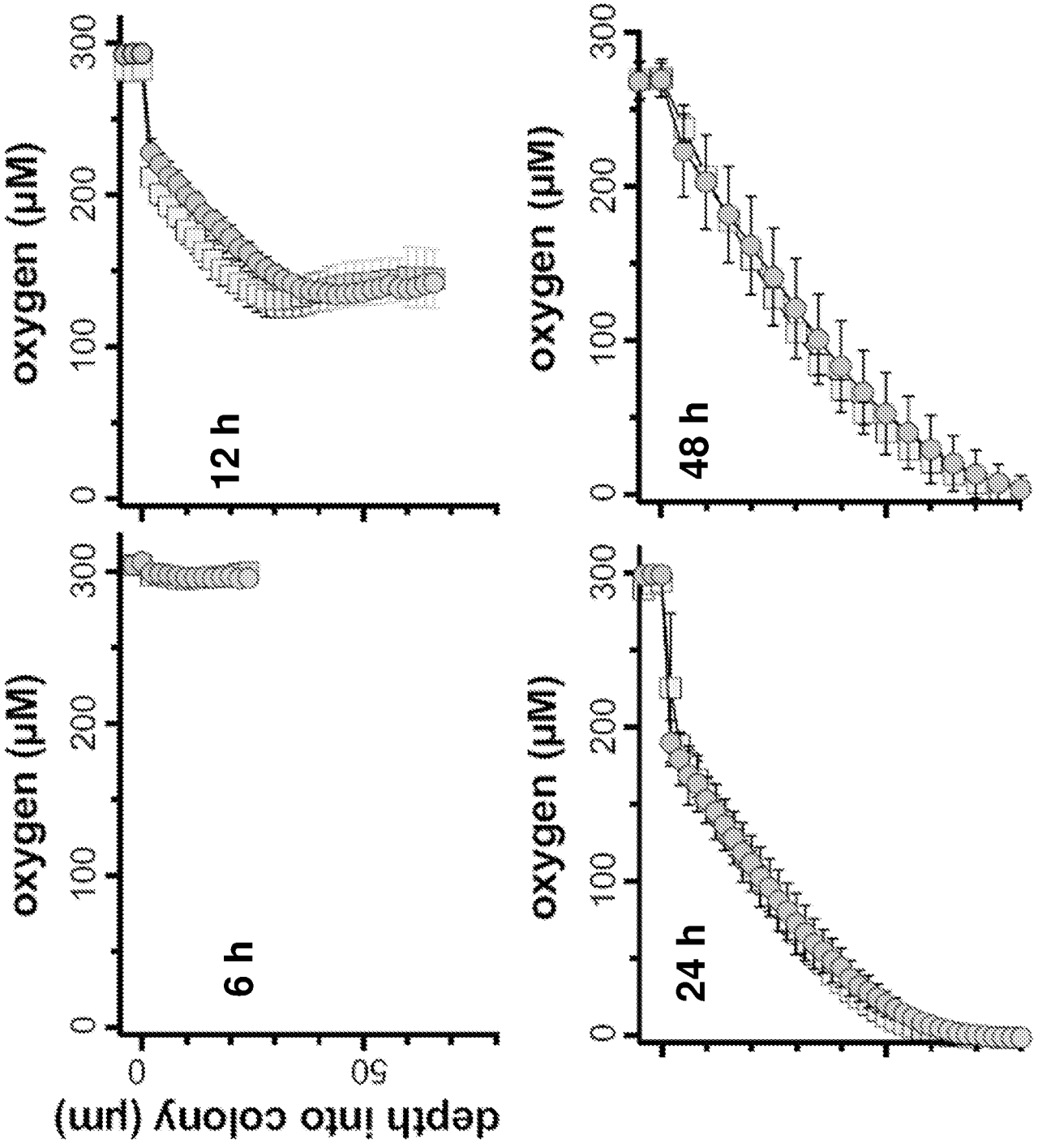


Figure 3D

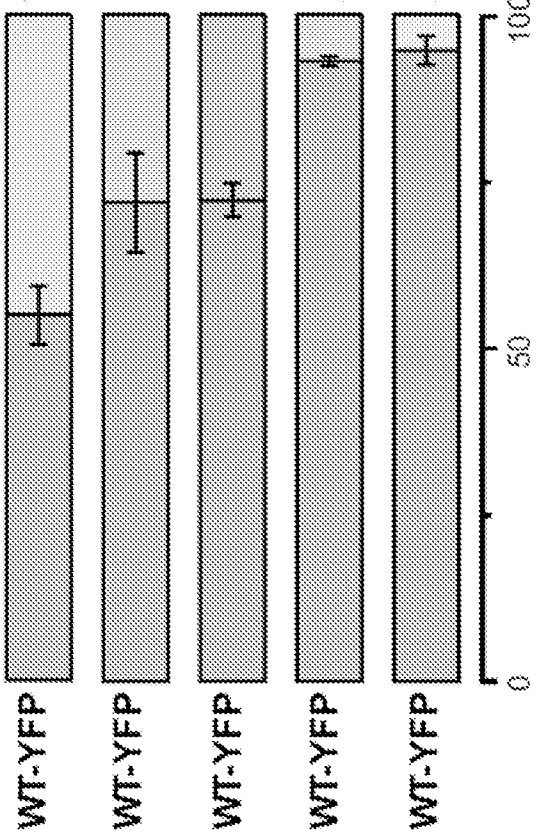


Figure 3(IA)

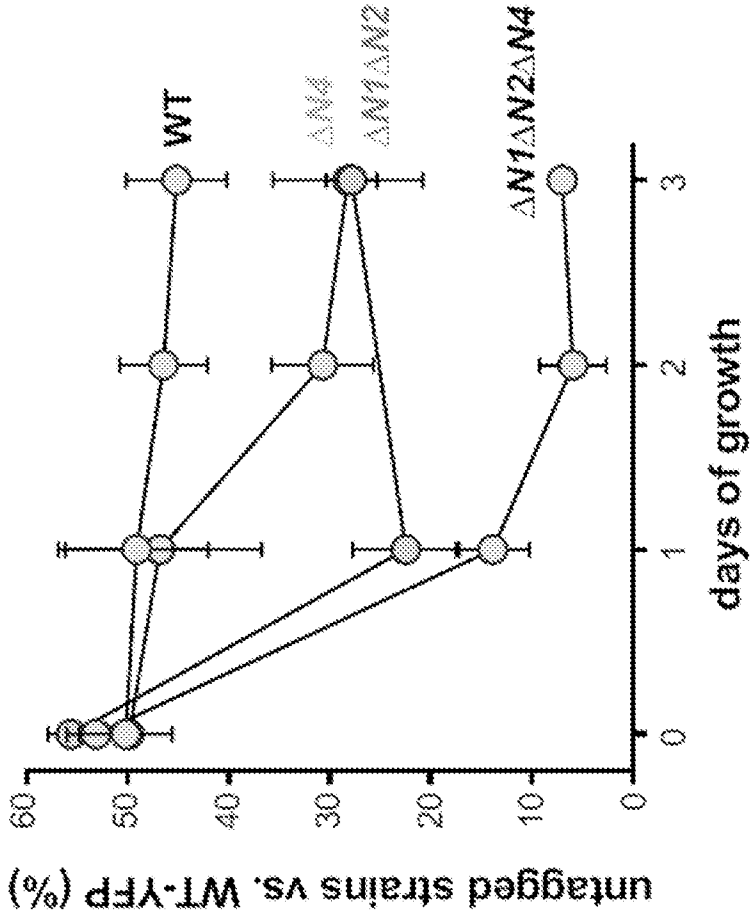


Figure 3(IB)

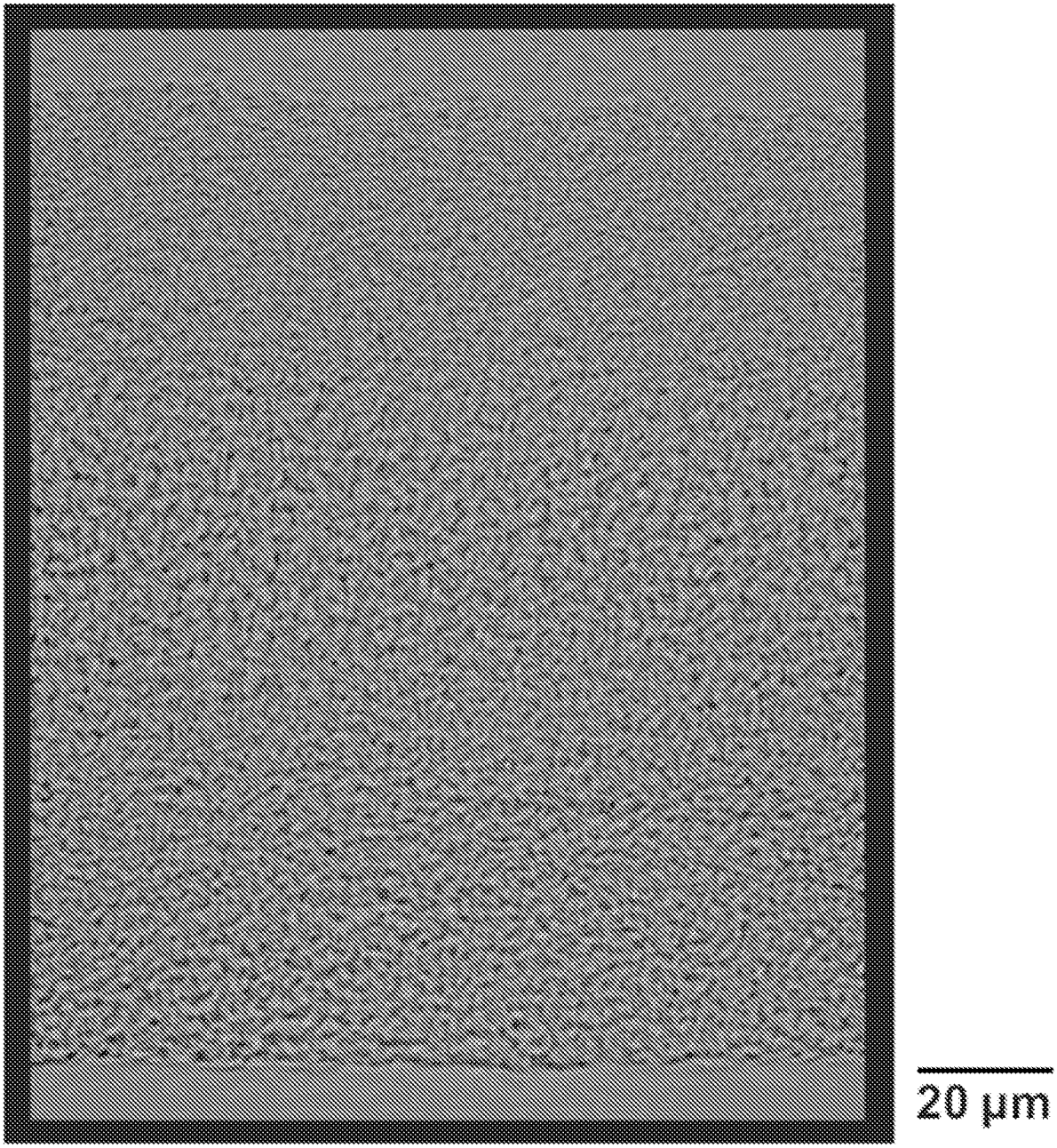
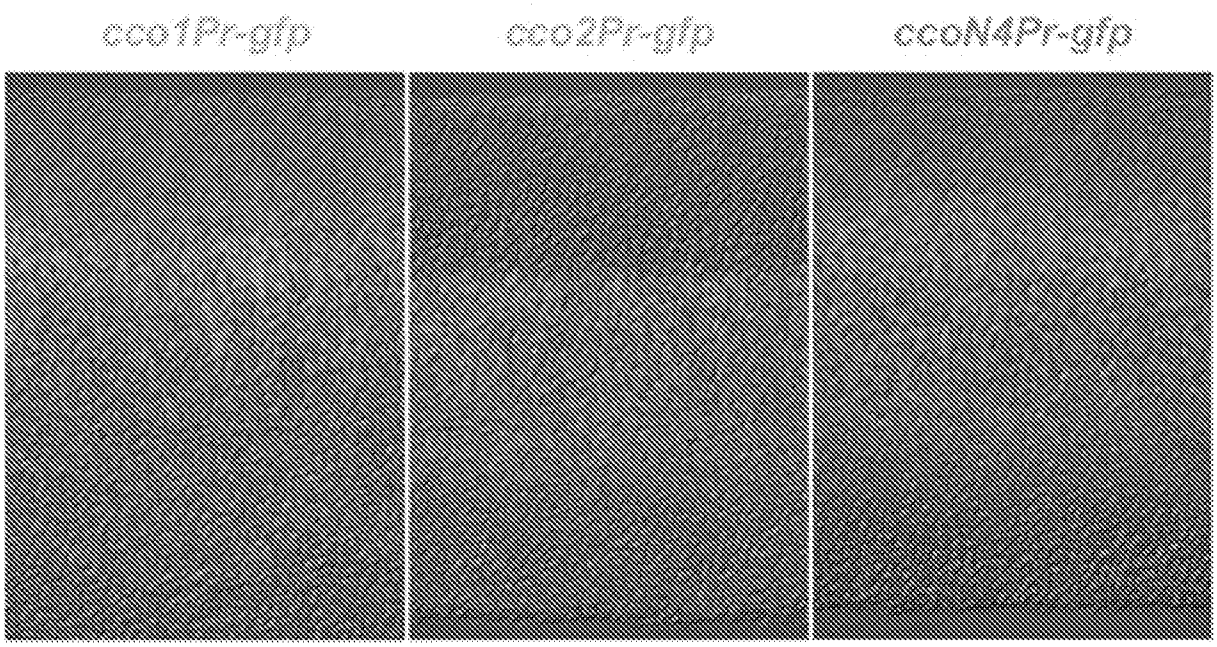


Figure 3(IC)


cco1Pr-gfp
cco2Pr-gfp
ccoN4Pr-gfp

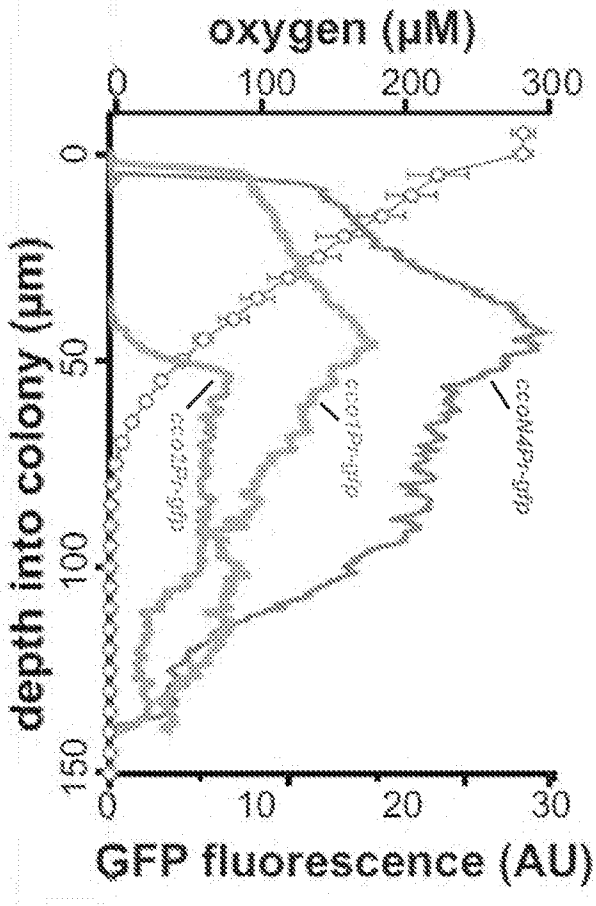

oxygen (μM)
0
100
200
300
depth into colony (μm)
0
50
100
150
cco1Pr-gfp
cco2Pr-gfp
ccoN4Pr-gfp
0
10
20
30
GFP fluorescence (AU)

Figure 4

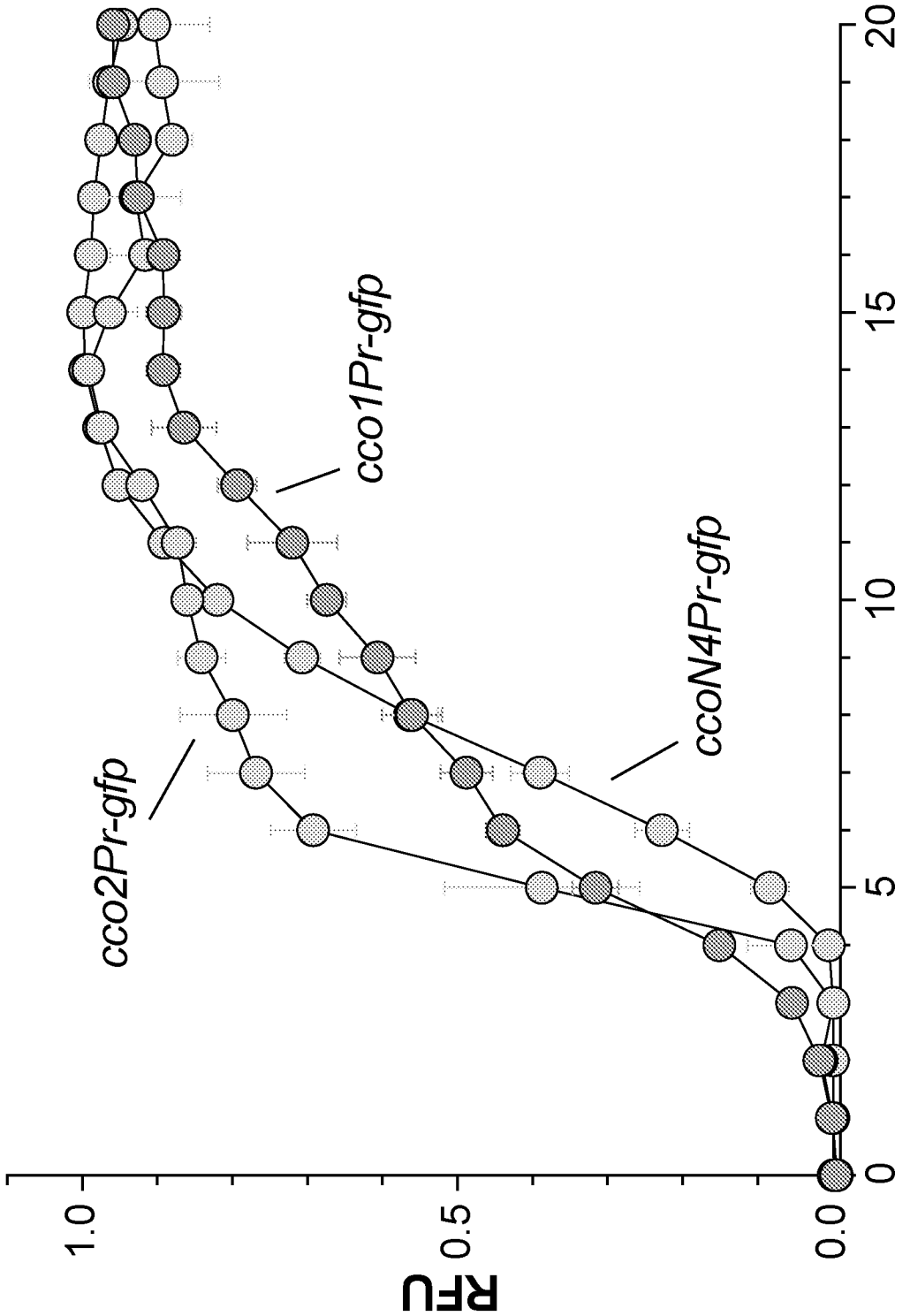

cco2Pr-gfp
cco1Pr-gfp
ccoN4Pr-gfp
RFU
1.0
0.5
0.0
0
5
10
15
20
time (hours)

Figure 4(IA)

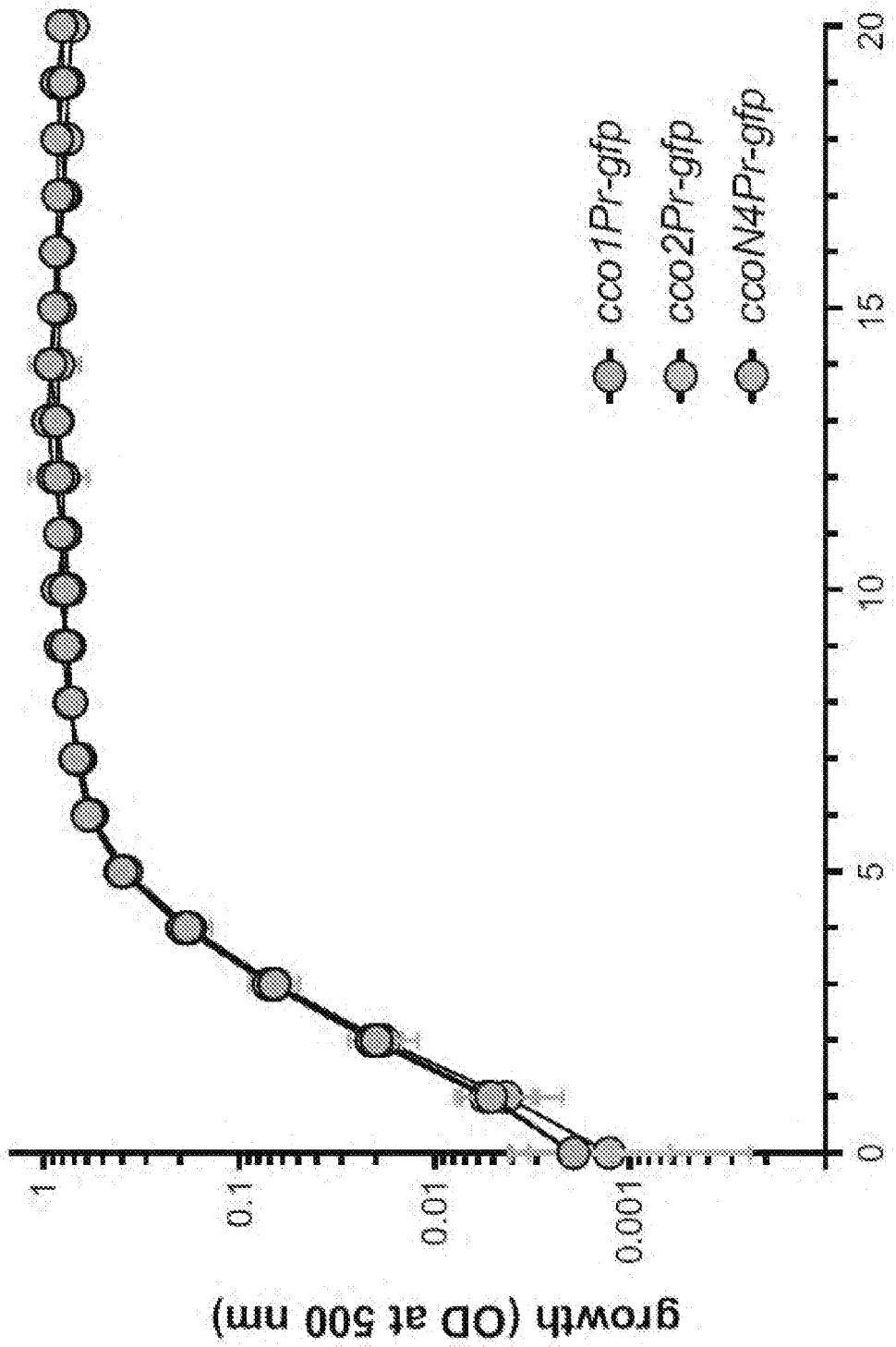

growth (OD at 500 nm)
1
0.1
0.01
0.001
0
5
10
15
20
time (hours)
cco1Pr-gfp
cco2Pr-gfp
ccoN4Pr-gfp

Figure 4(IB)

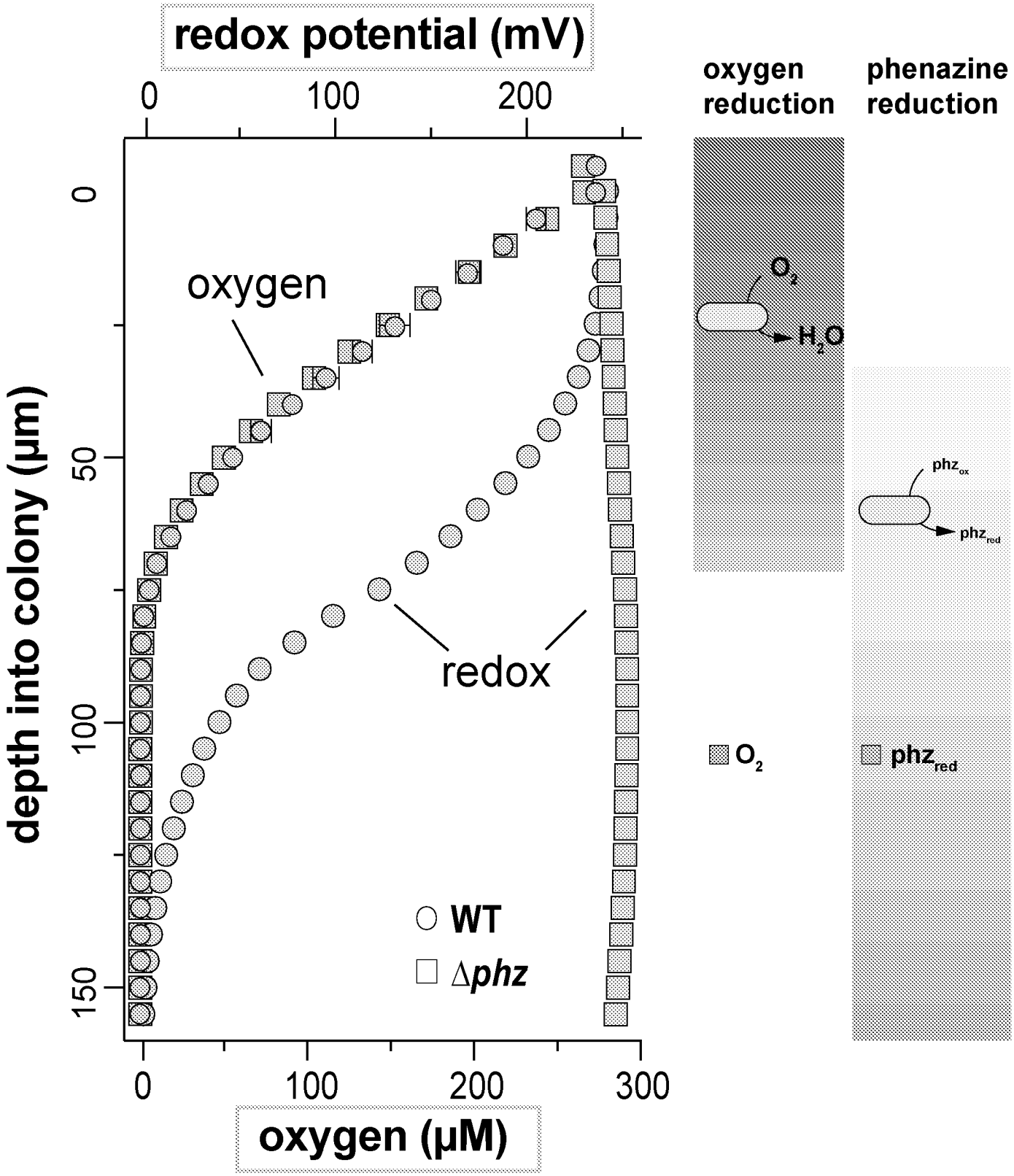

redox potential (mV)
0
100
200
oxygen
reduction
phenazine
reduction
oxygen
redox
depth into colony (µm)
0
50
100
150
O_2
H_2O
phz_{ox}
phz_{red}
WT
Δphz
O_2
phz_{red}
0
100
200
300
oxygen (µM)

Figure 5A

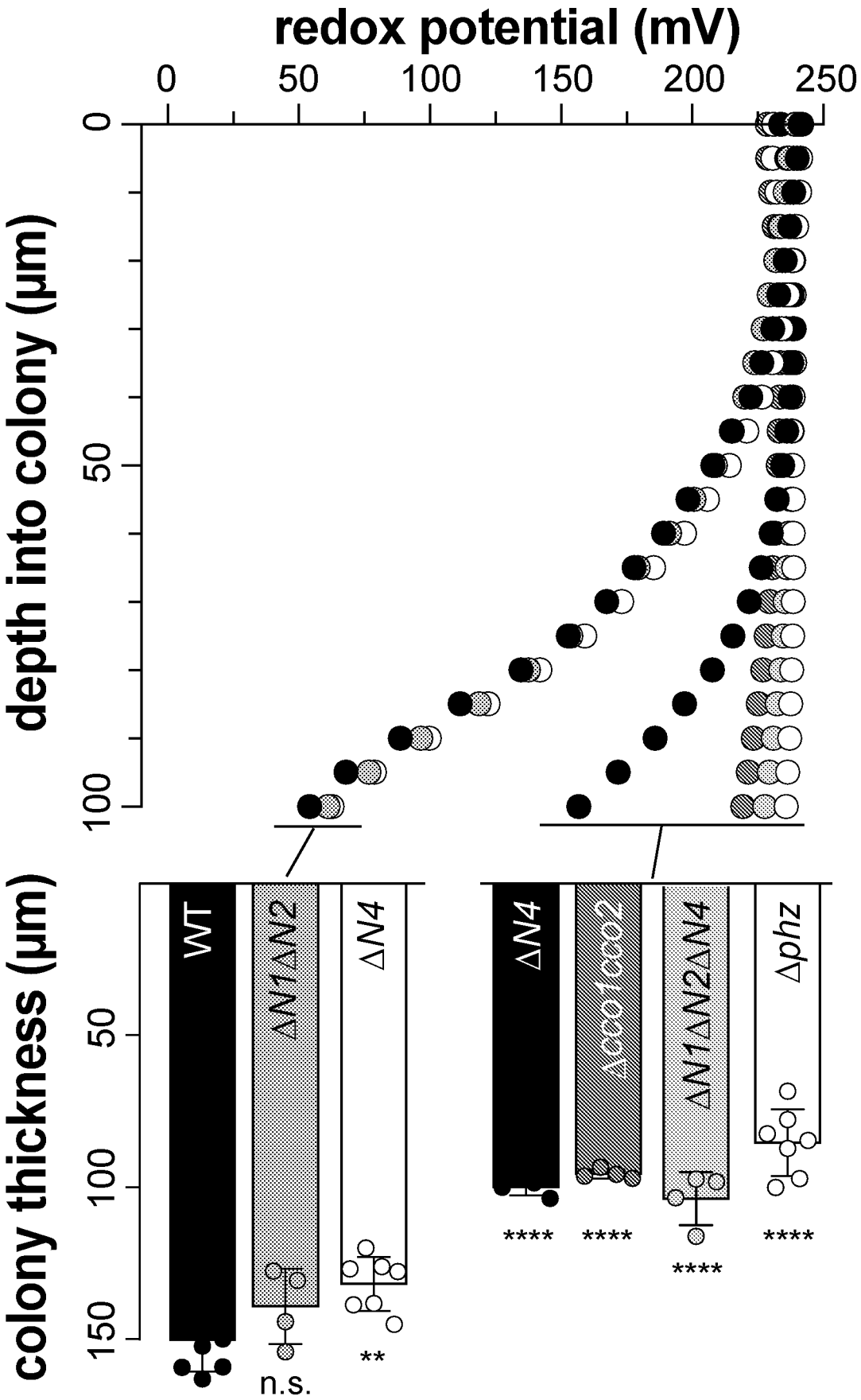

redox potential (mV)
0
50
100
150
200
250
depth into colony (µm)
0
50
100
colony thickness (µm)
50
100
150
WT
ΔN1ΔN2
ΔN4
ΔN4
Δeco1ecoA2
ΔN1ΔN2ΔN4
Δphz
n.s.
**
****
****
****
****

Figure 5B

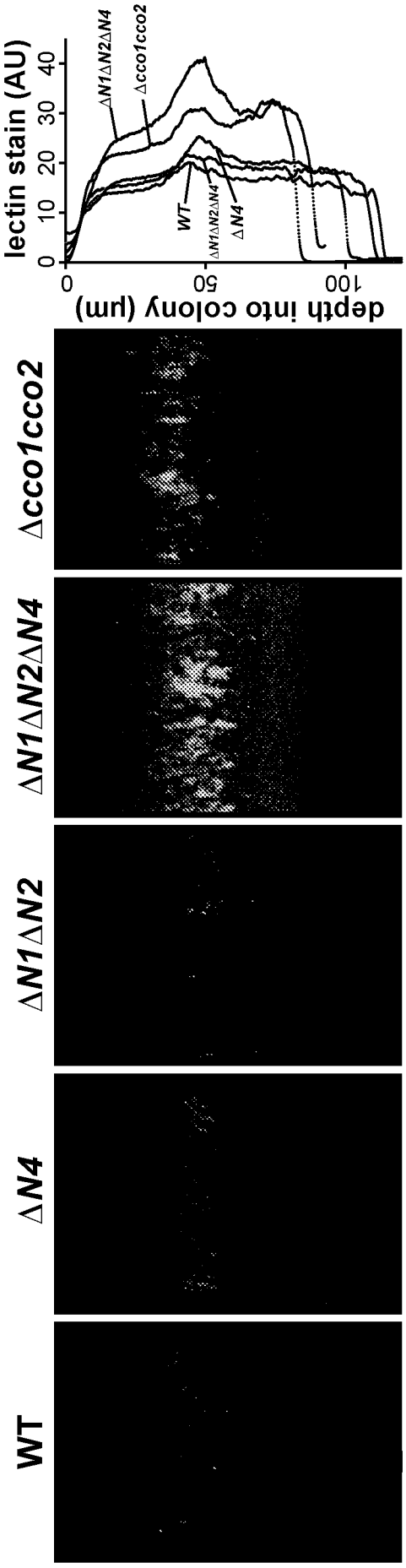

lectin stain (AU)
0
10
20
30
40
ΔN1ΔN2ΔN4
Δcco1cco2
WT
ΔN1ΔN2ΔN4
ΔN4
0
50
100
depth into colony (μm)
Δcco1cco2
ΔN1ΔN2ΔN4
ΔN1ΔN2
ΔN4
WT

Figure 5C

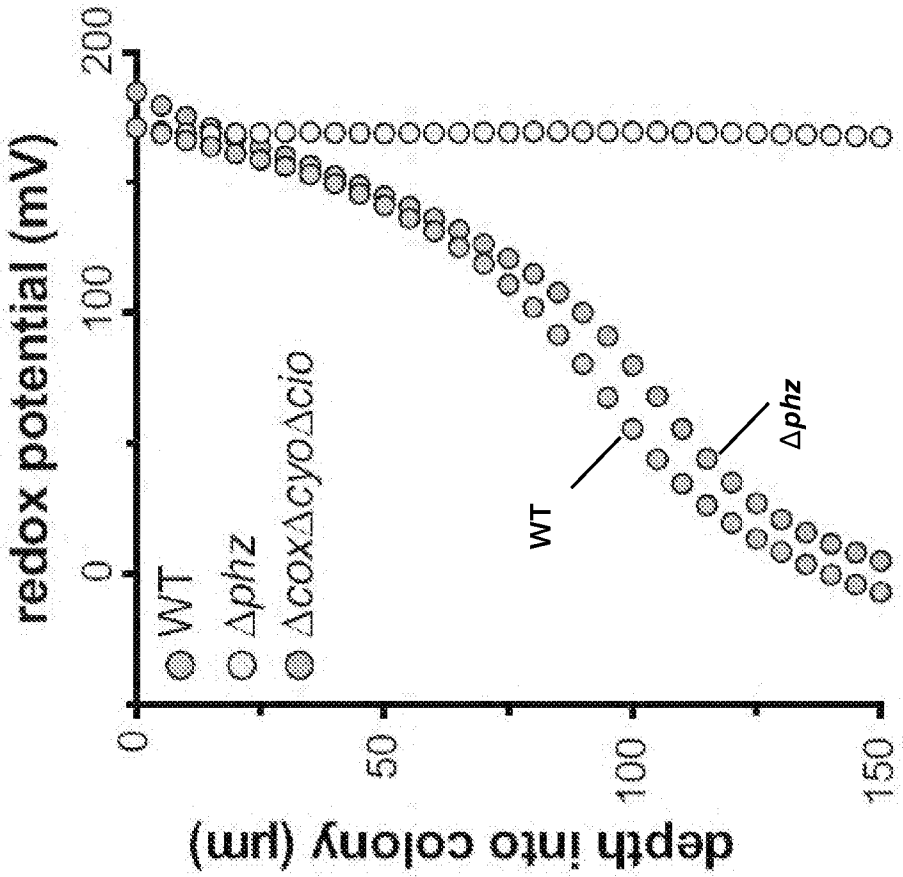


Figure 5(IB)

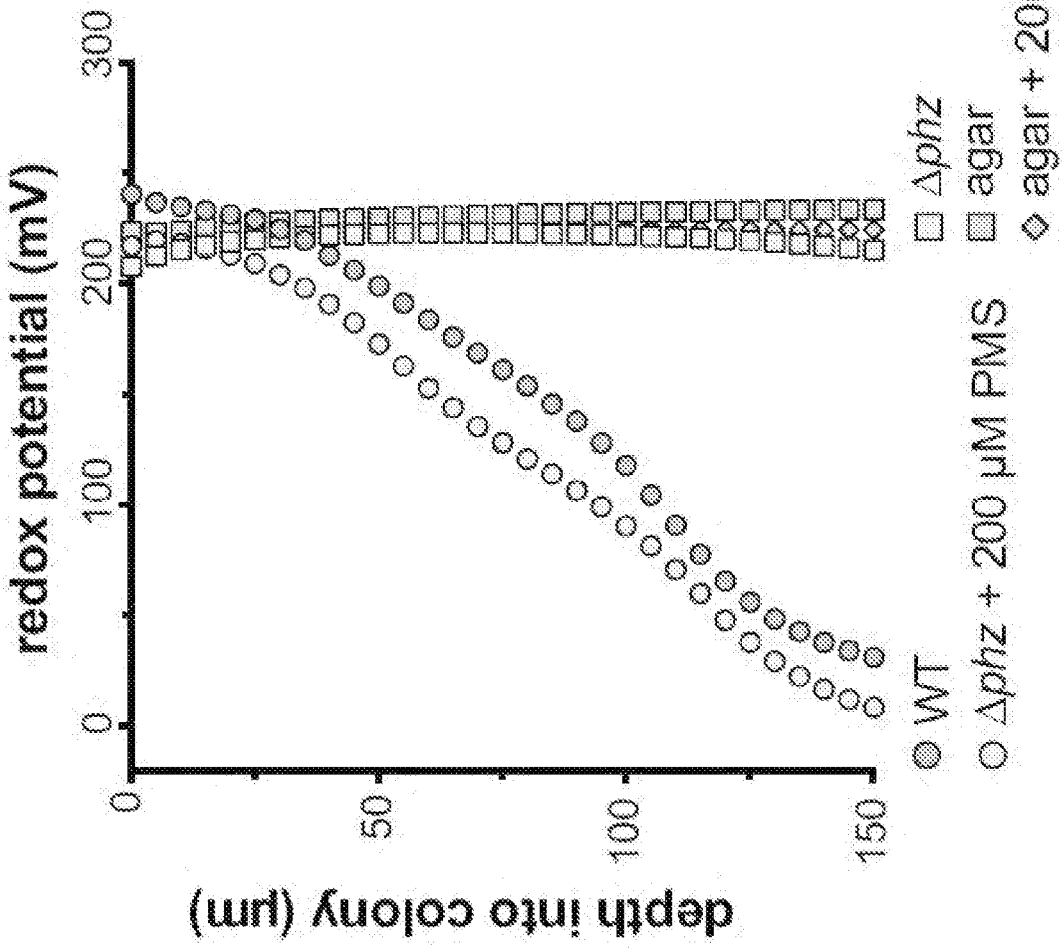


Figure 5(IA)

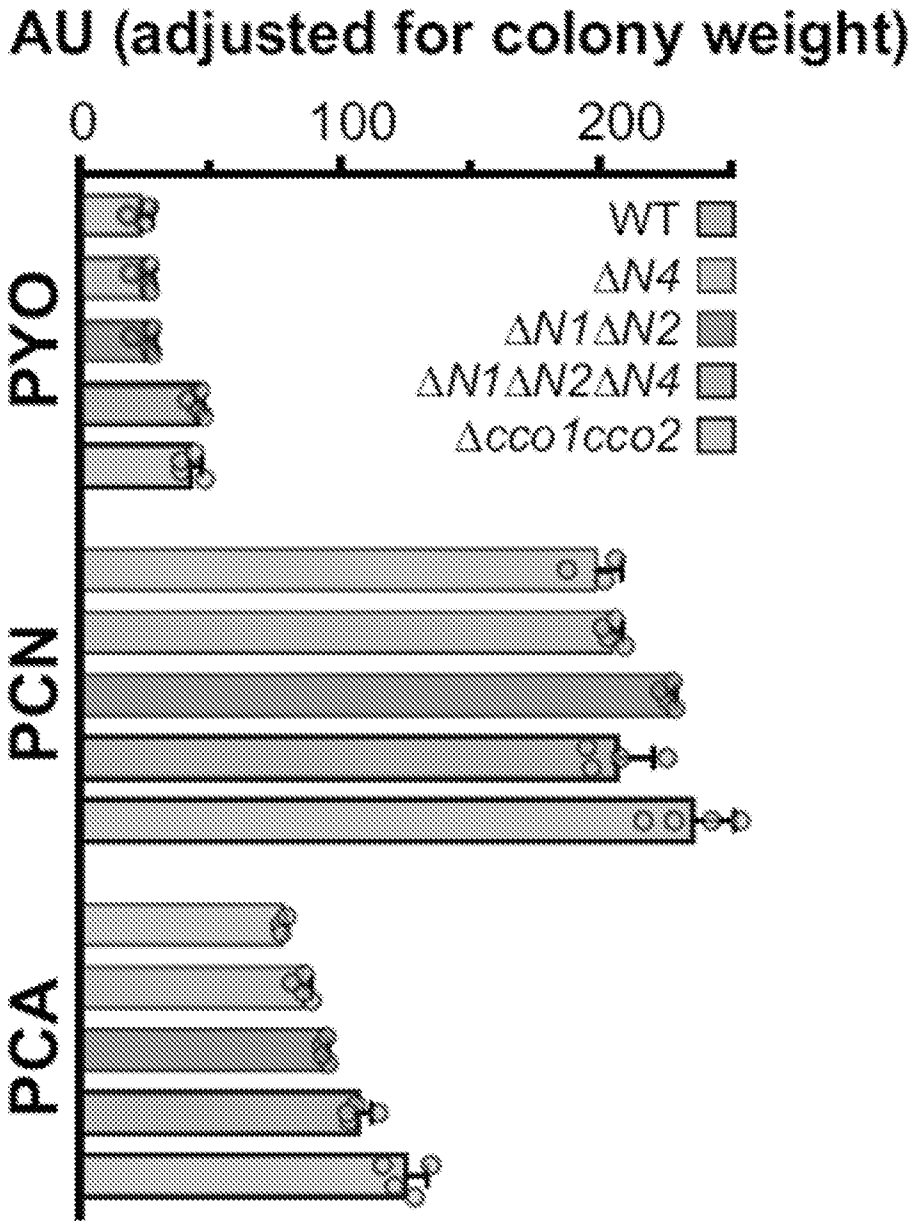

AU (adjusted for colony weight)
0
100
200
WT
ΔN4
ΔN1ΔN2
ΔN1ΔN2ΔN4
Δcco1cco2
PYO
PCN
PCA

Figure 5(IC)

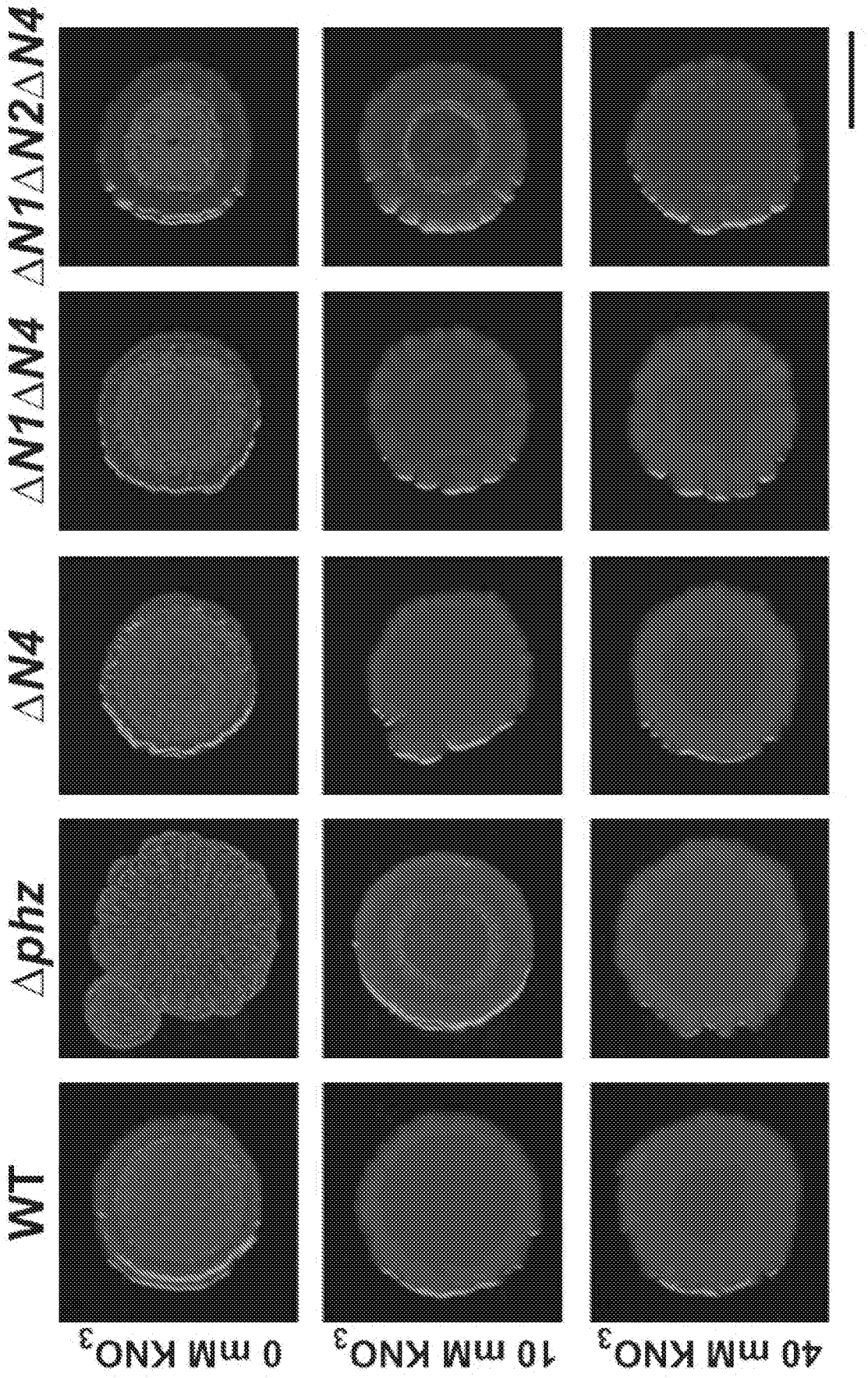


Figure 5(ID)

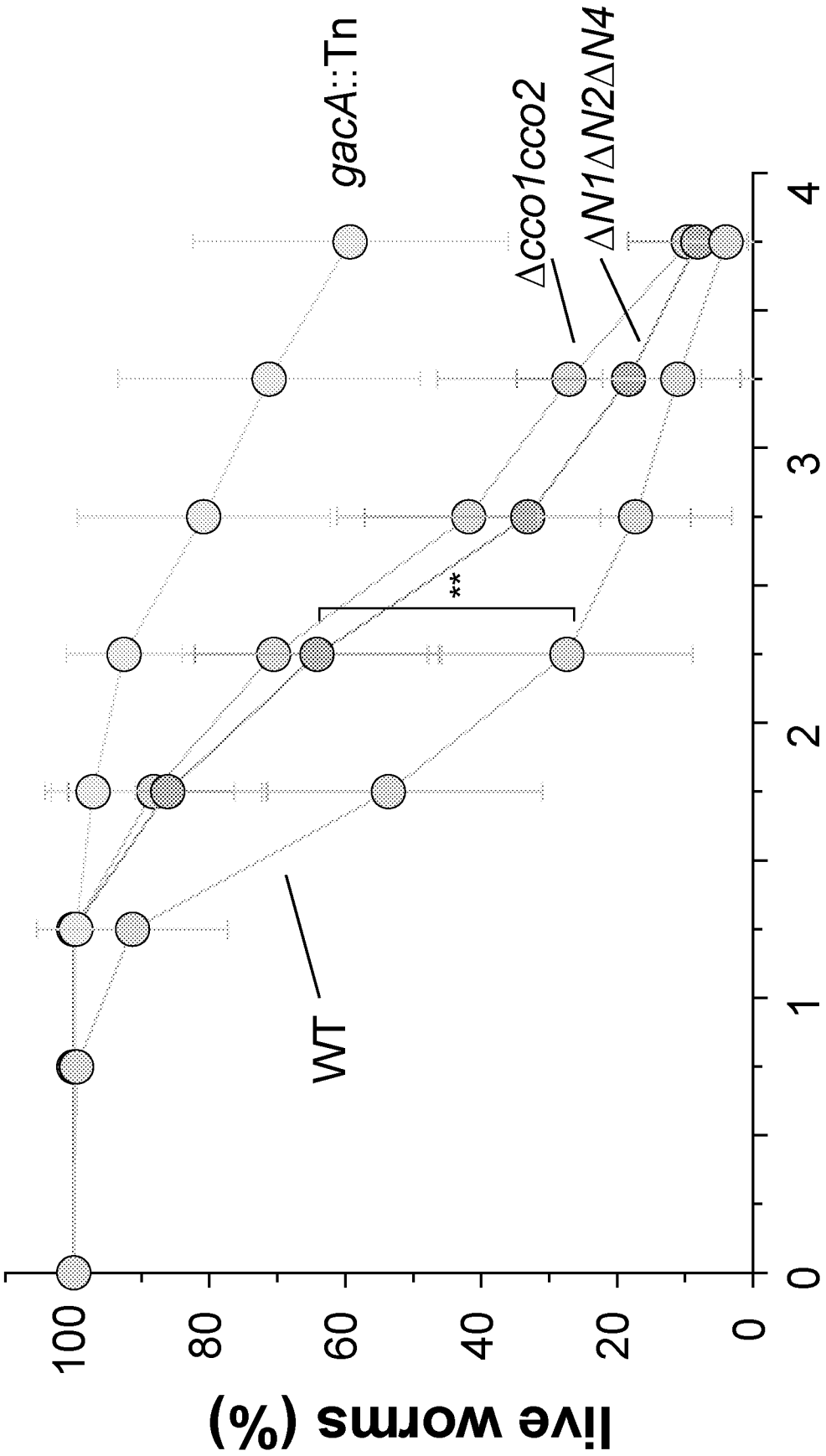

live worms (%)
100
80
60
40
20
0
0
1
2
3
4
time (days)
WT
gacA::Tn
Δcco1cco2
ΔN1ΔN2ΔN4
**

Figure 6A

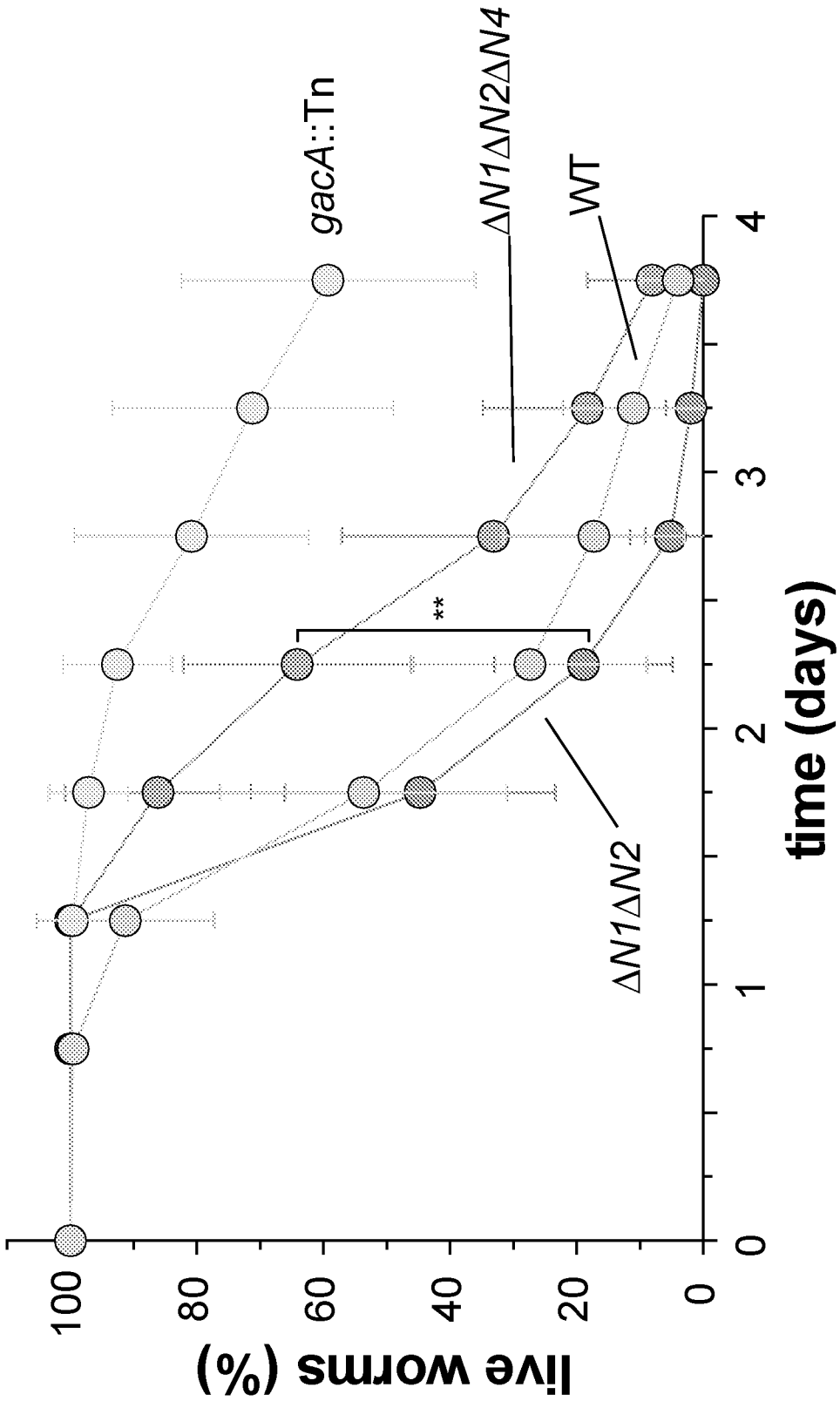

live worms (%)
100
80
60
40
20
0
0
1
2
3
4
time (days)
gacA::Tn
ΔN1ΔN2ΔN4
WT
ΔN1ΔN2
**

Figure 6B

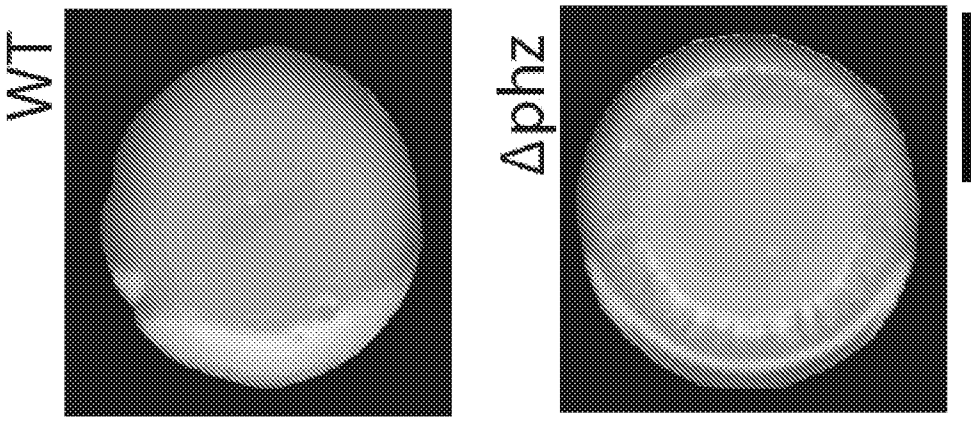


Figure 7A

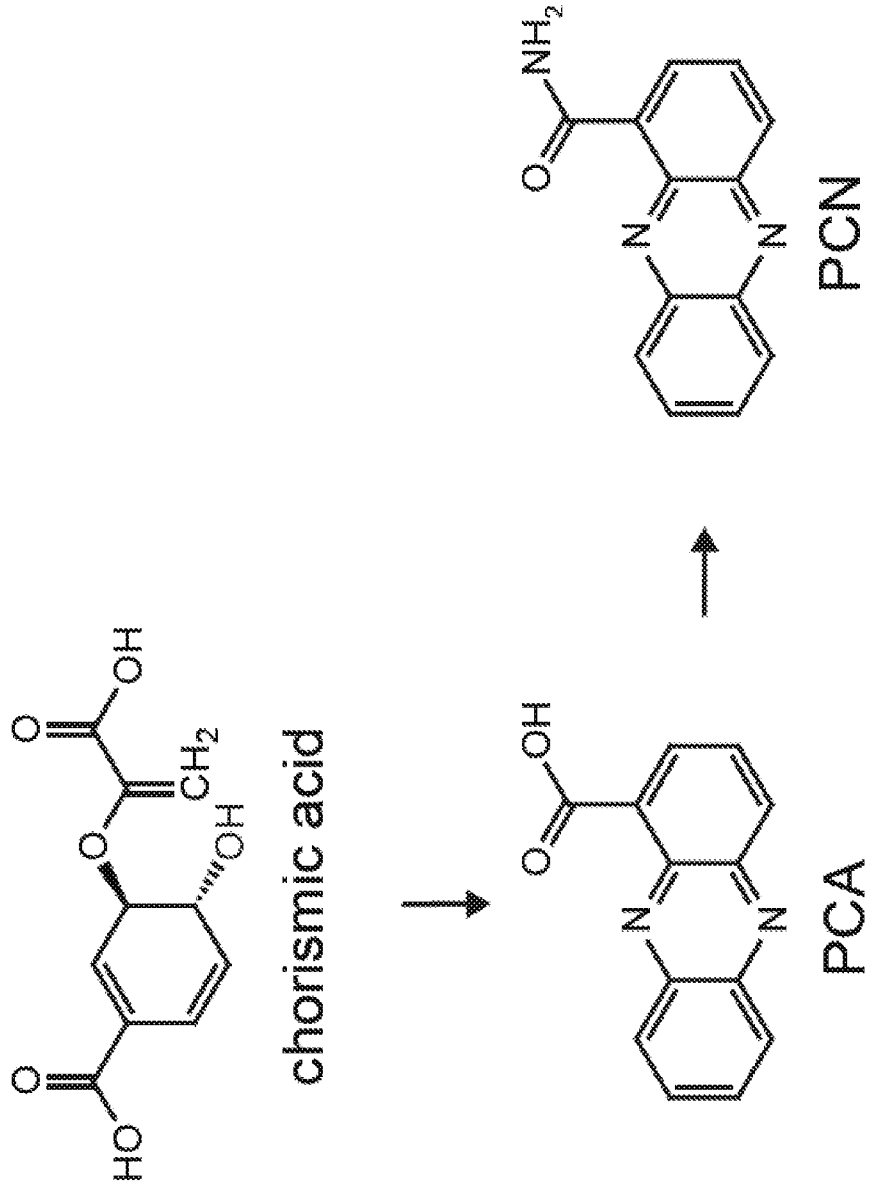


Figure 7B

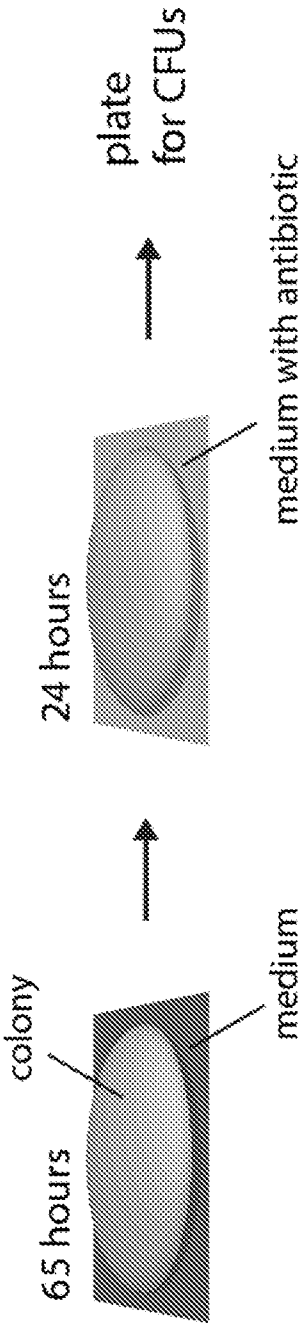

65 hours
colony
medium
24 hours
medium with antibiotic
plate
for CFUs

Figure 7C

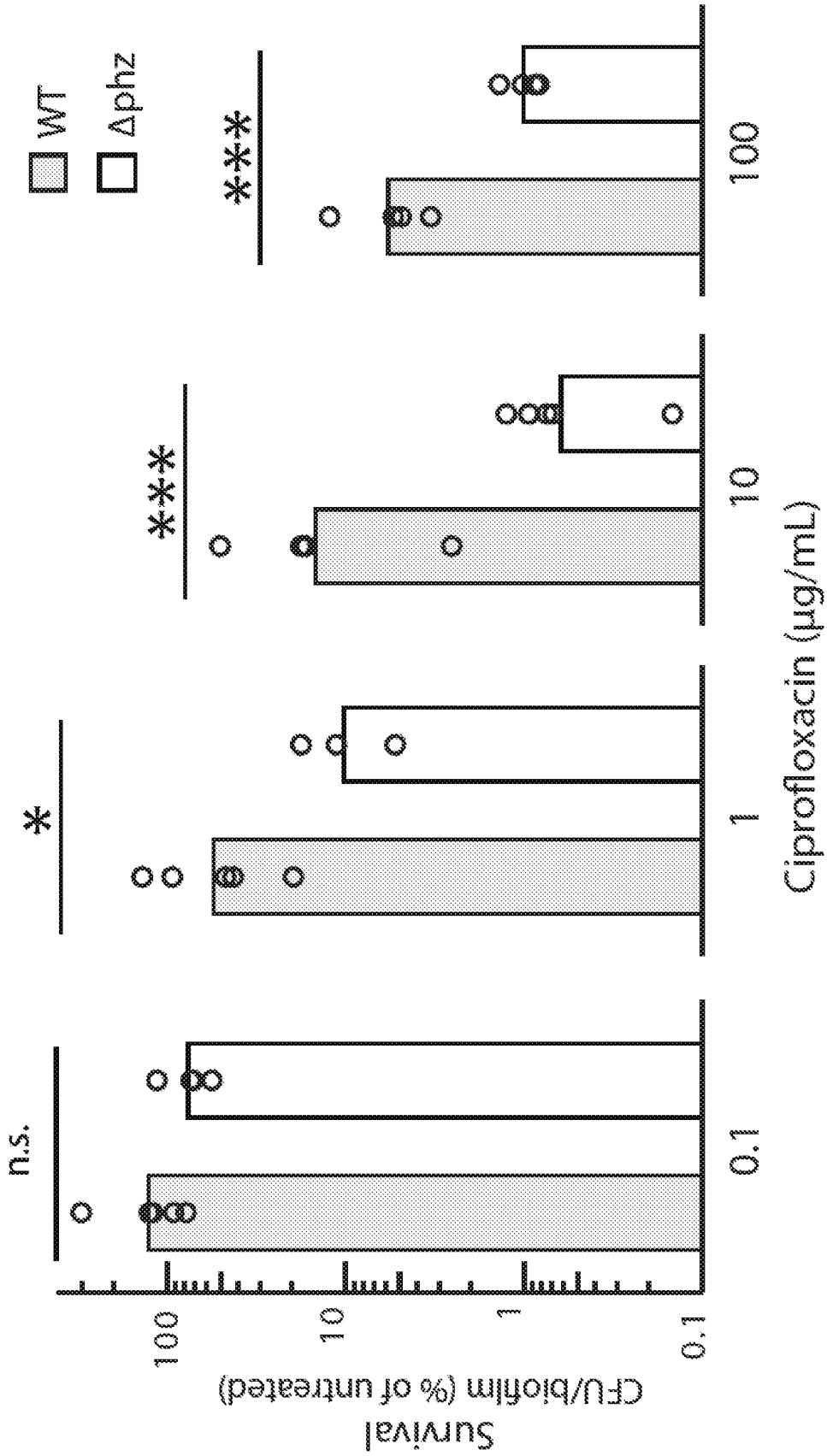

Survival
CFU/biofilm (% of untreated)
100
10
1
0.1
n.s.
*
***
****
WT
Δphz
0.1
1
10
100
Ciprofloxacin (μg/mL)

Figure 7D



Figure 8A

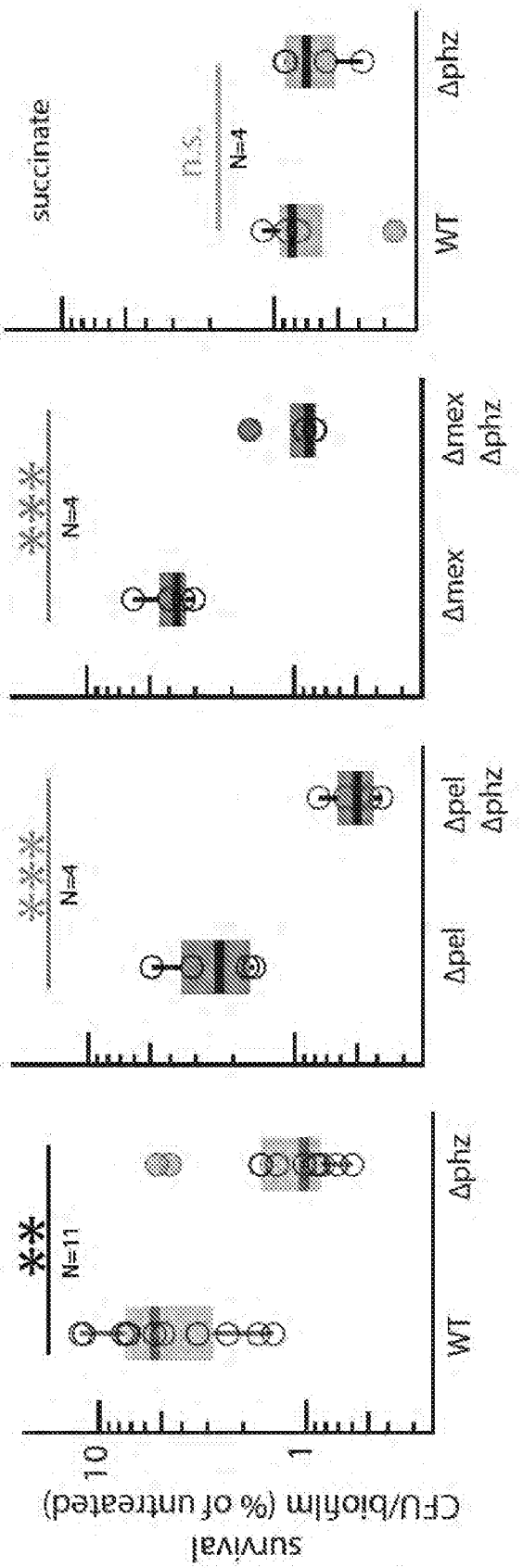


Figure 8B

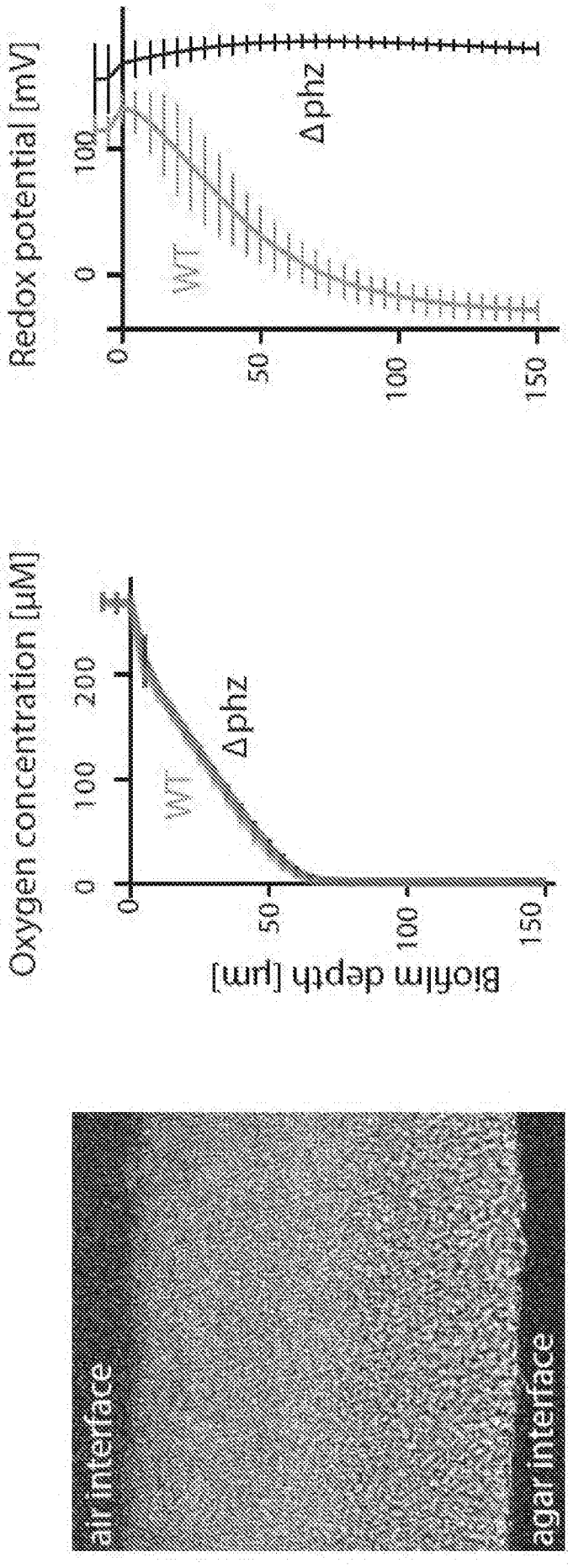

Redox potential [mV]
100
0
0
50
100
150
WT
Δphz
Oxygen concentration [μM]
0
100
200
0
50
100
150
WT
Δphz
Biofilm depth [μm]
air interface
agar interface

Figure 9A

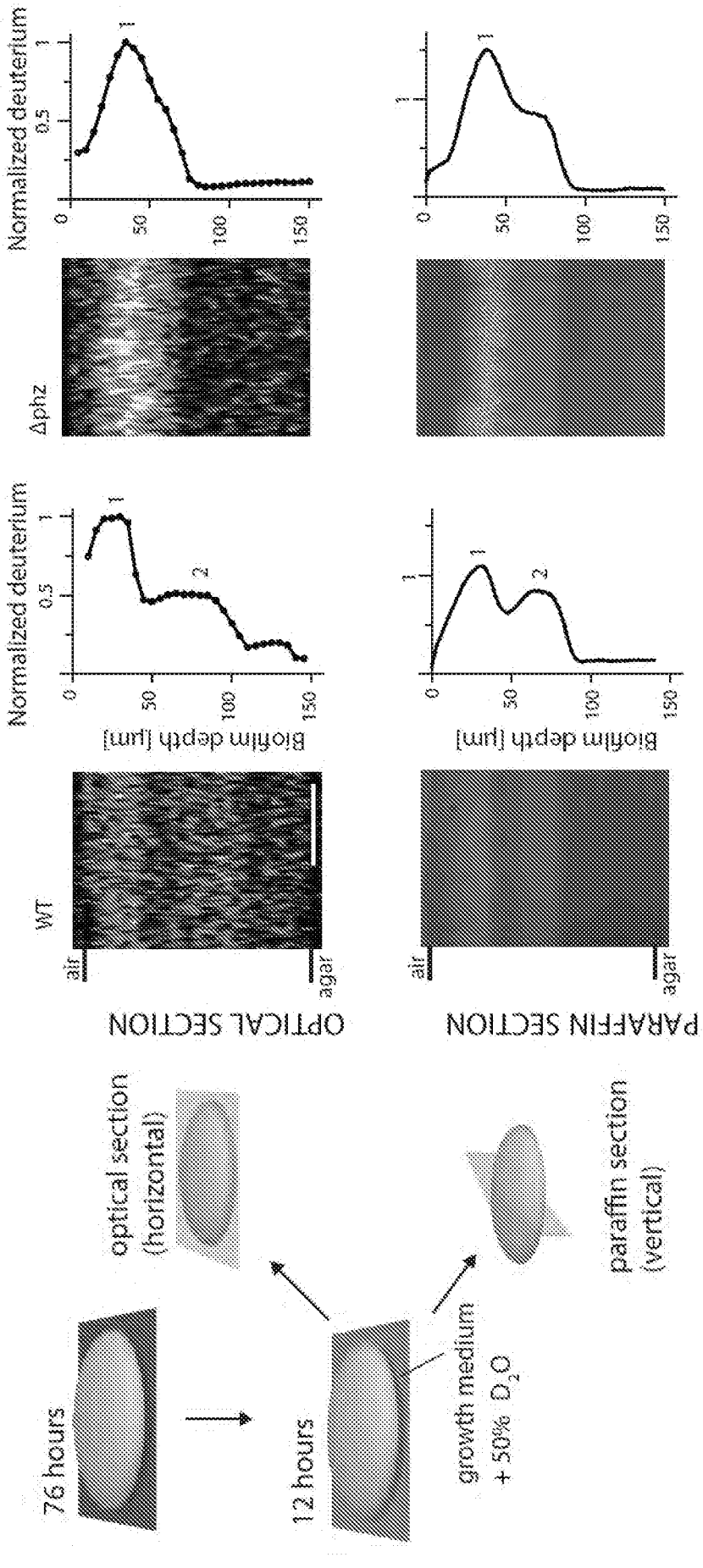

76 hours
12 hours
growth medium
+ 50% D_2O
optical section
(horizontal)
paraffin section
(vertical)
OPTICAL SECTION
PARAFFIN SECTION
WT
Δphz
air
agar
Normalized deuterium
Biofilm depth [μm]
0
0.5
1
50
100
150
1
2

Figure 9B

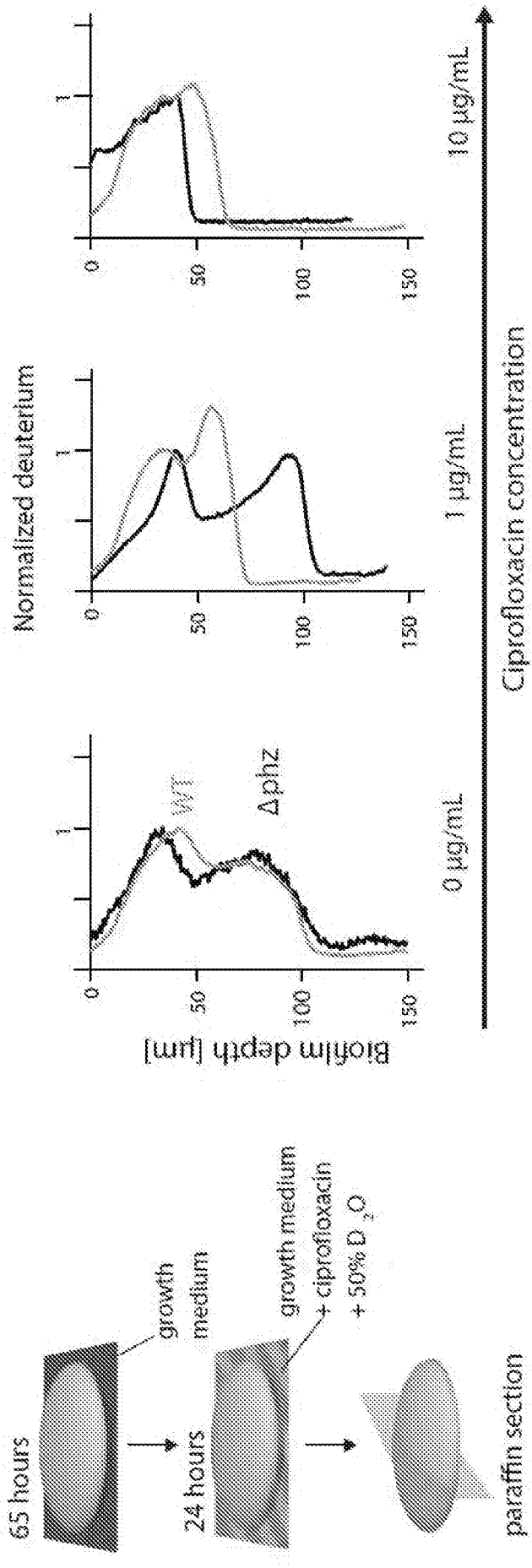

65 hours
growth medium
24 hours
growth medium + ciprofloxacin + 50% D2O
paraffin section
Biofilm depth [µm]
Normalized deuterium
WT
Δphz
0 µg/mL
1 µg/mL
10 µg/mL
Ciprofloxacin concentration

Figure 9C

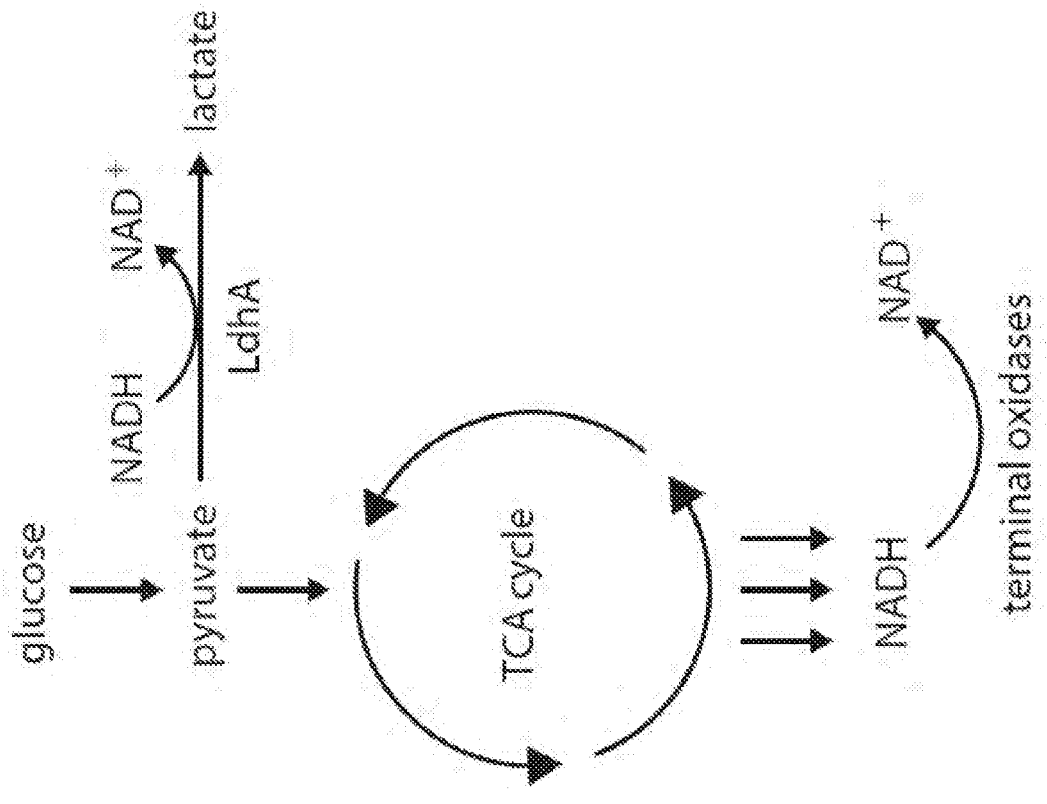


Figure 10A

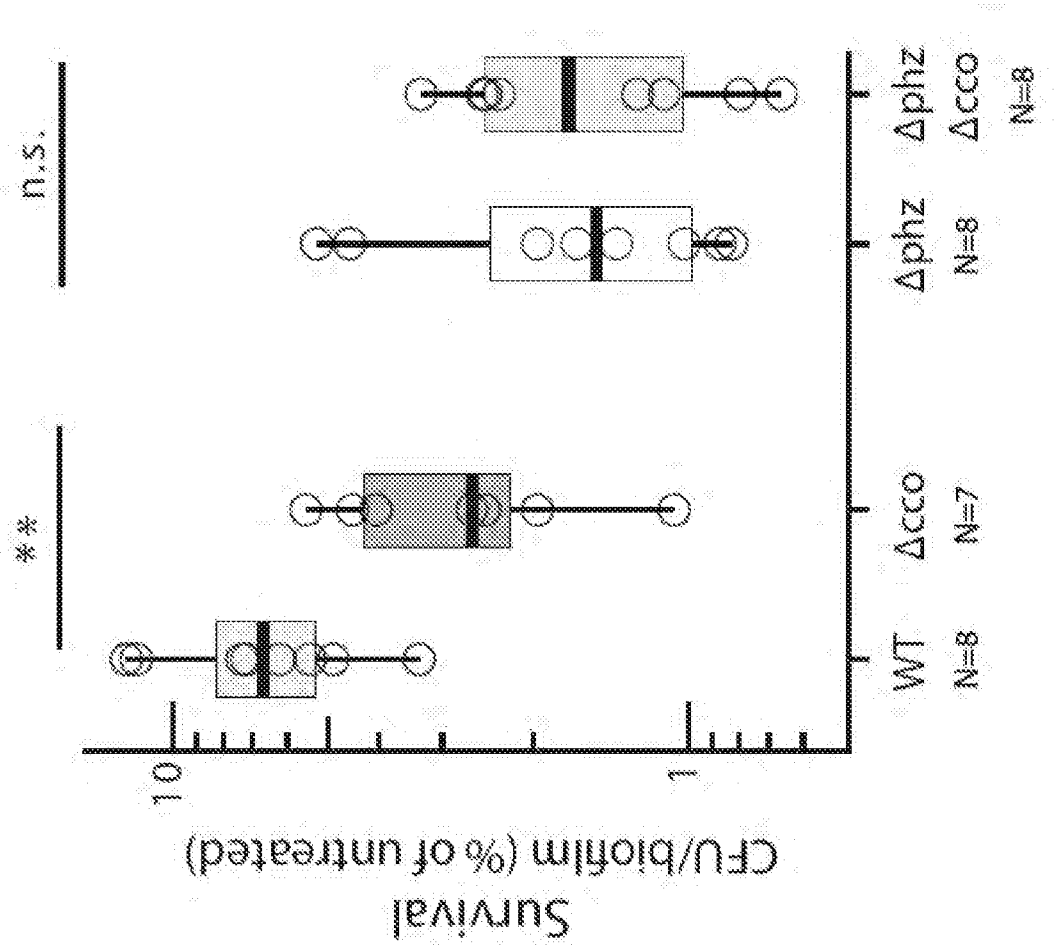


Figure 10B

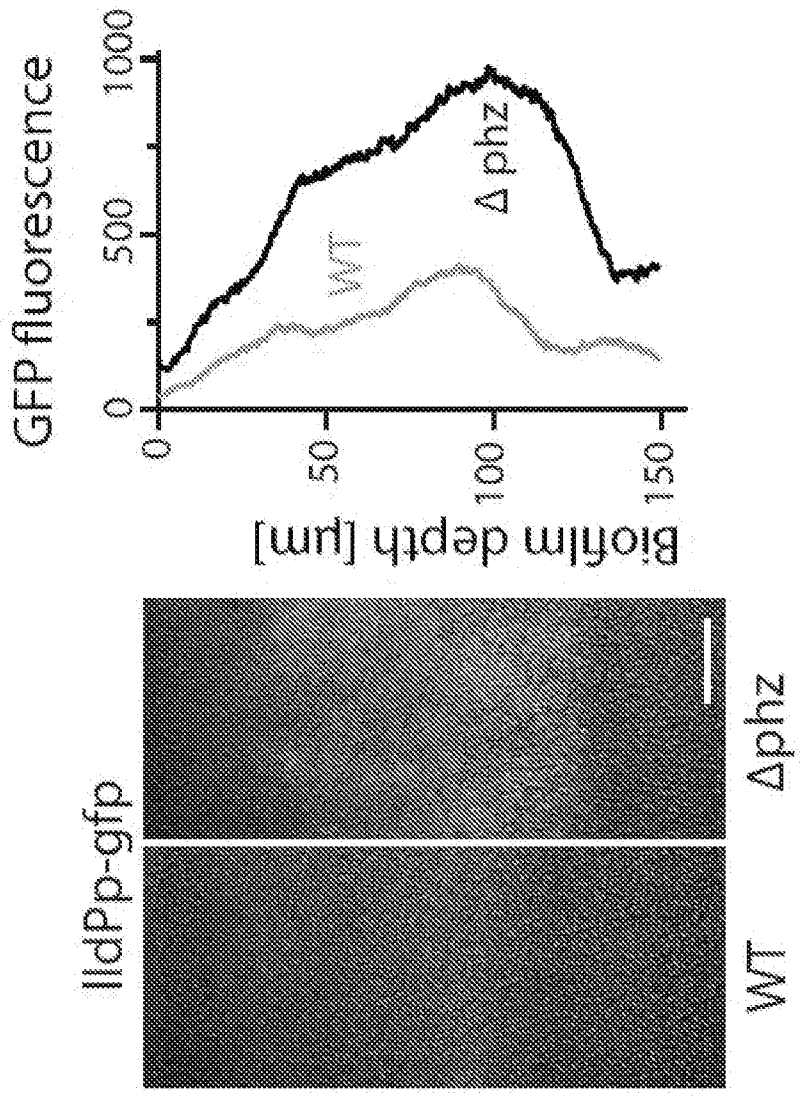

GFP fluorescence
0
500
1000
WT
Δ phz
0
50
100
150
Biofilm depth [μm]
lldPp-gfp
WT
Δphz

Figure 10C

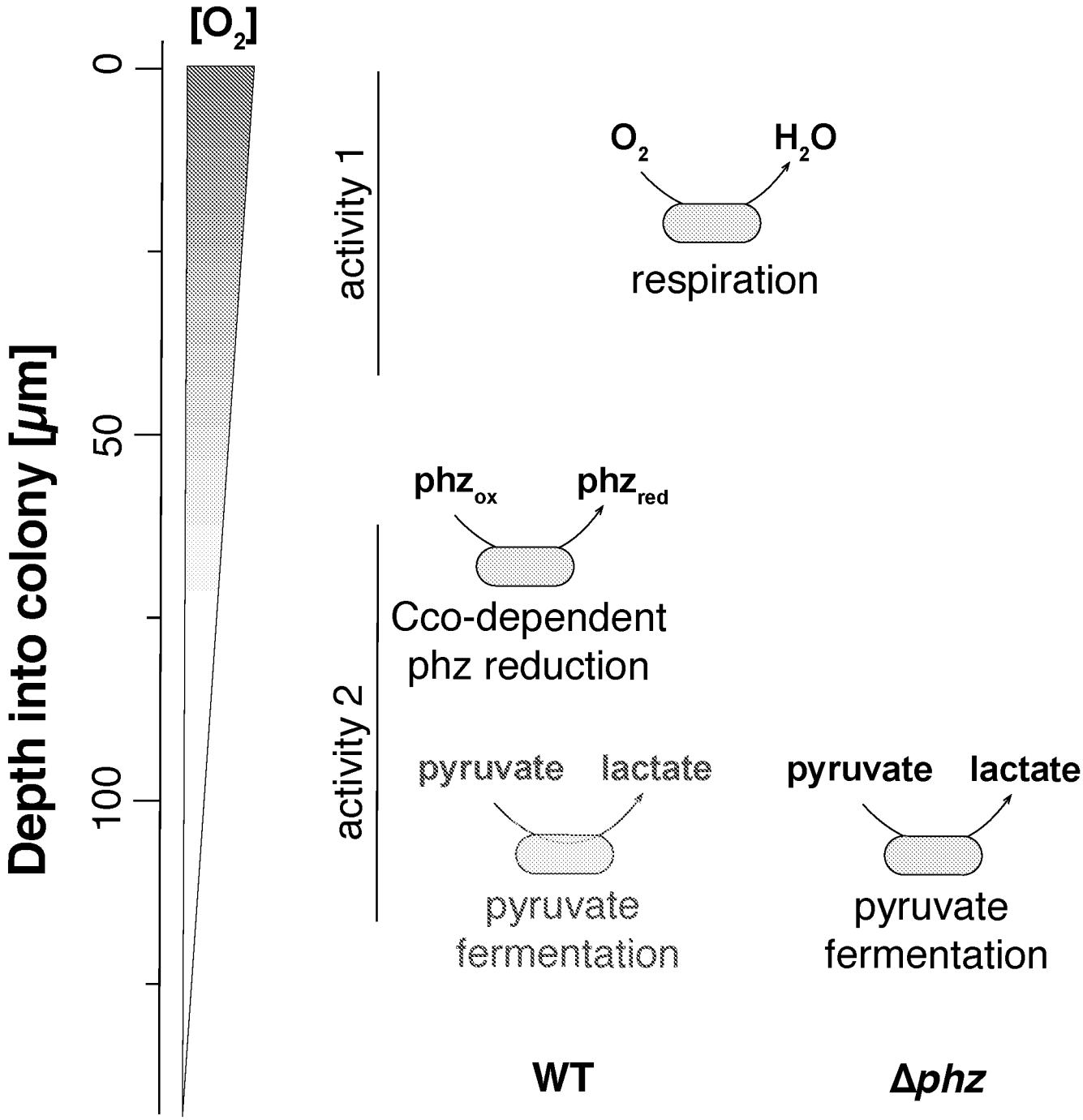

[O2]
0
50
100
Depth into colony [μm]
activity 1
activity 2
O2
H2O
respiration
phzox
phzred
Cco-dependent
phz reduction
pyruvate
lactate
pyruvate
fermentation
pyruvate
lactate
pyruvate
fermentation
WT
Δphz

Figure 10D

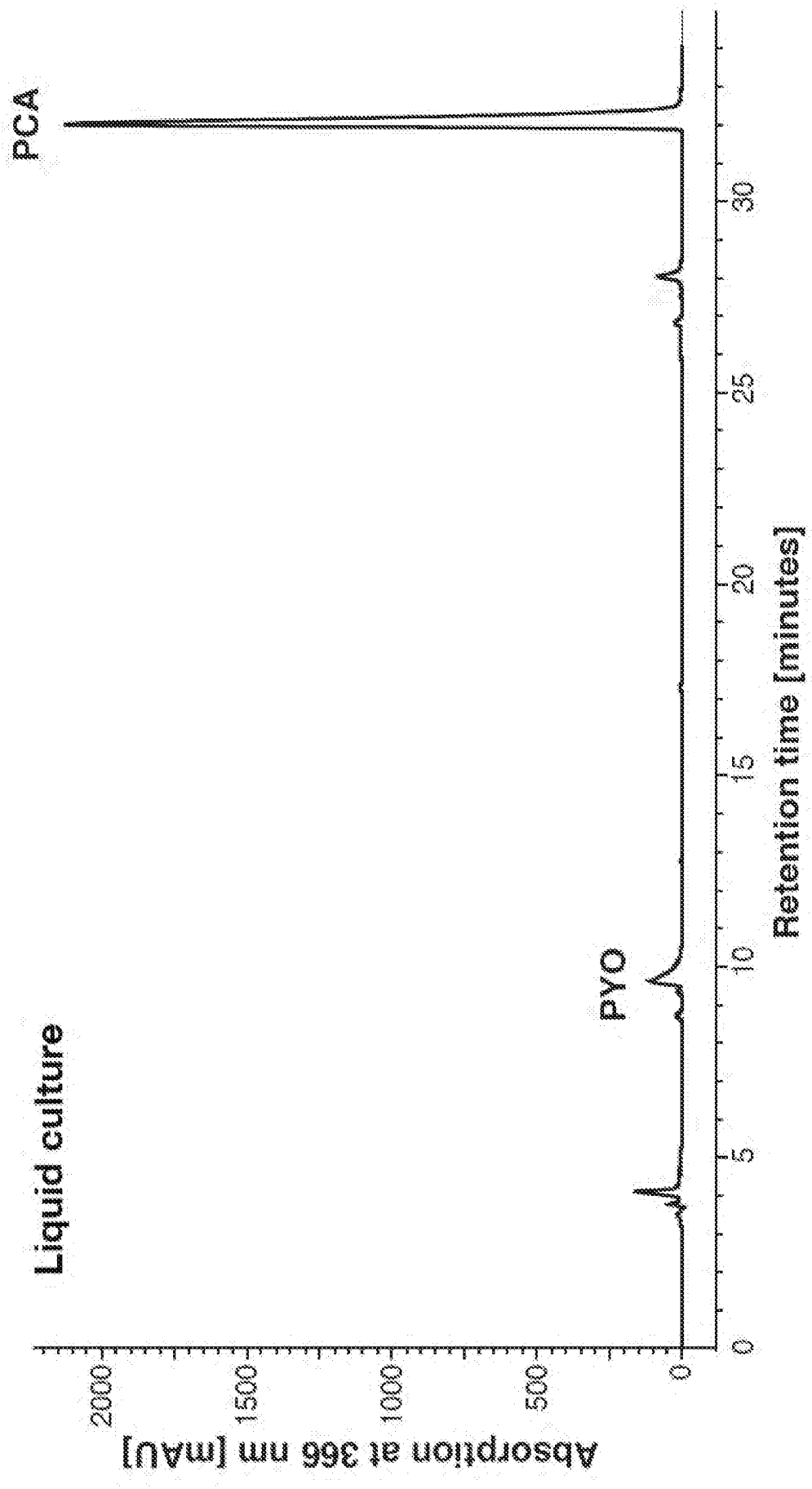

Liquid culture
PCA
PYO
Absorption at 366 nm [mAU]
2000
1500
1000
500
0
0
5
10
15
20
25
30
Retention time [minutes]

Figure 11A

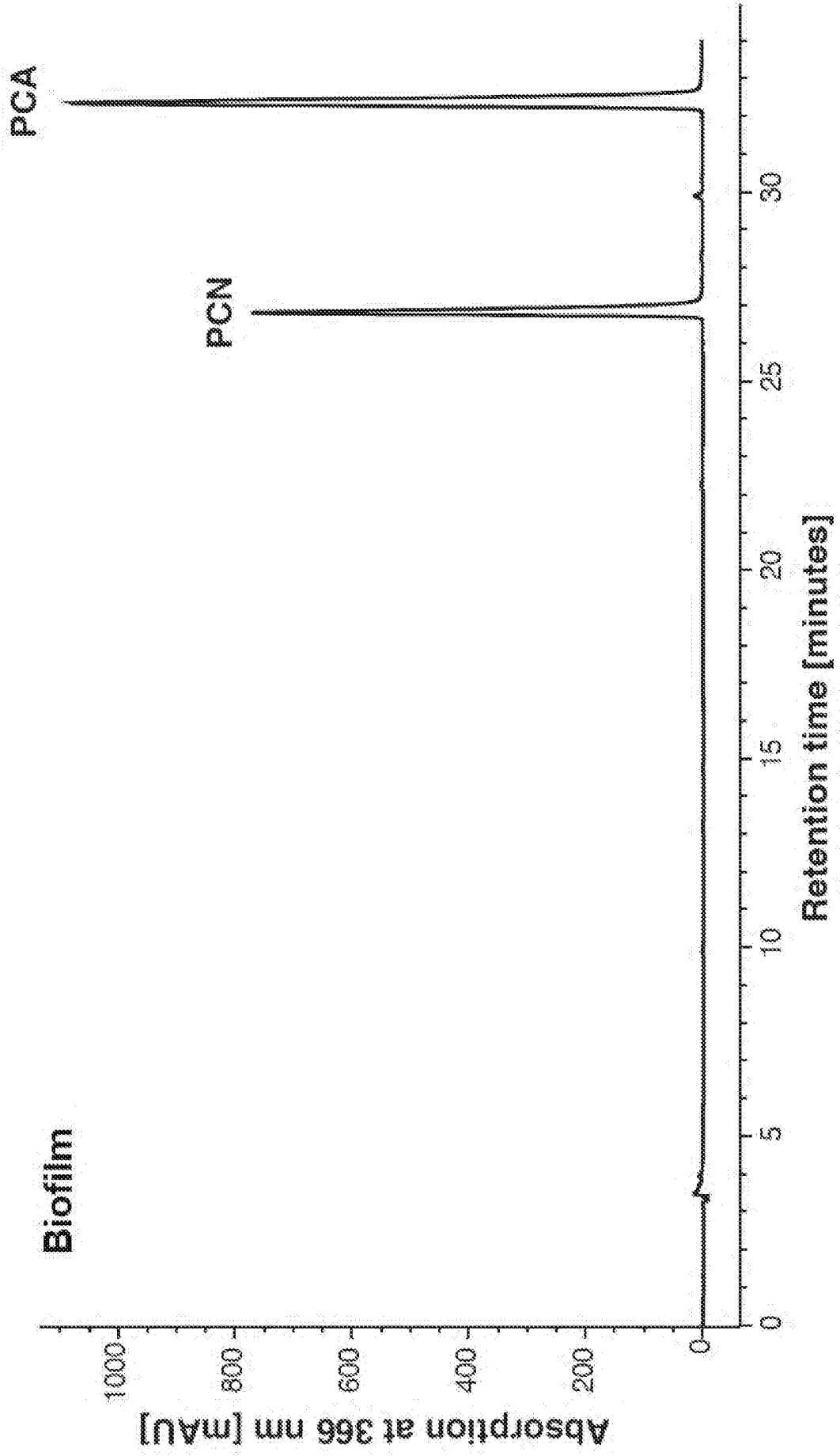

Biofilm
PCN
PCA
Absorption at 366 nm [mAU]
1000
800
600
400
200
0
0
5
10
15
20
25
30
Retention time [minutes]

Figure 11B

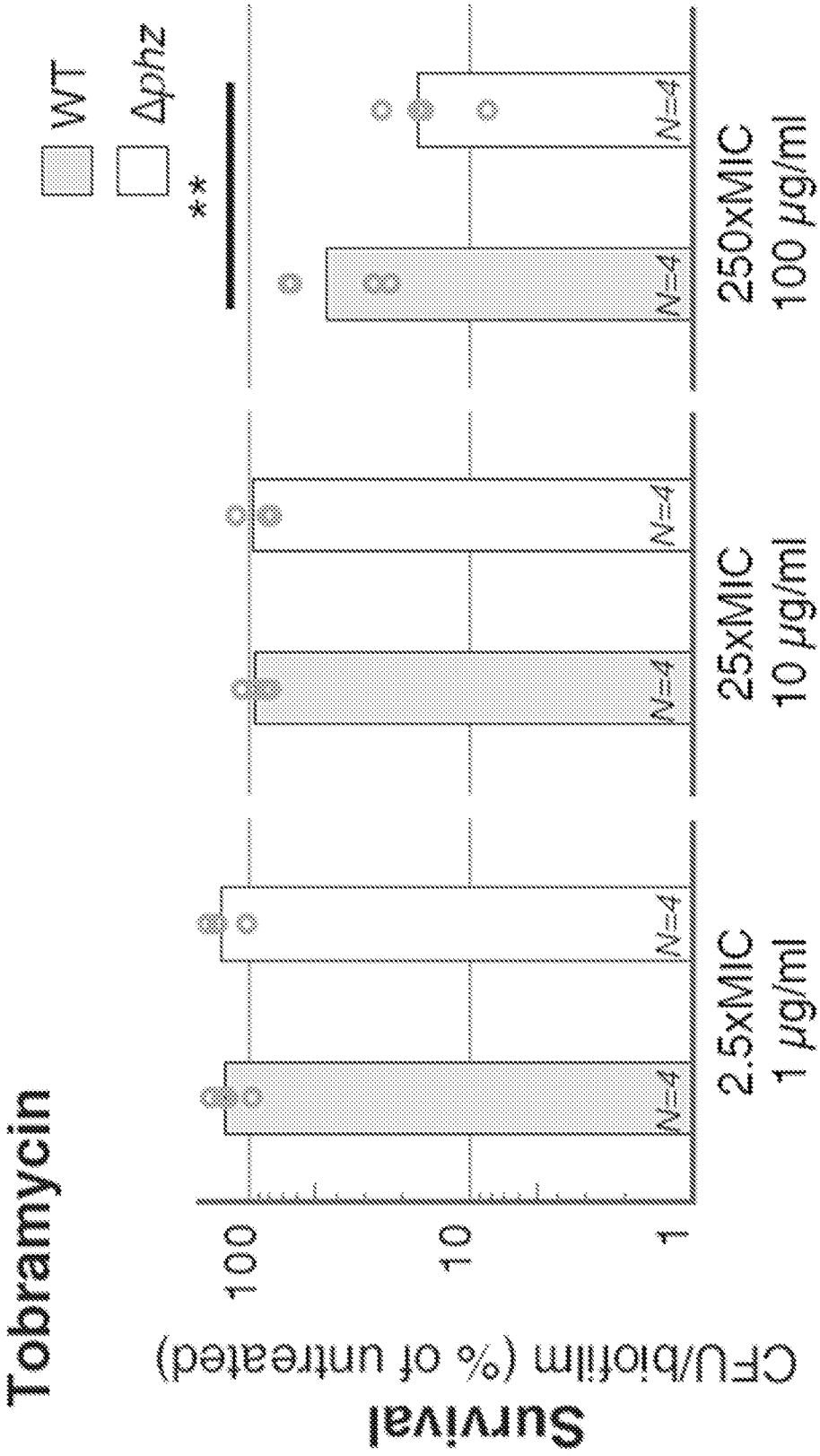

Tobramycin
Survival
CFU/biofilm (% of untreated)
100
10
1
WT
Δphz
**
N=4
2.5xMIC
1 μg/ml
25xMIC
10 μg/ml
250xMIC
100 μg/ml

Figure 12A

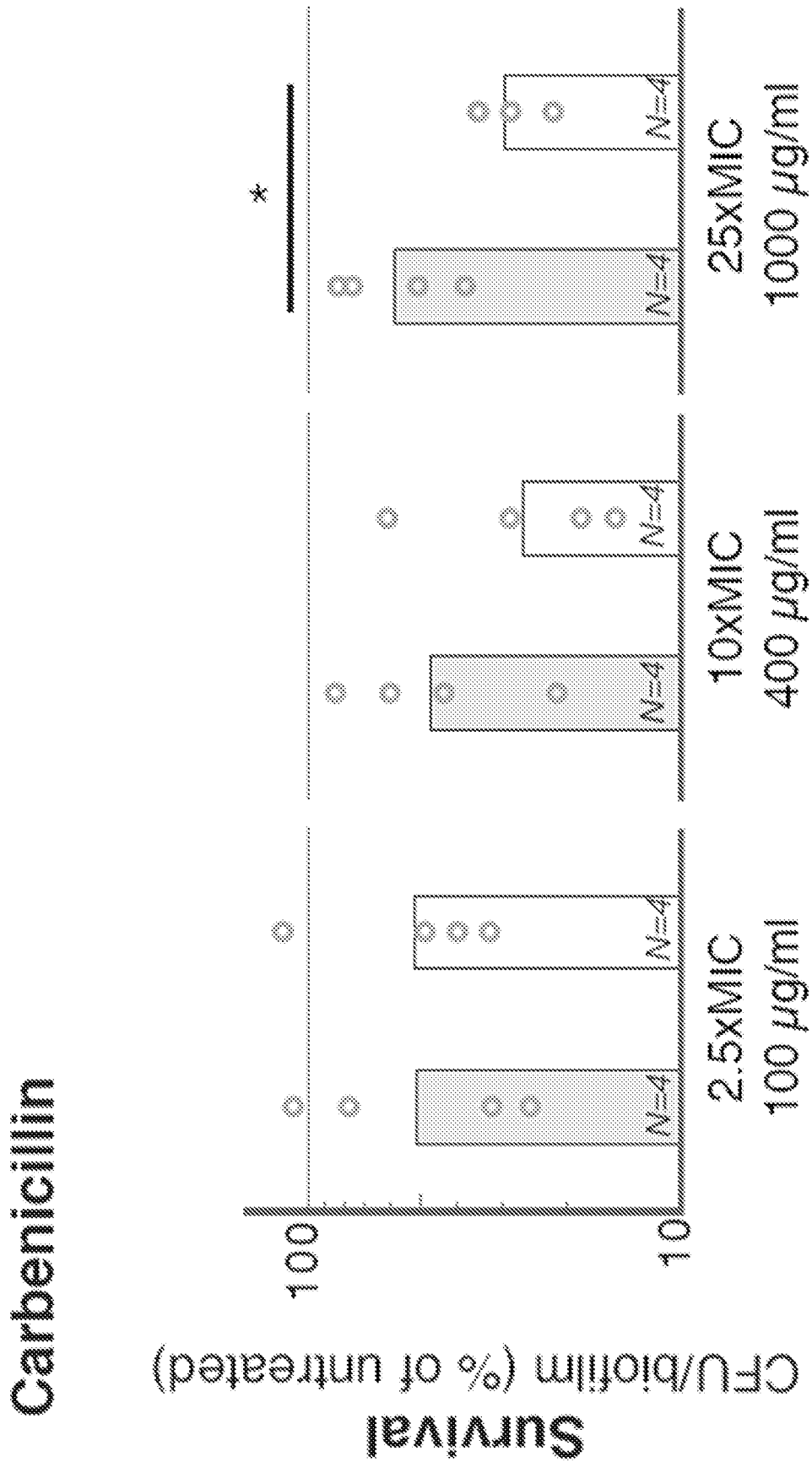

Carbenicillin
Survival
CFU/biofilm (% of untreated)
100
10
N=4
N=4
N=4
N=4
N=4
N=4
*
2.5xMIC
100 µg/ml
10xMIC
400 µg/ml
25xMIC
1000 µg/ml

Figure 12B

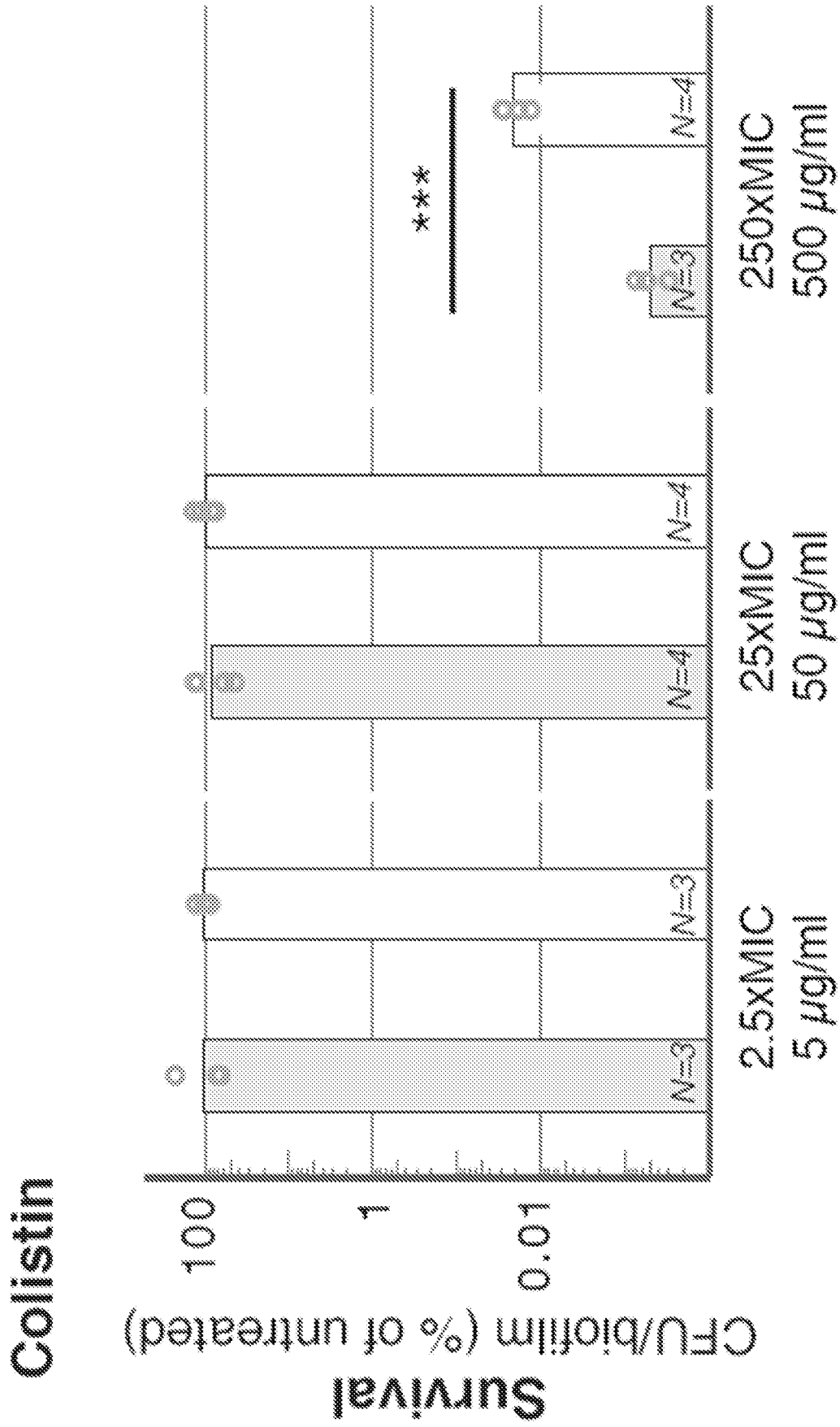

Colistin
Survival
CFU/biofilm (% of untreated)
100
1
0.01
N=3
N=3
N=4
N=4
N=4
N=3
***
2.5xMIC
5 μg/ml
25xMIC
50 μg/ml
250xMIC
500 μg/ml

Figure 12C

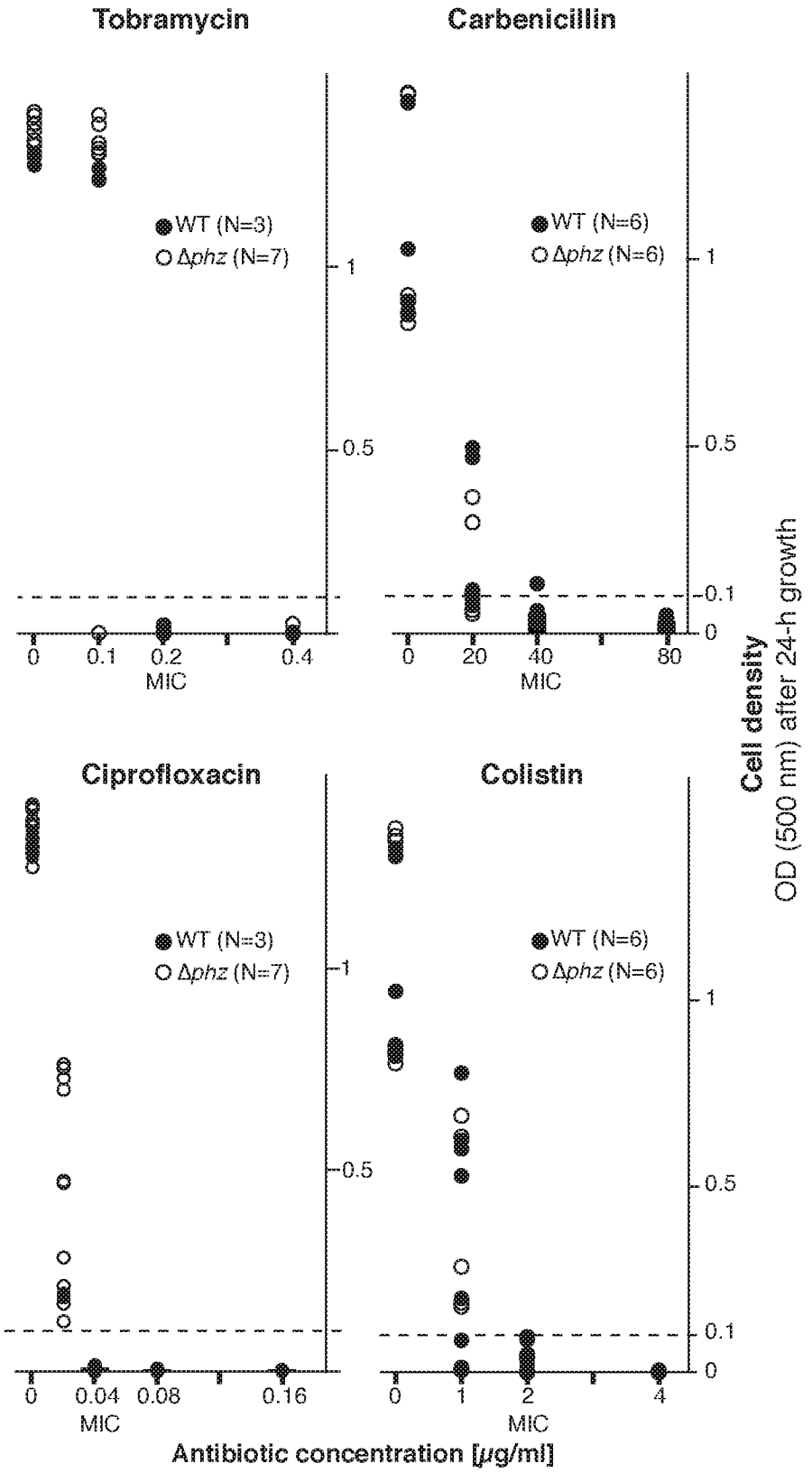

Tobramycin
Carbenicillin
WT (N=3)
Δphz (N=7)
WT (N=6)
Δphz (N=6)
1
0.5
0.1
0
0
0.1
0.2
0.4
0
20
40
80
MIC
MIC
Ciprofloxacin
Colistin
WT (N=3)
Δphz (N=7)
WT (N=6)
Δphz (N=6)
1
0.5
0.1
0
0
0.04
0.08
0.16
0
1
2
4
MIC
MIC
Cell density
OD (500 nm) after 24-h growth
Antibiotic concentration [μg/ml]

Figure 12D

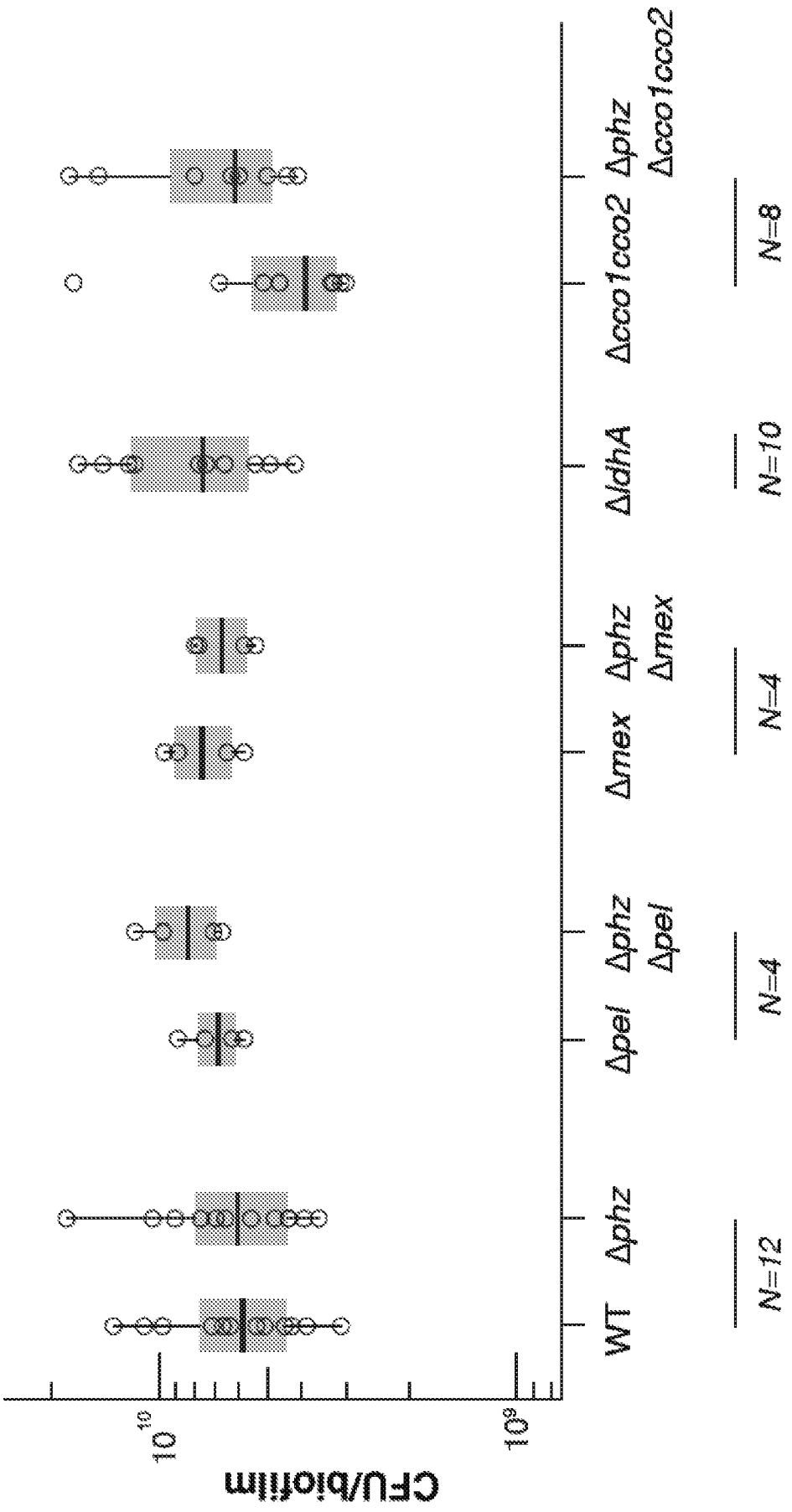

CFU/biofilm
10^{10}
10^{9}
WT
Δphz
Δpel
Δpel Δphz
Δmex
Δmex Δphz
ΔldhA
Δcco1cco2
Δcco1cco2 Δphz
N=12
N=4
N=4
N=4
N=10
N=8

Figure 13

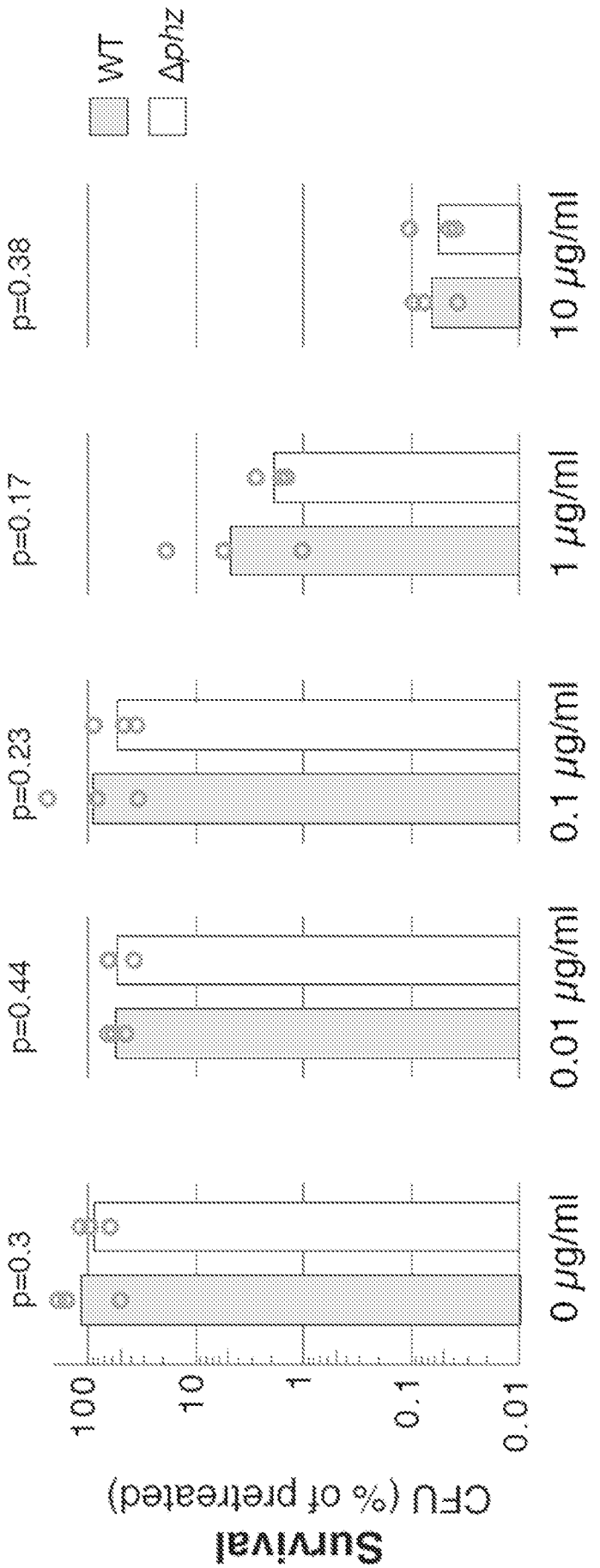

WT
Δphz
p=0.38
p=0.17
p=0.23
p=0.44
p=0.3
100
10
1
0.1
0.01
Survival
CFU (% of pretreated)
0 μg/ml
0.01 μg/ml
0.1 μg/ml
1 μg/ml
10 μg/ml
Ciprofloxacin concentration

Figure 14

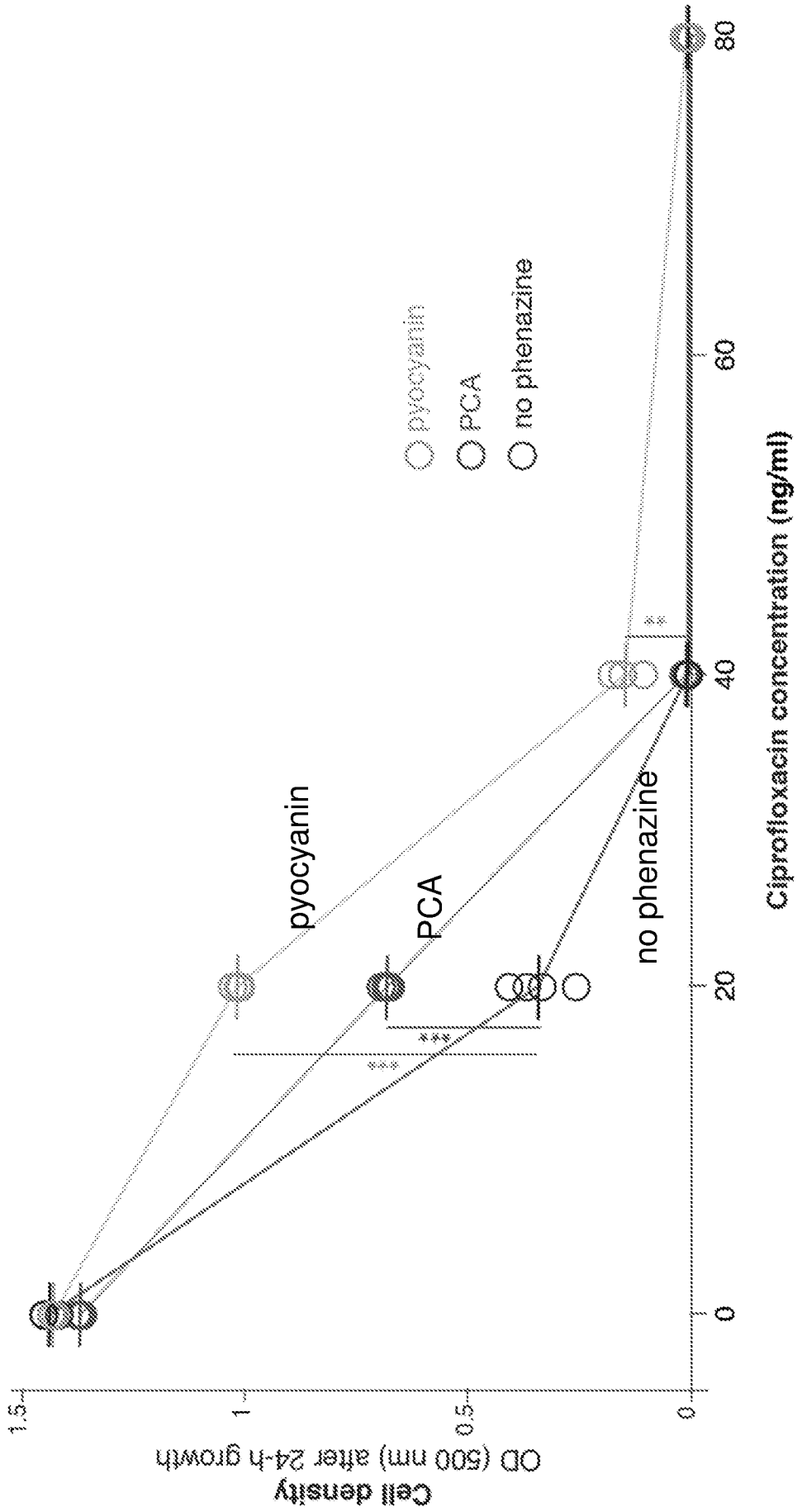

Cell density
OD (500 nm) after 24-h growth
1.5
1
0.5
0
0
20
40
60
80
Ciprofloxacin concentration (ng/ml)
pyocyanin
PCA
no phenazine
pyocyanin
PCA
no phenazine
***
***
**

Figure 15

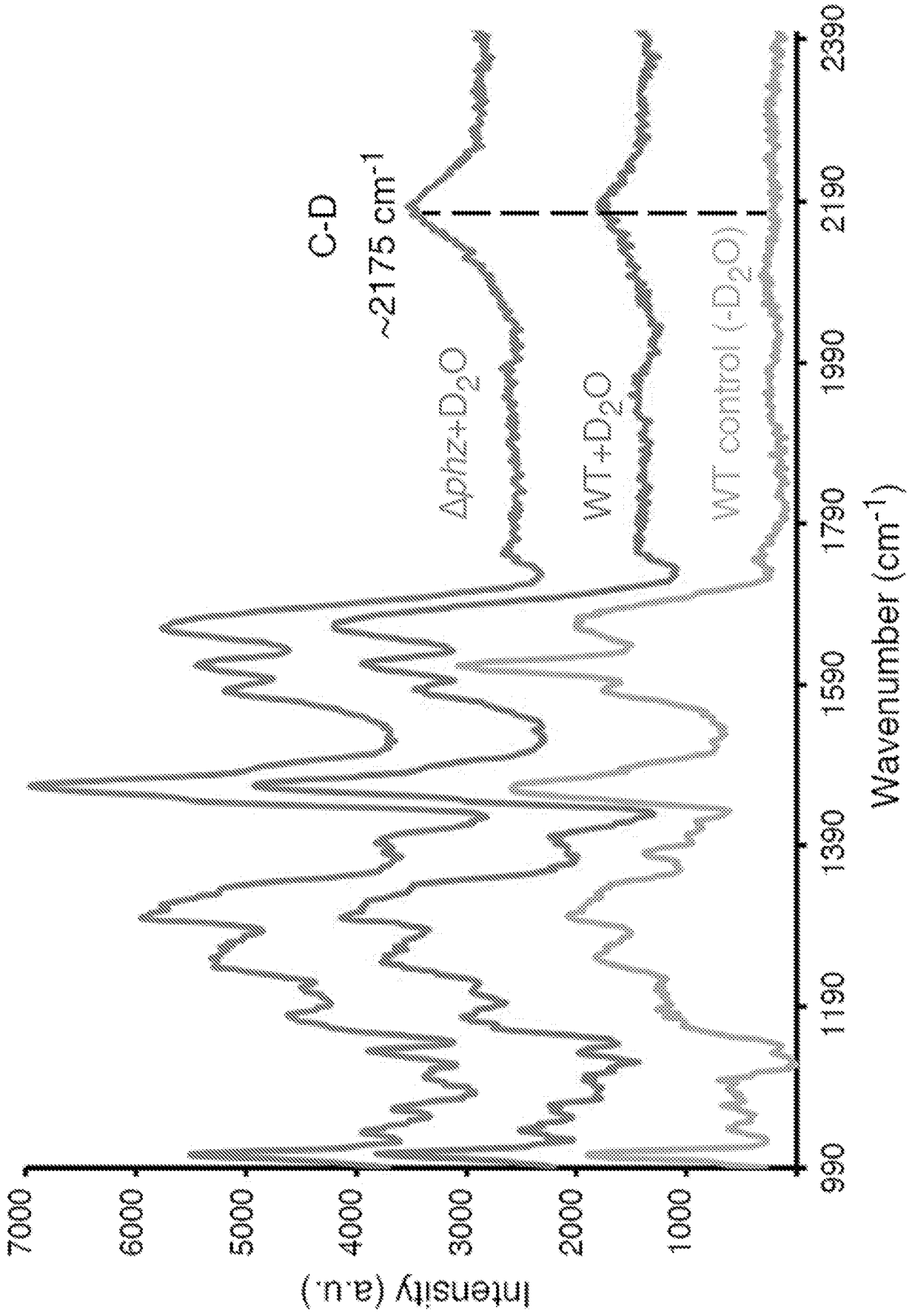

C-D
~2175 cm-1
Δphz+D2O
WT+D2O
WT control (-D2O)
Intensity (a.u.)
Wavenumber (cm-1)
7000
6000
5000
4000
3000
2000
1000
990
1190
1390
1590
1790
1990
2190
2390

Figure 16A

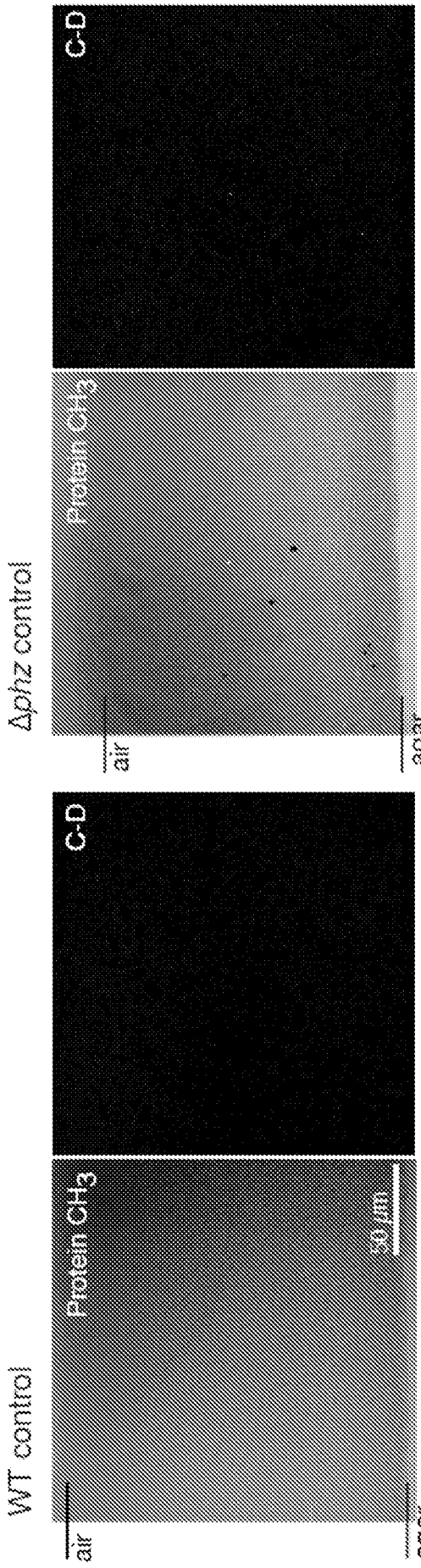

Δphz control
C-D
Protein CH_3
air
agar
WT control
C-D
Protein CH_3
50 μm
air
agar

Figure 16B

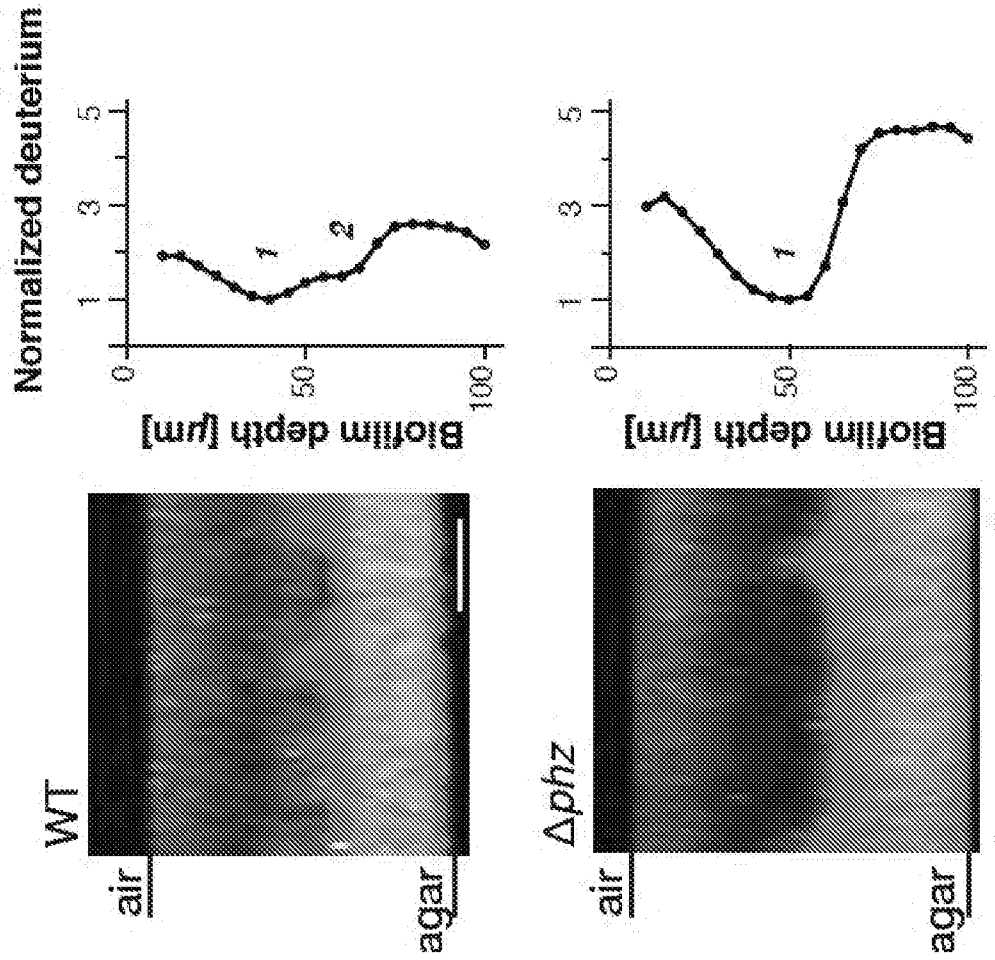


Figure 17B

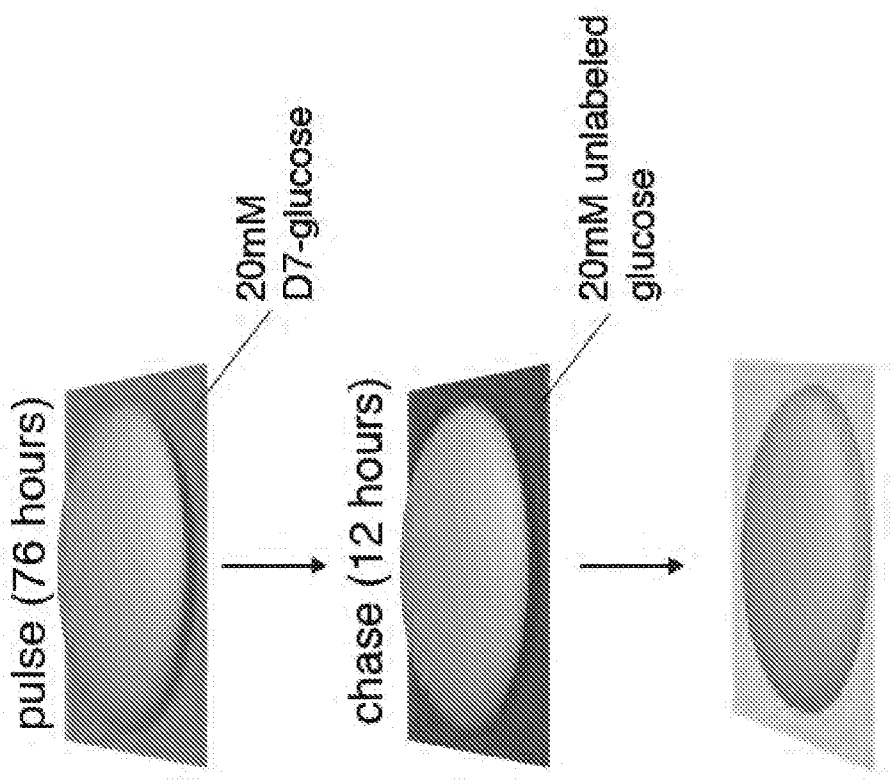


Figure 17A

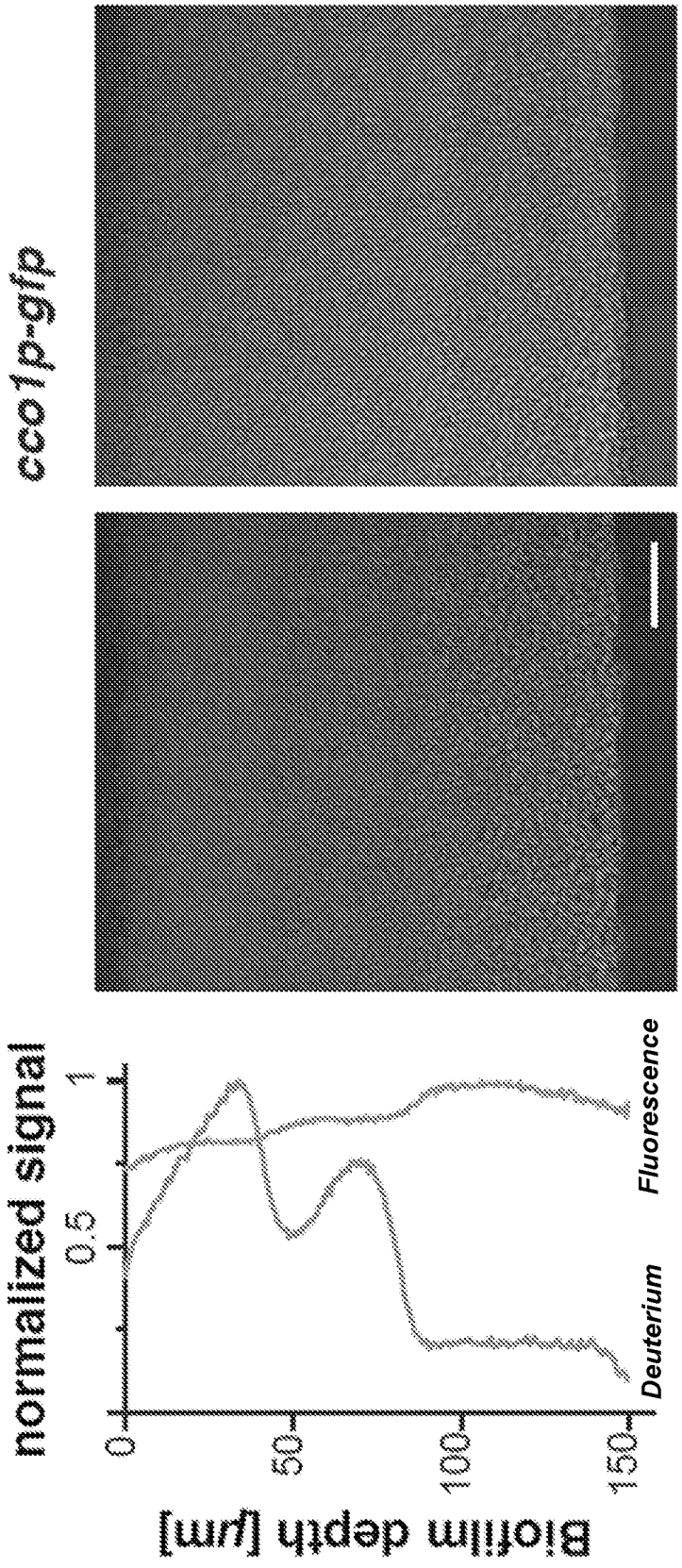

Deuterium
Fluorescence
cco1p-gfp
normalized signal
0
0.5
1
0
50
100
150
Biofilm depth [μm]
Fluorescence
Deuterium

Figure 18A

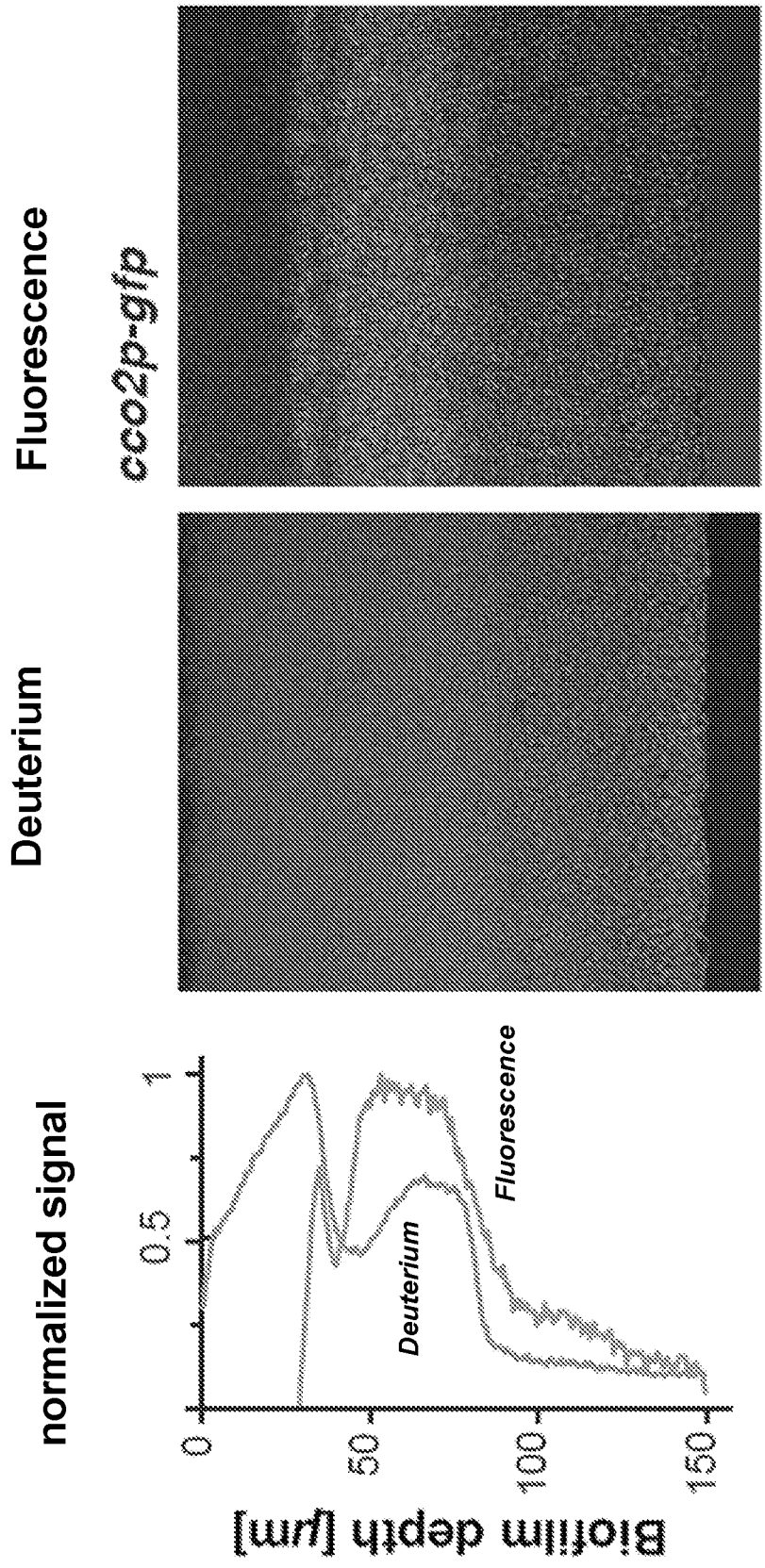

Fluorescence
cco2p-gfp
Deuterium
normalized signal
0
0.5
1
Deuterium
Fluorescence
0
50
100
150
Biofilm depth [μm]

Figure 18B

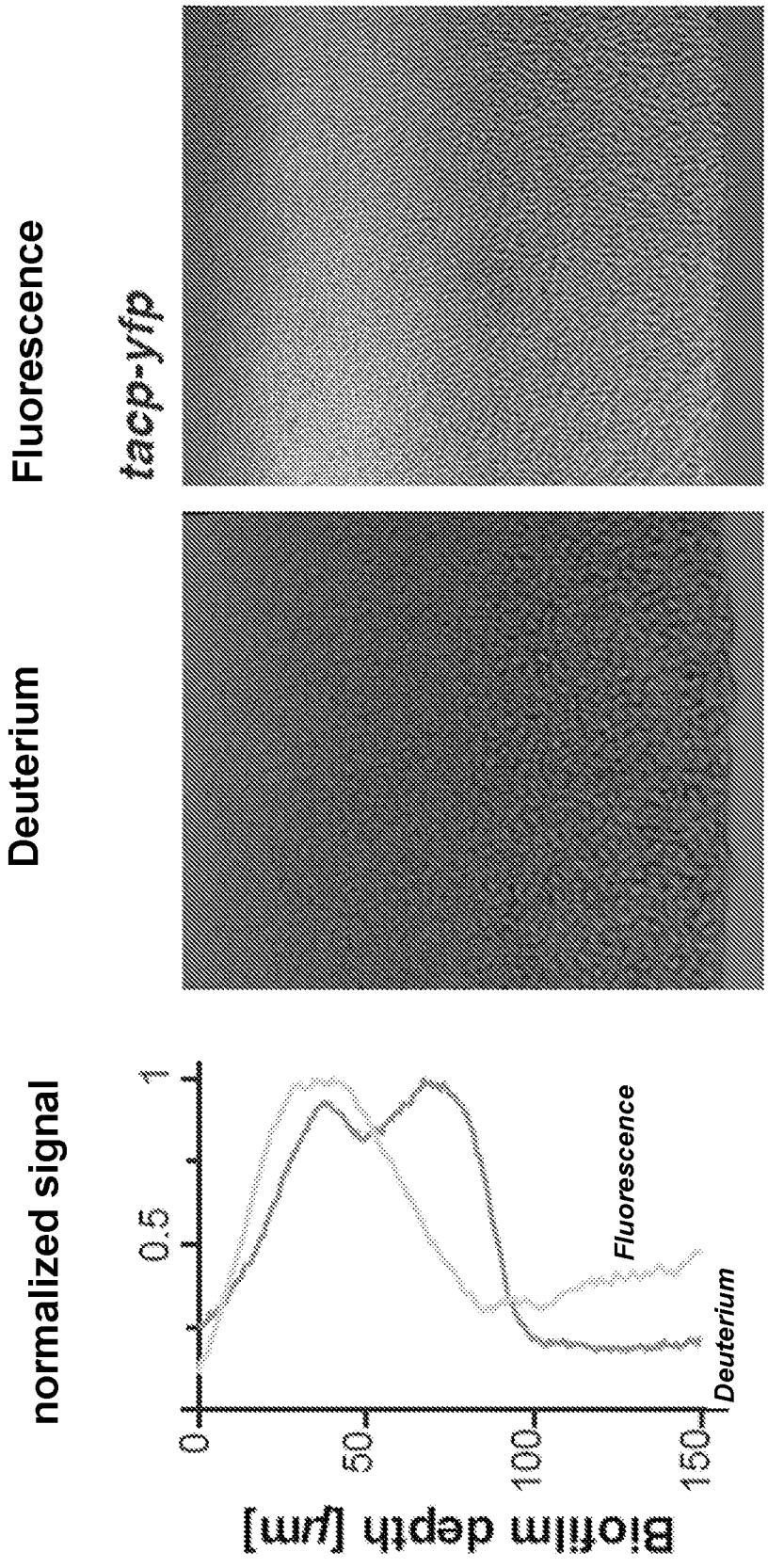

Fluorescence
tacp-yfp
Deuterium
normalized signal
0
0.5
1
0
50
100
150
Biofilm depth [μm]
Fluorescence
Deuterium

Figure 18C

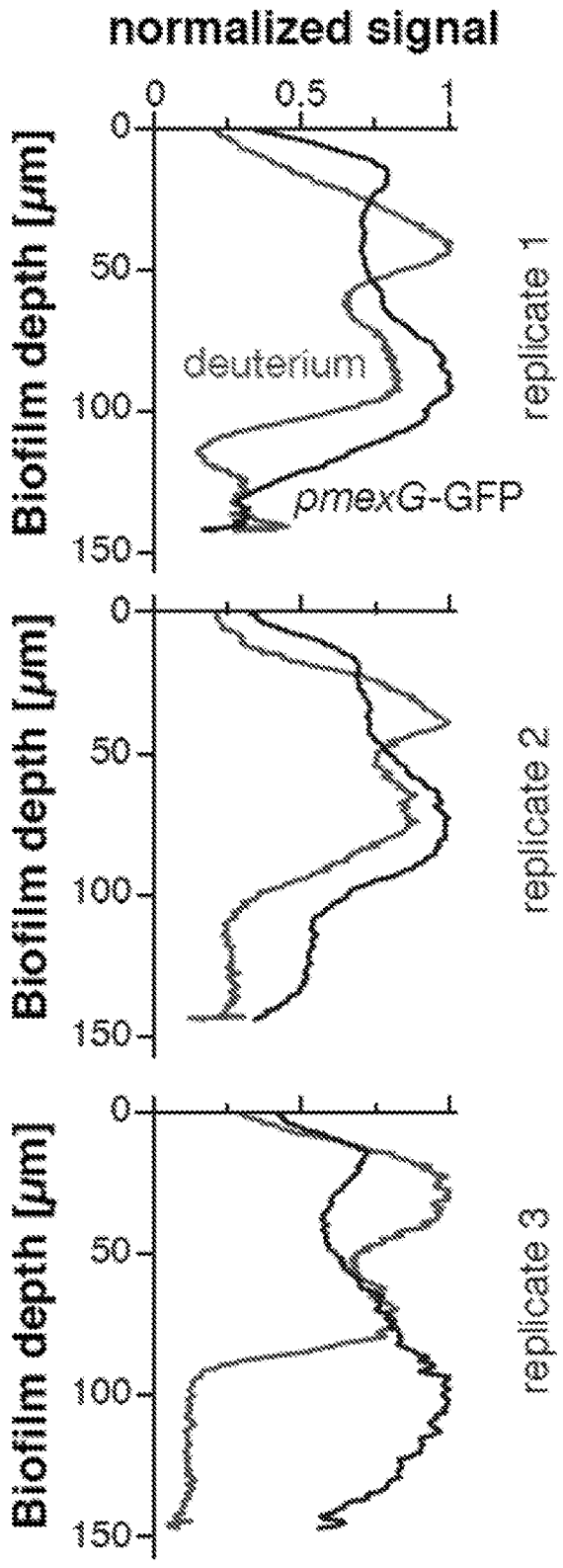

normalized signal
0
0.5
1
Biofilm depth [μm]
0
50
100
150
deuterium
pmexG-GFP
replicate 1
replicate 2
replicate 3

Figure 18D

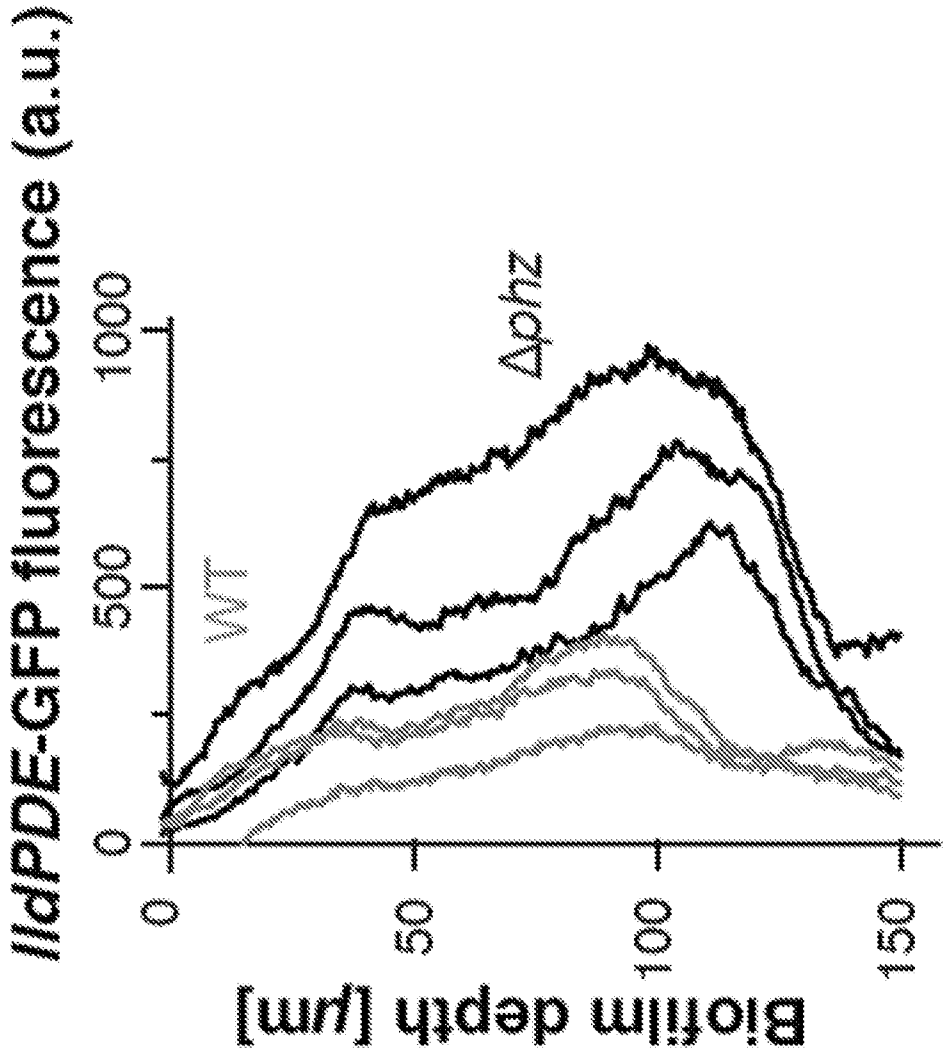

IIdPDE-GFP fluorescence (a.u.)
0
500
1000
WT
Δphz
0
50
100
150
Biofilm depth [μm]

Figure 18E

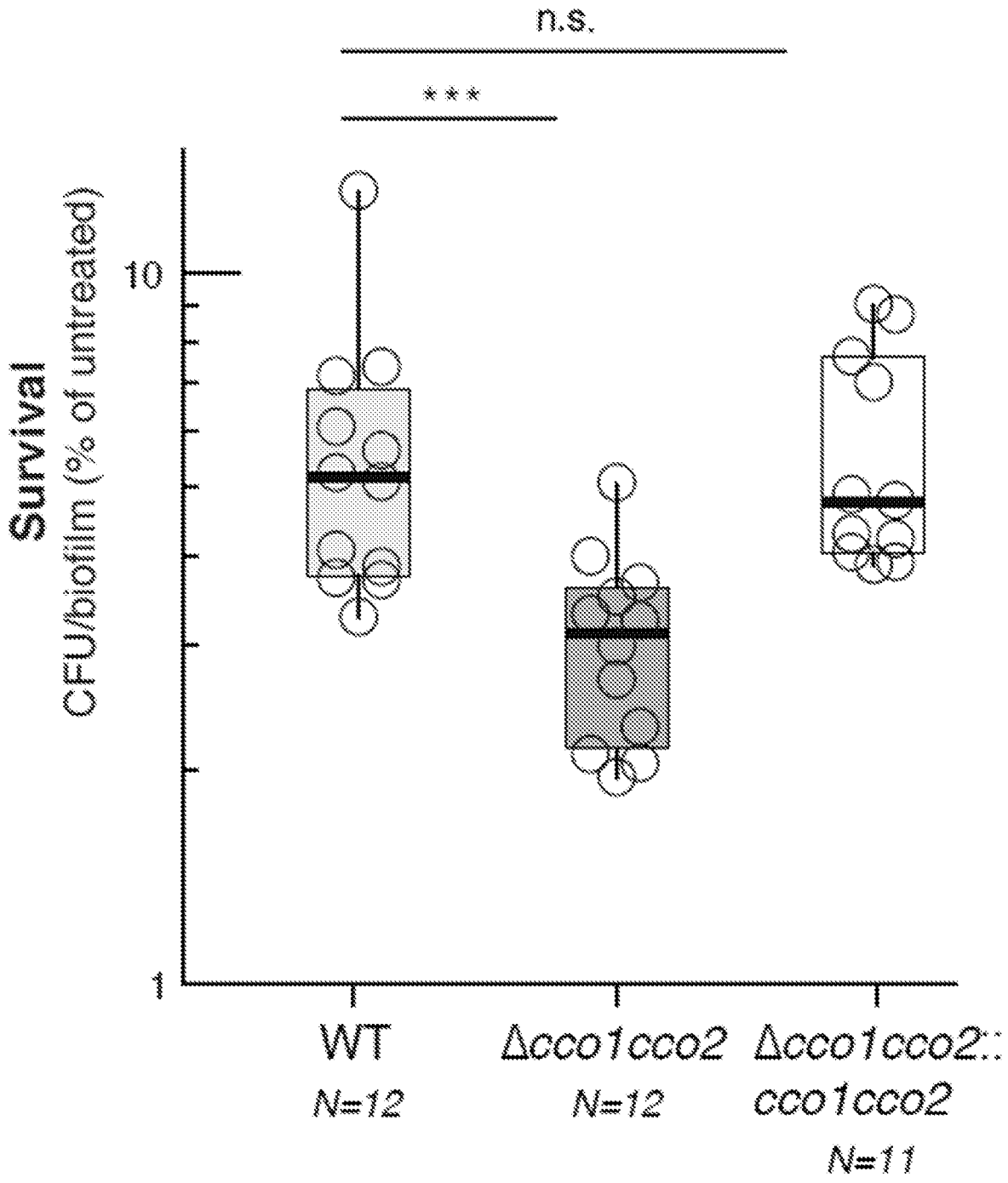

n.s.
***
Survival
CFU/biofilm (% of untreated)
10
1
WT
N=12
Δcco1cco2
N=12
Δcco1cco2::
cco1cco2
N=11

Figure 19A

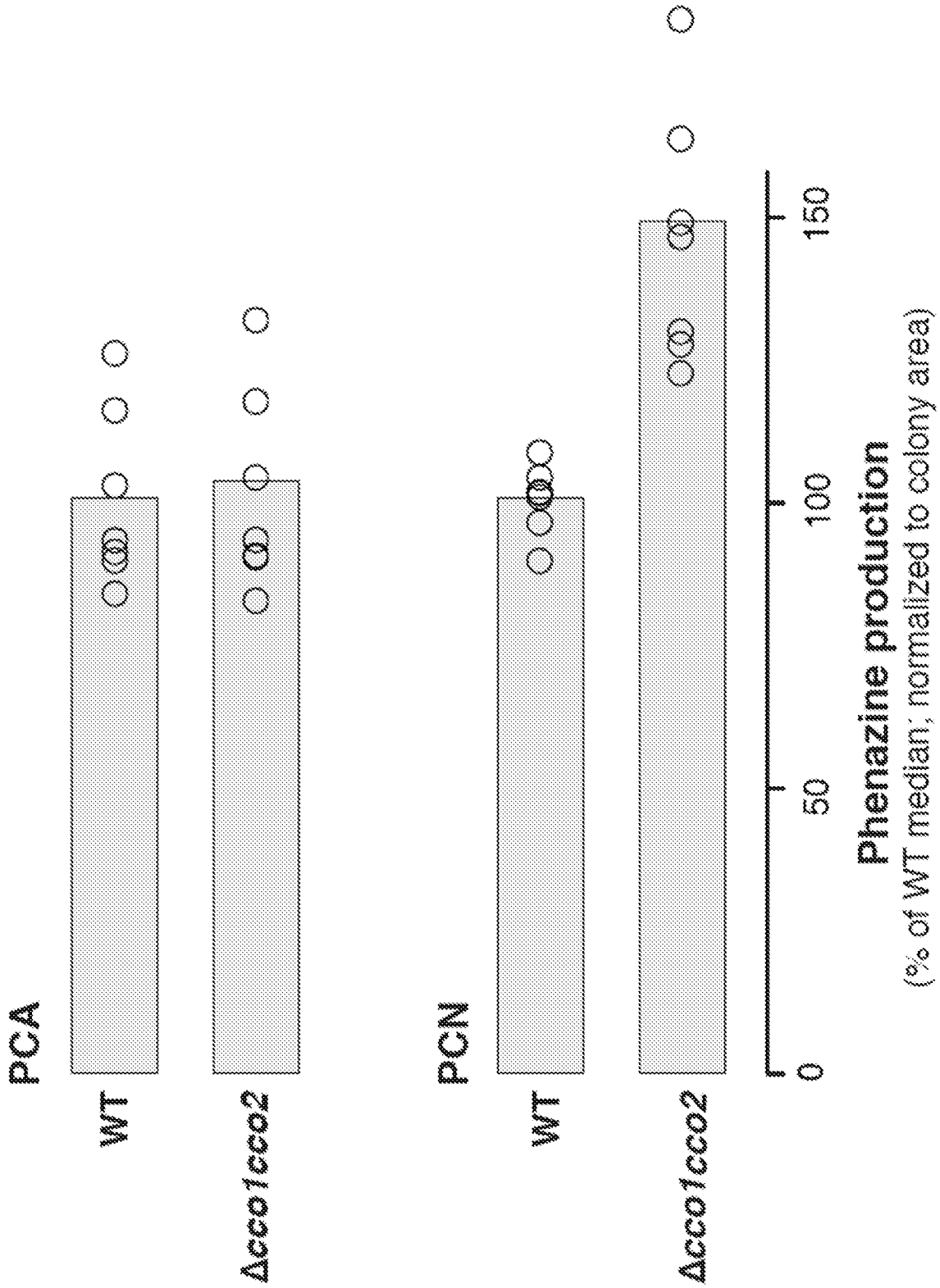

PCA
WT
Δcco1cco2
PCN
WT
Δcco1cco2
0
50
100
150
Phenazine production
(% of WT median; normalized to colony area)

Figure 19B

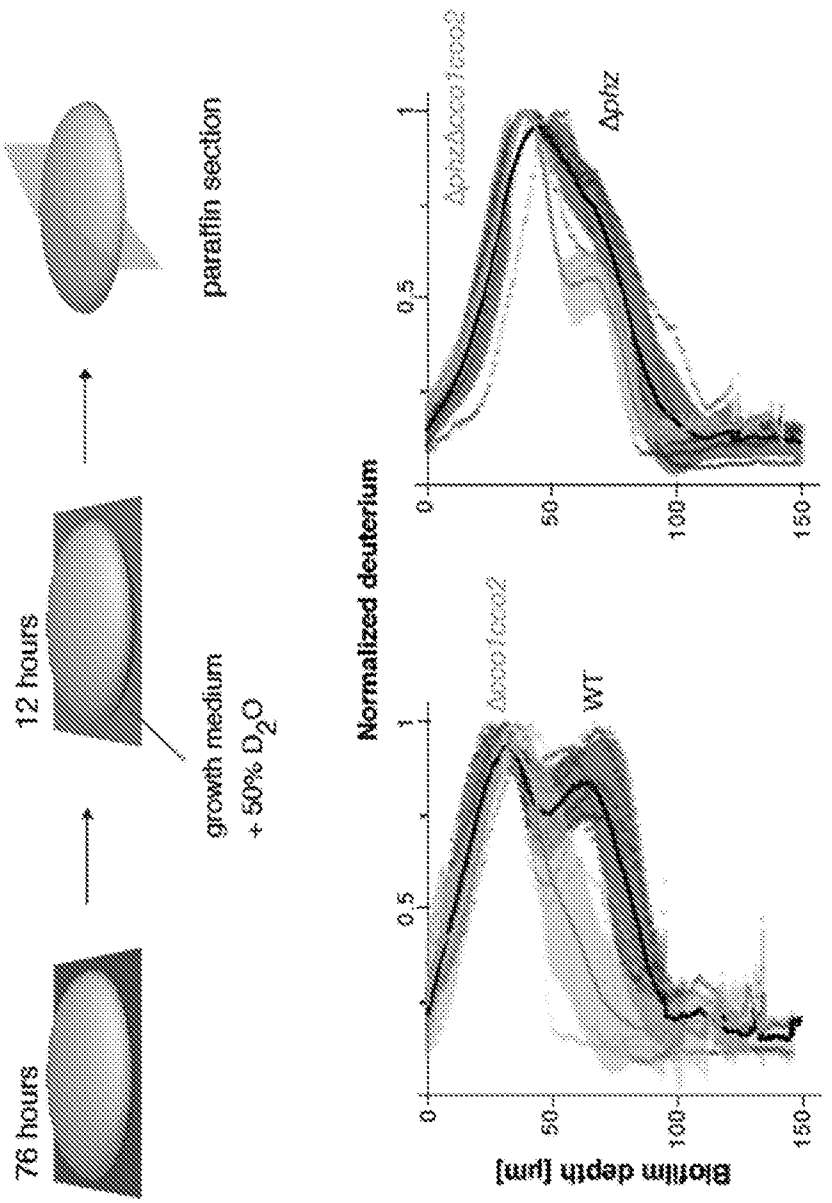

76 hours
12 hours
growth medium
+ 50% D_2O
paraffin section
Normalized deuterium
Biofilm depth [µm]
WT
Δsca1 sca2
Δpiz
Δpiz Δsca1 sca2
0
0.5
1
50
100
150

Figure 20

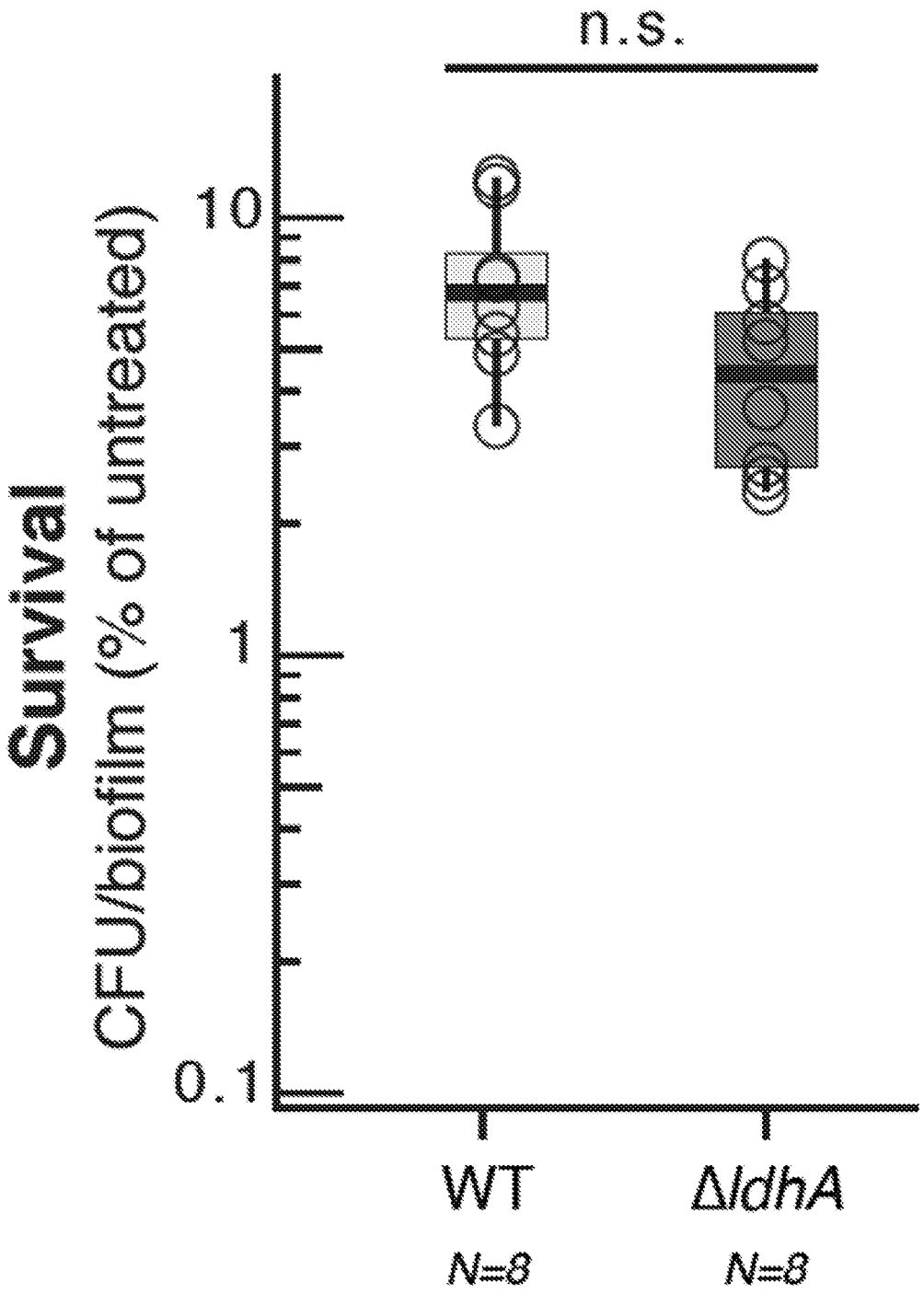


Figure 21

INTERNATIONAL SEARCH REPORT

International application No.
PCT/US19/17233

A. CLASSIFICATION OF SUBJECT MATTER

IPC - A61K 31/01, 31/04, 31/015, 31/19, 31/197, 31/198, 31/375, 33/26, 33/40, 39/104, 45/06 (2019.01)
CPC - A61K 31/01, 31/04, 31/015, 31/19, 31/197, 31/198, 31/375, 33/26, 33/40, 39/104, 45/06; A01N 37/44, 41/12, 43/08, 43/50, 59/16; A61L 15/22; C12Q 1/18; C12R 1/385; C07K 14/21, 14/195

According to International Patent Classification (IPC) or to both national classification and IPC

B. FIELDS SEARCHED

Minimum documentation searched (classification system followed by classification symbols)
See Search History document

Documentation searched other than minimum documentation to the extent that such documents are included in the fields searched
See Search History document

Electronic data base consulted during the international search (name of data base and, where practicable, search terms used)
See Search History document

C. DOCUMENTS CONSIDERED TO BE RELEVANT

Category*	Citation of document, with indication, where appropriate, of the relevant passages	Relevant to claim No.
X -- Y	US 2016/0089396 A1 (NEWSOUTH INNOVATIONS PTY LIMITED) 31 March 2016; paragraphs [0010], [0014], [0022], [0027]-[0028], [0035], [0057], [0062], [0070], [0077], [0089]-[0090], [0104], [0106], [0110], [0123], [0127], [0132], [0138], [0169]	1-4, 6, 14/1-4, 15-17, 18/1-4, 19/18/1-4, 21/1-4, 22/1-4, 23/1-4, 24/1-4, 25/1-4, 26/1-4, 27/1-4, 28/1-4, 29, 31/1-4, 32, 35/1-4, 36/1-4, 37/1-4, 38/37/1-4, 39-42, 44, 52/39-42, 53-55, 56/39-42, 57/56/39-42, 59/39-42, 60/39-42, 61/39-42, 62/39-42, 63/39-42, 64/39-42, 65/39-42, 66/39-42, 67, 69/39-42, 70, 73/39-42, 74/39-42, 75/39-42, 76/75/39-42, 77-78, 79/77-78, 80/79/77-78, 81/79/77-78, 82/79/77-78, 83/77-78, 84/77-78, 85/77-78, 86/77-78, 87/77-78, 88/77-78, 89/77-78, 90/77-78, 92/1-4 -------- ...cont. next page...

☒ Further documents are listed in the continuation of Box C. ☐ See patent family annex.

* Special categories of cited documents:
"A" document defining the general state of the art which is not considered to be of particular relevance
"E" earlier application or patent but published on or after the international filing date
"L" document which may throw doubts on priority claim(s) or which is cited to establish the publication date of another citation or other special reason (as specified)
"O" document referring to an oral disclosure, use, exhibition or other means
"P" document published prior to the international filing date but later than the priority date claimed
"T" later document published after the international filing date or priority date and not in conflict with the application but cited to understand the principle or theory underlying the invention
"X" document of particular relevance; the claimed invention cannot be considered novel or cannot be considered to involve an inventive step when the document is taken alone
"Y" document of particular relevance; the claimed invention cannot be considered to involve an inventive step when the document is combined with one or more other such documents, such combination being obvious to a person skilled in the art
"&" document member of the same patent family

Date of the actual completion of the international search	Date of mailing of the international search report
27 March 2019 (27.03.2019)	19 APR 2019
Name and mailing address of the ISA/ Mail Stop PCT, Attn: ISA/US, Commissioner for Patents P.O. Box 1450, Alexandria, Virginia 22313-1450 Facsimile No. 571-273-8300	Authorized officer Shane Thomas PCT Helpdesk: 571-272-4300 PCT OSP: 571-272-7774

INTERNATIONAL SEARCH REPORT

International application No.
PCT/US19/17233

C (Continuation). DOCUMENTS CONSIDERED TO BE RELEVANT

Category*	Citation of document, with indication, where appropriate, of the relevant passages	Relevant to claim No.
X -- Y	US 2016/0089396 A1 (NEWSOUTH INNOVATIONS PTY LIMITED) 31 March 2016; paragraphs [0010], [0014], [0022], [0027]-[0028], [0035], [0057], [0062], [0070], [0077], [0089]-[0090], [0104], [0106], [0110], [0123], [0127], [0132], [0138], [0169]	...cont. from prev. page... 20/18/1-4, 30, 58/56/39-42, 68
X	US 2015/0072025 A1 (HOPE MEDICAL ENTERPRISES, INC. DBA HOPE PHARMACEUTICALS) 12 March 2015; paragraphs [0017], [0020], [0232], [0234]; claims 39-41	1, 5, 7-10, 34, 39, 43, 45-48, 72
X -- Y	US 2004/0037897 A1 (BENJAMIN, N et al.) 26 February 2004; paragraphs [0008], [0016], [0030], [0037], [0040], [0043], [0089]	1, 11-13, 39, 49-51 ---------- 30, 68
X	WO 2014/070769 A1 (THE UNIVERSITY OF NORTH CAROLINA AT CHAPEL HILL) 08 May 2014; page 10, lines 11-13, 25-26; page 13, lines 18-19; page 18, line 24; page 34, line 4; Figure 4	1, 33, 39, 71, 77-78, 91/77-78
Y	WO 2017/067516 A1 (MICROBIOLOGY INSTITUTE OF SHAANXI) 27 April 2017; abstract	20/18/1-4, 58/56/39-42
A	(HIRAI, T et al.) Expression of multiple cbb3 cytochrome c oxidase isoforms by combinations of multiple isosubunits in Pseudomonas aeruginosa. Proceedings of the National Academy of Sciences of the U.S.A. 8 November 2016, Epub 24 October 2016, Vol. 113, No. 45; pages 12815-12819; DOI: 10.1073/pnas.1613308113	1-92
A	WO 2016/145192 A1 (UNIVERSITY OF CINCINNATI) 15 September 2016; entire document	1-92
A	WO 2017/147067 A1 (BOARD OF REGENTS, THE UNIVERSITY OF TEXAS SYSTEM) 31 August 2017; entire document	1-92
P, X	WO 2018/094278 A1 (RENOVION, INC.) 24 May 2018; entire document	1-92
P, X	WO 2018/237221 A1 (NOSOCOMIAL VACCINE CORPORATION et al.) 27 December 2018; entire document	1-92